INVESTIGATING THE ROLE OF TAB182 IN THE DNA DAMAGE RESPONSE AND REPLICATION STRESS PATHWAYS

By

ELLIS LOUISE RYAN

A thesis presented to the College of Medical and Dental Sciences, the University of Birmingham, for the degree of DOCTOR OF PHILOSOPHY

School of Cancer Sciences
College of Medical and Dental Sciences
University of Birmingham
December 2015

UNIVERSITY OF
BIRMINGHAM

University of Birmingham Research Archive

e-theses repository

This unpublished thesis/dissertation is copyright of the author and/or third parties. The intellectual property rights of the author or third parties in respect of this work are as defined by The Copyright Designs and Patents Act 1988 or as modified by any successor legislation.

Any use made of information contained in this thesis/dissertation must be in accordance with that legislation and must be properly acknowledged. Further distribution or reproduction in any format is prohibited without the permission of the copyright holder.

ABSTRACT

It is well established that adenoviruses degrade components of the cellular DNA damage response, such as p53, DNA ligase IV and Mre11, in order to avoid detection from the host cell and thus, promote viral replication. Here we show TAB182, a protein of previously unknown function, is degraded following adenovirus serotype 5 and 12 infection. Similarly to other DNA damage proteins, the degradation of TAB182 is dependent on the adenoviral E1B55K and E4orf6 proteins, together with the cellular Cullin 5 (during Ad5 infection) and Cullin 2 (during Ad12 infection). Interestingly, siRNA-mediated knockdown of TAB182 appears to be beneficial for adenovirus infection, as denoted by an increased expression of the adenoviral E1A protein and Cyclin E during adenovirus infection. Together with other studies, we confirm that TAB182 interacts with the large, multi-subunit CNOT complex. This complex has no defined function in mammalian cells, but is known to play a role in gene regulation in yeast. Interestingly, components of the CNOT complex are also degraded during adenovirus infection, whether adenovirus degrades TAB182 as well as CNOT for the same advantage is currently unknown.

Cells deficient in TAB182 are hypersensitive to agents that induce DNA replication stress and also exhibit abnormal replication dynamics following release from hydroxyurea-induced fork stalling. In particular, they display increased fork restart and elevated new origin firing following release from hydroxyurea treatment, suggesting that TAB182 prevents fork recovery and suppresses new origin firing following replication stress. Depletion of some components of the CNOT complex is able to rescue the phenotypes observed in TAB182 deficient cells, suggesting that TAB182 and the CNOT complex may act in concert at the replication fork. TAB182 deficient cells display less DNA gaps and breaks but increased

levels of 53BP1 bodies in G1 and micronuclei, which are markers of genome instability, following replication stress. Whether TAB182 acts directly at the replication fork, or in conjunction with other proteins known to be involved in replication restart such as helicases, nucleases or chromatin remodelling complexes, remains to be elucidated.

ACKNOWLEDGEMENTS

Firstly, I express my sincere gratitude to my supervisors Dr Roger Grand and Professor Grant Stewart. It is hard to put into words how grateful I am for Roger's guidance and support over the last four years, as well as a fantastic supervisor, he has also been a great friend to me, especially during the harder times of my PhD. A special thanks goes to Grant, who accepted me into his lab and was always on hand to offer scientific advice. I hope that in the future I am able to show even a fraction of the dedication to science that you do.

Thank you to members of the Stewart group both past and present. I am incredibly thankful to Natasha for her scientific discussions and dedication to helping me, especially during the writing of this thesis. Your vast knowledge and enthusiasm for science has been particularly inspiring to me. Thank you to John and Martin for their scientific input over the last four years. I extend my gratitude to Ed who was always there to provide positivity and advice on all things molecular biology. A massive thank you to Phil who provided me with a tremendous amount of support regarding cloning, and also to Eva for scientific discussion.

I could not have got through the last four years without the support of my dear friends. To Laura and Tegan, thank you for being there for me over the past four years, I am happy to have made two life-long friends from this process. Thank you to Amy and Lucas, who were successfully able to distract me during the harder times of this PhD. To Anna, who has selflessly and without reservation supported me since we started our undergraduate degree together in 2007, thank you for being such a wonderful friend. Thank you to Dom, Harry and 'the Smiths', because even when you didn't know it, you were a massive support for me throughout this process. To my BFF Grace, I cannot express in words how grateful and indebted I am to you for your support, you were always there for me without hesitation,

you are truly selfless and an all-round wonderful human. I am infinitely grateful to Josh, without whom I'm not sure I would have made it through this process, thank you for your never-ending patience and encouragement.

To my beloved Nan, thank you for all of your support, the 'words' are done now! Finally I thank my wonderful parents, who provided me with all the love and support necessary to get me through my PhD. You were always there to believe in me when I no longer believed in myself, for that I am eternally grateful. To them I dedicate this thesis.

TABLE OF CONTENTS

LIST OF FIGURES

LIST OF TABLES

LIST OF ABBREVIATIONS

4-NQO	4-nitroquinoline 1-oxide
53BP1	p53-binding protein 1
9-1-1	Rad9-Rad1-Hus1
Ad	Adenovirus
Adv Pol	Adv DNA polymerase
AP	apurinic-apyrimidinic
AP1	activating protein 1
APE1	AP endonuclease 1
ATCC	American type culture collection
ATF2	AMP-dependent transcription factor 2
ATM	ataxia telangiectasia mutated
ATRIP	ATR-interacting protein
ATRX	X-linked α thalassaemia retardation syndrome protein
BAK	BCL2 antagonist killer
BAX	BCL2-associated X
BCL2	B-cell lymphoma 2
BER	base excision repair
BLM	Bloom syndrome protein
BRCA1	breast cancer type 1 susceptibility protein
BRCA2	breast cancer type 2 susceptibility protein
BSA	bovine serum albumin
BubR1	budding uninhibited by benzimidazoles-related 1
CAR	coxsackievirus and Ad receptor
CBP	CREB-binding protein
CCR4-NOT	chemokine (C-C motif) receptor 4 - NOT
CDC25	cell division cycle 25
CDC45	cell division cycle 45
Cdc6	cell division cycle 6

Cdc7	cell division cycle 7
CDK	cyclin dependent kinase
Cdt1	cell division cycle 10-dependent transcript 1
CFS	common fragile site
CldU	5-chloro-2'-deoxyuridine
CNOT	CCR4-NOT transcription complex
CPD	cyclobutane pyridine dimer
CR	conserved region
CRM1	chromosome region maintenance 1
CRT1	compromised recognition of TCV 1
CtBP	C-terminal binding protein
CtIP	CtBP interacting protein
Cul	Cullin
D-loop	displacement loop
DAPI	4', 6-diamidino-2-phenylindole
Daxx	death domain-associated protein
DBP	DNA binding protein
dCMP	deoxycitidine monophosphate
DDK	Dbf4-dependent kinase (Cdc7-Dbf4)
DDR	DNA damage response
DMEM	Dulbecco's modified Eagle's medium
DMSO	dimethyl sulphoxide
DNA	deoxyribonucleic acid
DNA-PK	DNA-dependent protein kinase
DNA2	DNA replication helicase/nuclease 2
dNTPs	deoxyribonucleotides
ds	double-stranded
DSB	double-strand break
dsDNA	double-stranded DNA
DTT	dithiothreitol

ECL	enhanced chemiluminescence
EME1	essential meiotic endonuclease 1 homologue 1
ERCC1	excision repair cross-complementation group 1
ERFS	early-replicating fragile site
EXO1	exonuclease 1
FA	Fanconi anaemia
FAAP24	Fanconi anaemia associated protein 24
FANCA	Fanconi anaemia complementation group A
FANCD2	Fanconi anaemia complementation group D2
FANCM	Fanconi anaemia complementation group M
FBH1	F-box helicase 1
FCS	foetal calf serum
FEN1	flap endonuclease 1
FHL2	four and a half LIM domain 2
G1	gap phase 1
G2	gap phase 2
GADD45	growth arrest and DNA damage inducible 45 alpha
GGR	global-genome repair
GST	gluthathione S-transferase
HAT	histone acetyltransferase
HCl	hydrochloric acid
HPV18	human papillomavirus
HR	homologous recombination
HRP	horseradish-peroxidase
HU	hydroxyurea
ICL	Interstrand Cross-Link
IDL	insertion/deletion loop
IdU	5-iodo-2'deoxyuridine
iPOND	isolation of proteins on nascent DNA
IR	ionising radiation

ITR	inverted terminal repeat
JARID1C	jumonji and AT-rich interaction domain 1C
LB	luria broth
M	mitosis
MAPK	mitogen-activated protein kinase
MCL1	myeloid cell leukaemia 1
MCM	mini chromosome maintenance
mDa	megadalton
MDC1	mediator of damage checkpoint 1
MDM2	mouse double minute 2
MLL	mixed lineage leukaemia
MMR	mismatch repair
MOI	multiplicity of infection
MRN	Mre11-Rad50-NBS1
mRNA	messenger RNA
MUS81	Mus81 endonuclease homologue
MutLα	MLH1/PMS2
MutSα	MSH2-MSH6
MutSβ	MSH2-MSH3
Myt1	myelin transcription factor 1
NAC	nascent associated polypeptide complex
NAE	NEDD8-activating enzyme
NER	nucleotide excision repair
NETN	NP-40-EDTA-Tris HCl-NaCl
NF-κB	nuclear factor-kappa B
NF1	nuclear factor 1
NF2	nuclear factor 2
NHEJ	non-homologous end-joining
Oct-1	octamer-binding protein 1
ORC	origin recognition complex

ORF	open reading frame
PAR	poly (ADP-ribose)
PARP1	poly (ADP-ribose) polymerase 1
PBS	phosphate buffered saline
PCNA	proliferating cell nuclear antigen
PCR	polymerase chain reaction
PFA	paraformaldehyde
PFGE	pulse-field gel electrophoresis
PFU	plaque forming units
PI	propidium iodide
Plk3	polo-like kinase 3
PML	promyelocytic leukaemia
POD	PML oncogenic domain
PP2A	protein phosphatase 2A
pRB	retinoblastoma protein
pre-RC	pre-replicative complex
PRMT3	protein arginine N-methyltransferase 3
pTP	TP precursor
RAP80	receptor-associated protein 80
Rbx1	RING-box 1
RFB	replication fork barrier
RFC	replication factor C
RFC2	Rad17-replication factor C
RGD	Arg-Gly-Asp
RNA	ribonucleic acid
RNAPII	elongating polymerase II (is this right?)
RNF8/168	RING finger protein 8/168
RNR	ribonucleotide reductase
rNTP	ribonucleotide
ROS	reactive oxidative species

RPA	replication protein A
S	DNA synthesis
Sal I-HF	High fidelity Sal I
SDSA	synthesis-dependent strand annealing
SMAC	second mitochondria-derived activator of caspases
SMARCAL1	SWI/SNF-related matrix-associated actin-dependent regulator of chromatin subfamily A
SSB	single-strand break
ssDNA	single-stranded DNA
SUMO	small ubiquitin-like modifier
TAB182	tankyrase 1 binding protein 1 of 182kDa
TAF	TBP-binding protein
TBP	TATA-binding protein
TCR	transcription-coupled repair
TFIID	transcription factor IID
Tip60	HIV-1 tat interacting protein 60kDa
TLS	translesion synthesis
TOPBP1	topoisomerase II binding protein 1
TOPI	topoisomerase I
TOPII	topoisomerase II
TP	terminal protein
Ub	ubiquitin
UTB	urea-Tris HCl-β-mercaptoethanol
UV-C	ultra violet C
UV-DDB	UV DNA damage binding protein
VRC	viral replication centre
WRN	Werner syndrome protein
XLF	XRCC-like factor
XPB	xeroderma pigmentosum complementation group B
XPC	XPC-Rad23B-Centrin2
XPD	xeroderma pigmentosum complementation group D

XPF	xeroderma pigmentosum complementation group F
XPG	xeroderma pigmentosum complementation group G
XRCC1	X-ray repair cross-complementing protein 1
XRCC3	X-ray repair cross-complementing protein 3
XRCC4	X-ray repair cross-complementing protein 4

CHAPTER ONE

INTRODUCTION

1. INTRODUCTION

1.1 ADENOVIRUS

1.1.1 Adenovirus Identification and Classification

Adenovirus was first discovered in 1953 when Rowe and colleagues isolated the virus from adenoid tissue undergoing spontaneous degeneration in children (Rowe, Huebner et al. 1953). The name 'adenovirus' therefore derives from the origin of its initial isolation. A year later, a number of publications presented evidence to suggest a novel 'agent' was responsible for patients diagnosed with 'acute respiratory illness' that was not attributed to the common cold, these cases would later be recognised as the result of adenovirus infection (Hilleman and Werner 1954, Ginsberg, Gold et al. 1955). The next major discovery was by Trentin and colleagues who showed that adenovirus serotype 12 (Ad12) was able to directly induce tumours in new-born hamsters (Yabe, Trentin et al. 1962). This was the first example of a human virus that was able to cause cancer. In addition to its ability to cause tumours in new-born rodents, adenovirus can also transform mammalian cells in culture; every adenovirus serotype is known to have the capacity to transform primary rodent cells *in vitro* (McBride and Wiener 1964, Pope and Rowe 1964).

The *adenoviridae* family contains five accepted genera comprised of *Mastadenoviridae, Atadenoviridae, Aviadenoviridae, Siadenoviridae* and *Ictadenoviridae*. These genera encompass a wide range of host vertebrate species from humans in the *Mastadenoviridae* genus, to fish in the *Ictadenoviridae* genus. *Mastadenoviridae* is the genus in which all human adenovirus serotypes belong which is currently believed to include at least 55 serotypes. These serotypes can be further categorised into six species grouped A to

Group	Serotypes	Oncogenicity in Rodents	Transformation in tissue culture
A	12, 18, 31	High	Yes
B1	3, 7, 16, 21, 50	Moderate	Yes
B2	11, 14, 34, 35, 55	Moderate	Yes
C	1, 2, 5, 6	Low/None	Yes
D	8, 9, 10, 13, 15, 17, 19, 20, 22-30, 32, 33, 36-39, 42-49, 51, 53, 54	Low/None	Yes
E	4	Low/None	Yes
F	40, 41	Not reported	Yes
G	52	Not reported	Unknown

Table 1.1: Classification of Human Adenoviruses. The adenovirus serotypes identified to date are indicated, classified into groups A to G. The potential for these serotypes to cause oncogenicity in rodents and transformation in tissue culture is also indicated. Adenovirus serotypes used in this study are highlighted in red.

G (Table 1.1). The species to which each serotype is grouped is largely dependent on their oncogenicity in rodents, their ability to agglutinate erythrocytes and their DNA sequence (Russell 2009).

Certain adenovirus serotypes are known to cause gastrointestinal, respiratory and ocular disease (Bennett, Hamilton et al. 1957, Brandt, Kim et al. 1969, Uhnoo, Wadell et al. 1984). The incidence of adenovirus infection in immunocompromised hosts is significantly increased, particularly in patients receiving allogeneic stem cell transplantations. Adenovirus infection in immunocompromised individuals is associated with encephalitis, haemorrhagic cystitis, gastroenteritis, pneumonitis and hepatitis, all of which carry a significant mortality rate (Carrigan 1997).

1.1.2 Adenovirus Structure and Genome

Adenovirus is an icosahedral, non-enveloped virus of approximately 150 megadaltons (mDa) in weight, and 70nm in diameter. In 1959 electron microscopy gave the first indication of the structure of the adenovirus virion; the adenovirus capsid was shown to be composed of 252 subunits; 240 hexons and 12 pentons (Horne, Brenner et al. 1959). Six years later further imaging by electron microscopy revealed fibres that protruded from the penton bases of the capsid of the virus (Valentine and Pereira 1965). More recently, X-ray crystallography has revealed the atomic structure of most of the adenovirus structural proteins (Roberts, White et al. 1986, Athappilly, Murali et al. 1994, Zubieta, Schoehn et al. 2005). Each virion is composed of multiple copies of a total of 11 structural proteins. The icosahedral capsid is formed from the structural proteins hexon (II), penton base (III) and the protruding knob fibre (IV), which are known to be essential for binding to the coxsackievirus and Ad receptor (CAR) of the host cell (Bergelson, Cunningham et al. 1997). The capsid is

also composed of the more minor structural capsid proteins IIIa, IV, VIII and IX. The core complex contains the proteins V, VII, Mu and the terminal protein (TP). Each adenovirus virion also contains 10 copies of the adenovirus protease protein (Anderson 1990).

The adenoviral genome is a linear, double-stranded deoxyribonucleic acid (dsDNA) of approximately 35kbp in size. The adenoviral genome is characterised by inverted terminal repeats (ITRs) which are approximately 100 bp long (actual length varies between serotypes). The TP is covalently linked to each 5' end via the ITR region of the adenovirus genome, its function being to prime the genome for DNA replication (Rekosh, Russell et al. 1977). The remaining core proteins V, VII and Mu are non-covalently bound to the viral genome. Protein V is believed to provide a structural link between the core complex and the viral capsid via protein VI (Matthews and Russell 1998). Proteins VII and Mu are associated with the viral DNA (Vayda, Rogers et al. 1983, Chatterjee, Vayda et al. 1985).

1.1.3 Adenovirus DNA Replication

The initial interaction between adenovirus and the host cell involves the binding of the protruding fibre knob to the cellular receptor CAR (Bergelson, Cunningham et al. 1997). For most adenovirus serotypes, viral entry into the host cell is achieved by clathrin-mediated endocytosis following the binding of a penton base protein (containing an Arg-Gly-Asp (RGD) motif) to a cellular αv integrin (Wickham, Mathias et al. 1993). The viral protease L3/p23 is responsible for the degradation of the adenoviral structural protein IV, therefore disrupting the viral capsid in preparation for exit of the viral DNA (Greber, Webster et al. 1996). The virus is then transported from the cytoplasm to the nucleus, a process thought to be achieved through the association with the cellular protein p32. p32 shuttles between the mitochondria and nucleus as part of the cellular transport system, a system that is believed

to be hijacked by the virus in order to enter the host cell nucleus (Matthews and Russell 1998).

The adenovirus infectious cycle can be categorised into the early and late phase, which is separated by adenoviral DNA replication. The early phase of the adenovirus infectious cycle takes 6-8 hours and involves the transcription of the early proteins E1, E2, E3 and E4 (see Sections 1.1.4, 1.1.5 and 1.1.6 for a detailed discussion on the E1 and E4 proteins). In order to replicate its genome, adenovirus uses three viral proteins produced from transcription of its early E2 genes. These are the TP precursor (pTP), Adv DNA polymerase (Adv Pol) and the DNA binding protein (DBP) (van der Vliet and Levine 1973, Coombs, Robinson et al. 1979). Adenovirus also utilises three cellular proteins during DNA replication, two transcription factors: nuclear factor 1 (NF1) and octamer-binding protein 1 (Oct-1), as well as the type 1 topoisomerase (TOP) nuclear factor 2 (NF2) (Nagata, Guggenheimer et al. 1982, Nagata, Guggenheimer et al. 1983, Pruijn, van Driel et al. 1986). Adenovirus DNA replication begins from both ends of the DNA termini whereby a covalent bond is formed between the 5' terminal nucleotide deoxycitidine monophosphate (dCMP) and a serine residue of pTP, in a reaction catalysed by Ad pol. This dCMP/pTP complex then acts as a primer for nascent DNA synthesis. DBP stimulates the binding of the transcription factor NF1 to AdV Pol, whilst the transcription factor Oct-1 interacts with pTP; together these proteins form the pre-initiation complex required for the initiation of DNA replication (Nagata, Guggenheimer et al. 1982). DBP also promotes DNA elongation and together with NF2, stimulates efficient elongation (Nagata, Guggenheimer et al. 1983). During the termination of DNA replication, pTP is cleaved by a viral protease leading to the generation of viral DNA that is ready to be packaged into virions and transported out of the cell

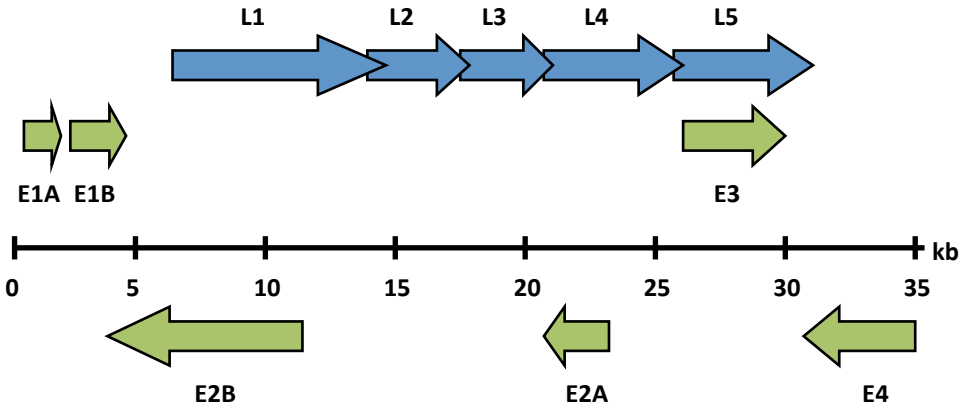

Figure 1.1: Adenovirus Genome Organisation. Schematic to outline the organisation of the adenovirus genome. Early adenovirus transcripts are indicated in green, late adenovirus transcripts are indicated in blue. Direction of the arrows represent the direction of transcription (modified from Russell, 2000).

(Dunsworth-Browne, Schell et al. 1980, Stillman, Lewis et al. 1981, Schaack, Ho et al. 1990). In order for this to occur, transcription and translation of the adenovirus intermediate (IX and Iva2) and late genes (L1-L5) is initiated, which produces the structural proteins required for the maturation of the virus (Figure 1.1).

1.1.4 The Adenovirus E1A Protein

The adenovirus E1A protein is the first messenger RNA (mRNA) to be transcribed following entry of the virus into the nucleus and produces two major mRNA products of 289 and 243 amino acid residues in length in adenovirus serotype 5. E1As from other virus serotypes vary in length (Avvakumov, Sahbegovic et al. 2002). These proteins contain three conserved regions (CRs) known as CR1, CR2 and CR4, whilst the 289 amino acid protein contains an additional conserved region designated CR3 (Figure 1.2). The E1A protein is known to induce the immortalisation of primary rodent cells but the expression of E1B (or a complementary oncogene such as mutant Ras) is required in order to completely transform cells (Graham, van der Eb et al. 1974, Houweling, van den Elsen et al. 1980, Ruley 1983). The E1A protein activates viral transcription and influences a number of cellular genes involved in gene expression and cell growth, with the ultimate aim of replicating the adenoviral genome. These genes include transcriptional co-repressors, co-activators, cell cycle regulatory proteins and the transcriptional machinery (Gallimore and Turnell 2001, Berk 2005).

The first E1A-binding protein to be characterised was the retinoblastoma protein (pRB) tumour suppressor (Whyte, Buchkovich et al. 1988). The CR1 and CR2 regions of E1A are responsible for the binding of E1A to pRB, along with the related proteins p107 and p130. AdE1A displaces pRB from E2F promoters and in turn stimulates E2F-dependent

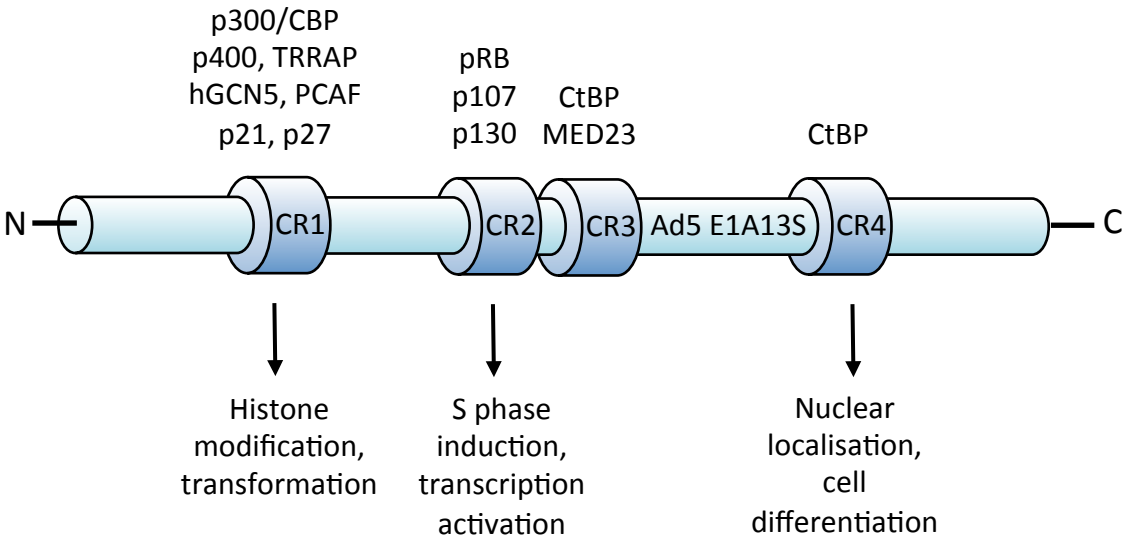

Figure 1.2: Representation of Ad5 E1A13S. Schematic shows the Ad5 E1A13S protein and the four conserved regions (CR1-4) of the protein. Protein binding partners are depicted (above), together with the cellular functions of these regions (adapted from Zheng 2010).

transcription of the viral gene E2 and a number of cellular genes, the end result of which being S phase entry, which drives viral DNA replication (Bagchi, Raychaudhuri et al. 1990, Grand, Ibrahim et al. 1998). In adenovirus transformed cells where there is no viral replication, the role of AdE1A is to drive cellular proliferation, largely through interaction with the same proteins (Gallimore and Turnell 2001).

Another way in which the adenovirus E1A protein is able to drive cell cycle progression is through the interaction with the transcriptional co-activators p300 and CREB-binding protein (CBP) (Eckner, Ewen et al. 1994, Arany, Newsome et al. 1995). These transcriptional co-activators possess histone acetyltransferase (HAT) activity which is thought to control the transcriptional activation of other key cell cycle mediator proteins such as p53 and nuclear factor-kappa B (NF-κB), again with the ultimate aim to drive cells into S phase (Ogryzko, Schiltz et al. 1996, Lill, Grossman et al. 1997).

Other E1A interacting proteins include the transcriptional co-repressor C-terminal binding protein (CtBP) and components of the general transcription machinery such as the TATA-binding protein (TBP) and a number of TBP-associated factors (TAFs), as well as the transcription factors AMP-dependent transcription factor 2 (ATF2) and cJUN (Figure 1.2) (Maguire, Shi et al. 1991, Chatton, Bocco et al. 1993, Hateboer, Timmers et al. 1993, Geisberg, Lee et al. 1994, Mazzarelli, Atkins et al. 1995, Song, Loewenstein et al. 1995, Zheng 2010).

1.1.5 The Adenovirus E1B Proteins

The E1B gene encodes one mRNA transcript which is alternatively spliced to give rise to five different E1B proteins characterised as E1B19K, E1B55K and the less abundant

proteins E1B84R, E1B93R and E1B156R (in Ad5). The main functions of the E1B proteins are thought to counter the pro-apoptotic environment that the E1A protein induces.

The E1B55K protein has been shown to directly inhibit the transcriptional activity of p53 through binding to p53 at p53-responsive promoters (Yew and Berk 1992, Yew, Liu et al. 1994). In addition, the E1B55K protein has intrinsic E3 small-ubiquitin-like modifier (SUMO) ligase activity which has been shown to conjugate a SUMO to p53. This SUMO modification induces the localisation of p53 to promyelocytic leukaemia (PML) nuclear bodies, inhibiting its mobility and therefore its function (Muller and Dobner 2008, Pennella, Liu et al. 2010). The E1B55K protein then facilitates nuclear export and the subsequent degradation of p53 (Figure 1.3) (Muller and Dobner 2008).

In addition to E1B55K acting alone, E1B55K also interacts with the E4orf6 viral protein, the results of which are two-fold: firstly, the E1B55K and E4orf6 proteins act together to induce the degradation of a number of cellular proteins which would otherwise be detrimental to viral DNA replication. Secondly, the E1B55K and E4orf6 proteins inhibit cellular mRNA export and translation whilst facilitating the transport of late viral mRNAs. Ad5E1B55K and Ad5E4orf6, together with the cellular proteins RING-box 1 (Rbx1), Cullin5 (Cul5) and Elongins B and C form an E3 ubiquitin ligase complex that is able to ubiquitinate target proteins and thus direct them for proteasomal-mediated degradation (Querido, Blanchette et al. 2001). Such targets include p53 and various DNA damage and repair proteins (see Section 1.3.2). The E1B55K and E4orf6 proteins also have roles in the late stages of adenovirus infection, where they are involved in the inhibition of cellular mRNA transport and the facilitation of late viral mRNA transport from the nucleus

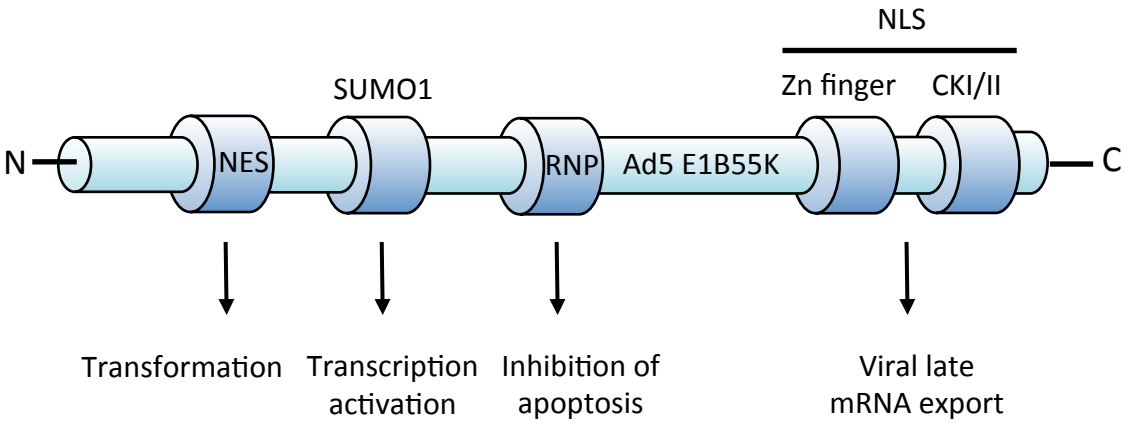

Figure 1.3: Representation of Ad5 E1B55K. Schematic shows the Ad5 E1B55K protein and its associated motifs. The biological functions of these motifs are indicated below the schematic. NES, nuclear export signal; RNP, ribonucleoprotein motif; Zn finger, C_2H_2 zinc finger; CKI/II, casein kinase I/II; NLS, nuclear localisation signal (adapted from Zheng 2010).

(Babiss and Ginsberg 1984, Babiss, Ginsberg et al. 1985, Pilder, Moore et al. 1986, Gonzalez, Huang et al. 2006). The E1B55K/E4orf6 E3 ubiquitin ligase has been shown to accumulate at viral replication centres (VRCs) within the nucleus and has also been shown to continuously shuttle between the nucleus and the cytoplasm, suggesting that these proteins are required for viral mRNA export (Ornelles and Shenk 1991, Dobbelstein, Roth et al. 1997). Indeed, E1B55K is known to be required for the transport of viral mRNAs from the nucleus via the chromosome region maintenance 1 (CRM1) export pathway, but the precise roles of the ubiquitin E3 ligase complex in viral mRNA export is yet to be defined (Babiss, Ginsberg et al. 1985, Dosch, Horn et al. 2001, Kindsmuller, Groitl et al. 2007, Woo and Berk 2007). Both proteins have also been implicated in the inhibition of cellular mRNA export, although the precise roles of these proteins during cellular mRNA export are yet to be discovered (Figure 1.3) (Beltz and Flint 1979, Babiss and Ginsberg 1984, Halbert, Cutt et al. 1985, Pilder, Moore et al. 1986).

The E1B19K protein is a distant homolog of the anti-apoptotic B-cell lymphoma 2 (BCL2) family of proteins (Rao, Debbas et al. 1992, Chiou, Tseng et al. 1994, Subramanian, Tarodi et al. 1995). In infected cells, the expression of the adenoviral E1A protein induces the degradation of the BCL2 homolog myeloid cell leukaemia 1 (MCL1) protein, which ordinarily resides bound to the pro-apoptotic protein BCL2 antagonist killer (BAK) (Debbas and White 1993, Sabbatini, Chiou et al. 1995). The now dissociated BAK protein oligomerises with the BCL2-associated X (BAX) pro-apoptotic protein, resulting in the formation of mitochondrial membrane pores from which the pro-apoptotic proteins that activate caspases, such as cytochrome c and second mitochondria-derived activator of caspases (SMAC), are released. This results in the activation of the caspase-dependent cell death pathway and ultimately

apoptosis. Since the activation of this pathway would be catastrophic for the production of viral progeny, the E1B19K protein counteracts this process by binding to the pro-apoptotic proteins BAK and BAX, inhibiting the activation of the caspase-dependent apoptotic pathway and thus allowing the virus to survive in the host cell (Debbas and White 1993, Sabbatini, Chiou et al. 1995, Zheng 2010).

1.1.6 The Adenovirus E4 Protein

The adenovirus E4 transcription unit encodes at least 18 distinct mRNAs which are alternatively spliced to produce seven known open reading frames (orfs) designated orf1, orf2, orf3, orf3/4, orf4, orf6 and orf6/7 (Virtanen, Gilardi et al. 1984). It is well established that the E4 region is required for lytic infection, since adenovirus mutants with deletions in total E4 have significantly reduced growth. Interestingly, the mutants in each individual orf did not recapitulate the impact to viral growth observed in the total E4 mutant (Halbert, Cutt et al. 1985). It was later revealed that mutations in orf3 or orf6 can compensate for each other, perhaps explaining the previous result (Bridge and Ketner 1989, Huang and Hearing 1989). The E4 proteins have a diverse range of functions during adenovirus infection including the regulation of transcription, mRNA nucleocytoplasmic transport, DNA replication, virion assembly and host-cell shut off.

E4orf4 has a number of roles during adenovirus infection including the negative regulation of E1A expression, the regulation of hypophosphorylation of various viral and cellular proteins and the induction of apoptosis. E4orf4 was shown to repress E1A-mediated transactivation of E2 and E4 promoters (Bondesson, Ohman et al. 1996, Mannervik, Fan et al. 1999). E4orf4 directly binds to the protein phosphatase 2A (PP2A) protein through the β subunit of PP2A, leading to the hypophosphorylation of a number of viral and cellular

proteins including E1A and the c-Fos component of the activating protein 1 (AP1) transcription factor (Muller, Kleinberger et al. 1992, Kleinberger and Shenk 1993). The actions of E4orf4 suggest that a negative feedback loop exists between E1A and E4orf4; the expression of E1A induces the initiation of E4orf4 transcription, which in turn downregulates the response to E1A both directly through the negative regulation of E1A transcription and the repression at E2 and E4 promoters, and indirectly through the hypophosphorylation of viral and cellular proteins. This negative feedback loop is thought to exist in order to limit the toxicity of viral infection and in turn increase viral efficiency. The adenovirus E4orf4 protein has also been shown to induce apoptosis, the expression of E4orf4 protein was shown to induce apoptosis independently of p53 (Marcellus, Lavoie et al. 1998). Interestingly, the induction of apoptosis was seen exclusively in transformed cell lines, suggesting that E4orf4 may be a potential therapeutic target (Shtrichman, Sharf et al. 1999).

Apart from the adenovirus E1A and E1B proteins, E4orf1 is the only other known adenovirus protein to confer transforming capabilities in rodent cells, albeit only during Ad9 infection (Javier, Raska et al. 1992, Javier 1994).

The E4orf2 protein has been detected at early time points post-infection in HeLa cells, the function of this protein to date is unknown (Dix and Leppard 1995). The E4orf3/4 protein has never been detected in infected cells, however it is predicted to exist based on the analysis of mRNA in Ad2 infected cells (Virtanen, Gilardi et al. 1984).

The E4orf6/7 gene product is a fusion protein with known roles as a viral transactivator together with E1A. The E4orf6/7 protein is known to bind to E2F, where it dimerises and associates with E2F binding sites in the viral Ad5 E2 early promoter and the cellular E2F1 promoter (Obert, O'Connor et al. 1994, Schaley, O'Connor et al. 2000).

Interestingly, expression of the E4orf6/7 protein alone is sufficient to displace pRB and p107 from E2F dimers, the consequence of which being cellular E2F binding to the adenovirus E2 promoter (O'Connor and Hearing 2000).

As previously discussed (see Section 1.1.5), E4orf6 cooperates with the E1B55K protein and together with a number of cellular proteins, forms an E3 ubiquitin ligase complex which targets various proteins for degradation. In addition, both E4orf6 and E1B55K have been implicated in the later stages of infection during late viral mRNA transport. E4orf6 can also act independently of E1B55K during adenovirus replication. The E4orf6 protein has been shown to interact with p53 and inhibit p53-mediated transcriptional activation. Binding of E4orf6 to p53 inhibits the ability of p53 to bind to the transcription factor IID (TFIID), thus inhibiting transcriptional activation (Dobner, Horikoshi et al. 1996).

The adenovirus E4orf3 protein has a number of roles during adenovirus infection. E4orf3 is involved in the splicing of the viral major late transcript (Nordqvist, Ohman et al. 1994). E4orf3 has also been shown to be responsible for the reorganisation of a number of cellular proteins to discrete nuclear structures known as PML nuclear bodies or PML oncogenic domains (PODs). A number of proteins are known to associate with these structures, the most notable of which is the PML protein, the recruitment of a number of PML nuclear bodies is dependent on this protein. During adenovirus infection, E4orf3 is responsible for the rapid reorganisation of PODs into track-like structures through the interaction with the PML isoform PMLII (Hoppe, Beech et al. 2006). The precise function of PML bodies, and the reason for the reorganisation of these bodies during adenovirus infection is to date unknown, however they have been implicated in the regulation of gene expression, the DNA damage response and apoptosis (Zhong, Salomoni et al. 2000, Dellaire

and Bazett-Jones 2004, Takahashi, Lallemand-Breitenbach et al. 2004). E4orf3 is also responsible for the localisation of E4orf6 to PML nuclear bodies (Leppard and Everett 1999). E4orf3 also stimulates the reorganisation of p53 to PML bodies where it induces H3K9me3 heterochromatin formation at p53 target promoter regions, silencing p53 target genes (Soria, Estermann et al. 2010). Finally, as well as E1B55K, E4orf3 has been shown to also bind to p53, relocating it from the nucleus to the cytoplasm. The function of the E4orf3 interaction with p53 is thought to 'liberate' p53 from E1B55K, subsequently allowing it to be degraded by the E1B55K/E4orf6 E3 ubiquitin ligase complex (Konig, Roth et al. 1999). E4orf3 also prevents the concatemerisation of the viral genome through the recruitment of DNA damage proteins to VRCs (see Section 1.3.3).

1.2 THE DNA DAMAGE RESPONSE, REPAIR AND REPLICATION STRESS

The cellular genome is under constant assault from agents that can damage genomic DNA. DNA damage occurs from both exogenous agents as well as endogenous cellular processes. Examples of exogenous agents that are able to induce DNA damage include exposure to ultra-violet C (UV-C) irradiation, which leads to the formation of bulky lesions within DNA, such as cyclobutane pyrimidine dimers (CPDs) or 6-4 photoproducts (Wood 1999, Douki and Cadet 2001). Exposure to ionising radiation (IR) generates a number of DNA lesions including double-strand breaks (DSBs), single-strand breaks (SSBs) and oxidative base damage (Alexander and Stacey 1958). Other examples of agents that are able to induce DNA damage include heterocyclic amines and aflatoxins which can be found in contaminated food, and polycyclic aromatic hydrocarbons found in tobacco smoke (Jackson and Bartek 2009). Examples of endogenous cellular processes generating DNA damage include the

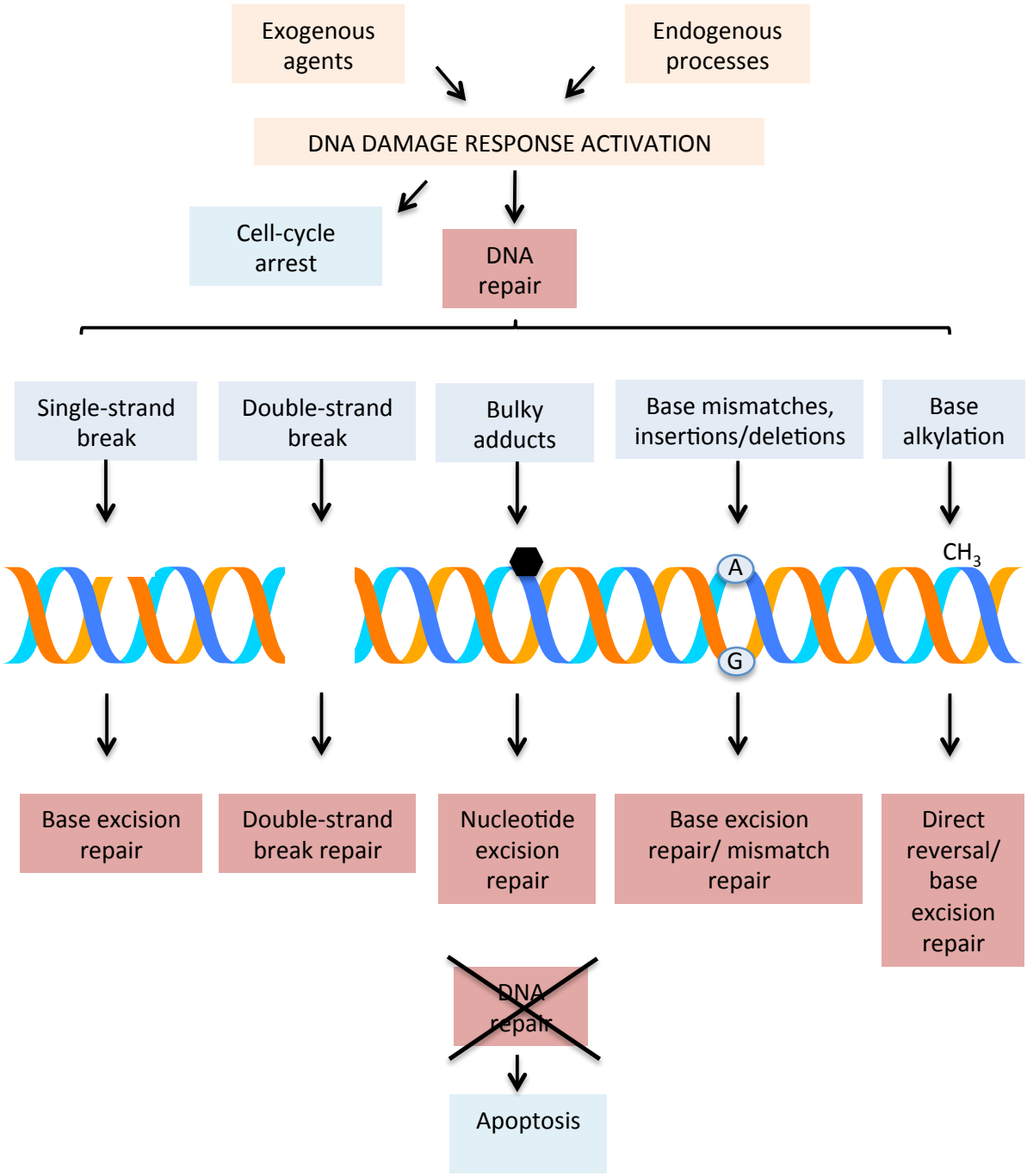

Figure 1.4: DNA Damage, Repair, and the Maintenance of Genome Stability. DNA damage can be generated from both exogenous agents as well as endogenous cellular processes. Activation of the DNA damage response induces cell cycle arrest to prevent DNA replication until the damage is repaired. In the event of irreparable DNA damage, apoptosis mechanisms are triggered. DNA damage includes the generation of DNA strand breaks, bulky adducts, base mismatches and base alkylations. The pathways through which such lesions are repaired are also highlighted.

introduction of SSBs from the oxidative attack of reactive oxygen species (ROS) produced as a by-product of normal cellular metabolism, the abortive activity of enzymes that generate 'nicks' in the DNA during DNA replication or transcription, such as topoisomerase I (TOPI) and topoisomerase II (TOPII), leading to SSBs and DSBs respectively, and the erroneous action of DNA polymerases during DNA replication, leading to DNA base mismatches (Weiss, King et al. 1977, Ward, Evans et al. 1987).

The rapid detection and repair of DNA damage is essential for cellular survival and the maintenance of genome stability. Unrepaired DNA lesions can lead to the accumulation of mutations and ultimately genomic instability, a defined hallmark for cancer development or cell death (Hanahan and Weinberg 2011). It is therefore not surprising that a complex and coordinated set of signalling networks and repair pathways exist in order to protect the integrity of the genome (Figure 1.4). In the following paragraphs, the process of DNA damage detection, repair and the cellular response to replication stress will be discussed.

1.2.1 The DNA Damage Response

1.2.1.1 The ATM Kinase and the Detection of Double-Strand Breaks

DSBs can be defined as discontinuities in both strands of the DNA double helix and can occur both endogenously and from environmental sources. DSBs can occur endogenously through the abortive activity of TOPII, the collapse of stalled replication forks and from the collision of an elongating replication fork with a SSB during DNA replication (Liu, Liu et al. 1980, Michel, Ehrlich et al. 1997). Environmental sources of DSBs include exposure to IR (Alexander and Stacey 1958). It is thought that a single unrepaired DSB can result in cell death, and therefore DSBs are considered to be highly genotoxic (Rich, Allen et

al. 2000). At a frequency of 10 endogenous DSB events per cell occurring every day, it would be detrimental to genome integrity if these breaks were not efficiently repaired (Lieber 2010).

The MRN complex, comprising Mre11, Rad51 and Nbs1 proteins, is responsible for the rapid detection of DSBs. Following detection, the transducer kinase ataxia telangiectasia mutated (ATM) is rapidly recruited to the site of the break (Falck, Coates et al. 2005, Lee and Paull 2005). Two events are required for the complete activation of ATM: firstly, the MRN complex is required to activate ATM, secondly, ATM is acetylated by HIV-1 tat interacting protein 60kDa (Tip60) (Sun, Jiang et al. 2005). In its inactive form, ATM resides in homodimers but, following its activation, it becomes autophosphorylated whereby it dissociates to form active monomers (Bakkenist and Kastan 2003). Following the complete activation of ATM by the MRN complex and Tip60, ATM is then able to phosphorylate downstream components of the DNA damage response (DDR) such as H2AX, and components of the cell cycle checkpoint such as p53 and Chk2, ultimately resulting in the activation of the cell cycle checkpoint and the subsequent halting of the cell cycle, which prevents DNA replication from occurring until the DNA damage has been accurately repaired (Figure 1.5)(Banin, Moyal et al. 1998, Canman, Lim et al. 1998, Khanna, Keating et al. 1998, Matsuoka, Huang et al. 1998, Rogakou, Pilch et al. 1998, Matsuoka, Rotman et al. 2000).

Following DSB formation, the histone H2A variant H2AX, a minor chromatin constituent composed of approximately 2-25% of the total H2A pool, becomes rapidly phosphorylated by ATM (termed γH2AX) (Rogakou, Pilch et al. 1998). This leads to the recruitment of the mediator of DNA damage checkpoint 1 (MDC1) to the site of the break,

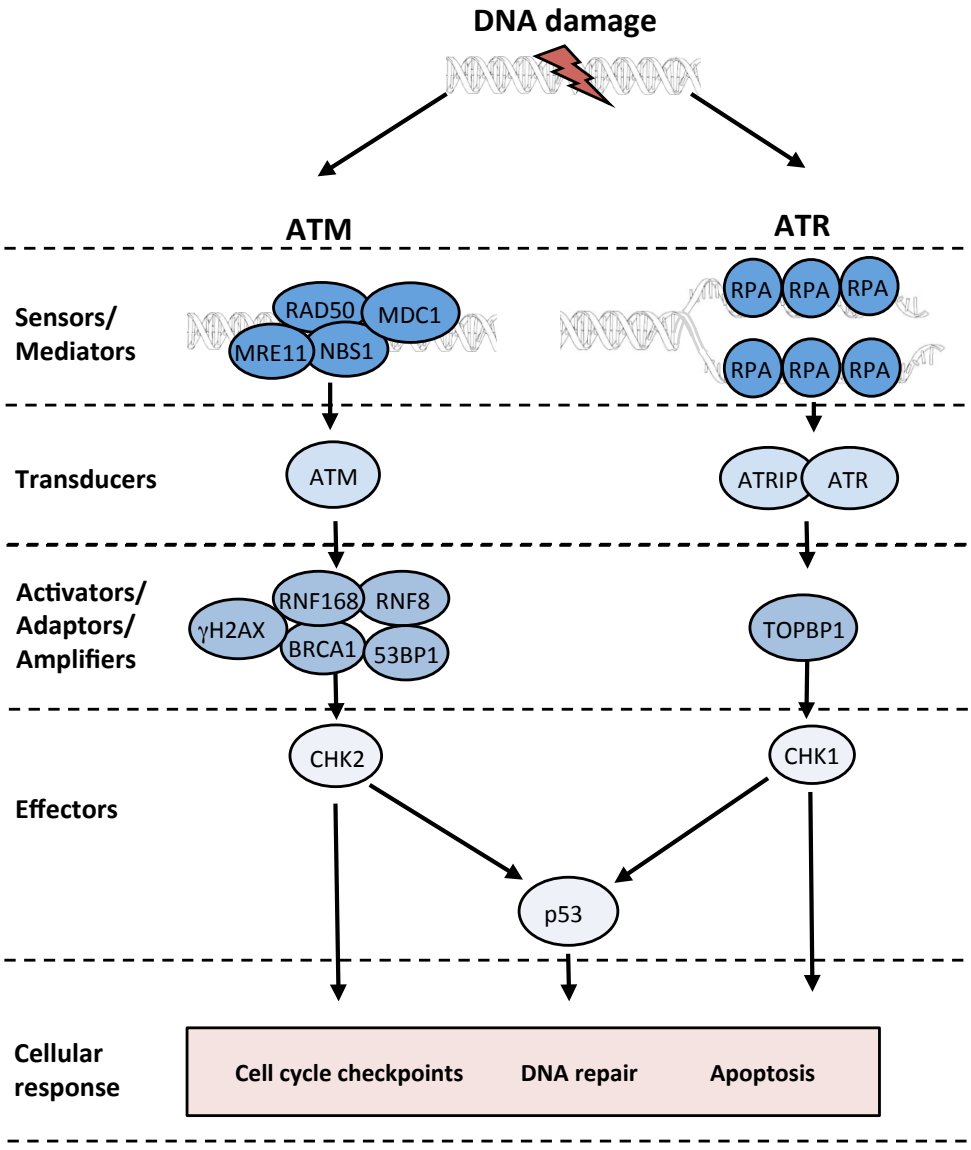

Figure 1.5: Activation of the ATM and ATR Kinases in Response to DNA Damage. The MRN complex is recruited to sites of double-strand breaks facilitating the recruitment and subsequent activation of ATM, together with Tip60. Activated ATM is able to phosphorylate p53 and Chk2, resulting in cell cycle arrest. Activated ATM also rapidly phosphorylates H2AX (termed γH2AX), which leads to the recruitment of MDC1 to the site of the break, which is subsequently phosphorylated by ATM. MDC1 recruits additional ATM to the site of the break, propagating the DNA damage signal, and also recruits RNF8 to the site of the break. RNF8, together with MDC1 catalyses the formation of ubiquitin chains onto γH2AX. RNF168 is then recruited to the site of the break and further ubiquitinates γH2AX. At this point repair factors such as 53BP1 and BRCA1 are recruited to the site of the break. RPA is responsible for the rapid detection of ssDNA. Binding of RPA to ssDNA recruits the ATR kinase through its association with ATRIP. TOPBP1 localises to the region through 9-1-1 complex and RFC2 clamp loader complex association. TOPBP1 is responsible for the activation of ATR through interactions with ATR and the 9-1-1 complex. Activated ATR then activates a number of downstream repair proteins and induces cell cycle arrest through the activation of Chk1 (adapted from Turnell and Grand 2012).

where it is subsequently phosphorylated by ATM (Goldberg, Stucki et al. 2003). MDC1 is then able to associate with γH2AX, ATM and the MRN complex, the results of which are two-fold (Stucki, Clapperton et al. 2005). Firstly, MDC1 is able to recruit additional ATM to the site of the damage, where it is able to propagate the DNA damage signal through the phosphorylation of additional H2AX (Lou, Minter-Dykhouse et al. 2006). It is thought that this action is able to 'spread' the DNA damage signal along up to 2 megabases of DNA (Celeste, Petersen et al. 2002). Secondly, MDC1 is able to form a 'scaffold' onto which other proteins involved in the DDR can access the site of the break. Following the recruitment and phosphorylation of MDC1 at the site of the damage, the E3 ubiquitin ligase ring finger protein 8 (RNF8) is recruited to the site of the break where it associates with phosphorylated MDC1 (Huen, Grant et al. 2007, Kolas, Chapman et al. 2007, Mailand, Bekker-Jensen et al. 2007). RNF8 and MDC1 then interact with the E2 conjugating enzyme Ubc13, which together are responsible for the addition of K63 ubiquitin chains onto γH2AX, amplifying the DNA damage signal further (Bin and Elledge 2007). The ubiquitination of γH2AX in turn recruits the E3 ubiquitin ligase RNF168 to the site of the damage, which is also able to ubiquitinate γH2AX, further propagating the signal (Doil, Mailand et al. 2009, Stewart, Panier et al. 2009, Mattiroli, Vissers et al. 2012). In addition to the amplification of the DNA damage signal, the ubiquitination of γH2AX at the site of the DSB also leads to the recruitment of DNA repair proteins such as receptor-associated protein 80 (RAP80), breast cancer type 1 susceptibility protein (BRCA1) and p53-binding protein 1 (53BP1), amongst others, ultimately leading to the repair of the DSB (Figure 1.5)(Wang, Matsuoka et al. 2002, Bin and Elledge 2007).

1.2.1.2 ATR Kinase Activation

The transducer kinase ATR can be activated by a number of different types of DNA damage including DSBs, and also following replication stress, the common structure known to activate ATR being single-stranded DNA (ssDNA)(Figure 1.5)(Zou and Elledge 2003, Jazayeri, Falck et al. 2006). The ssDNA binding protein, replication protein A (RPA), is responsible for the rapid coating of regions of ssDNA, which subsequently recruits the ATR kinase to the ssDNA site through the interaction with the ATR binding partner ATR-interacting protein (ATRIP)(Zou and Elledge 2003). The Rad9-Rad1-Hus1 (9-1-1) complex and the Rad17-replication factor C 2 (RFC2) clamp loader complex are subsequently recruited to the ssDNA-RPA complex, which results in topoisomerase II binding protein 1 (TOPBP1) recruitment to the site of ssDNA (Bermudez, Lindsey-Boltz et al. 2003, Zou and Elledge 2003, Parrilla-Castellar, Arlander et al. 2004). TOPBP1 is then able to activate ATR through associations with ATRIP and the Rad9 component of the 9-1-1- complex (Kumagai, Lee et al. 2006, Mordes, Glick et al. 2008). Activated ATR is subsequently able to phosphorylate downstream effector proteins, including those involved in DNA repair (H2AX, BRCA1 and Bloom syndrome protein (BLM)) and cell cycle arrest (p53 and Chk1) (Lakin, Hann et al. 1999, Liu, Guntuku et al. 2000, Tibbetts, Cortez et al. 2000, Ward and Chen 2001, Davies, North et al. 2004). Induction of cell cycle arrest prevents the replication of damaged DNA and allows time for the replication barrier and/or DNA damage to be repaired (Figure 1.5).

1.2.2 DNA Repair and Genome Integrity

1.2.2.1 DSB Repair

DSB repair is essential for the maintenance of genome integrity since failure to efficiently repair DNA damage can lead to gross chromosomal translocations and genome instability. There are two main DSB repair mechanisms in place to rapidly and efficiently repair DSBs when they arise; these repair mechanisms are non-homologous end-joining (NHEJ) and homologous recombination (HR) repair (Weibezahn and Coquerelle 1981). NHEJ involves the direct end-to-end ligation of DNA ends with relatively limited DNA end processing. This mechanism of DSB repair can on occasion lead to loss of genetic information since DNA end processing involved in this type of repair can lead to the loss of nucleotides. In addition, NHEJ also has the capacity to induce genome rearrangements and chromosomal translocations since DNA ends may be joined with other DNA ends erroneously (Liang, Han et al. 1998, Heidenreich, Novotny et al. 2003). In contrast, HR repair involves extensive DNA end processing (end-resection) followed by a 'search' for homologous regions in the undamaged, sister strand of the DNA; once found, this region of homology is used as a template for DNA repair. Since HR repair involves end-processing with no loss of genetic information, HR is considered to be an error-free form of DSB repair. However, since HR repair requires the homologous sister strand for efficient repair, this form of repair is restricted to S and G2 phases of the cell cycle, as opposed to NHEJ which can occur during all phases (Bezzubova, Silbergleit et al. 1997, Liang, Han et al. 1998, Takata, Sasaki et al. 1998).

1.2.2.1.1 Non-Homologous End-Joining (NHEJ)

The initiation of NHEJ begins with the rapid recognition of the DSB by the Ku70/80 heterodimer, which forms a ring-like structure around each end of the DSB (Figure 1.6) (Blier, Griffith et al. 1993, Walker, Corpina et al. 2001). The formation of the ring-like structure around the DNA allows the structure to translocate along the DNA away from the break, which allows other NHEJ proteins access to the site of the break (Yoo and Dynan 1999). Following the recruitment of the Ku70/80 heterodimer to the break, the catalytic subunit of the DNA-dependent protein kinase (DNA-PKcs) associates with the Ku70/80 heterodimer, together forming the DNA-PK holoenzyme (Suwa, Hirakata et al. 1994). The active DNA-PK holoenzyme autophosphorylates itself, as well as phosphorylating a number of downstream mediators of NHEJ including Ku70/80, X-ray repair cross-complementing protein 4 (XRCC4) and Artemis (Lees-Miller, Chen et al. 1990, Yu, Wang et al. 2003, Goodarzi, Yu et al. 2006). The role of the autophosphorylation of DNA-PK is to allow the dissociation of the holoenzyme allowing access of other NHEJ proteins to the site of the DSB including DNA ligase IV, Artemis, XRCC4 and XRCC-like factor (XLF) (Chan and Lees-Miller 1996, Ding, Reddy et al. 2003).

DNA ends of the DSB need to be returned to their conventional 3'OH and 5'P DNA termini before they can be re-ligated by NHEJ. The end-processing enzymes used in this process are dependent on the termini created during the DNA damage. For example, the major processing enzyme during NHEJ is believed to be Artemis, which is responsible for the processing of DNA overhangs and hairpins (Ma, Pannicke et al. 2002). NHEJ is complete when DNA ligase IV, together with XRCC4 and XLF join the processed ends of the DSB

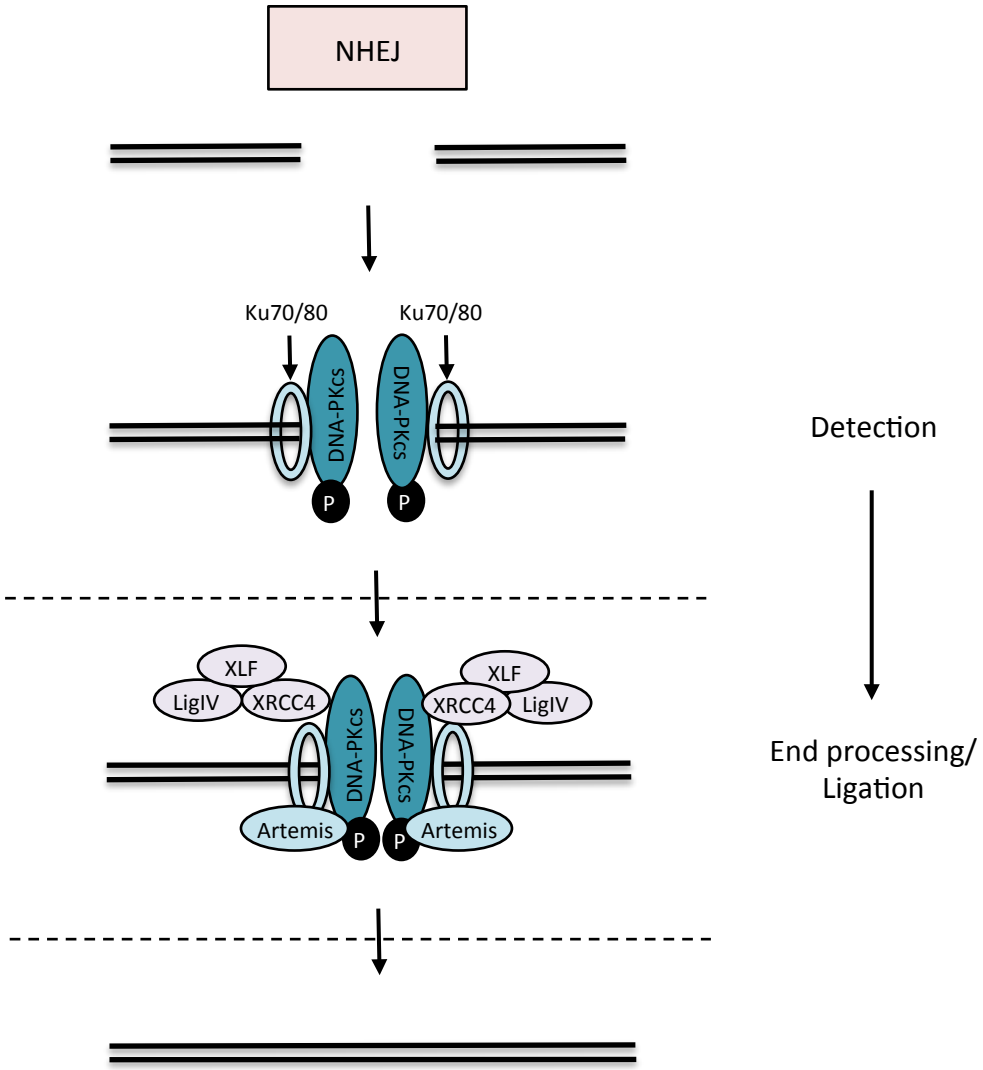

Figure 1.6: Non-Homologous End-Joining. The Ku70/Ku80 heterodimer is responsible for the detection of DSBs during NHEJ. Following initial detection, the Ku70/Ku80 heterodimer translocates along the DNA allowing access to the break for other DSB repair machinery. DNA-PK is then recruited to the site of the break and together with Ku70/Ku80, forms the DNA-PK holoenzyme. The autophosphorylation of DNA-PK results in the accumulation of other DSB repair proteins at the site of the break such as Artemis, DNA ligase IV, XRCC4 and XLF. A variety of end-processing factors including Artemis, are able to process DNA ends and make them compatible for ligation. DNA ligase IV, in conjunction with XRCC4 and XLF are responsible for DNA end ligation.

(Figure 1.6) (Leber, Wise et al. 1998, Matsumoto, Suzuki et al. 2000, Calsou, Delteil et al. 2003, Ahnesorg, Smith et al. 2006, Hentges, Ahnesorg et al. 2006, Tsai, Kim et al. 2007, Yano, Morotomi-Yano et al. 2008).

1.2.2.1.2 Homologous Recombination Repair

The process of HR repair begins with the resection of each end of the DSB to produce a region of ssDNA, which is orchestrated by the MRN complex together with CtBP interacting protein (CtIP) (Figure 1.7) (Sartori, Lukas et al. 2007, Huertas and Jackson 2009). The E3 ubiquitin ligase BRCA1 is responsible for the targeting of CtIP to the DSB site (Yu, Fu et al. 2006). The helicase BLM and the exonucleases: exonuclease 1 (EXO1) and DNA replication helicase/nuclease 2 (DNA2) are responsible for the further resection of the DNA ends (Nimonkar, Genschel et al. 2011). The 3' ssDNA overhang created from resection of the DNA ends is rapidly coated with RPA, with two major consequences. Firstly, the coating of RPA on the ssDNA activates ATR and its downstream proteins. Secondly, RPA binding to ssDNA induces the next steps in the HR process. RPA is displaced from the ssDNA-RPA by Rad51 in a breast cancer type 2 susceptibility protein (BRCA2)-dependent manner, which forms a nucleoprotein filament with the ssDNA (Wong, Pero et al. 1997, Pellegrini, Yu et al. 2002). The ssDNA-Rad51 nucleoprotein, then invades the undamaged, sister chromatid strand, displacing the DNA, which forms a displacement loop (D-loop)(Baumann, Benson et al. 1996, Sugiyama and Kowalczykowski 2002). The nucleoprotein filament then undergoes a search for the homologous region on the sister chromatid, which is subsequently used as a template to repair the damaged strand. The structure formed can be resolved in one of two ways. Firstly, if the D-loop has been 'captured' by the second DNA end, a double Holliday

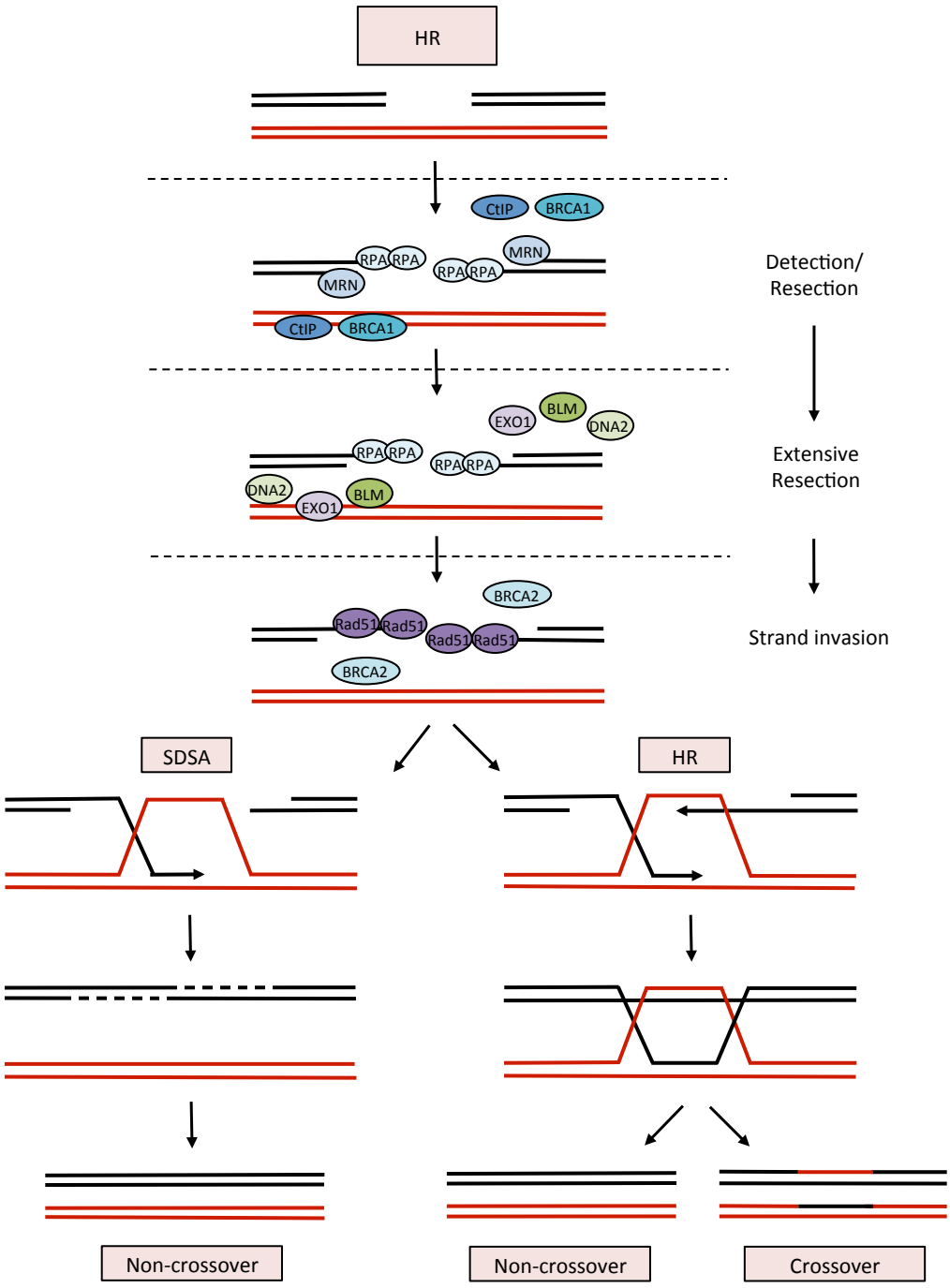

Figure 1.7: Homologous Recombination Repair. During homologous recombination repair, MRN in conjunction with CtIP and BRCA1, are responsible for the initial 5'-3' resection of the DNA at the site of the DSB. Extensive resection is carried out by BLM, EXO1 and DNA2. RPA rapidly binds the 3' overhang ssDNA generated by resection which is displaced by the recombinase Rad51 in conjunction with BRCA2, forming a nucleoprotein filament with the ssDNA. The nucleoprotein filament invades the undamaged homologous sister chromatid and uses the homologous sequence as a template for DNA synthesis. The resulting structure can be resolved either by the classical recombination repair pathway, whereby the D-loop captures the second DNA end, or by synthesis-dependent strand annealing (SDSA), where the D-loop is dissolved before second-end capture, resulting exclusively in non-crossover events. The classical recombination repair pathway results in the formation of double Holliday junctions, which are resolved by a range of endonucleases, resulting in both cross-over and non-crossover products.

junction is formed which can be resolved by the endonucleases MUS81 endonuclease homologue (MUS81)/ essential meiotic endonuclease 1 homologue 1 (EME1), SLX1/SLX4 and GEN1 (Boddy, Gaillard et al. 2001, Ip, Rass et al. 2008, Fekairi, Scaglione et al. 2009). The endonucleases are responsible for the cleavage of the junction and depending on the endonuclease employed, this results in either a chromatid crossover event, whereby genetic information between the chromatids is exchanged, or a non-crossover product (Wu and Hickson 2003). Secondly, if the end of the double Holliday junction is not 'captured' by the second DNA end, the newly repaired DNA strand can anneal to the other side of the break, a process known as synthesis-dependent strand annealing (SDSA). SDSA always results in the generation of a non-crossover product (Figure 1.7) (Adams, McVey et al. 2003, Ira, Satory et al. 2006).

1.2.2.2 Single-Strand Break Repair

A single-strand break (SSB) can be defined as a discontinuity in a single-strand of the double-stranded DNA helix. SSBs are thought to be one of the most common DNA lesions to occur in the genome, with approximately 10,000 endogenously-induced SSBs per cell per day (Lindahl 1993). SSBs are not the most genotoxic DNA lesion to the cell; however, it is important that these lesions are repaired by the cell repair machinery since SSBs have the capacity to become DSBs if met by a replication fork during DNA replication (Kuzminov 2001) (see Section 1.2.4.2).

One of the most common sources of SSB lesions is endogenous oxidative attack from ROS deriving from normal cell metabolism (Weiss, King et al. 1977, Ward, Evans et al. 1987). SSBs can also occur indirectly from the excision of damaged or incorrect bases during base excision repair (BER) (Lindahl 1974). This form of repair is responsible for the removal of

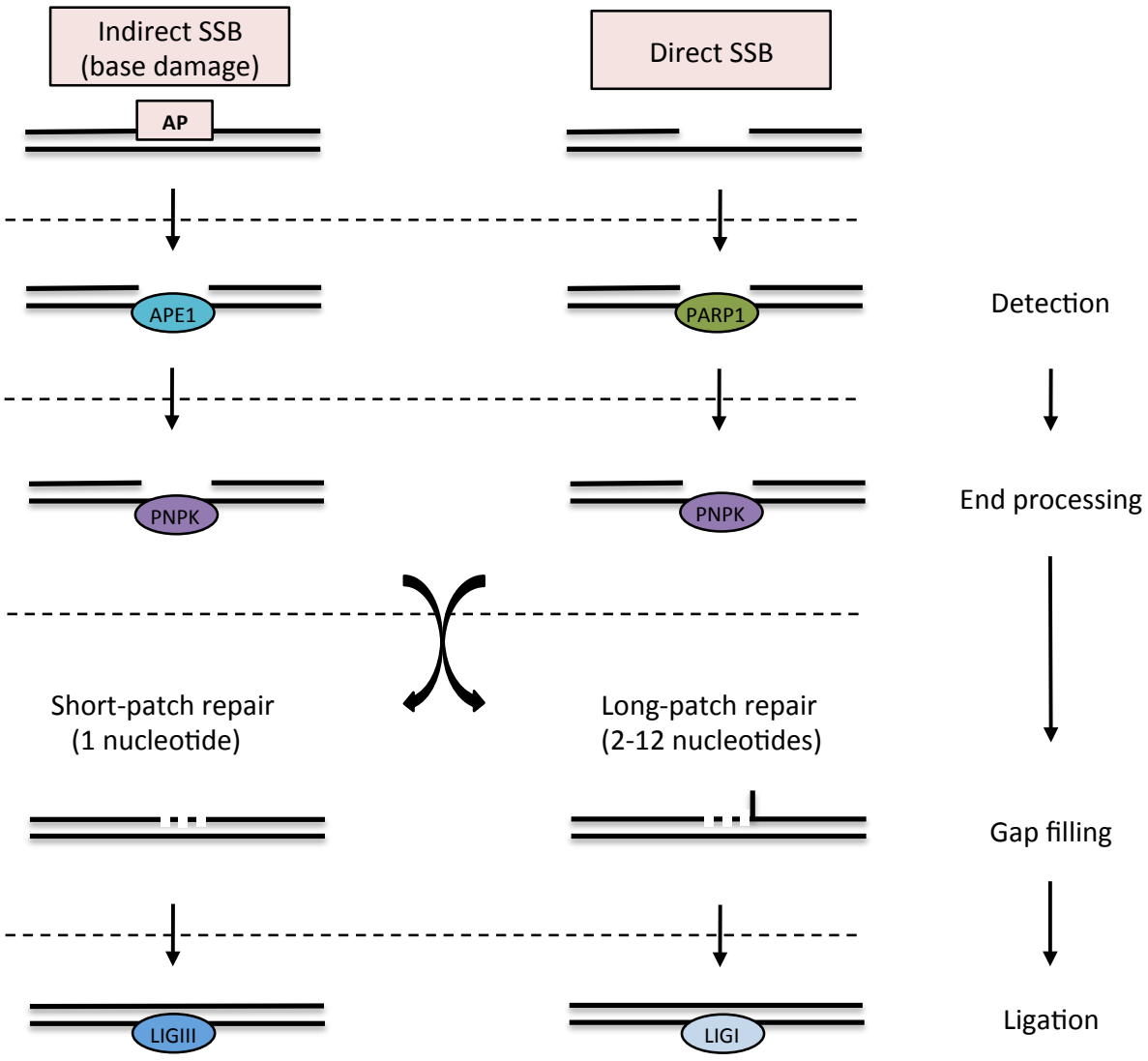

Figure 1.8: Single-Strand Break Repair. Single-strand breaks can be generated indirectly by the endonuclease activity of APE1, which acts to cleave abasic (AP) sites during base excision repair. Alternatively, single-strand breaks can be generated directly and are recognised by PARP1. As with DSBs, SSBs possess damaged termini which need to be processed before SSB repair can proceed. A number of end-processing factors exist to process the termini, one example being PNPK. Following DNA end-processing, DNA gap filling can occur either incorporating 1 nucleotide (termed short-patch repair) or 2-12 nucleotides (termed long-patch repair). FEN1 removes displaced 5' single strand DNA flaps associated with long-patch repair. DNA is ligated by either DNA ligase I or DNA ligase III.

alkylated, deaminated and oxidised bases from the DNA backbone. Nucleotide excision repair (NER) also leads to the indirect formation of SSBs through the removal of bulky, helix distorting lesions from the DNA backbone. SSBs can also occur from abortive TOP1 activity during DNA replication and transcription. The function of TOP1 is to reduce super-helical torsion produced during DNA replication and transcription by creating a 'nick' in the DNA. Ordinarily, TOP1 acts to rapidly reseal the 'nick' in the DNA backbone however, occasionally, if the 'nick' collides with the DNA replication or transcriptional machinery, or if TOP1 is close to a DNA lesion, the end result can be TOP1 abortive activity and ultimately the generation of an irreversible TOP1-associated SSB (Pourquier, Pilon et al. 1997).

1.2.2.2.1 Base Excision Repair

As previously discussed, SSBs can also occur indirectly from the excision of damaged or incorrect bases during BER (Lindahl 1974). During BER, DNA base modifications are excised by DNA glycosylases which act to excise these modifications leaving an apurinic-apyrimidinic (AP) site (Figure 1.8). There are known to be two types of DNA glycosylases; mono-functional glycosylases which possess glycosylase activity alone, and bi-functional glycosylases which possess glycosylase activity and AP lyase activities (Lindahl 1974). Mono-functional glycosylases excise the damaged base leaving an AP site, which is subsequently incised by AP endonuclease I (APE1), leaving a SSB (Demple, Herman et al. 1991). The intrinsic AP lyase activities of the bi-functional glycosylases cleave abasic sites in a β-elimination or β,δ- elimination reaction, leading to a single nucleotide gap containing a 5'-P and 3'-αβ unsaturated aldehyde or 5' and 3'-P, respectively (O'Connor and Laval 1989).

Poly (ADP-ribose) polymerase 1 (PARP1) is responsible for the recognition of SSBs that have occurred directly (e.g through sugar damage); upon recognition and binding of

PARP1 to the SSB, PARP1 becomes activated (Figure 1.8) (Benjamin and Gill 1980, Alkhatib, Chen et al. 1987, Gradwohl, Menissier de Murcia et al. 1990, Satoh and Lindahl 1992, Weinfeld, Chaudhry et al. 1997). The activation of PARP1 induces its poly (ADP-ribose)(PAR) polymerase activity, causing the addition of PAR polymers to itself and other proteins including histones (Ueda, Omachi et al. 1975, Tanaka, Hayashi et al. 1978, Kanai, Miwa et al. 1982, Mendoza-Alvarez and Alvarez-Gonzalez 1993, Altmeyer, Messner et al. 2009, Messner, Altmeyer et al. 2010).

The PARylation of PARP1 and its target proteins leads to the recruitment of a number of proteins to the SSB. One such protein is X-ray repair cross complementing protein (XRCC1), which acts as a scaffold for other proteins involved in BER (Caldecott, Aoufouchi et al. 1996, Masson, Niedergang et al. 1998, El-Khamisy, Masutani et al. 2003). Before the SSB can be repaired, the DNA ends of the break must be restored to their conventional 3'OH and 5'P ends. This is achieved by various end-processing proteins, the protein involved in the end-processing is dependent on the type of damage to the termini. For example, polynucleotide kinase phosphatase (PNKP) is necessary for the processing of 3'P and 5'OH termini induced by ROS, and so is a particularly important processing enzyme considering the abundance of these lesions (Jilani, Ramotar et al. 1999, Whitehouse, Taylor et al. 2001). Following the restoration of the DNA termini to their conventional forms, single-strand gap filling can occur which can either incorporate one nucleotide (short-patch repair) or 2-12 nucleotides (long-patch repair)(Dianov, Price et al. 1992, Klungland and Lindahl 1997). The removal of displaced 5' nucleotides produced during long-patch repair are resolved/removed by flap endonuclease 1 (FEN1) (Prasad, Dianov et al. 2000). The DNA polymerases involved in short-patch and long-patch repair are numerous and are

responsible for DNA gap filling during BER. Finally, the end step of SSB repair is the ligation of the newly synthesised DNA which is performed by DNA ligase III (usually associated with short-patch repair)/DNA ligase I (normally associated with long-patch repair) (Figure 1.8) (Brookman, Tebbs et al. 1994, Caldecott, McKeown et al. 1994, Caldecott, Tucker et al. 1995, Pascucci, Stucki et al. 1999, Sleeth, Robson et al. 2004).

1.2.2.2.2 Nucleotide Excision Repair

SSBs can also occur during NER through the removal of bulky, helix-distorting lesions caused during exposure to chemicals which cause bulky chemical-induced adducts, and agents such as UV-C, which induce CPDs and 6-4 photoproducts (Wood 1999, Douki and Cadet 2001).

There are two forms of NER termed global-genome repair (GGR) NER and transcription-coupled repair (TCR). GGR NER involves the repair of bulky lesions in transcriptionally inactive areas of the genome, whereas TCR occurs in transcriptionally active genes (Mellon, Spivak et al. 1987). The XPC-Rad23B-Centrin 2 (XPC) complex is able to detect bulky lesions during GGR NER, i.e. the detection of (6-4) photoproducts (Sugasawa, Ng et al. 1998, Araki, Masutani et al. 2001). For the recognition of smaller DNA lesions that cannot be detected by the XPC complex, there is the UV DNA damage binding protein (UV-DDB) composed of DDB1 and DDB2/XPE to facilitate their recognition (Payne and Chu 1994, Hwang, Toering et al. 1998). The recognition of bulky lesions during TCR is performed by the elongating polymerase II (RNAPII), the recognition involves the stalling of the polymerase during transcription from the collision with the bulky lesion (Donahue, Yin et al. 1994). Following the recognition of the bulky lesion by either GGR NER or TCR, the two DNA repair pathways merge and the proceeding steps of NER occur in both forms of NER (Figure 1.9).

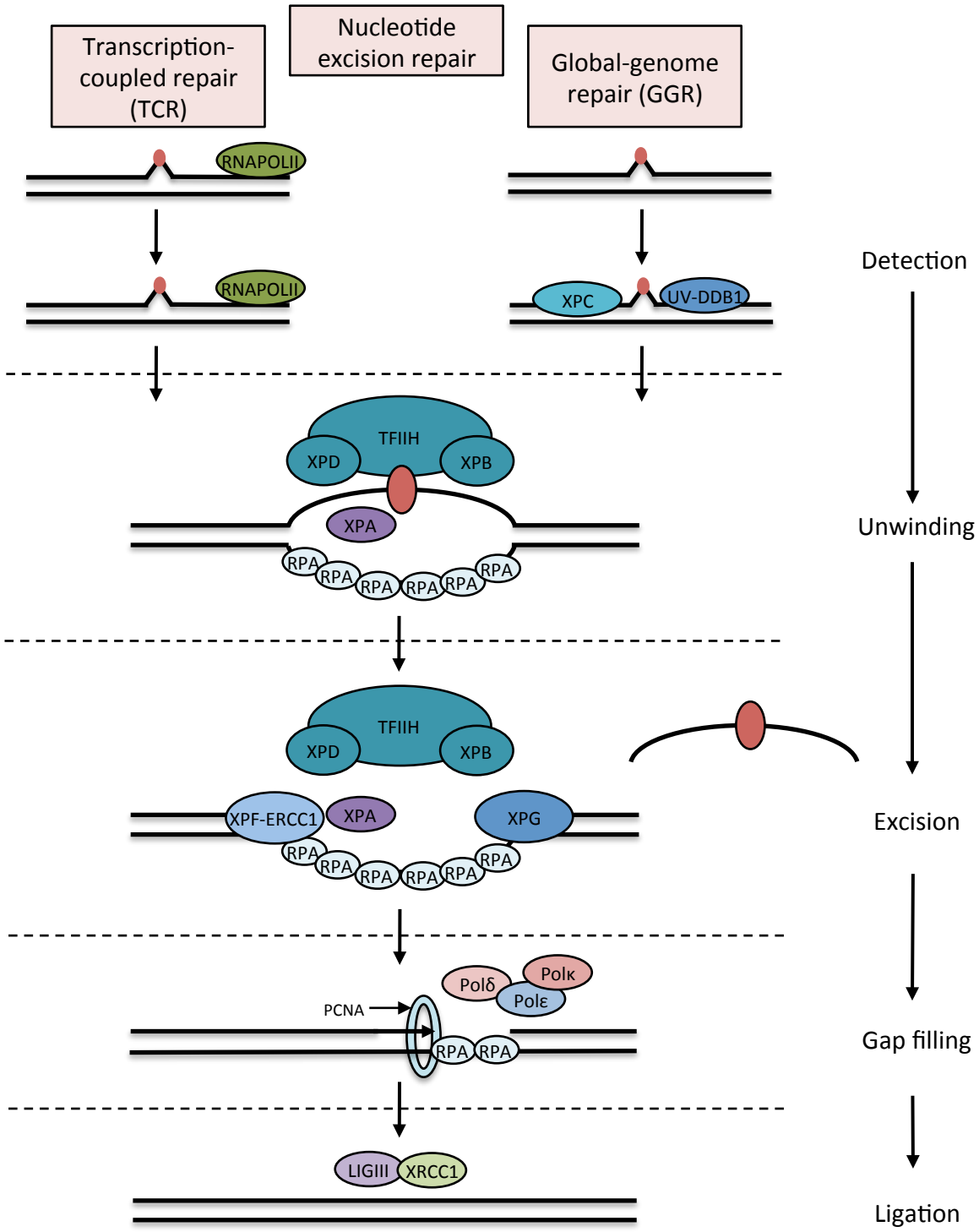

Figure 1.9: Nucleotide Excision Repair. The XPC-Rad23B-Centrin 2 and UV-DDB complexes are responsible for the detection of bulky DNA lesions during global-genome repair (GGR), whilst RNA polymerase II detects bulky DNA lesions during transcription-coupled repair (TCR). Following initial detection the two pathways of nucleotide excision (NER) repair converge. The multi-subunit TFIIH transcription factor associates with the lesion and this stimulates the helicase activity of two of its subunits; XPB and XPD, resulting in the unwinding of the DNA to allow access for the repair machinery. XPA associates with the lesion present on the single stranded DNA coated with RPA. This then activates the XPF-ERCC1 and XPG endonucleases which make an incision on the DNA 5' and 3' of the lesion, respectively. Pol ε. Pol δ and Pol κ together with PCNA are responsible for DNA gap filling. DNA is ligated by the DNA ligase III-XRCC1 complex.

Following the recognition of the bulky lesion, the two helicase subunits of the transcription factor TFIIH, termed xeroderma pigmentosum (XP) XPB and XPD, are responsible for the unwinding of the DNA, which allows access of the repair machinery to the DNA lesion (Volker, Mone et al. 2001, Tapias, Auriol et al. 2004). TFIIH is then responsible for recruiting XPA and RPA which activate XPF- excision repair cross-complementation group 1 (ERCC1) and XPG (5' endonuclease and 3' endonuclease, respectively) which are responsible for the excision of the 22-30nt long DNA strand containing the bulky lesion (Li, Elledge et al. 1994, Odonovan, Davies et al. 1994, Park and Sancar 1994, Saijo, Kuraoka et al. 1996, Volker, Mone et al. 2001). The DNA polymerases Pol δ, Pol ε and Pol κ are responsible for filling the gap in the DNA left behind from the endonucleases together with proliferating cell nuclear antigen (PCNA)(Shivji, Kenny et al. 1992). The ligase III-XRCC1 complex facilitates the ligation step in NER (Figure 1.9) (Shivji, Kenny et al. 1992, Moser, Kool et al. 2007).

1.2.2.3 Mismatch Repair

DNA base mismatching occurs from errors made by DNA polymerases during DNA replication. Deviations from the Watson-Crick base-pairs G-C and A-T are repaired by mismatch repair (MMR) (Watson and Crick 1953). In addition to base-pair mismatches, MMR is also responsible for the repair of insertion/deletion loops (IDLs) which are a consequence of multiple unpaired nucleotides. To preserve the integrity of the genome, various measures are in place to ensure that the mismatch is removed from the newly-synthesised DNA strand rather than the parental strand. The MMR machinery is able to recognise the newly-synthesised DNA strand through the recognition of 'nicks' in the DNA left from Okazaki

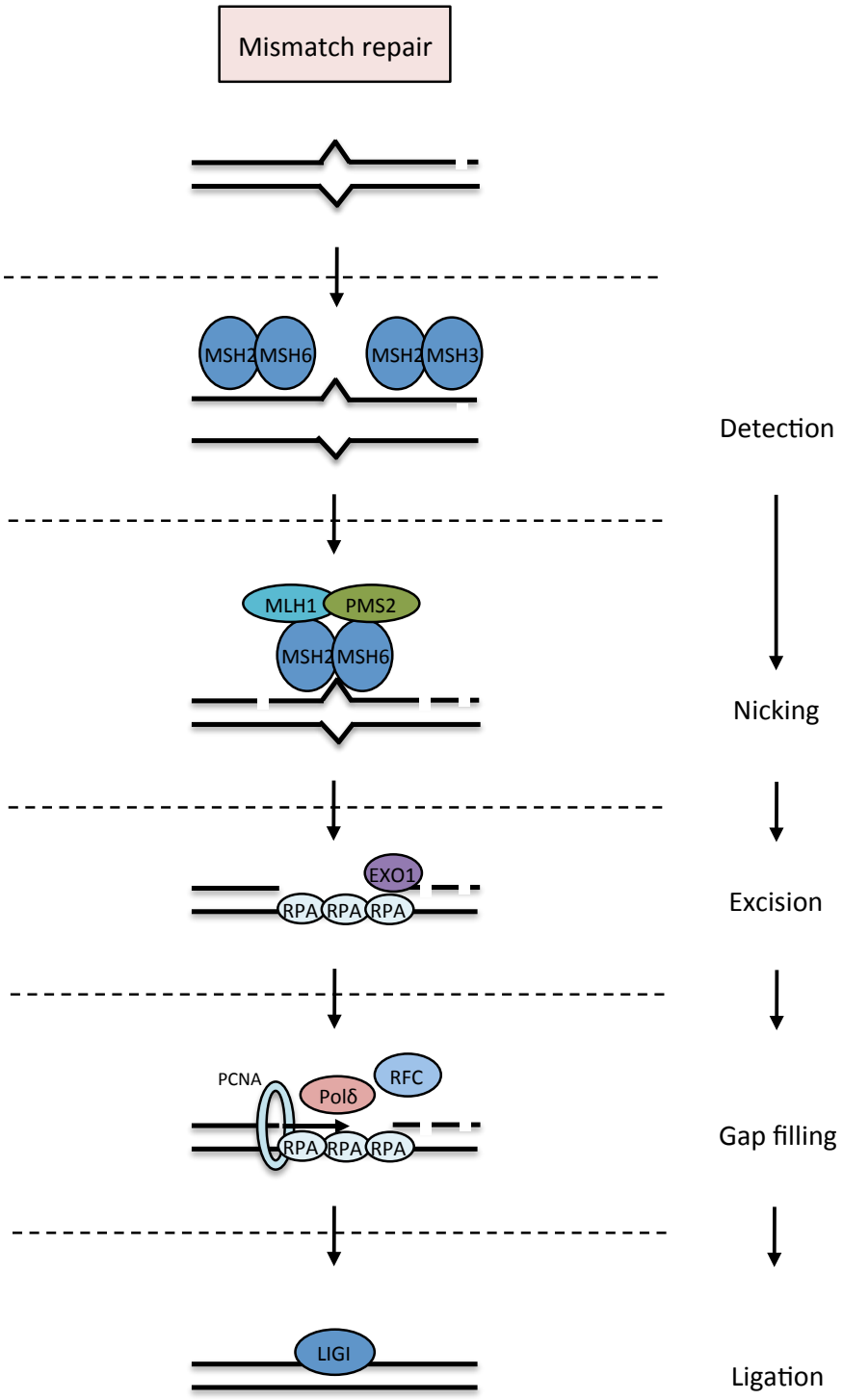

Figure 1.10: Mismatch Repair. DNA mismatches are detected by MSH2-MSH6 heterodimer and deletion/insertion loops by the MSH2-MSH3 complex. MLH1/PMS2 is then recruited to the mismatch where it forms a complex with MSH2-MSH6 or MSH2-MSH3, respectively. PMS2 has endonuclease activity which is able to generate a nick 5' to the mismatch so that it can be subsequently removed by EXO1. DNA gap filling is achieved by RFC-loaded PCNA and DNA Pol δ. Finally DNA is ligated by DNA ligase I.

fragment formation on the lagging DNA strand (Lacks, Dunn et al. 1982, Holmes, Clark et al. 1990, Thomas, Roberts et al. 1991). DNA base-pair mismatches and IDLs are detected by MSH2-MSH6 (MutSα) and MSH2-MSH3 (MutSβ), respectively (Figure 1.10) (Drummond, Li et al. 1995, Acharya, Wilson et al. 1996, Palombo, Iaccarino et al. 1996, McCulloch, Gu et al. 2003). Following the detection of the mismatch by MutSα and MutSβ, the MLH1/PMS2 (MutLα) complex is recruited which forms a ternary complex with MutSα and MutSβ. The formation of the ternary complex induces a change in the conformation which is necessary for the movement of the complex away from the site of the mismatch (Gradia, Acharya et al. 1997). This induces the endonuclease activity of the PMS2 subunit of MutLα which is responsible for creating a 'nick' 5' to the mismatch, and the mismatch is then subsequently removed by the exonuclease EXO1 (Genschel, Bazemore et al. 2002, Kadyrov, Dzantiev et al. 2006). DNA gap filling is achieved by the DNA polymerase Pol δ which is dependent on PCNA and replication factor C (RFC) (Longley, Pierce et al. 1997, Gu, Hong et al. 1998). Ligation by DNA ligase I of the newly synthesised strands completes MMR (Figure 1.10) (Zhang, Yuan et al. 2005).

1.2.2.4 Interstrand Cross-Link Repair

Interstrand cross-links (ICLs) can be defined as the covalent linkage between the two strands of the double helix. ICLs are highly toxic to the cell since they prevent the separation of DNA strands during DNA replication and transcription. The Fanconi anaemia (FA) pathway is responsible for the resolution of ICLs (Raschle, Knipscheer et al. 2008). FANCM is responsible for recognition of ICLs during DNA replication. FANCM forms a heterodimeric complex with FA-associated protein 24kDa (FAAP24), which is necessary for the specificity and stability of the FANCM protein (Ciccia, Ling et al. 2007). Following recognition of the ICL

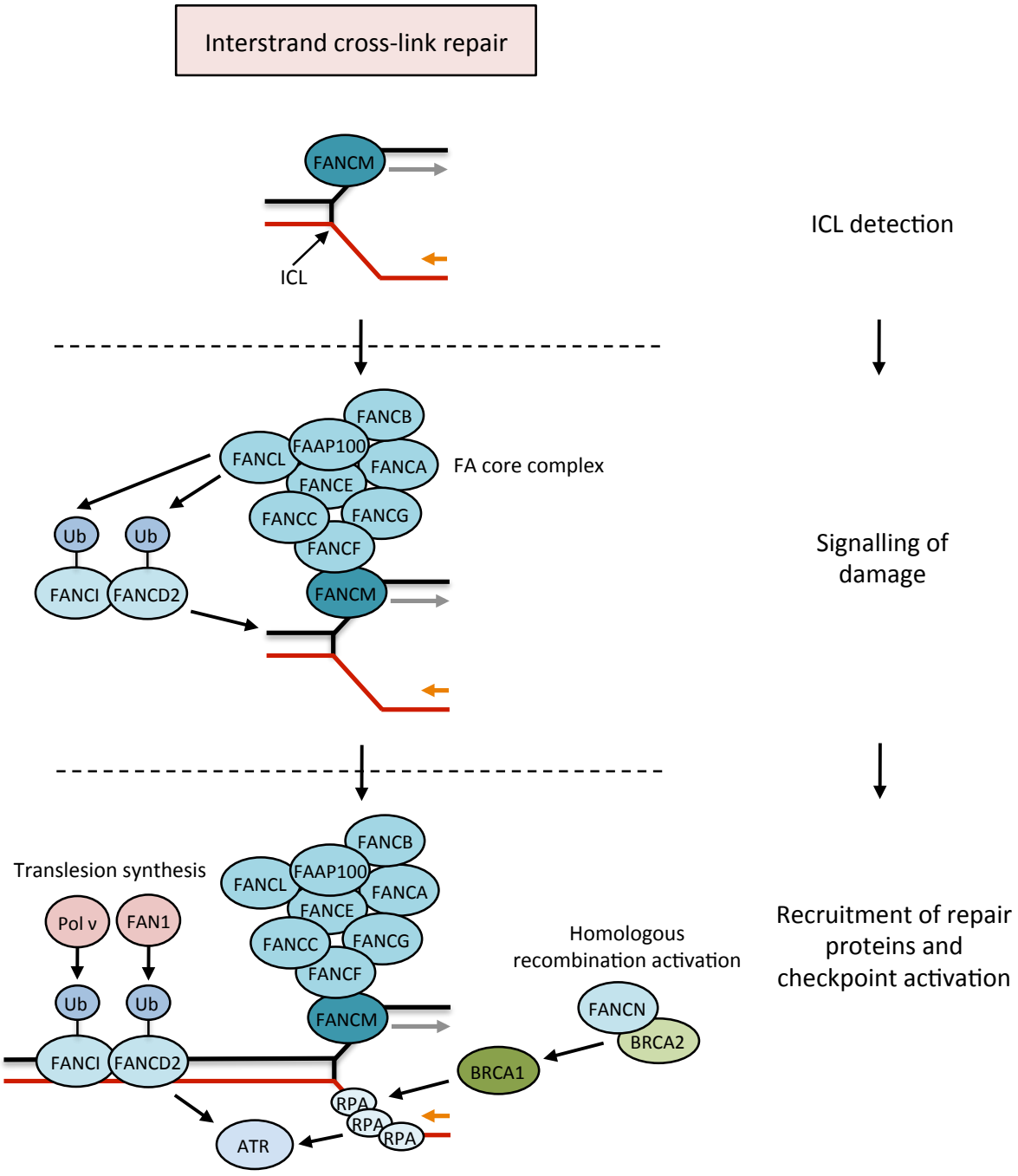

Figure 1.11: Interstrand Cross-Link Repair. ICLs are recognised by FANCM which leads to the recruitment of the FA core complex and the subsequent monoubiquitination of the ID complex (FANCI and FANCD2). The ID complex is retained at the chromatin which leads to the recruitment of repair proteins such as nucleases and polymerases. BRCA1 and BRCA2 are responsible for the initiation of homologous recombination (adapted from Deans and West 2011).

by FANCM, the FA core complex (comprised of FANCA/B/C/E/F/G/L) is recruited to the ICL. The FA core complex has E3 ubiquitin ligase activity which together with the E2-conjugating enzyme UBE2T, is responsible for the monoubiquitination of FANCI (I) and FANCD2 (D), which together form the ID complex (Machida, Machida et al. 2006). The monoubiquitination of FANCI and FANCD2 leads to the retention of these proteins at chromatin, where they can coordinate ICL repair through the recruitment of other FA proteins such as FANCD1, FANCJ, FANCN, FANCO and FANCP, as well as nucleases (such as FAN1) and polymerases (such as Pol ν) that are necessary for ICL repair (MacKay, Declais et al. 2010, Moldovan, Madhavan et al. 2010). The removal of the ICL involves the generation of two incisions on one DNA strand flanking the ICL, resulting in the 'unhooking' of the ICL. Translesion synthesis then occurs over the ICL on the intact strand, followed by further incisions to remove the lesion and homologous recombination to repair the DSB formed by the incision events (Moldovan, Madhavan et al. 2010). The downstream FA proteins BRCA1 (FANCS) and BRCA2 (FANCD1) are responsible for the regulation of homologous recombination which is required for the stabilisation of the replication fork during ICL repair (Figure 1.11)(Deans and West 2011).

1.2.3 The Cell Cycle

There are four phases of the cell cycle; gap-phase 1 (G1), DNA synthesis (S), gap-phase 2 (G2) and mitosis (M) (Figure 1.12). Progression through the cell cycle is controlled by Cyclin dependent kinases (CDKs) together with Cyclins that are the regulatory subunits of CDKs which are responsible for kinase activity and substrate specificity. When cells are in G0 or G1, mitogenic signals stimulate the expression of Cyclin D proteins which associate with

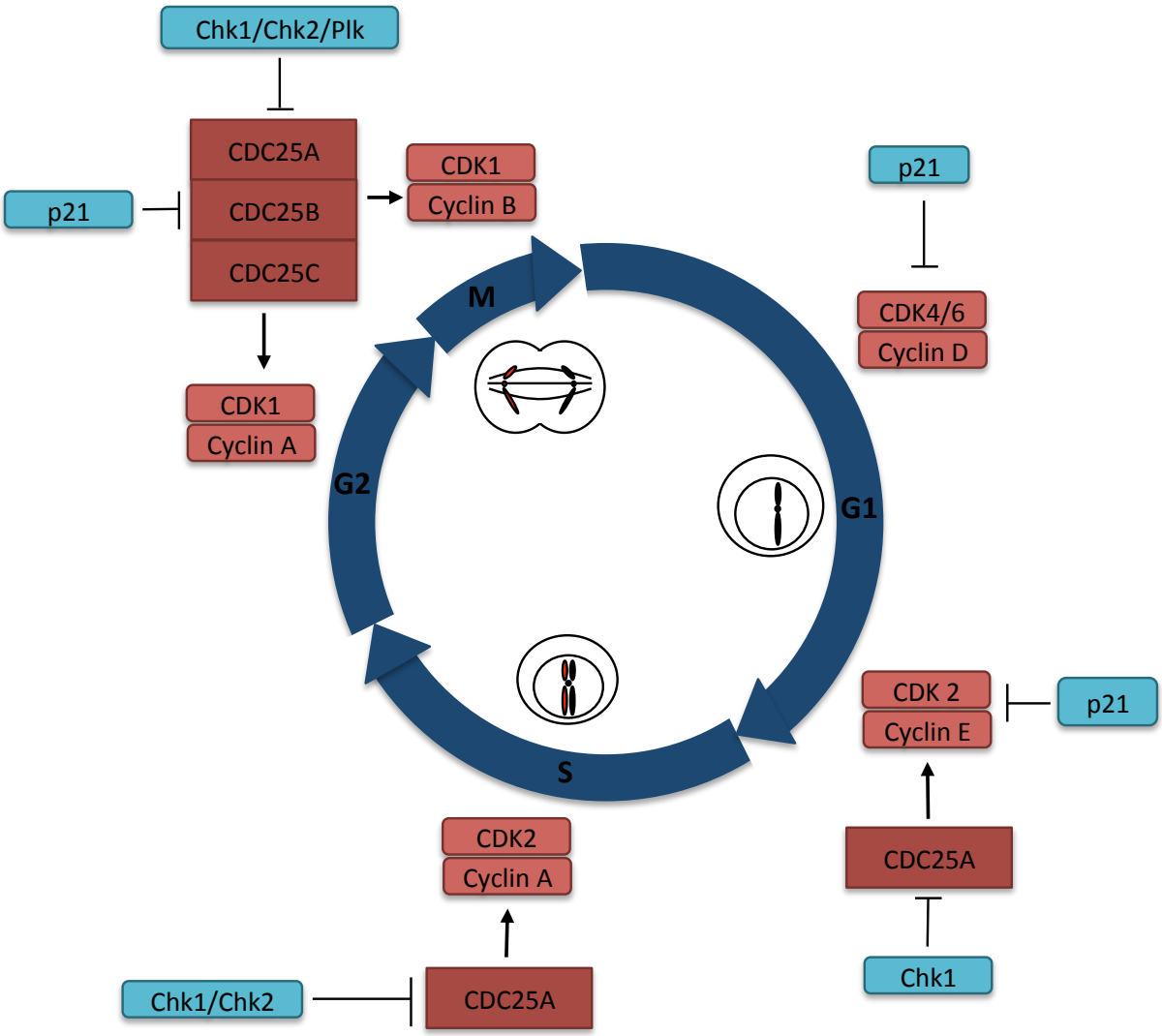

Figure 1.12: The Cell Cycle and Cell Cycle Checkpoints. Progression through the four phases of the cell cycle (G1, S, G2 and M) is controlled by Cyclin-CDK complexes. Progression through G1 is governed by Cyclin D-CDK4/6 and Cyclin E-CDK2 complexes. The formation of the Cyclin A-CDK2 complex marks the S/G2 transition. Formation of the Cyclin A-CDK1 complex promotes the G2/M transition. Finally, the Cyclin B-CDK1 complex marks the G2/M transition. The CDC25 phosphatases are responsible for the removal of inhibitory phosphatases on the Cyclin-CDK complexes. p21 is able to inhibit Cyclin-CDK complexes during G1. Chk1/Chk2 are able to phosphorylate CDC25A during G1/S phase, inhibiting its activity and in turn the Cyclin-CDK complex. During G2/M, the Chk1/Chk2/Plk/MAPK kinases are able to inhibit CDC25A/B/C and in turn G2/M Cyclin-CDK complexes.

CDK4 and CDK6, activating their kinase activities (Matsushime, Quelle et al. 1994, Meyerson and Harlow 1994). The formation of the active Cyclin D-CDK4/6 complexes leads to the phosphorylation of the tumour suppressor pRB and its homologues p107 and p130 (Cao, Faha et al. 1992, Ewen, Sluss et al. 1993, Kato, Matsushime et al. 1993, Beijersbergen, Carlee et al. 1995, Mayol, Garriga et al. 1995, Ezhevsky, Nagahara et al. 1997). Phosphorylation of pRB leads to its dissociation from E2F transcription factors which it binds to when in its non-phosphorylated form (Chellappan, Hiebert et al. 1991). Free E2F is able to stimulate the transcription of, amongst a number of proteins, Cyclin E that associates with CDK2 (Ohtani, DeGregori et al. 1995). The Cyclin E-CDK2 complex also phosphorylates pRB leading to further dissociation of pRB from E2F, which leads to the transcriptional activation of S phase genes and the G1/S phase transition (Lundberg and Weinberg 1998, Harbour, Luo et al. 1999). At the later stages of DNA replication (S phase), Cyclin A binds to CDK2 and this marks the S/G2 transition. During S and G2 phases, transcription factors activate the transcription of Cyclin B1 (required for M phase), which is driven by the Cyclin A-CDK2 complexes. Cyclin A then associates with CDK1, promoting the G2/M transition where it is then subsequently degraded. During G2, Cyclin B1-CDK1 complexes remain inactive through the phosphorylation of CDK1 on Tyr15 and Tyr14 by the Wee1 and myelin transcription factor 1 (Myt1) kinases, respectively (Parker and Piwnicaworms 1992, Liu, Stanton et al. 1997). The cell division cycle 25 C (CDC25C) phosphatase is responsible for the dephosphorylation of CDK1, thus activating the Cyclin B1-CDK1 complex which triggers the G2/M transition (Malumbres and Barbacid 2009). Active Cyclin B1-CDK1 complexes are then able to phosphorylate CDC25A/B/C, forming a positive feedback loop for the activation of more Cyclin B1-CDK1 complexes (Figure 1.12) (Izumi and Maller 1993).

1.2.3.1 The Cell Cycle Checkpoints

1.2.3.1.1 The G1 Checkpoint

The G1 checkpoint is in place to prevent damaged DNA from being replicated during the subsequent S phase. G1 checkpoint arrest is achieved through DNA damage-activated signalling cascades that ultimately lead to the inhibition of the Cyclin D-CDK4/6 and Cyclin E-CDK2 complexes and thus halt the cell cycle at G1. Following the detection of DNA damage, ATM becomes phosphorylated leading to the activation of Chk2 (see Section 1.2.1.1), which in turn leads to the phosphorylation of the transcriptional activator p53 (by both Chk2 and ATM directly)(Banin, Moyal et al. 1998, Canman and Kastan 1998, Shieh, Ahn et al. 2000). Subsequently p53 becomes transcriptionally activated and stabilised through the phosphorylation-mediated disruption of p53 mouse double minute 2 (MDM2) binding, which prevents MDM2-mediated nuclear export and degradation of p53 (Dumaz and Meek 1999, Schon, Friedler et al. 2002). The activation and stabilisation of p53 leads to the transcriptional activation of a number of target genes including p21, which inhibits G1/S entry through its role as a CDK inhibitor, subsequently inhibiting the Cyclin D-CDK4/6 and Cyclin D-CDK2 complexes and preventing the transition into S phase (He, Siddik et al. 2005). ATM-mediated Chk2 activation also leads to the removal of CDC25A, a phosphatase that normally acts to remove the inhibitory phosphatases from CDK2 and thus inhibit the Cyclin E-CDK2 complexes, preventing the G1/S transition. There is also evidence to suggest that ATR is able to directly phosphorylate p53 to induce cell cycle arrest following DNA damage, inducing further inhibition of the Cyclin E-CDK2 complexes (Tibbetts, Brumbaugh et al. 1999).

1.2.3.1.2 The S Phase Checkpoint

The S phase checkpoint exists to ensure that damaged DNA is not replicated. Activation of the S phase checkpoint through the ATR/Chk1 signalling pathway targets the Cyclin-CDK and CDC7-DBF4 protein kinase (DDK) complexes which act to inhibit the firing of primed origins (Heffernan, Unsal-Kacmaz et al. 2007, Zegerman and Diffley 2010). The checkpoint also exists in order to preserve the integrity of the replication forks following replication stress, allowing time for DNA repair before it is met by an ongoing replication fork (see Section 1.2.4.2.2 for a detailed discussion of the S phase checkpoint during replication). The S phase checkpoint also detects DSBs that occur during S phase that are not associated with active replicons. DSBs that occur during S phase are recognised by the ATM/Chk2 signalling pathway (see Section 1.2.1.1), which is ultimately activated to induce the degradation of the S phase promoting phosphatase CDC25A. Degradation of CDC25A leads to the maintenance of the inhibitory phosphorylation, normally removed by CDC25A, of the CDK2 component of the Cyclin E/A-CDK2 complexes, leading to the inhibition of these complexes. This inhibition prevents cell division cycle 45 (CDC45) loading at pre-replication complexes (see Section 1.2.4.1), and therefore inhibits firing of any remaining origins that have been primed for replication initiation (Falck, Mailand et al. 2001). Activation of the ATR/Chk1 pathway also leads to the proteasome-mediated degradation of CDC25A, thus also contributing to the activation of the S phase checkpoint (Zhao, Watkins et al. 2002, Sorensen, Syluasen et al. 2003).

1.2.3.1.3 The G2/M Checkpoint

The G/M checkpoint is in place to prevent the segregation of damaged chromosomes which have either incurred unrepaired damage during G2 phase, or S or G1 phase. At the

G2/M checkpoint, the CDC25 phosphatases (CDC25A, CDC25B, CDC25C) are phosphorylated leading to the inactivation of the Cyclin B1-CDK1 complex which is necessary for the progression into M phase. Following the activation of Chk1 and/or Chk2 by ATR and ATM kinases respectively, active Chk1/Chk2 is able to phosphorylate CDC25C, stimulating the 14-3-3 family of proteins to bind to CDC25C; this sequesters CDC25C to the cytoplasm, where it is no longer able to remove the inhibitory phosphorylation from CDK1 of the Cyclin B1-CDK1 complex (Kumagai and Dunphy 1999, Lopez-Girona, Furnari et al. 1999). Proteins of the mitogen-activated protein kinase (MAPK) pathway have also been shown to be able to phosphorylate CDC25A, CDC25B and CDC25C, also leading to 14-3-3 binding and sequestering of these proteins to the cytoplasm (Bulavin, Higashimoto et al. 2001, Reinhardt, Aslanian et al. 2007). ATM/ATR-mediated phosphorylation of polo-like kinase 3 (Plk3) has also been shown to further inhibit CDC25 function during the G2/M checkpoint (Bahassi, Hennigan et al. 2004). p53 is also involved in G2/M checkpoint arrest through the transcriptional activation of cell cycle inhibitors such as p21, 14-3-3σ and growth arrest and DNA damage inducible 45 alpha (GADD45). p21 is able to inhibit CDK1 directly, 14-3-3σ is responsible for the relocalisation of CDK1 to the cytoplasm, and GADD45 prevents CDK1-Cyclin B1 binding (Hermeking, Lengauer et al. 1997, Wang, Zhan et al. 1999, Zhan, Antinore et al. 1999).

1.2.4 DNA Replication

1.2.4.1 DNA Replication Initiation

The initiation of DNA replication is a two-step process involving origin licensing followed by origin firing. Origin licensing begins during the late phases of mitosis and

continues through to the G1 phase of the cell cycle. The onset of origin licensing occurs when the hexameric origin recognition complex 1-6 (ORC 1-6) recruits cell division cycle 10-dependent transcript 1 (Cdt1) and cell division cycle 6 (Cdc6) proteins to replication origins (Bell and Stillman 1992, Gavin, Hidaka et al. 1995, Piatti, Lengauer et al. 1995, Nishitani, Lygerou et al. 2000). Together, these proteins load the helicase component, mini chromosome maintenance (MCM) 2-7 protein complexes onto origins of replication; the proteins loaded at these origins together form a complex termed the pre-replicative complexes (pre-RCs) (Evrin, Clarke et al. 2009). Cyclin A/CDK2 activity marks the G1/S phase transition where origin firing is initiated. In mammalian cells, the pre-RC component Cdc6 becomes phosphorylated upon S phase entry, leading to its dissociation from the pre-RC complex into the cytoplasm (Petersen, Lukas et al. 1999). Origin firing during S phase also involves the activation of the MCM 2-7 hexamer and is achieved by the subsequent association of Cdc45 and MCM10 with the pre-RC complex, which then associates with GINS to form the active helicase complex (Ilves, Petojevic et al. 2010). Treslin and TOPBP1 associate with pre-RCs which forms the pre-initiation complex (Kumagai, Shevchenko et al. 2010). Entry into S phase and subsequent origin firing also involves the activation of the DDK protein kinase, which is able to phosphorylate a number of pre-initiation complex proteins (Heller, Kang et al. 2011). The active helicase is then able to unwind DNA at the origin site. GINS and Cdc45 are thought to be involved in the recruitment of DNA replication machinery, which includes PCNA, Polα primase, RPA, and the leading and lagging strand DNA polymerases Pol ε and Pol δ, to the origin (Aparicio, Stout et al. 1999, De Falco, Ferrari et al. 2007). The loading of the DNA replication machinery behind the active helicase leads to the

formation of the replisome which is able to move bi-directionally along the DNA, continuing to replicate the DNA over the entire genome.

1.2.4.2 Replication Stress

Replication stress can be defined as any perturbation in the process, coordination and timing of DNA synthesis. One way of inducing replication stress is the slowing or stalling of the replication fork during DNA synthesis in response to a particular replication fork barrier (RFB). There are a number of RFBs that have the capacity to lead to replication stress, including unresolved DNA lesions, DNA-bound proteins and secondary structures (Zeman and Cimprich 2014). A number of exogenous agents can also induce replication stress including agents that inhibit DNA elongation such as the DNA polymerase inhibitor aphidicolin, and the ribonucleotide reductase (RNR) inhibitor hydroxyurea (HU) (Yarbro 1968, Krokan, Wist et al. 1981). RNR catalyses the conversion of NDPs into dNDPs, which is the rate limiting step in the production of dNTPs (Jordan and Reichard 1998). HU treatment therefore depletes dNTP pools which stalls replication forks (Bianchi, Pontis et al. 1986). Prolonged exposure to HU stalled replication forks collapse into DSBs. It is essential that the cell is able to respond effectively to replication stress since unresolved replication stress can ultimately lead to fork collapse, incomplete DNA replication and DNA breakage.

Replication fork stalling can be defined as a temporary 'pause' in replication fork progression in response to a RFB. Following the removal of the RFB, the stalled replication fork is able to resume fork progression. Fork collapse can be defined as a replication fork which is no longer able to complete replication in response to replication stress. Fork collapse is normally associated with the dissociation of the replisome, and deterioration of the replication fork into a DSB, which occurs passively (normally after long replication blocks)

or actively via MUS81 endonuclease cleavage (Hanada, Budzowska et al. 2007). To prevent fork collapse, replication forks must be stabilised and their replisomes retained with the fork (see Section 1.2.4.2.2 for discussion on fork stabilisation). Replication forks subjected to long periods of fork stalling become inactivated and are no longer able to undergo fork restart. In this instance, global new origin firing is responsible for the completion of DNA replication (Woodward, Gohler et al. 2006, Ge, Jackson et al. 2007, Petermann, Orta et al. 2010).

The replication fork has a number of defence mechanisms that act to resolve replication stress. Firstly, the simplest mechanism to avoid replication stress is to resolve any DNA lesions before they are met by the replication fork. This can be performed by any number of DNA repair mechanisms depending on the type of damage incurred (see Section 1.2.2). Secondly, if the damage is not resolved before association with the replication fork, activation of the replication checkpoint can act to temporarily stall the replication fork, which can then be stabilised and restarted following clearance of the damage. Finally, if the two previous mechanisms fail to clear the RFB and replication remains stalled, complex restart mechanisms are employed which act to restart and complete replication (see Section 1.2.4.2.3).

1.2.4.2.1 Sources of Replication Stress

There are numerous RFBs that can lead to replication stress including DNA damage, DNA-bound protein and DNA structures amongst others. The generation of replication stress most commonly results in the formation of ssDNA as a result of DNA helicase activity continuing to unwind the double helix when the polymerase has stalled. The type of replication fork arrest induced by these RFBs is dependent on the lesion/structure formed (Figure 1.13) (Zeman and Cimprich 2014).

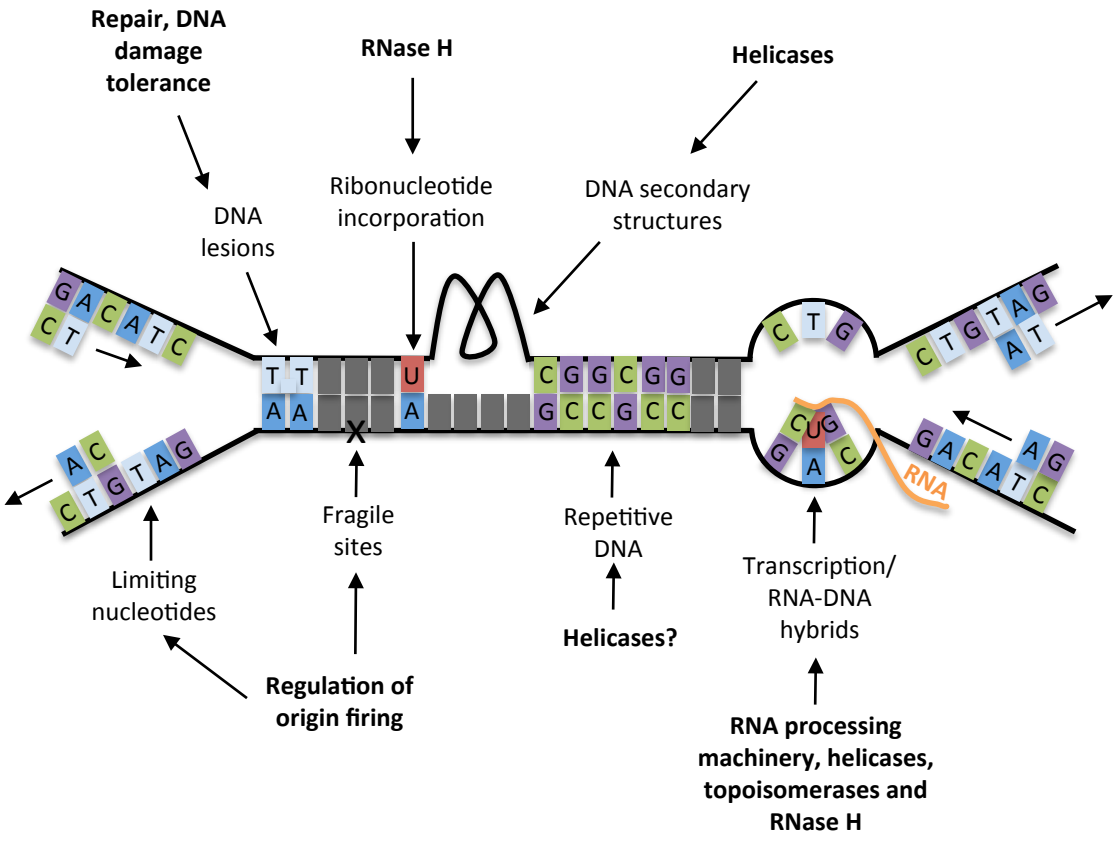

Figure 1.13: Sources of Replication Stress. There are a number of replication fork barriers that can perturb the progression of DNA synthesis and lead to replication stress. These include limited nucleotide pools, DNA lesions, fragile sites, ribonucleotide incorporation, DNA secondary structures, repetitive DNA and transcription/RNA-DNA hybrids. The mechanisms by which these replication fork barriers are resolved are highlighted in bold (adapted from Zeman and Cimprich 2004).

One common unresolved RFB is DNA damage, which includes lesions such as bulky adducts, alkylated bases, pyrimidine dimers and abasic sites. These unresolved lesions pose a problem for the replicating polymerases, since they cannot replicate past these sites. The translesion synthesis (TLS) pathway acts to resolve this problem by employing a group of 'error-prone' polymerases, termed TLS polymerases, which are able to incorporate nucleotides opposite the damaged base allowing replication to proceed (Cordeiro-Stone, Zaritskaya et al. 1997, Gibbs, McGregor et al. 1998, Gerlach, Aravind et al. 1999). Blocking of the replication machinery resulting in uncoupling of polymerase and helicase activities induces the monoubiquitination of PCNA on lysine 164 which is catalysed by the E2 ubiquitin-conjugating enzyme Rad6 and the E3 ubiquitin ligase Rad18 (Hoege, Pfander et al. 2002, Stelter and Ulrich 2003). The ubiquitination of PCNA aids the association with TLS polymerases which are then able to by-pass the lesion, but sometimes at the cost of mutagenesis (Hoege, Pfander et al. 2002, Stelter and Ulrich 2003, Kannouche, Wing et al. 2004). Poly-ubiquitination of PCNA leads to a mode of damage by-pass that is less characterised but is considered to be error-free (Moldovan, Pfander et al. 2007).

Single-strand gaps and DSBs also pose a serious threat to DNA replication. The consequence of a replication fork meeting a single-strand gap or DSB is thought to be a broken fork with one arm becoming a DSB, and two double-strand ends respectively (Cortes-Ledesma and Aguilera 2006). As a defence mechanism against the generation of passive DSBs, there is some evidence to suggest that the replication fork is able to slow down, in order to allow for DNA repair mechanisms to clear the damage before the fork arrives, which would ultimately lead to replisome dissociation at the break and incomplete replication (Chaudhuri, Hashimoto et al. 2012).

Mis-incorporation of ribonucleotides into the DNA backbone is a significant source of replication stress. Sometimes, the replicative polymerases, Pol δ and Pol ε, erroneously incorporate ribonucleotides (rNTPs) instead of deoxyribonucleotides (dNTPs) into the DNA backbone during DNA replication (McElhinny, Watts et al. 2010). Mis-incorporated rNTPs must be removed from the DNA backbone since polymerases cannot replicate past these. Mis-incorporated rNTPs are removed from the DNA backbone by the ribonucleotide repair pathway, whereby RNase H2 is responsible for the recognition and excision of the rNTP, together with the endonucleases FEN1 and EXO1 (Sparks, Chon et al. 2012). In the absence of RNase H2-mediated excision of rNTPs, the TLS polymerases are able to bypass them (Lazzaro, Novarina et al. 2012).

Replication stress can also be induced by DNA structures that deviate from the right-handed double helix B form of DNA. Such structures include hairpins, triplexes, cruciforms and G4 quadruplexes (Gacy, Goellner et al. 1995, Paeschke, Bochman et al. 2013). The formation of these structures leads to a significant challenge for the replication fork. These structures are thought to be resolved by specific helicases, which act to dissociate bound DNA structures, as well as nucleases (Mre11, FEN1, EXO1 and DNA2) which are thought to cleave secondary structures (Sun, Karow et al. 1998, Fry and Loeb 1999, Ghosal and Muniyappa 2005, Masuda-Sasa, Polaczek et al. 2008, Wu, Shin-ya et al. 2008, Vallur and Maizels 2010).

Since both replication and transcription occur on DNA, it is not surprising that the two machineries have the capacity to collide. Whilst DNA replication is restricted to occur only during S phase, and transcription normally occurs during G1 phase, the latter can also proceed during S phase. It is thought that replication and transcription occurring during S

phase is spatially separated from the DNA replication machinery in order to prevent collision. Interestingly, there are a number of human genes that are so large they need more than one cell cycle to be completely transcribed, in these cases the replication and transcriptional machinery are known to associate (Helmrich, Ballarino et al. 2011). Helicases and topoisomerases are known to unwind the DNA and ease the topological stress associated with replication and transcription machinery that are in close proximities (Bermejo, Capra et al. 2009, Tuduri, Crabbe et al. 2009).

The formation of R-loops can also cause significant replication stress; they can be defined as an RNA-DNA hybrid structure with a displaced ssDNA strand. These structures cannot be replicated and are a significant barrier to the replication machinery. The formation of R-loops can be resolved by specialised RNA-DNA helicases, that operate to unwind such RFBs, or through the enzyme RNase H, which dissolves the RNA portion of the structure (Huertas and Aguilera 2003, Alzu, Bermejo et al. 2012).

There are certain regions in the genome that are known to be difficult to replicate, such regions are predisposed, by default, to replication stress, and are termed fragile sites. Two types of fragile site exist, early-replicating fragile sites (ERFSs) and common fragile sites (CFSs). ERFSs, as the name suggests, replicate early, have a high G/C content and have a relaxed chromatin configuration (Barlow, Faryabi et al. 2013). CFSs replicate late, are A/T rich and have a condensed chromatin state (Smeets and van de Klundert 1990). Most significantly, CFSs are prone to the formation of secondary structures and the generation of DSBs induced by replication stress. CFSs are thought to be susceptible to replication stress because they have a reduced number of replication origins, which leads to incomplete replication due to lack of origin firing upon replication stress. These regions of replication

stress are targeted by the nucleases MUS81-EME1 or ERCC1, resulting in controlled DSB events. These controlled breaks are thought to maintain genomic stability (Naim, Wilhelm et al. 2013, Ying, Minocherhomji et al. 2013). More recently, the nuclease activity of MUS81 was shown to stimulate DNA synthesis at these regions in mitosis, a mechanism which is thought to preserve genomic stability (Minocherhomji, Ying et al. 2015).

The over-expression of oncogenes including Cyclin E, HRAS and c-Myc can also induce replication stress. It is thought that the over-expression or mutation of these genes leads to the depletion of nucleotide pools and replication/transcription machinery collision through increased origin firing and/or increased initiation events (Halazonetis, Gorgoulis et al. 2008, Jones, Mortusewicz et al. 2013, Srinivasan, Dominguez-Sola et al. 2013). Finally, limiting replication factors such as the replication machinery itself, nucleotides, histones and histone deposition machinery, which is responsible for the newly replicated DNA packaging, can also lead to replication stress via fork slowing (Figure 1.13) (Anglana, Apiou et al. 2003, Groth, Corpet et al. 2007, Poli, Tsaponina et al. 2012, Mejlvang, Feng et al. 2014).

1.2.4.2.2 Checkpoint Activation Following Replication Stress

As previously discussed, a number of factors can stall replication forks including DNA damage, DNA-protein adducts and secondary structures. If the RFB is not resolved before meeting the replication fork, the next mechanism of defence to protect against replication fork collapse is to activate the replication checkpoint which prevents further replication until the damage/lesion is repaired, only then will replication proceed. A common structure formed from replication stress is ssDNA, which often results from the uncoupling of the DNA polymerase and the DNA helicase, whereby the helicase continues to unwind the DNA following the stalling of the DNA polymerase (Pacek and Walter 2004). The generation of

large stretches of ssDNA activates the replication checkpoint through the activation of ATR kinase, which acts to stall the cell cycle and thus prevent further DNA replication during replication stress (see Section 1.2.1.2) (Byun, Pacek et al. 2005). The active ATR kinase phosphorylates and activates Chk1, which, when activated, is able to phosphorylate the CDC25A, CDC25B and CDC25C phosphatases. These phosphatases are responsible for the prevention of the activation of Cyclin E/A-Cdk2 and Cyclin B-Cdk1, which ultimately leads to arrest of the cell cycle allowing for repair/restart of the replication fork (Sanchez, Wong et al. 1997, Zhao, Watkins et al. 2002, Sorensen, Syluasen et al. 2003).

ATR is also thought to respond to replication stress with the ultimate aim of stabilising the stalled replication fork and preventing fork collapse. A number of mechanisms of fork stabilisation have been proposed including late origin firing inhibition, replisome stabilisation and fork remodelling by repair enzymes to promote fork restart. However, the exact mechanisms by which ATR stabilises stalled replication forks remain to be elucidated. In mammalian cells, the ATR-Chk1 replication checkpoint has been shown to be responsible for the inhibition of late origin firing through a Chk1-mediated mechanism (Feijoo, Hall-Jackson et al. 2001). There is also evidence to suggest that the suppression of late origin firing is controlled through the ATR-mediated repression of CDC45 chromatin binding, although DDK activity remains (Liu, Barkley et al. 2006, Tsuji, Lau et al. 2008). The ATR-mediated inhibition of CDK2 and the phosphorylation of mixed lineage leukaemia (MLL) histone methyltransferase are also responsible for the suppression of late origin firing during replication stress (Liu, Takeda et al. 2010). One mechanism involved in replication fork stabilisation was thought to be the stabilisation of components of the replisome by the checkpoint machinery. Studies in human cells showed that the amount of chromatin-

associated replisome components PCNA, POLE, POLD2 and CDC45 was reduced in ATR-deficient cells treated with replicative stress agents when compared to untreated cells, suggesting that the checkpoint is necessary for replisome stabilisation (Ragland, Patel et al. 2013). Furthermore, the association of the replisome component PCNA was impeded during early origin firing following inhibition of ATR in mammalian cells when compared to ATR competent cells, also suggesting that the checkpoint is important for replisome stability (Dimitrova and Gilbert 2000). There is also evidence to suggest that the S phase checkpoint during replication stress is not important for replisome stability at the fork (De Piccoli, Katou et al. 2012). Furthermore, recent isolation of proteins on nascent DNA (iPOND), using checkpoint-deficient cells, showed that ATR signalling plays no significant role in the stabilisation of the replisome but that it is essential for fork stability (Dungrawala and Cortez, unpublished data). In addition to the inhibition of late origin firing, activation of the replication checkpoint is also thought to stabilise stalled forks through the ATR-mediated activation of repair proteins such as Werner syndrome protein (WRN), BLM and SWI/SNF-related matrix-associated actin-dependent regulator of chromatin subfamily A-like protein 1 (SMARCAL1) (Pichierri, Rosselli et al. 2003, Davies, North et al. 2004, Couch, Bansbach et al. 2013). Activation of these proteins is required in order for fork restart and ultimately, fork stabilisation (see Section 1.2.4.2.3).

1.2.4.2.3 Restart Mechanisms of Stalled Replication Forks

There are certain scenarios where repair of the RFB is not achieved before meeting the replication fork, or repaired following the temporary stalling of the replication fork via

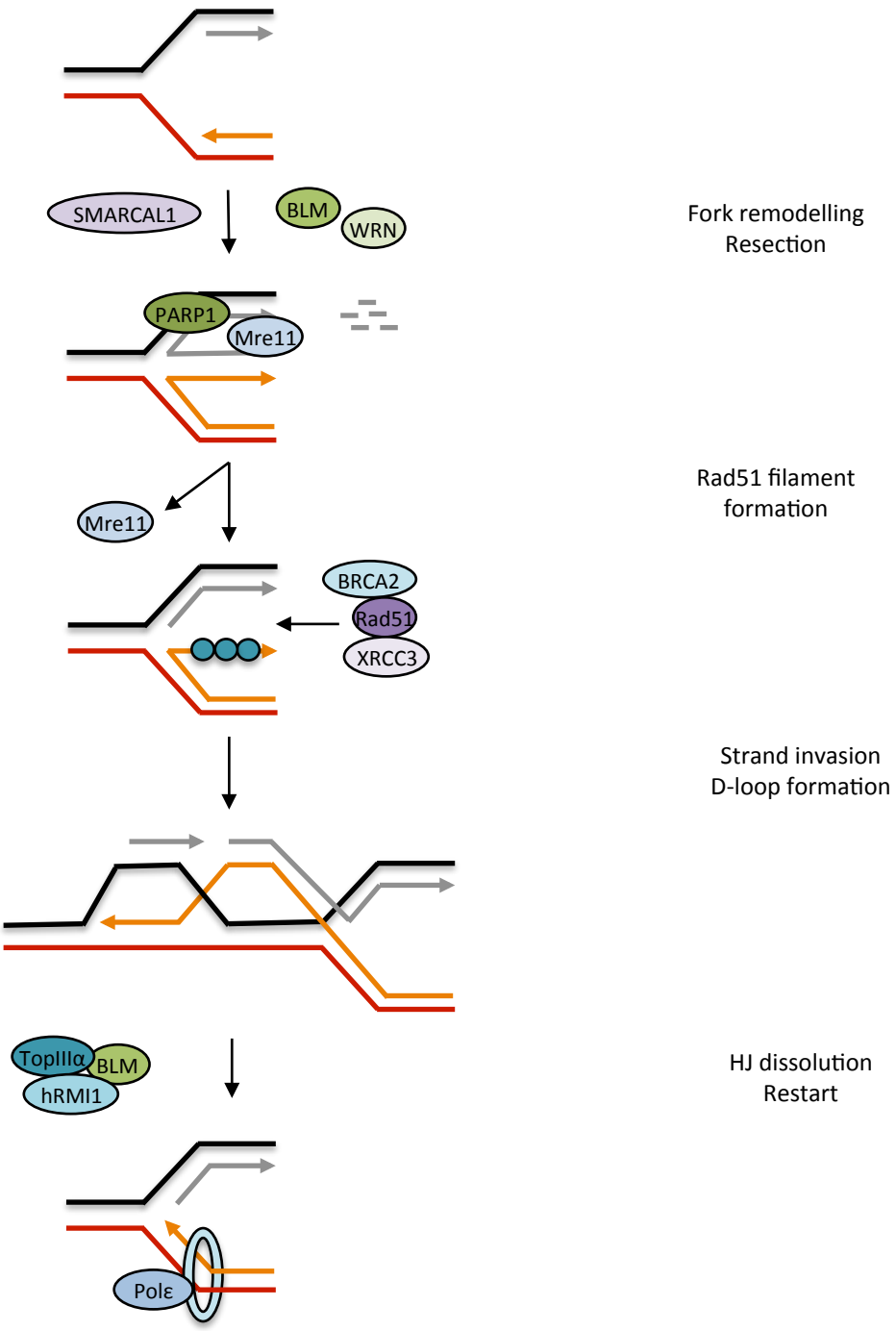

Figure 1.14: A Model for Replication Fork Restart. In this model SMARCAL1 is responsible for the reannealing of ssDNA that has formed as a consequence of helicase polymerase uncoupling. BLM and WRN are responsible for the reversal of the replication fork into a Holliday Junction. Mre11 is then recruited to the stalled fork by PARP1, which subsequently creates a 3' overhang suitable for the generation of a Rad51 filament. BRCA2 and XRCC3 then load Rad51 onto the 3' overhang. The Rad51 filament stimulates strand invasion and D-loop formation. The Holliday Junction may be resolved by BLM, resulting in a non-crossover product (adapted from Jones and Petermann 2012).

ATR-mediated mechanisms. It is at this point that replication restart mechanisms are employed in order to ensure the complete replication of the genome. The exact mechanism by which stalled replication forks are restarted is currently unknown. A number of mechanisms for fork restart have been postulated, however, including the enzymatic reversal of stalled forks into a 'chicken-foot' structure that is competent for replication (Postow, Ullsperger et al. 2001). The remodelling of stalled forks by various ATR-activated repair proteins has also been implicated in fork restart, although this mechanism may overlap with fork reversal. HR as a mechanism of restart has also been hypothesised, as well as DSB-mediated restart mechanisms, which will be described in the following paragraphs (Figure 1.14) (reviewed in (Jones and Petermann 2012)).

Reversal of Replication Forks

Replication fork reversal can be defined as the processing of a replication fork which comprises a typical three-way fork, into a four-way junction through the annealing of the newly synthesised DNA strands, and the re-annealing of the parental strands, producing a structure which has essentially 'back-tracked' along the replicating DNA (Postow, Ullsperger et al. 2001). The consequences of fork reversal are thought to be three-fold. Firstly, in the context of a DNA lesion causing the replication stress, fork reversal can back-track the DNA lesion into the double-stranded region of the DNA, allowing the lesion to be excised by conventional excision mechanisms. Secondly, annealing of the two newly synthesised DNA strands limits the extent of exposed ssDNA, therefore promoting the stabilisation of the fork. Finally, fork regression allows lesion bypass through template switching. The concept of replication fork reversal was first suggested in 1976, when Higgins and colleagues proposed

the formation of the four-way replication fork to be a DNA damage tolerance mechanism, whereby the newly synthesised strands were used as a template for DNA replication in order to bypass a DNA lesion on the parental strand (Higgins, Kato et al. 1976). Although there has been evidence for fork reversal in prokaryotes, only relatively recently has there been evidence to suggest fork reversal is a mechanism used by higher eukaryotes. There was no convincing data to confirm this until 2012, when fork reversal was demonstrated *in vivo* in yeast and mammalian cell lines following topoisomerase 1 poisoning in a mechanism that is dependent on PARP1 (Chaudhuri, Hashimoto et al. 2012). Further work from this group demonstrated that the helicase RECQ1 promotes the restart of reversed replication forks following TOP1 inhibition. This RECQ1 activity is inhibited by PARP1-mediated ADP ribosylation (Berti, Chaudhuri et al. 2013). Further evidence for fork reversal came from the work of Thangavel and colleagues who showed that WRN and DNA2 were responsible for the degradation of the 'fourth arm' of the reversed replication fork allowing fork restart by a novel mechanism (Thangavel, Berti et al. 2015). Recent studies have demonstrated that fork reversal occurs not just in response to TOP1 inhibitors, but also following treatment with DNA synthesis inhibitors, interstrand cross-linking inducers and base-damaging agents, showing that fork reversal is a *bona fide* mechanism to respond to replication stress (Zellweger, Dalcher et al. 2015). In addition, this work showed that Rad51 was essential for the conversion of ssDNA into reversed forks in response to TOP inhibitors, depletion of nucleotides and interstrand crosslinks (Zellweger, Dalcher et al. 2015).

Fork Remodelling During Replication Restart

Recent developments from *in vivo* studies of fork reversal have furthered our understanding of replication restart following replication stress. However, a number of proteins have been implicated in replication restart via *in vitro* studies, including additional proteins that may be required for fork reversal, and also proteins that have been implicated in branch migration via fork remodelling. Of course, it is possible that fork reversal and branch migration are interlinked and both processes are necessary to carry out fork restart. Indeed, Holliday junctions are structurally similar to reversed forks, and it could be that there is a dual function for these proteins both in HR and fork reversal. Other proteins that have been implicated in restart include the DNA helicases BLM, WRN, Fanconi anaemia complementation group M (FANCM), SMARCAL1 and F-box helicase 1 (FBH1) whose fork remodelling activities are thought to promote fork restart. Defects in BLM and WRN proteins have been shown to slow fork progression, and cells deficient in these proteins undergo reduced fork restart following treatment with replication inhibitors (Davies, North et al. 2007, Sidorova, Li et al. 2008). It is possible that the helicase activity of these proteins may be a prerequisite for HR-mediated fork restart; both BLM and WRN have been implicated in the regression of stalled forks via the formation of D-loop intermediates and Holliday junctions (Machwe, Xiao et al. 2006, Ralf, Hickson et al. 2006). Evidence also suggests that BLM and WRN are capable of unwinding secondary structures in DNA that would otherwise be difficult to replicate (Sun, Karow et al. 1998, Fry and Loeb 1999). SMARCAL1 is another helicase that may play a role in replication restart. It is an annealing helicase which is recruited to stalled replication forks in response to replication stress. Defects in SMARCAL1 lead to replication fork restart problems and an accumulation of ssDNA; this suggests that

SMARCAL1 may restart stalled replication forks by re-annealing ssDNA which has resulted from helicase polymerase uncoupling (Bansbach, Betous et al. 2009, Ciccia, Bredemeyer et al. 2009). Interestingly, cells lacking functional FANCM exhibit increased replication speeds in the presence and absence of DNA damage, suggesting that the FANCM helicase has the ability to slow replication (Luke-Glaser, Luke et al. 2010). Interestingly, in DT40 cells loss of functional FANCM resulted in an increase in replication fork restart following camptothecin treatment (Schwab, Blackford et al. 2010). Although there is mounting evidence to suggest that restart of stalled replication forks is achieved through fork remodelling, it is still unclear how this would be achieved considering the need for replisome dissociation from the DNA in order for the fork to be remodelled. How the replisome would be reloaded at the replication fork in this scenario is currently unclear. It has therefore also been hypothesised that remodelling of the fork into Holliday Junctions by the DNA helicases may be a prerequisite for HR-mediated fork restart.

Fork Restart via Homologous Recombination

There is increasing evidence to suggest that homologous recombination plays an important role in the restart of stalled forks. HR-mediated fork restart involves the processing of the stalled fork to form Holliday junctions and D-loop intermediates by a mechanism that is functionally distinct from HR-mediated DSB repair. Indeed, defects in a number of HR proteins have been shown to induce replication-associated DSBs including BRCA2, Fanconi anaemia complementation group A (FANCA), Fanconi anaemia complementation group D2 (FANCD2), Mre11 and Rad51 (Sonoda, Sasaki et al. 1998, Costanzo, Robertson et al. 2001, Lomonosov, Anand et al. 2003, Sobeck, Stone et al. 2006).

In addition, following treatment with various inhibitors of replication, the loss of the HR proteins Mre11, Rad51 and X-ray repair cross-complementing protein 3 (XRCC3) has been shown to negatively affect replication restart, suggesting that these proteins are necessary for this process (Trenz, Smith et al. 2006, Bryant, Petermann et al. 2009, Petermann, Orta et al. 2010). The HR resection protein Mre11 is known to be recruited to the sites of stalled replication forks (Franchitto and Pichierri 2002, Mirzoeva and Petrini 2003, Robison, Elliott et al. 2004). Mre11 could, therefore, be recruited to stalled forks to process them to produce the lagging strand gap or 3' overhang necessary for subsequent Rad51 loading and strand invasion. The Rad51 paralogue XRCC3 has also been shown to facilitate fork restart following the release from replication blocks (Bishop, Ear et al. 1998). In addition, PARP1 has been shown to facilitate replication restart through the recruitment of Mre11 to the replication fork, where it is thought to promote restart through its resection activities (Bryant, Petermann et al. 2009). In support of the idea of HR-mediated fork restart, Rad51 has also been shown to be necessary for replication fork restart following long replication blocks which lead to collapse into DSBs (Petermann, Orta et al. 2010). Another HR protein, BRCA2, has also been implicated in HR-mediated fork restart. BRCA2 was shown to limit Mre11-dependent DNA resection at stalled forks, and also to regulate Rad51 loading and filament formation during replication restart (Hashimoto, Chaudhuri et al. 2010, Schlacher, Christ et al. 2011). During HR-mediated restart, the resulting Holliday Junction formed could be resolved in a process involving BLM and TOPIIIα, which would allow replication to proceed without recombination due to crossing-over (Wu and Hickson 2003). As previously discussed, it is also possible that HR proteins have crossover functions in both HR and fork

reversal, since there has been no direct *in vivo* evidence to suggest that Holliday Junctions and homologous-recombination mechanisms exist during replication restart.

The Role of Double-Strand Break Formation in Fork Restart

In addition to HR-mediated restart that is achieved in the absence of a DSB, it has been suggested that, following long replication blocks, fork-associated DSBs are created by the endonuclease activity of MUS81-EME1 (Hanada, Budzowska et al. 2007). It is not entirely clear whether these fork-associated DSBs are repaired by the canonical DSB repair machinery or whether a more specific, fork-associated DSB repair mechanism is employed. It is thought that fork-associated DSBs that occur passively, i.e. through replication and transcription machinery collision rather than in an MUS81-EME1 dependent manner, are repaired by standard DSB repair mechanisms. Evidence to suggest that the induction of DSBs promotes replication fork restart comes from a study using MUS81-deficient cells, which, when released from long replication blocks (24 hours), failed to restart efficiently (Hanada, Budzowska et al. 2007). Conflicting reports suggest that replication cannot be restarted following the generation of DSBs induced by long replication blocks, and can only restart following short incubations that do not result in the generation of DSBs (Petermann, Orta et al. 2010). Replication restart following long replication blocks appears to be as a result of new origin firing rather than restart of forks that have collapsed into DSBs (Petermann, Orta et al. 2010).

1.3 ADENOVIRUS AND THE DNA DAMAGE RESPONSE

The first indication for a relationship between adenovirus and the DDR was seen when Ad12 infection was shown to induce specific chromosomal breaks in human embryo kidney cells (Stich, Hsu et al. 1964, Zur Hausen 1967, Mcdougal.Jk 1970, Mcdougal.Jk 1971). At the initial stages of adenovirus infection, the host cell initiates a DDR response following the detection of viral DNA or cellular stress. This DDR response can be measured from the levels of phosphorylated DDR proteins such as H2AX and RPA32 (Carson, Schwartz et al. 2003). One consequence of the activation of the cellular DDR is the 'repair' of viral DNA to form viral concatemers which can no longer be packaged into virions; it is therefore essential that adenovirus is able to circumvent the cellular DNA damage response (Weiden and Ginsberg 1994). Adenovirus has evolved sophisticated mechanisms which lead to efficient evasion from the cellular DDR which will be described in more detail in the following passages (Turnell and Grand 2012).

1.3.1 Concatenation of Adenovirus Genomes

It is well established that adenovirus has to circumvent a number of barriers to aid efficient viral infection, including detection by the host cells immune response and evasion of apoptosis. In addition, it is becoming increasingly apparent that adenovirus must circumvent the cellular DDR in order to effectively replicate its genome. During adenovirus infection, the double-stranded DNA ends of the linear adenovirus genome can be recognised by the host cell as 'damaged' DNA in the form of cellular DSBs. The outcome of this is the activation of the DDR and subsequent 'repair' of the double-stranded viral DNA ends through the DSB repair pathway (Weiden and Ginsberg 1994).

The first study to document the 'end-to-end' joining of viral double-stranded genomes showed that infection with Ad5 mutant viruses containing large E4 deletions resulted in the formation of large concatemers of viral DNA (Weiden and Ginsberg 1994). Concatemers can be defined as covalently joined monomers of DNA, joined in a non-specific orientation. The net effect of this concatermerisation is two-fold; joining of the viral ends results in the loss of the ITR regions and thus viral origins of DNA replication, and secondly, the large viral concatemers formed from end-to-end ligation results in a product that is too large to be packaged into viral capsids (Weiden and Ginsberg 1994).

To date, a number of studies have shown that the cellular DDR proteins DNA ligase IV, DNA-PKcs, and the MRN complex components Mre11 and NBS1 to be important for concatermisation of viral genomes (Boyer, Rohleder et al. 1999, Riballo, Critchlow et al. 1999, Stracker, Carson et al. 2002). Significantly, studies using the Ad5 E4 mutant virus *dl*1004 showed that infection with this mutant exhibited defective viral DNA replication and late protein synthesis as a consequence of the formation of concatemers (Stracker, Carson et al. 2002). Since the process of viral concatermisation involves the direct end-to-end ligation of viral genomes with some loss of genetic information, it was speculated that the DDR, and more specifically NHEJ machinery, played an important role in viral concatermisation. Further investigations showed that *dl*1004 infection in cell lines expressing mutant Mre11, DNA Ligase IV and DNA-PKcs were able to rescue the formation of viral concatemers, suggesting that these components of the NHEJ machinery are required for viral concatemerisation (Stracker, Carson et al. 2002). Later studies further demonstrated the relationship between concatemer formation and defective DNA replication and late protein synthesis, showing that the activity of the MRN complex had a direct effect on viral

DNA replication and not through the activation of the DDR and concatemer formation (Lakdawala, Schwartz et al. 2008).

1.3.2 Adenovirus-Mediated Degradation of Cellular Proteins

In a cellular context, ubiquitin ligases are known to have important roles in the control of homeostasis through the addition of ubiquitin (Ub) onto target proteins. The proteins involved in this system include the E1 activating enzymes, the E2 conjugating enzymes and the E3 ligase enzymes. In brief, the E1 activating enzyme binds and activates ubiquitin in an ATP-dependent manner, which is then passed onto a specific E2 conjugating enzyme recruited by E1. Together with the E3 ligase enzyme, E2 conjugates ubiquitin onto lysine residues of target proteins. The end result is usually being marked for proteasome-mediated degradation (reviewed in (Nakayama and Nakayama 2006). It is well established that the Ad5 and Ad12 viral proteins E1B55K and E4orf6 interact with the cellular proteins Rbx1, Cullin 2/5 and Elongins B and C to form an E3 ubiquitin ligase complex (Querido, Blanchette et al. 2001). It is thought that the E1B55K protein acts as a substrate recognition unit whilst the E4orf6 protein assembles the cellular proteins in the complex (Baker, Rohleder et al. 2007, Blackford, Patel et al. 2010, Forrester, Sedgwick et al. 2011, Orazio, Naeger et al. 2011, Gupta, Jha et al. 2013). The assembly of the E3 ubiquitin ligase complex results in the targeting of various cellular factors that are detrimental to virus replication and survival, for proteasome-mediated degradation. The cellular proteins targeted by adenovirus for proteasome-mediated degradation will be discussed in the following passages.

The first indication that adenovirus employed cellular proteins to form an E3 ubiquitin ligase complex came from Querido and colleagues who demonstrated that the degradation of p53 was achieved through the Ad5 E1B55K/E4orf6 viral proteins ‘hijacking’

the cellular E3 ligase components Rbx1, Cul5, and Elongins B and C (Querido, Marcellus et al. 1997, Steegenga, Riteco et al. 1998). During p53 ubiquitination, the Ad5 E1B55K protein acts as the substrate recognition protein whilst the E4orf6 protein binds to Elongins B and C via its BC box motifs (Blanchette, Cheng et al. 2004).

Shortly after this discovery, the MRN complex component Mre11 was shown to be targeted for proteasome-mediated degradation by adenovirus with the ultimate aim of destabilising the cellular DNA damage response and thus promoting viral replication (Stracker, Carson et al. 2002). Since the other MRN complex components, Rad50 and NBS1, become destabilised in the absence of Mre11, targeting Mre11 for degradation essentially targets the entire complex (Stewart, Maser et al. 1999, Zhong, Bryson et al. 2005). As previously discussed, the MRN complex recognises DSBs and activates ATM, initiating the DDR (Lee and Paull 2005). Targeting this complex, therefore, prevents the activation of the DDR and thus is essential for viral replication.

Other DNA damage proteins known to be degraded during adenovirus infection include DNA ligase IV, BLM and TOPBP1. The NHEJ DSB repair pathway component DNA ligase IV was shown to be a target for proteasome-mediated degradation by Ad5 (Baker, Rohleder et al. 2007). The degradation of DNA ligase IV prevents viral concatermisation and is therefore also beneficial for viral replication. Interestingly, group B, D and E adenoviruses only appear to degrade DNA ligase IV but not p53, Mre11 or TOPBP1, the reason for this is unclear (Forrester, Sedgwick et al. 2011). BLM is a DDR component that is known to have DNA-end processing activity. BLM is degraded in a E1B55K/E4orf6/Cullin 5-dependent manner during Ad5 infection, although the precise function of the degradation of this protein during adenovirus infection is unclear (Orazio, Naeger et al. 2011). It is known that

BLM is not required for viral concatemer formation (Orazio, Naeger et al. 2011). The DDR protein TOPBP1 was also shown to be degraded during Ad12 infection (Blackford, Patel et al. 2010). TOPBP1 is responsible for the activation of ATR and therefore adds another layer of complexity to the inhibition of the DDR during adenovirus infection. Interestingly, TOPBP1 is degraded exclusively by Ad12 in an E4orf6-dependent, E1B55K-independent manner, suggesting that E4orf6 can in fact act as a substrate recognition unit as well as a cellular linker protein (Blackford, Patel et al. 2010). Quite why it is necessary for the group A adenoviruses (which includes Ad12) but not the group C viruses (Ad5) to degrade TOPBP1 is unknown at present.

Most recently, adenovirus has been shown to degrade the lysine acetyltransferase Tip60 in an E1B55K, E4orf6 and proteasome-dependent manner. Tip60 has been implicated in the DNA damage response through its activation of the ATM and ATR kinases. In addition it is also able to inhibit the DDR through promoting the dephosphorylation of H2AX. It has been shown that Tip60 is able to bind directly to the immediate early promoter of the adenovirus E1A gene, thus inhibiting its expression. It is, therefore, important that Tip60 is degraded during adenovirus infection in order to evade the inhibition of E1A gene expression (Gupta, Jha et al. 2013).

Adenovirus 5 has also been shown to degrade proteins not involved in the DDR including the cell surface receptor integrin α3 (Dallaire, Blanchette et al. 2009). This degradation is E1B55K/E4orf6/Cul5 dependent (Dallaire, Blanchette et al. 2009). The function of integrin α3 during adenovirus infection is as an alternative Ad receptor, making this protein a target for proteasome-mediated degradation in order to prevent re-infection (Salone, Martina et al. 2003, Dallaire, Blanchette et al. 2009).

The death domain-associated protein (Daxx) is another target during adenovirus infection. Daxx is thought to be involved in the regulation of a number of functions including apoptosis and transcription. Daxx is degraded during Ad5 infection in an E1B55K-dependent, E4orf6-independent manner (Schreiner, Wimmer et al. 2011). Further studies from this group showed that X-linked α-thalassaemia retardation syndrome protein (ATRX), which has been previously shown to form a complex with Daxx and to be involved in chromatin remodelling, is also degraded during Ad5 infection (Xue, Gibbons et al. 2003, Schreiner, Burck et al. 2013).

It has also been suggested that adenoviruses can inhibit the DDR independently of protein degradation. Both Ad5 E4orf3 and E4orf6 proteins have been shown to interact with DNA-PK resulting in a reduction in the levels of DNA-PK autophosphorylation during double-strand break repair (Boyer, Rohleder et al. 1999, Hart, Yannone et al. 2005). Intriguingly, Ad5 E4orf6 has also been shown to enhance the DDR through the inhibition of PP2A, leading to phosphorylation of H2AX, activation of PARP and apoptosis (Hart, Ornelles et al. 2007).

1.3.3 Relocalisation of Cellular Proteins during Adenovirus Infection

In addition to inhibiting the cellular DDR through the proteasome-mediated degradation of key DDR proteins, adenovirus is also able to interfere with the DDR by affecting the localisation of various DDR proteins. During adenovirus infection, a number of DDR proteins are localised to VRCs including RPA32, ATR, ATRIP, TOPBP1, Rad17 and Rad9 (Stracker, Lee et al. 2005, Blackford, Bruton et al. 2008, Carson, Orazio et al. 2009). Although the role for adenoviral-mediated relocalisation to VRCs is currently unknown, it has been suggested that the relocalisation inhibits the function of the DDR proteins, therefore circumventing the activation of the DDR and promoting viral DNA replication. Alternatively it

is possible that these proteins may be required to play a transient role in the replication of viral DNA (Stracker, Lee et al. 2005, Blackford, Bruton et al. 2008, Carson, Orazio et al. 2009).

As well as relocalisation to VRCs, adenovirus infection can also induce the relocalisation of DDR proteins into nuclear track structures which derive from PML bodies (Puvion-Dutilleul, Chelbi-Alix et al. 1995, Everett 2001). As previously discussed (see Section 1.1.6), E4orf3 is responsible for the rapid reorganisation of PML bodies into PML nuclear tracks, where it is known to relocalise p53 and PML to these sites (Carvalho, Seeler et al. 1995, Konig, Roth et al. 1999). The function of this relocalisation is largely unknown, although it is thought that E4orf3-mediated p53 relocalisation induces H3K9me3 heterochromatin formation at p53 target promoter regions, silencing p53 target genes (Soria, Estermann et al. 2010). A number of other proteins, which associate with PML bodies, are degraded during adenovirus infection and this is distinct from PML reorganisation. Examples include the MRN complex which is relocalised to PML nuclear tracks following IR exposure, and this is thought to inhibit the activation of ATR and ultimately promote the degradation of the MRN complex (see Section 1.3.2)(Evans and Hearing 2005). Another example is Daxx, where its E4orf3-mediated association with PML nuclear tracks is thought to inhibit its repression of transcriptional activity (Li, Leo et al. 2000).

During adenovirus infection, DDR proteins can also be relocalised to aggresomes. Ordinarily, misfolded proteins are transported along microtubules to microtubule-organising centres, by the motor protein dynein, where they are sequestered into these large cytoplasmic bodies known as aggresomes. The proteins within these structures are then usually targeted for degradation. During Ad5 infection, a large number of aggresomes are formed where the adenoviral proteins E1B55K, E4orf3, E4orf6, Cul5 and the MRN complex

have been shown to localise (Zantema, Fransen et al. 1985, Araujo, Stracker et al. 2005). It is thought that the MRN complex is initially localised to nuclear tracks and then subsequently relocalised to aggresomes together with adenoviral proteins where Mre11 is subsequently degraded (Liu, Shevchenko et al. 2005). p53 has also been shown to be relocalised to aggresomes in an E4orf3 dependent manner, suggesting that adenovirus is able to exploit the cellular aggresome system in order to induce degradation of DDR proteins that would otherwise be detrimental for viral DNA replication (Liu, Shevchenko et al. 2005). Interestingly, not all E1B55K proteins from various adenovirus serotypes localises to aggresomes, suggesting that the relocalisation of E1B55K to these structures is not necessary for degradation of target proteins (Blanchette, Wimmer et al. 2013). In the case of Ad4 and Ad12 infection, the MRN complex is not relocalised into PML nuclear tracks by E4orf3 and is instead relocalised to VRCs (Stracker, Lee et al. 2005, Carson, Orazio et al. 2009). This could prove detrimental for viral DNA replication since the localisation of the MRN complex to VRCs could initiate a DDR. In order to circumvent this, Ad4 and Ad12 viruses have evolved to also degrade TOPBP1, in order to inhibit ATR signalling at these regions and therefore prevent the activation of the DDR (Blackford, Patel et al. 2010).

1.4 THE CCR4-NOT COMPLEX

The chemokine (C-C motif) receptor 4 -NOT (CCR4-NOT) complex is a large, highly conserved, multi-subunit complex with a number of cellular functions, mainly in the control of gene expression. The CCR4-NOT complex has been implicated in mRNA regulation,

Yeast Protein Name	Human Orthologue	Function
NOT1	CNOT1	Scaffold
NOT2	CNOT2	Unknown
NOT3/NOT5	CNOT3	Unknown
NOT4	CNOT4	E3 ligase activity
CCR4	CNOT6	Deadenylase
	CNOT6L	Deadenylase
CAF1	CNOT7	Deadenylase
	CNOT8	Deadenylase
RCD1/CAF40	CNOT9 (RQCD1)	Unknown
Unknown	CNOT10	Unknown
Unknown	CNOT11 (C2orf29)	Unknown
CAF130	Unknown	Unknown

Table 1.2: Classification of Human CNOT Subunits. The yeast subunits of the CCR4-NOT complex are indicated, together with the human CNOT complex orthologues. If known, the function of each subunit is also shown.

transcription elongation, chromatin modifications and DNA repair. The majority of studies on the CCR4-NOT complex have been performed in yeast (both *S. cerevisiae* and *S. pombe*),where the complex comprises 9 core subunits: CCR4, CAF1, CAF40, CAF130 and NOT1-5. Whilst much less is known about the human CCR4-NOT complex, the orthologues CCR4-NOT transcription complex (CNOT1-CNOT10) have been identified in human cells. Table 1.2 represents yeast CCR4-NOT complex components along with their human orthologues.

Two major enzymatic functions of the CCR4-NOT complex have been identified in yeast and mammals, deadenylation and ubiquitination. The ubiquitination activity of the CCR4-NOT complex is performed by the NOT4 component of the complex, which has been shown to have E3 ubiquitin ligase activity (Albert, Hanzawa et al. 2002). In *S. cerevisiae*, NOT4 has been shown to stably interact with the CCR4-NOT complex; interestingly, however, in human cells, the NOT4 (hCNOT4) protein has been shown to exist in a protein complex distinct from the CCR4-NOT complex (Lau, Kolkman et al. 2009, Panasenko and Collart 2011). The deadenylase activity of the CCR4-NOT complex is achieved through the CCR4 subunit in *S. cerevisiae*, which has 3' exoribonuclease activity that targets poly(A) substrates (Chen, Chiang et al. 2002). The *S. cerevisiae* CCR4-NOT protein Caf1 is the linker protein between CCR4 and the core complex components (Tucker, Staples et al. 2002). It has also been shown to have 3'-5' exonuclease activity in vitro (Daugeron, Mauxion et al. 2001). The CCR4 and CAF1 human orthologs CNOT6/CNOT6L and CNOT7/CNOT8 respectively, are responsible for deadenylase activities of the CNOT complex in human cells.

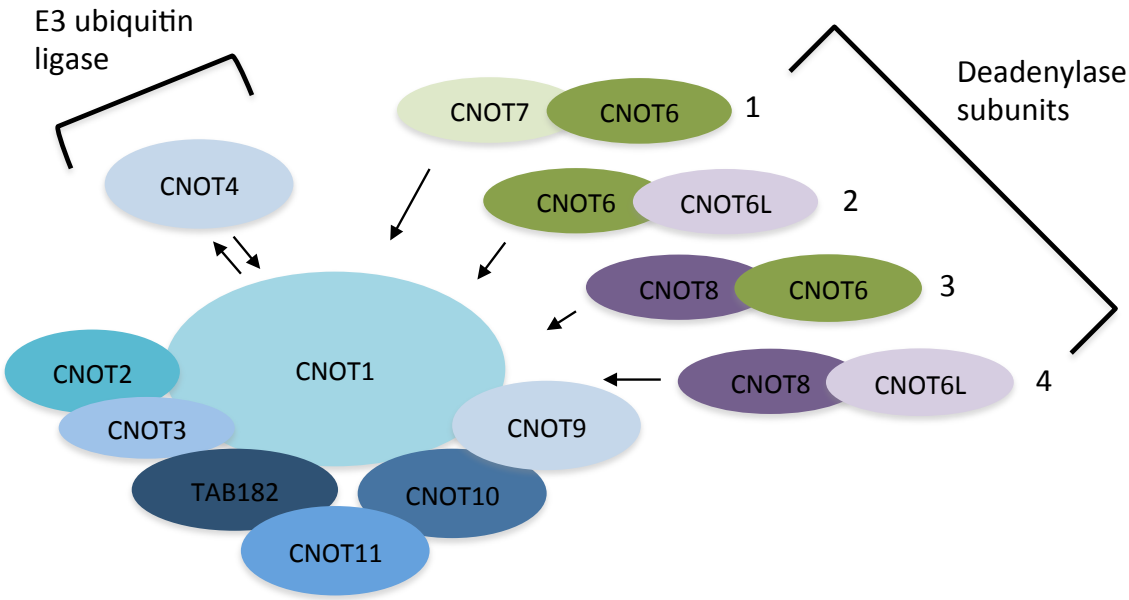

Figure 1.15: The Human CNOT Complex. The human CNOT complex comprises of the core subunits CNOT1, CNOT2, CNOT3, CNOT9, CNOT10, CNOT11 and TAB182. CNOT4, the E3 ubiquitin ligase component of the CNOT complex, transiently associates with the complex. Four deadenylase complexes also transiently associate with the complex, these are known to be CNOT7/CNOT6, CNOT6/CNOT6L, CNOT8/CNOT6 and CNOT8/CNOT6L.

The human CNOT complex exists in a number of different conformations which are dependent on the associated deadenylase. The CNOT complex comprises the core proteins CNOT1, CNOT2, CNOT3, CNOT9, CNOT10, CNOT11 and TAB182. The deadenylases CNOT6, CNOT6L, CNOT7 and CNOT8 transiently associate with the core complex. Interestingly, studies by Lau and colleagues found that the deadenylases CNOT7 and CNOT8 do not associate with each other, suggesting that these proteins form distinct CNOT complexes. Furthermore, the deadenylases CNOT6 and CNOT6L were found to stably interact with CNOT7 but not CNOT8, and deadenylases CNOT6 and CNOT6L do not interact with each other, suggesting that these deadenylases are mutually exclusive. Finally, this group showed that the ubiquitin ligase component of the CNOT complex, CNOT4, does not stably interact with the complex, but instead associates transiently, suggesting that the association of CNOT4 with the complex is a regulated event (Figure 1.15)(Lau, Kolkman et al. 2009).

1.4.1 The CCR4-NOT Complex and the DNA Damage Response

A number of studies have implicated the CCR4-NOT complex in the DDR in both *S. cerevisiae* and *S. pombe*. In the vast majority of these studies, sensitivity assays were performed using yeast strains that were mutant for various components of the CCR4-NOT complex. CCR4 (hCNOT6/hCNOT6L) was shown to be sensitive to IR, UV-C, HU, 4-nitroquinoline 1-oxide (4-NQO) and camptothecin in both *S. cerevisiae* and *S. pombe* (Bennett, Lewis et al. 2001, Westmoreland, Marks et al. 2004, Mulder, Winkler et al. 2005, Traven, Hammet et al. 2005, Woolstencroft, Beilharz et al. 2006, Deshpande, Hayles et al. 2009). Caf1 (hCNOT7/hCNOT8) was shown to be sensitive to IR, HU, 4-NQO, camptothecin and MMS in both *S. cerevisiae* and *S. pombe* (Mulder, Winkler et al. 2005, Woolstencroft,

Beilharz et al. 2006, Deshpande, Hayles et al. 2009). NOT1, NOT2, NOT3, NOT4 and NOT5 mutant *S. cerevisiae* strains have been shown to be sensitive to HU (Mulder, Winkler et al. 2005). Together these data suggest that the CCR4-NOT complex is involved in the response to a number of forms of DNA damage and/or replication stress. The mechanism for sensitivity to various DNA damaging agents in CCR4-NOT complex mutant strains is currently unclear and in some cases conflicting. There have been reports that the deadenylase activity of the CCR4-NOT complex is responsible for the sensitivity to DNA damaging agents in *S. cerevisiae* (Traven, Hammet et al. 2005, Woolstencroft, Beilharz et al. 2006). Some groups have reported that defective RNR accumulation is responsible for DNA damage sensitivity in CCR4-NOT complex *S. cerevisiae* and *S. pombe* mutant strains, whilst one group suggest that defective RNR accumulation does not contribute to DNA damage sensitivity observed in CCR4-NOT *S. cerevisiae* mutant strains (Mulder, Winkler et al. 2005, Traven, Hammet et al. 2005, Takahashi, Kontani et al. 2007).

To date, little is known about the CNOT complex and the DDR in mammalian cells. To our knowledge, only one publication exists by Morita and colleagues to suggest a role for CNOT6L in the DDR. This group showed that depletion of CNOT6L inhibited cell cycle progression from G1 to S phase, combined with a reduced expression of Cyclin D1 and Cyclin A. These phenotypes were later attributed to CNOT6L being responsible for deadenylation of p27KIP1 mRNA (Morita, Suzuki et al. 2007).

1.5 TAB182

Tankyrase 1 binding protein 1 of 182 KDa (TAB182), or TNKS1BP1, was first identified in 2002 when it was found to interact with the telomeric poly(ADP-ribose) polymerase Tankyrase 1. In this study, a number of assays were performed to elucidate the function of TAB182 and its interaction with Tankyrase 1. Subcellular fractionation of TAB182 showed that it was located in both the nucleus and the cytoplasm, the nuclear and cytoplasmic cellular localisation of TAB182 was further validated by the transfection of labelled TAB182 protein and endogenous TAB182 targeting antibodies. Through immunofluorescence analysis of a synchronised cell population, TAB182 was found to associate with mitotic chromosomes (Seimiya and Smith 2002). The TAB182 protein is known to have a tankyrase binding domain (TBD) and two nuclear localisation signals (NLS) at the C-terminus of the protein (Figure 1.16). One study also identified TAB182 as a subunit of the CNOT complex, although its role in this complex is unclear at present (Lau, Kolkman et al. 2009). According to the literature, a function for TAB182 is yet to be identified.

1.5.1 TAB182 and the DNA Damage Response

TAB182 was first implicated in the DDR following its discovery in a mass spectrometry screen used to identify novel ATM/ATR substrates following exposure to IR (Matsuoka, Ballif et al. 2007). To date, no other studies have suggested a role for TAB182 in the DDR.

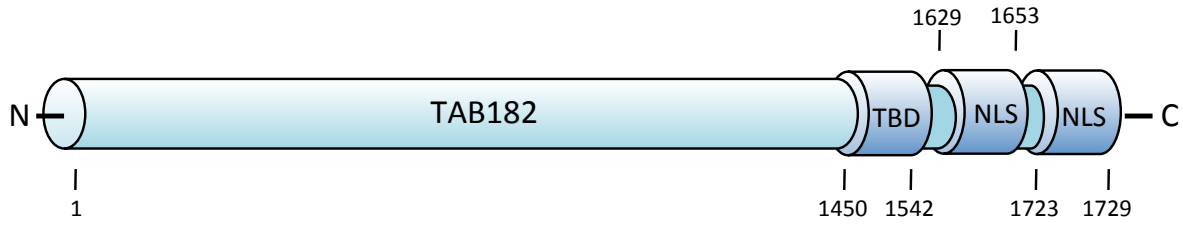

Figure 1.16: Schematic of TAB182 Protein. Schematic of the full-length TAB182 protein. Showing amino acid numbers, tankyrase binding domain (TBD) and the two nuclear localisation signals (NLS) it contains.

1.6 AIMS

Previous work in our laboratory has shown TAB182 to be degraded following Ad5 infection. Since more than 80% of adenoviral targets are known to be DDR proteins, this lead to the speculation that TAB182 may also be involved in the DDR. Furthermore, TAB182 was identified in a mass spectrometry screen as a potential substrate of ATM/ATR, further implicating a role in the DDR (Matsuoka, Ballif et al. 2007). Therefore the aims of this study were as follows:

1. To confirm the degradation of TAB182 during adenovirus infection and investigate the mechanism by which this occurs.
2. To investigate a role for TAB182 in the DDR and replication stress pathways.
3. To identify TAB182 interacting proteins in order to further elucidate the function of TAB182.

CHAPTER TWO

MATERIALS AND METHODS

2. MATERIALS AND METHODS

2.1 TISSURE CULTURE TECHNIQUES

2.1.1 Human Cell Lines

The cell lines used in this study are summarised in Table 2.1. HeLa cells were used for the majority of the experiments throughout this study. HeLa cells respond to adenovirus infection in a manner similar to other human tumour cell lines, such as A549 and U2OS. They have low levels of p53 due to the presence of HPV E6, which facilitates p53 degradation. However, the p53 gene in these cells is wild-type and expression of the protein is induced by adenovirus E1A during viral infection as has been reported for other human cell lines (Grand, Grant et al. 1994).

2.1.2 Tissue Culture Media

Unless otherwise stated, all cell lines were cultured in Dulbecco's modified Eagle's medium (DMEM) (Invitrogen) supplemented with 2mM L-glutamine and 10% foetal calf serum (FCS) (both Invitrogen). When necessary, media was supplemented with 3,000 mg of streptomycin and 30,000 units of penicillin. All media was stored at 4°C for up to 3 months.

2.1.3 Maintenance of Human Cell Lines

All cell lines were passaged by removing existing media, washing twice in phosphate buffered saline (PBS) and incubating with 0.05% trypsin (Invitrogen) at 37°C for a maximum of 5 minutes. Detachment was confirmed by microscopy and any remaining adherent cells were removed by gentle tapping. Following detachment, cells were collected in fresh culture

Cell line	ATCC number	Information
HeLa	CCL-2.2	Human cervical adenoma cell line expressing human papillomavirus 18 (HPV-18) transforming genes
Cullin2- H1299	N/A	Human non-small cell lung carcinoma cell line with inducible knockdown of Cul2 expression in the presence of 1µg/ml puromycin
Cullin5- H1299	N/A	Human non-small cell lung carcinoma cell line with inducible knockdown of Cul5 expression in the presence of 1µg/ml puromycin and 500µg/ml hygromycin B

Table 2.1: Human Cell Lines used throughout this Study. The human cell lines used throughout the duration of this study are indicated, along with American type culture collection (ATCC) numbers and any additional information.

medium heated to 37°C and replated at the desired confluency. All cell lines were passaged in sterile flow hoods and stored in humidified incubators at 37°C supplied with 5% CO_2.

2.1.4 Cryopreservation of Cell Lines

Cell lines were trypsinised as above and pelleted by centrifugation at 1400rpm for 5 minutes. Cell pellets were resuspended in 10% dimethyl sulphoxide (DMSO) (Sigma-Aldrich) with DMEM supplemented with 10% FCS. Resuspended cells were transferred to cryovials and gradually cooled to -80°C in isopropanol overnight. Cells were transferred to liquid nitrogen tanks for long-term storage at -180°C. When required, cells were rapidly thawed at 37°C . Cells were pelleted by centrifugation at 1400rpm for 5 minutes, resuspended in fresh culture media and replated.

2.2 CELL BIOLOGY TECHNIQUES

2.2.1 Viruses

All viruses used in this study are listed in Table 2.2

2.2.2 Viral Infections

Cells were grown to 80% confluency prior to adenoviral infections. Cells, grown in 6cm dishes, were infected with the appropriate virus in DMEM (no FCS) at a multiplicity of infection (MOI) of 5 plaque forming units (pfu) per cell. Dishes were incubated at 37°C for 2 hours, agitating every 15 minutes to ensure the efficient distribution of media over the dish. Following incubation, virus-containing media was removed and replaced with DMEM supplemented with 10% FCS. Virus-infected cells were incubated at 37°C until required.

Name	Information	Source
Ad5	Adenovirus serotype 5	Professor J. S. Mymryk
Ad12	Adenovirus serotype 12	Professor J. S. Mymryk
Ad5*dl*1520	Ad5E1B55K$^-$ mutant	Baker and Berk, 1987
Ad12*dl*620	Ad12E1B$^-$ mutant	Byrd et al., 1987
Ad5*dl*155	Ad5E4- mutant	Professor Thomas Dobner
H5*pm*4155	Ad5E4orf3$^-$Ad5E4orf6$^-$ mutant	Professor Thomas Dobner
H5*in*351	Ad5E4orf1$^-$ mutant	Professor Thomas Dobner
H5*pm*4166	Ad5E4orf4$^-$ mutant	Professor Thomas Dobner
H5*dl*356	Ad5E4orf7$^-$ mutant	Professor Thomas Dobner
H5*in*352	Ad5E4orf2$^-$ mutant	Professor Thomas Dobner
H5*pm*4154	Ad5E4orf6$^-$ mutant	Professor Thomas Dobner
H5*dl*150	Ad5E4orf3$^-$ mutant	Professor Thomas Dobner

Table 2.2: Adenovirus Serotypes and Mutant Viruses used in this Study. The adenovirus serotypes and mutant viruses used throughout this study and their sources are indicated.

2.2.3 Transfection of Cell Lines with siRNA

24 hours prior to transfection, cells were plated into 6cm dishes at 30-40% confluency in DMEM supplemented with 10% FCS. The following day, a siRNA transfection mix was prepared as follows. Per transfection, 1ml of Opti-MEM (Invitrogen) was added to 10µl of oligofectamine (Invitrogen) and 1.8µl siRNA (50µM stock). The transfection mix was incubated at room temperature for 30 minutes. During the incubation, media was removed from cells plated the day previous, washed once in Opti-MEM and 1ml of Opti-MEM added to each dish. Following the 30 minute incubation, the transfection mix was added to each dish and incubated at 37°C for 16 to 18 hours. The Opti-MEM transfection mix was then removed and replaced with DMEM supplemented with 10% FCS. Cells were incubated at 37°C until required. A list of all the siRNAs used in this study is outlined in Table 2.3.

2.2.4 Transient DNA Transfections

HeLa cells were transfected with plasmids containing the adenovirus genes as follows: pXC15-*Ad5E1B55K*, pCMV-*Ad5E4orf6*, pcDNA3*Ad12E1B54K*, and pcDNA3*Ad12E4orf6* (all E4orf6 constructs were HA tagged). GFP-*TAB182*, HA-*CNOT6* and HA-*CNOT6L* plasmids were also used to transfect HeLa cells during this study. 24 hours prior to transfection, cells were plated at 80-90% confluency into 6-well plates supplemented with 10% FCS in DMEM. The following day, 150µl of Opti-MEM was added to 2.5µg of DNA in a 1.5ml eppendorf tube (per reaction). In another eppendorf tube, 150µl of Opti-MEM was added to 7.5µl of Lipofectamine 2000 (Invitrogen) (per reaction). The contents of both eppendorf tubes were mixed together and left to incubate for 30 minutes at room temperature. The Opti-MEM/DNA/Lipofectamine-2000 mix was added to cells plated in

Target	siRNA	Sense sequence	Supplier
Non-silencing control	Custom	CGUACGCGGAAUACUUCGAdTdT	Dharmacon
CNOT4	SMARTpool	CCAAUUCUCUCAAUAGUAC UAACAGAGUCACAGUCGUU CGUCUUUGUUGUAGGUUUA GGUAGUAGAUGGCAGAACA	Dharmacon
CNOT6	SMARTpool	GAAAGAACGUGGCUAUAAU GAGCACAGGUGGAGUAGAA GGGCAGAGCUUGAAAUAAG GCUAUAAUGUUCUUUGUGA	Dharmacon
CNOT6L	SMARTpool	UGACAGCGCUGCACCUAAA CCAAUUACACCUUUGAUUU GAGCAGGUAUGAAGCCUAU GGUAUUAGAGGUCCACAAA	Dharmacon
TAB182	SMARTpool	GAGUUUGGGAAGAGCGCUU AGGACCAGGAAUUCGGAAA CAGAAGCUUUGGAACGAGA CACCAAGGCCUGCGGUUGA	Dharmacon

Table 2.3: siRNAs used during this Study. The siRNAs used to knockdown the expression of various genes in this study are shown. The target protein, siRNA type, sense sequence and source are indicated.

media the day previous and incubated at 37°C for 6-7 hours. Cells were then washed once in PBS and supplemented with DMEM with 10% FCS and incubated at 37°C until required.

2.2.5 UV-C and IR Irradiation of Cells

HeLa cells were mock-irradiated or irradiated with ionising γ-rays using a ^{137}C source delivering approximately 1 Gy/20 seconds. Prior to UV-C irradiation, HeLa cells were washed twice with PBS and any residual PBS removed. Cells were mock-irradiated or irradiated with the required dose of UV-C irradiation from a 254nm UV-C light source. Following irradiation, DMEM supplemented with 10% FCS was added. Following both UV-C and IR irradiation, cells were left in a 37°C incubator to recover until harvested.

2.2.6 Drug Treatments of Cell Lines

0.5µM of Bortezomib (LC Laboratories) was added to HeLa cells 24 hours prior to each harvesting point. 4µM of MLN4924 (Active Biochem Labs) was added to HeLa cells immediately after infecting with adenovirus and left throughout the duration of the infection. HU (Sigma-Aldrich) was dissolved at the required concentration in DMEM and added at different time-points prior to harvesting depending on the experiment. 5µM of the ATR inhibitor (VE-821 Selleck)(in DMSO) was added 2 hours prior to labelling DNA fibres. 1µM of the Chk1 inhibitor (Go6976 Calbiochem)(in DMSO) was added 2 hours prior to labelling DNA fibres. 25µM of the CDK inhibitor (Cdk1/2i III Merck)(in DMSO) was added 2 hours prior to labelling DNA fibres.

2.2.7 Flow Cytometry

Following treatment with the indicated damaging agent, cells were harvested at the indicated time points as follows. Media was removed and added to a 50ml Falcon tube, cells were washed in PBS, and the PBS also added to the falcon tube (keeping all media and washes ensures no mitotic cells are lost). Cells were trypsinised as previously described and the harvested cells also added to the Falcon tube. All cells were pelleted by centrifugation at 1400rpm for 5 minutes. Cells were resuspended in PBS and pelleted by centrifugation at 1400rpm for a further 5 minutes. Cells were resuspended in 3mls ice-cold PBS, followed by the addition of 7mls of ice-cold 100% ethanol drop-wise whilst vortexing (preventing cells from clumping). Cells were stored at -20°C for at least 1 hour or up to 2 weeks.

To process cells for propidium iodide (PI) staining, cells were washed 3 times in ice-cold PBS and the cells pelleted by centrifugation at 1600rpm for 5 minutes between each wash. Cells were incubated in 10mls of ice-cold 0.25% Triton-X100 (Sigma-Aldrich) in PBS for 15 minutes at 4°C. Cells were washed in 10mls of ice-cold PBS and pelleted by centrifugation at 1600rpm for 5 minutes. Cells were incubated in 1µg/ml PI (Sigma-Aldrich) together with 0.1mg/ml RNase A (Sigma-Aldrich) in PBS for at least 30 minutes. Flow cytometry was performed on a BD Accuri C6 flow cytometer and analysed using BD C Flow Plus software.

2.2.8 DNA Fibre Labelling

24 hours prior to labelling, HeLa cells were plated in a 6 well plate at 30-40% confluency. Cells were pulse-labelled with 25µM 5-Chloro-2'-deoxyuridine (CldU) (Sigma-Aldrich) for 20 minutes at 37°C. Cells were washed 3 times in PBS to remove any remaining CldU. Cells were then treated with 2mM HU for 2 hours at 37°C and washed 3 times in PBS

to remove any remaining HU. Cells were pulse-labelled with 250µM 5-Iodo-2'-deoxyuridine (IdU) (Sigma-Aldrich) for 45 minutes at 37°C. IdU was removed and cells washed 2 times in ice-cold PBS. Cells were trypsinised as above and resuspended in ice-cold PBS to a concentration of 50 x 10^4 cells/ml. 2µl of cells resuspended in PBS were spotted onto glass slides and left for 4 minutes, and subsequently lysed in 7µl of spreading buffer (200mM Tris HCl pH 7.4, 50mM EDTA, 0.5% SDS) for 2 minutes. Glass slides were tilted to allow DNA to spread down the slide, excess liquid was allowed to run off the slide, and left to air-dry for 2 minutes. Slides were fixed in methanol / acetone (3:1) for 10 minutes and air-dried for 5 to 10 minutes. Slides were stored at 4°C for up to 1 year.

2.2.9 Metaphase Spread Analysis

HeLa cells were treated with 0.1mg/mL colcemid (Sigma-Aldrich) approximately 2-4 hours before harvesting. Cells were then trypsinised and collected, along with all media and washes into Falcon tubes, and cells subsequently pelleted by centrifugation at 900rpm for 5 minutes. Cells were washed once in PBS and again pelleted by centrifugation. Following resuspension of cell pellets in 1-2ml PBS, 8-10mls of pre-warmed 0.03M sodium citrate was added drop-wise with gentle agitation. Cells were incubated at 37°C for 1 hour, transferred to a polypropylene tube and pelleted by centrifugation at 900rpm for 5 minutes. The supernatant was discarded and resuspended in 1-2mls PBS, followed by the addition of 6-8ml of 3:1 methanol: acetic acid drop-wise with gentle agitation. Cells were pelleted by centrifugation at 900rpm for 5 minutes. The resuspension of cells in 1-2mls of supernatant followed by the drop-wise addition of 3:1 methanol: acetic acid was repeated a further 2-3 times. At this stage it was possible to store the cells at -20°C for up to 2 weeks. To 'drop' the

cells onto slides, slides were immersed in acetic acid, blotted to remove any excess acetic acid, and using a pipette, two drops of fixed cells were dropped onto the slides. Slides were left to dry overnight. Slides were then stained in Giemsa diluted 1:20 with H_20 for 15 minutes, followed by a wash in H_20 for a further 3 minutes. The slides were allowed to dry overnight. Finally, mounting medium was added, along with a coverslip, and left for a minimum of 4 hours before viewing under the microscope.

2.3 PROTEIN BIOCHEMISTRY TECHNIQUES

2.3.1 Cell Lysate Preparation

Cells were harvested by removing media, washing once in warm PBS, and trypsinising as previously described. Cells were pelleted by centrifugation at 1400rpm for 5 minutes. Cell pellets were then washed in PBS and pelleted by centrifugation for a further 5 minutes. All PBS was removed from the cell pellets and the pellet resuspended in 80-200µl UTB lysis buffer (8M urea, 50mM Tris HCl, 150mM β-mercaptoethanol, pH 7.5). Cells were sonicated twice for 10 seconds and immediately placed on ice. Cell lysates were then centrifuged at 16000 rpm for 15 minutes to remove cell debris. Supernatants were transferred to a pre-chilled Eppendorf tube, snap-frozen in liquid nitrogen and stored at -80°C.

Cell lysate preparation for glutathione S-transferase (GST) pull-downs and co-immunoprecipitation assays was performed as follows. Cells were washed two times in ice-cold PBS, in the final PBS wash, cells were scraped off of the tissue culture dish using a cell scraper and pooled into 15ml Falcon tubes. Cells were pelleted by centrifugation at 2000 rpm at 4°C for 5 minutes. Cells were washed in ice-cold PBS a further two times, pelleting

the cells by centrifugation in between each wash. Cells were then lysed in 500-1000 µl NETN buffer (0.5% NP-40 (Sigma-Aldrich), 150mM NaCl (Sigma-Aldrich), 50mM Tris HCl pH 7.5, 0.5mM EDTA (Sigma-Aldrich)) depending on cell number. Cell lysates were homogenised using a Wheaton-Dounce homogeniser and centrifuged three times at 4°C, first at 3000 rpm for 5 minutes, followed by 13000 rpm for 15 minutes, and finally 45000 rpm for 30 minutes. The supernatant was retained in preparation for the GST pull-down or co-immunoprecipitation assays.

2.3.2 Protein Determination

Protein concentration of cell lysates were determined against a range of bovine serum albumin (BSA) (Sigma-Alrich) concentrations between 0-500ng/ml. 10µl of BSA standard was added in quadruplet to each well of a 96-well plate. Cell lysates were diluted 1:10 in water and also added in quadruplet to each well in a 96-well plate. Bradford reagent (Bio-Rad) was diluted 1:5 in water and 200µl of the diluted Bradford reagent was added to each well of both the BSA standards and cell lysates. Absorbance readings were measured using a micro-plate reader (Bio-Rad) at a wavelength of 595nm. Final protein concentrations were calculated against a BSA standard curve.

2.3.3 SDS-Polyacrylamide Gel Electrophoresis (SDS-PAGE)

For proteins over or under 50kDa molecular weight, 6% or 10% polyacrylamide gels were prepared respectively (Table 2.4). Gel apparatus (GE Healthcare) was constructed as per the manufacturer's instructions. Cell lysates were prepared for loading with the addition

of an equal volume of 2x Laemmli sample buffer (Bio-Rad), boiled for 5 minutes and centrifuged at 14,000 rpm for 1 minute. Typically 50µg of cell lysate was loaded onto each gel lane, along with molecular weight markers (GE healthcare) to determine protein size. Gels were run in buffer composed of 100mM Tris/Bicine and 1% SDS. Gels were run at 20mA from between 4 to 6 hours depending on protein size.

2.3.4 Visualisation of Proteins on Polyacrylamide Gels

Following the separation of proteins by SDS-PAGE, proteins were visualised using a Coomassie blue solution (0.1% Coomassie Brilliant Blue R-250 (Sigma-Aldrich), 40% methanol and 10% acetic acid). Gels were agitated in Coomassie blue solution for 10 minutes at room temperature. To destain, gels were agitated in destain (10% acetic acid and 20% methanol) overnight at room temperature.

2.3.5 Preparation of Proteins for Analysis by Mass Spectrometry

Samples were produced by co-immunoprecipitation or GST pull-down assay and the protocols followed until the point of the NETN washes (see Sections 2.3.6 and 2.4.3, respectively). Beads were denatured by incubating in 9M Urea/ 50mM ammonium bicarbonate at room temperature for 1 hour with agitation. Beads were pelleted by centrifugation at 3000 rpm at 4°C for 1 minute and supernatant transferred to a fresh eppendorf tube. A final concentration of 50mM dithiothreitol (DTT) was added to the supernatant and incubated at 56°C for 30 minutes. A final concentration of 100mM iodoacetamide was added and incubated at room temperature in the dark for 30 minutes.

	6%	10%
H_20	27.4ml	22ml
1M Tris/Bicine	4ml	4ml
30% Acrylamide	8ml	13.4ml
10% SDS	400µl	400µl
TEMED	80µl	80µl

Table 2.4: Polyacrylamide Gel Ingredients. Polyacrylamide gel ingredients used throughout this study are shown.

300µl of supernatant was added to FASP filters (Amicon, 30K cut off) and centrifuged at 14000 rpm for 15 minutes at room temperature. Flow-through was discarded and the remaining supernatant added to the FASP filter and centrifuged again at 14000 rpm for 15 minutes at room temperature. Filters were washed four times with 50mM ammonium bicarbonate, centrifuging at 14000 rpm for 15 minutes at room temperature between each wash, and discarding the flow-through each time. FASP filters were transferred to fresh collection tubes and mass spectrometry-grade trypsin (Promega), diluted in 50mM ammonium bicarbonate to a final volume of 300µl, added to the FASP filters (1µg per filter). FASP filters were left in an incubator at 37°C overnight. To collect tryptic peptides, FASP filters were centrifuged at 14000 rpm for 10 minutes at room temperature and the flow-through, containing the peptides, transferred to a fresh Eppendorf tube. FASP filters were washed in 300µl 50mM ammonium bicarbonate, centrifuged at 14000 rpm for 10 minutes at room temperature and the flow-through added to the previous flow-through. Peptides were dried in a vacuum centrifuge (Eppendorf) overnight. Peptides were resuspended in 40µl 1% acetonitrile/ 1% formic acid in sterile mass-spectrometry grade water (further details are given in Chapters 3 and 4).

2.3.6 GST Pull-Down Assay

In order to assess *in-vitro* protein-protein interactions, GST pull-down assays were performed. 10mg of cell lysate (as prepared in Section 2.3.1) was incubated with 25µg GST-fusion protein (see Table 2.5 for a list of GST-fusion proteins used in this study), rotating at 4°C for 3 hours. To isolate protein-protein complexes, 25µl of glutathione beads (Sigma-Aldrich) were then added and incubated for a further hour at 4°C. To capture protein-protein

complexes, glutathione beads were pelleted by centrifugation at 3000 rpm at 4°C for 1 minute, and the supernatant discarded. Glutathione beads were washed in NETN buffer, centrifuged at 3000 rpm at 4°C for 1 minute, this was repeated 4 times. Samples were then washed in Buffer B (2mM EDTA in PBS), centrifuged at 3000 rpm at 4°C for 1 minute, and taking care to remove all supernatant. To elute protein-protein complexes from the beads, 60µl of 25mM glutathione pH 8.2 (BDH Laboratories) was incubated with the samples for 1 hour at 4°C. Samples were centrifuged at 3000 rpm at 4°C for 1 minute and supernatant containing the protein-protein complexes was transferred into a fresh Eppendorf tube. A further 30µl of glutathione was added to the beads and incubated at 4°C for 30 minutes. The samples were centrifuged again at 3000 rpm at 4°C for 1 minute and supernatant pooled into the eppendorf tube. Samples were run on SDS-PAGE gels as follows. 25µl of Laemmli sample buffer was added to the supernatant and boiled for 5 minutes. Samples were centrifuged at 13000 rpm and loaded onto 6%/10% electrophoresis gels together with 50µg of cell lysate as a positive control, and resolved by SDS-PAGE.

2.3.7 Deadenylase Assays

The method is based on that described by Mittal and colleagues (Mittal, Aslam et al. 2011). Usually, whole cell lysates were immunoprecipitated as described in Section 2.3.1 and 2.4.3. After the final wash the immunoprecipitates were washed twice with deadenylation buffer (50mM Hepes-NaOH pH8.0, 0.15MNaCl, 2mMMgCl_2, 10%glycerol). The immunoprecipitated Protein G-agarose beads with the bound antibody-antigen complex were incubated in deadenylation buffer (25µl) with 2µl 5'fluoroscein-labelled substrate (Flc-5'-CCUUUCCAAAAAAA-3' final concentration 0.2µM, Sigma-Aldrich) at 37^{o} for 1 hour. After

GST-fusion protein	Incorporating	Source
GST	N/A	Phillip Gallimore
GST-TAB182C	Spanning the amino acids 824-864 fused to amino acids 1221-1729 of TAB182	Susan Smith

Table 2.5: GST-Fusion Proteins used in this Study. The GST-fusion proteins used in this study are indicated and the source.

that time 10µl of supernatant were mixed with 10µl RNA loading buffer (95% formamide, 0.025% SDS, 5mM EDTA, Blue-orange loading dye, Promega) and heated at 85^{o}C for 5 minutes. RNA was analysed by electrophoresis on a 20% acrylamide gel run in the presence of 8M urea and TBE. Fluoroscein-labelled ribonucleotide was visualised using a Fusion SL chemiluminescence imaging system (Vilber Lourmat, Marne-la-Vallée, France). On occasion the assay was carried out on whole cell lysates, solubilised in NETN buffer and clarified by high speed centrifugation.

2.4 IMMUNOCHEMISTRY TECHNIQUES

2.4.1 Antibodies

All the antibodies used in this study are listed in Table 2.6.

2.4.2 Western Blotting

Following separation of proteins by SDS-PAGE, proteins were transferred onto nitrocellulose membrane using the following method. The gel and nitrocellulose membrane (VWR Laboratories) were soaked in transfer buffer (20% methanol, 50mM Tris, 190mM glycine) and placed in between two pieces of 3MM filter paper (Whatman) and two pieces of sponge. This was then placed inside a plastic cassette and placed in a transfer tank filled with transfer buffer (all transfer apparatus was supplied by Hoeffer Scientific). Proteins were left to transfer at 200mA at room temperature for 16-18 hours overnight. Following the transfer, the nitrocellulose membrane was stained to visualise proteins with Ponceau S solution

Antigen	Antibody	Species	Application	Dilution	Source
53BP1	53BP1	Rabbit	IF/WB	1:1000	Novus
Ad5E1A	M73	Mouse	WB	1:500	Ed Harlow
Ad5E1B55K	2A6	Mouse	WB/IF	1:1000	Arnold Levine
Ad5E4ORF3	6A11	Mouse	WB	1:200	Thomas Dobner
Ad5E4ORF6	RSA1	Mouse	WB	1:200	Thomas Dobner
Ad12E1A	M13	Mouse	WB	1:20	In house
Ad12E1B55K	XPH9	Mouse	WB/IF	1:1000	In house
Ad5 Hexon	Ad5 Hexon	Rabbit	WB	1:1000	Vivien Mautner
Ad12 Knob	Ad12 Knob	Rabbit	WB	1:1000	Paul Freimuth
ATR	ATR	Goat	WB	1:1000	Santa Cruz
Aurora kinase	Aurora kinase	Mouse	WB	1:1000	Abcam
β-Actin	Actin	Mouse	WB	1:50000	Sigma-Aldrich
BLM	BLM	Rabbit	WB	1:1000	Bethyl
BubR1	BubR1	Mouse	WB	1:3000	Becton Dickinson
Chk1	Chk1	Mouse	WB	1:1000	Santa Cruz
pChk1 S317	pChk1 S317	Rabbit	WB	1:1000	Bethyl
pChk1 S345	pChk1 S345	Rabbit	WB	1:1000	Cell Signalling
Chk2	Chk2	Rabbit	WB	1:1000	Steve Elledge
Claspin	Claspin	Rabbit	WB	1:1000	Bethyl
CldU	BrdU	Rat	DNA fibres	1:750	AbD SeroTec
CNOT3	CNOT3	Rabbit	WB	1:1000	GeneTex
CNOT4	CNOT4	Rabbit	WB	1:1000	GeneTex
CNOT7	CNOT7	Rabbit	WB	1:1000	GeneTex
CtIP	CtIP	Mouse	WB	1:1000	Baer Richard
Cullin 2	Cullin 2	Rabbit	WB	1:1000	Abcam
Cullin 5	Cullin 5	Rabbit	WB	1:500	Santa Cruz
Cyclin A	Cyclin A	Rabbit	WB/IF	1:500	Santa Cruz
Cyclin B	Cyclin B	Rabbit	WB	1:500	Santa Cruz
Cyclin E	Cyclin E	Rabbit	WB	1:500	Santa Cruz
DBP	DBP	Mouse	IF	1:100	Pieter van der Vliet
DNA-PK	DNA-PK	Rabbit	WB	1:1000	Abcam
H3	H3	Rabbit	WB	1:3000	Abcam

Table 2.6: Antibodies used throughout this Study. Table shows the antibodies used throughout this study together with antigen, species, application, dilution and source.

Antigen	Antibody	Species	Application	Dilution	Source
pHistone H3 Ser10	pHistone H3 Ser10	Rabbit	WB/FACS	1:100	Cell signalling
H2AX	H2AX	Rabbit	WB	1:1000	Millipore
γH2AX S139	γH2AX S139	Mouse	WB/IF	1:1000	Millipore
HA	HA 12CAS	Mouse	WB	1:1000	Sigma-Aldrich
hnRNPUL1	hnRNPUL1	Rabbit	WB	1:1000	In house
IdU	BrdU	Mouse	DNA fibres	1:500	Becton Dickinson
Ku80	Ku80	Mouse	WB	1:1000	GeneTex
MDC1	MDC1	Rabbit	WB	1:1000	In house
MDM2	2A10	Mouse	WB	1:200	Arnold Levine
Mre11	Mre11	Mouse	WB	1:1000	Genetex
NBS1	NBS1	Rabbit	WB	1:10000	Genetex
pNBS1 S343	pNBS1 S343	Rabbit	WB	1:1000	Abcam
p53	DO1	Mouse	WB	1:2000	David Lane
PCNA	PCNA	Mouse	WB	1:1000	Santa Cruz
Rad9	Rad9	Rabbit	WB	1:1000	Santa Cruz
Rad18	Rad18	Rabbit	WB	1:1000	Bethyl
Rad50	Rad50	Mouse	WB	1:1000	GeneTex
Rad51	Rad51	Rabbit	WB	1:1000	Santa Cruz
RNR1	RNR1	Rabbit	WB	1:1000	GeneTex
RNR2	RNR2	Rabbit	WB	1:1000	GeneTex
p53R2	p53R2	Rabbit	WB	1:1000	GeneTex
RPA	RPA	Mouse	WB/IF	1:1000	Calbiochem
p21	p21	Mouse	WB	1:500	Santa Cruz
pRPA S4/8	pRPA S4/8	Rabbit	WB	1:1000	Bethyl
Tab182	Tab182	Rabbit	WB	1:500	In house
Tankyrase 1	Tankyrase 1	Rabbit	WB	1:1000	GeneTex
TOPBP1	TOPBP1	Rabbit	WB	1:1000	Bethyl
Mouse IgG	Anti-mouse HRP	Goat	WB	1:2000	DAKO Laboratories
Rabbit IgG	Anti-rabbit HRP	Swine	WB	1:3000	DAKO Laboratories
Rabbit IgG	Alexa fluor® 488 anti-rabbit	Donkey	FACS	1:50	Invitrogen
Rabbit IgG	Alexa fluor® 546 anti-rabbit	Goat	IF	1:1000	Invitrogen
Mouse IgG	Alexa fluor® 488 anti-mouse	Goat	IF	1:1000	Invitrogen
Rat IgG	Alexa fluor® 488 anti-mouse	Goat	DNA fibres	1:500	Invitrogen
Mouse IgG	Alexa fluor® 488 anti-mouse	Goat	DNA fibres	1:500	Invitrogen

Table 2.6 Cont'd: Antibodies used throughout this Study. Table shows the antibodies used throughout this study together with antigen, species, application, dilution and source.

(Sigma-Aldrich) for 1 minute and washed with deionised water three times to remove excess Ponceau S stain. Following visualisation of proteins, stain was completely removed by incubating the nitrocellulose membrane in TBS-T (20mM Tris HCl, 150mM NaCl, 0.1% Tween pH 7.6) with gentle agitation. Nitrocellulose membranes were blocked against non-specific antibody binding by incubating the membranes in 5% milk powder (Marvel) in TBS-T for 30 minutes at room temperature, with agitation. Primary antibodies were diluted in 5% milk or 5% BSA at the required concentration (see Table 2.6), and incubated with nitrocellulose membranes overnight at 4°C with agitation. To remove excess primary antibodies, nitrocellulose membranes were washed with TBS-T three times for 10 minutes with agitation. Nitrocellulose membranes were then incubated with horseradish-peroxidase (HRP)-conjugated secondary antibodies (Dako) for 1 hour with agitation. To remove excess secondary antibodies, nitrocellulose membranes were washed three times with TBS-T for 10 minutes each time with agitation. Antigens were detected by incubation in enhanced chemoluminescence (ECL) (GE Healthcare) for 1 minute and visualised using autoradiography film (Kodak).

2.4.3 Co-Immunoprecipitation

To assess *in-vivo* protein-protein interactions, co-immunoprecipitation assays were performed as follows. 5mg of cell lysate (as prepared in Section 2.3.1) was incubated with 10µl of primary antibody at 4°C rotating overnight. Cell lysates were then centrifuged at 45000 rpm at 4°C for 10 minutes and the supernatant collected. To capture protein-protein complexes, 40µl of Protein-G agarose beads (Sigma-Aldrich) were added to the cell lysates and rotated at 4°C for 1 hour. Following incubation, the samples were centrifuged at 3000

rpm for 1 minute at 4°C and the supernatant discarded. The beads were then washed 4 times in NETN buffer, centrifuging at 3000 rpm for 1 minute at 4°C and discarding the supernatant between each wash. 50µl of Laemmli sample buffer was added to the beads and boiled for 5 minutes. The samples were centrifuged at 13000 rpm for 1 minute, loaded onto polyacrylamide gels and resolved by SDS-PAGE.

2.4.4 Immunofluorescence

Cells were plated onto poly-L-lysine coated coverslips and incubated at 37°C overnight. Cells were washed twice in ice-cold PBS and permeabilised by incubation in ice-cold pre-extraction buffer (10mM pipes pH 6.8, 300mM sucrose, 20mM NaCl, 3mM $MgCl_2$ and 0.5% Triton X-100) for 5 minutes. Cells were fixed in ice-cold 3.6% paraformaldehyde (PFA) in PBS for a further 10 minutes. Cover slips were washed three times in ice-cold PBS and incubated in 10% FCS in PBS for 1 hour at room temperature or overnight at 4°C. Primary antibodies were diluted to the required concentration (see Table 2.6) in 1% FCS/PBS and 100µl of diluted primary antibody was added to each coverslip and incubated at room temperature for 1 hour in a moistened chamber. Coverslips were washed three times in PBS to remove any residual primary antibody. Coverslips were incubated with secondary antibodies (Alexa-Fluor, Invitrogen) diluted to the required concentration in 2% FCS/PBS (see Table 2.6) for 1.5 hours at room temperature in a dark moistened chamber. The coverslips were then washed in PBS a further three times. Coverslips were mounted onto glass slides using Vectashield Mounting medium with 4', 6-diamidino-2-phenylindole (DAPI) (Vector Laboratories). Upon the addition of Vectashield, gentle pressure was applied to the coverslips to remove any excess, and the edges of the coverslips were sealed using nail

varnish. Glass slides were stored at 4°C in a light-proof box. Cells were viewed using a Nikon Eclipse E600 microscope using Velocity software.

2.4.5 Immunostaining of DNA Fibres

Slides were washed twice in H_20, rinsed once in 2.5M hydrochloric acid (HCl) and denatured in 2.5M HCl for 1 hour 15 minutes. Slides were rinsed twice in PBS, followed by two washes in blocking solution (1% bovine serum albumin (BSA), 0.01% Tween 20 in PBS). Slides were incubated in blocking solution for a further 30 minutes. Slides were incubated with rat anti-BrdU (AbD SeroTec) (which specifically cross-reacts with CldU) and mouse anti-BrdU (Becton Dickinson) (which specifically cross reacts with IdU) antibodies in blocking solution for 1 hour. Slides were washed 3 times in PBS and incubated in 5% PFA for 10 minutes to fix the antibodies. Slides were washed a further 3 times in PBS followed by 3 washes in blocking solution. Slides were incubated in anti-rat and anti-mouse secondary antibodies (Alexafluor) for 1.5 hours. Slides were washed twice in PBS, followed by three washes in blocking solution and twice more in PBS. Slides were mounted in mounting medium (Sigma-Aldrich) and stored at -20°C for up to one week. DNA fibres were viewed using a Nikon Eclipse E600 microscope and Velocity software.

2.4.6 Immunostaining of Cells for Flow Cytometry

Cells were harvested for analysis by flow cytometry as described in Section 2.2.7. To ensure complete removal of ethanol, cells were washed three times in ice-cold PBS, pelleting the cells by centrifugation at 1600rpm for 5 minutes between each wash. Cells were

incubated in 10mls ice-cold 0.25% Triton-X100 in PBS for 15 minutes at 4°C. Following the incubation, cells were pelleted by centrifugation at 1600rpm for 5 minutes. Cells were then washed in ice-cold 1% BSA in PBS and pelleted by centrifugation. Cells were then incubated with p-Histone H3 Ser10 antibody in 1% BSA for 1 hour at room temperature. Following the incubation, cells were washed twice in 1% BSA, pelleting the cells by centrifugation between each wash. Cells were then further incubated with alexa-488 anti-rabbit secondary antibody in 1% BSA for 30 minutes at room temperature in the dark. Following the incubation, cells were washed once in 1% BSA in PBS and pelleted by centrifugation at 1600rpm for 5 minutes. From this point the cells were stained according to the PI protocol outlined in Section 2.2.7. As before, flow cytometry was performed using a BD Accuri C6 flow cytometer and analysed using BD C Flow Plus software.

2.5 MOLECULAR BIOLOGY TECHNIQUES

2.5.1 Media and Antibiotics

Luria Broth (LB) (Sigma-Aldrich): was prepared at 25g per litre (pH 7.3-7.5) and autoclaved to sterilise prior to use.

LB-agar plates: 1.2% agar (Sigma-Aldrich) was added to LB prior to sterilisation. Following sterilisation, LB-agar was heated to melt, antibiotic added when sufficiently cooled, and poured into agar plates. LB-agar plates were stored at 4°C.

Antibiotics: Ampicillin (Sigma-Aldrich) was added to LB and LB agar plates at a concentration of 50μg/ml.

2.5.2 Transformation of Bacteria

Transformation of plasmids into Stbl2 competent cells (Thermo-Fisher Scientific) was achieved as follows. Stbl2 competent cells were thawed on ice, 20-50ng of DNA was added to 50µl of cells in a pre-chilled polypropylene tube. This was left on ice for 30 minutes, heat shocked at 42°C for 25 seconds, and immediately placed back on ice for 2 minutes. 450µl of SOC media (Invitrogen) was then added and left to incubate in an orbital shaker at 220rpm at 30°C for 1.5 hours. 20-50µl of the sample was spread onto LB-agar plates containing the appropriate antibiotic. LB-agar plates were incubated at 37°C overnight.

2.5.3 Small-Scale Preparation of DNA

Colonies were picked from LB-agar plates using a sterile pipette tip and used to inoculate 3mls of LB supplemented with the appropriate antibiotic in a shaking incubator at 37°C at 220rpm overnight. Overnight cultures were centrifuged to pellet bacteria at 12000 rpm for 1 minute. Small-scale preparation of DNA was performed using the Sigma GenElute^{TM} Plasmid Miniprep Kit as follows. Bacterial pellets were resuspended in 200µl of re-suspension buffer supplemented with RNAse A. 200µl of lysis buffer was added to the re-suspension to lyse the bacteria for no longer than 5 minutes. 300µl of neutralisation solution was added and bacterial debris pelleted by centrifugation at 13000 rpm for 10 minutes. Following centrifugation, the supernatant was added to a mini-prep binding column that had been prepared by the addition of 500µl of column preparation solution. Columns were spun at 13000 rpm for 1 minute to allow lysate to flow through. The columns were then washed with 750µl wash solution and centrifuged again at 13000 rpm for 1 minute. The columns

were transferred into a fresh collection tube, 100µl of elution solution added and centrifuged at 13000 rpm for 1 minute. DNA was stored at -20°C until required.

2.5.4 Large-Scale Preparation of DNA

Colonies were picked from LB-agar plates using a sterile pipette tip and used to inoculate 3mls of LB supplemented with the appropriate antibiotic in a shaking incubator at 37°C at 220rpm overnight. The total volume of this culture was used to inoculate 250mls of LB supplemented with the appropriate antibiotic in a shaking incubator at 37°C at 220rpm overnight. Overnight cultures were centrifuged to pellet bacteria at 12000 rpm for 1 minute. Large-scale preparation of DNA was performed using the Invitrogen PureLink^{TM} HiPure Plasmid Filter Purification Kit as follows. Bacterial pellets were resuspended in 20mls of resuspension buffer supplemented with RNAse A. The bacteria were lysed in 20mls of lysis buffer for no longer than 5 minutes. 10mls of precipitation buffer was added to the lysate to neutralise the reaction. The precipitated lysate was transferred to a maxi column that had been pre-prepared by the addition of 30mls of equilibration buffer, and allowed to drip through the column by gravity. Columns were washed with 50mls of wash buffer and allowed to run through the column by gravity. Columns were transferred into fresh collection tubes and 15mls of elution buffer was added to elute the DNA. The eluted DNA was split equally into two Falcon tubes and 5.2mls of isopropanol added to each tube. DNA was pelleted by centrifugation at 5000 rpm for 1 hour at 4°C. DNA pellets were resuspended in 5mls 70% ethanol (Fisher Scientific) and pelleted by centrifugation at 5000 rpm for 1 hour at 4°C. The supernatant was removed, DNA pellets were air-dried, resuspended in 200-500µl TE buffer (depending on DNA pellet size), and stored at -20°C until required.

2.5.5 DNA Concentration Quantification

DNA concentrations were measured using a Nanodrop 1000 spectrophotometer (Thermo-Fisher Scientific). DNA concentrations were measured in ng/µl and the $OD_{260nm/280nm}$ recorded.

2.5.6 Cloning

2.5.6.1 PCR of TAB182 Gene Sequence from cDNA

2µl of cDNA (originally generated from a lymphoblastoid cell line prepared from cells of a normal individual) (kindly donated by Dr Phil Byrd) was used to amplify the complete TAB182 cDNA using forward and reverse primers (shown in Table 2.7). The polymerase chain reaction (PCR) reaction was set up as follows: 10-20ng of cDNA, 0.5µM forward and reverse primers, 1.5 units of Q5 High-Fidelity DNA polymerase (New England Biolabs), 200mM dNTPs, 1 X Q5 reaction buffer in a 50µl reaction. A Veriti 96-well Thermal Cycler (Applied Biosystems) was used for the PCR reaction under the following conditions: an initial denaturation step of 98°C for 30 seconds was followed by 30 cycles of 98°C for 5 seconds, 62°C for 15 seconds, 72°C for 4 minutes. A final extension of 5 minutes at 72^{o}C followed the 30 cycles.

2.5.6.2 Agarose Gel Electrophoresis

The visualisation of PCR products was achieved by running the product on 0.8% agarose gels. 0.8g agarose (Sigma-Aldrich) and 1µg/ml ethidium bromide (total concentration) was added to 100mls of 1x TBE (20mM Na_2EDTA, 880mM Tris and 890mM

orthoboric acid) and heated until all agarose was dissolved. Once dissolved, the agarose mixture was poured into gel tanks and allowed to cool. Once cooled, gel tanks were flooded with 1x TBE buffer. 1µl of PCR product, together with 2µl of loading buffer (0.25% w/v bromophenol blue, 30% glycerol) and 7µl 0.25x TBE buffer was mixed and loaded onto the agarose gel along with DNA molecular weight marker (Roche). Agarose gels were run at 120V for 30 minutes to 1 hour depending on PCR product size. PCR products were visualised using a G:BOX (Syngene).

2.5.6.3 Restriction Digest and Ligation

Restriction digests were performed on plasmid DNA (pEGFP-C3) or on PCR products (full-length TAB182) with engineered restriction sites (Sal I). PCR products were digested for 2 hours at 37^{o}C in 80µl 1x CutSmart buffer (New England Biolabs) containing 20 units of High-Fidelity Sal I (Sal I-HF) restriction endonuclease (New England Biolabs). 5µg of pEGFP-C3 plasmid DNA was digested with 20 units of Sal I-HF in 100µl 1x CutSmart buffer and 10 units of calf intestinal phosphatase (New England Biolabs) to remove 5' phosphates from the ends of linear molecules generated. Ligation reactions were set up with 50ng Sal I-HF digested and phosphatased pEGFP-C3 DNA and 50ng of Sal I-HF digested TAB182 cDNA. Ligation reactions were performed in 12µl 1x ligation buffer containing 1µl (400 units) T4 DNA ligase (New England Biolabs). The ligation reaction was incubated at 16^{o}C overnight. 3µl of the ligation reaction was transformed into 50µl of high efficiency NEB 5-alpha competent *E.coli* bacteria (New England Biolabs). Tranformation reactions were plated on LB-agar plates containing 30µg/ml kanamycin and incubated overnight at 37^{o}C.

2.5.6.4 Screening of Colonies via Bacterial PCR

Colonies were picked and grown in LB as previously described. 1µl of the culture was incubated with 0.5µl Taq polymerase (Roche), 0.75µl of dNTPs (10mM), 1µl forward and reverse primers, 2.5µl 5x buffer $+Mg^{2+}$, into a final volume of 25µl. The reaction mix was subjected to the same conditions as before (Section 2.5.6.1). PCR products were run on agarose gels and assessed as previously described.

2.5.6.5 DNA Sequencing

The DNA sequence of the ligated product was determined to check whether the gene sequence had acquired any mutations during the cloning process. Sequencing primers were designed to sequence the entire length of the eGFPC3-TAB182 gene (Table 2.7). Plasmid DNA along with sequencing primers was sent to Source Bioscience for sequencing. DNA sequences were analysed using FinchTV software and NCBI BLAST.

Primer	Sequence
pEGFP-C3 Forward	5' CCTGAGCAAAGACCCCAACGAGAAG 3'
pEGFP-C3 Reverse	5' CCCCCTGAACCTGAAACATAAAATG 3'
TAB182 Forward 1	5' ATGAAAGTGTCTACTCTCAGG 3'
TAB182 Forward 2	5' TTTGACACCCCCAGCTCGAT 3'
TAB182 Forward 3	5' TTCAACGGGGACCTGGCTAA 3'
TAB182 Forward 4	5' TCTTGGAGCCCCATAGCCTG 3'
TAB182 Forward 5	5' AGCAGGGAAGAAGGAGTGTCT 3'
TAB182 Forward 6	5' TGTGTTCTCTTTGCTGATGC 3'
TAB182 Forward 7	5' TGCTTCTCAGGACTATGGCCTT 3'
TAB182 Forward 8	5' ATTTGGGGAAGAGGGACCAC 3'
TAB182 Forward 9	5' AGTGATGCTAGCCAGGAGGT 3'
TAB182 Forward 10	5' CTGAGCTTGAGAGACATGAA 3'
TAB182 Forward 11	5' TGACCTGTGACCCAGACTCT 3'
TAB182 Forward 12	5' CTGTTGGAGGAGGAAGGAGC 3'
TAB182 Forward 13	5' AGTCAGGACTTCTCCTTCATT 3'
TAB182 Reverse 1	5' CATCTTGGCCAGGATCTCTT 3'
TAB182 Reverse 2	5' ATTCTCTGAGGAGGGGGCTGGACTT 3'
TAB182 Reverse 3	5' AGATGGAAACGTCCGAGTGAGAT 3'
TAB182 Reverse 4	5' AACTTCCTGACCCACTTGGA 3'
TAB182 Reverse 5	5' ATGCCCTACACAAGTCTTGA 3'
TAB182 Reverse 6	5' TTGCCCATACTTGCTGGTCCA 3'
TAB182 Reverse 7	5' AAACTCCCAGTCCTGCTCAT 3'
TAB182 Reverse 8	5' ATCTTCCAGGTCAGCACTGC 3'
TAB182 Reverse 9	5' TTCAGACCCTCCACTTTCCAAA 3'
TAB182 Reverse 10	5' ATGCTCCCTGGCTTCACTTG 3'
TAB182 Reverse 11	5' AGGCTCCAGCACCTCCTCTT 3'
TAB182 Reverse 12	5' CTCTGTAGAGTCCTGGAACA 3'
TAB182 Reverse 13	5' TCAGACCTTCTTCTTCTTCAGTTT 3'

Table 2.7: Sequencing Primers used in this Study. Table illustrates the primers used in this study. Primer name and sequence are shown.

CHAPTER THREE

THE ROLE OF TAB182 DURING ADENOVIRUS INFECTION

3. THE ROLE OF TAB182 DURING ADENOVIRUS INFECTION

3.1 INTRODUCTION

During adenovirus infection, the viral linear double-stranded genome can be recognised by the DDR as DSBs and acted upon by the DSB repair machinery in an attempt to 'repair' the adenoviral ends. The result of such 'repair' leads to the concatenation of viral genomes which are unable to be replicated (Weiden and Ginsberg 1994). To avoid this, adenovirus has developed sophisticated mechanisms to avoid detection from the DDR and therefore replicate its genome. Such mechanisms include the degradation of proteins involved in the DDR and repair pathways including p53, Mre11, DNA ligase IV, BLM, TOPBP1 and Tip60 (Querido, Blanchette et al. 2001, Stracker, Carson et al. 2002, Baker, Rohleder et al. 2007, Blackford, Patel et al. 2010, Orazio, Naeger et al. 2011, Gupta, Jha et al. 2013). Another mechanism of evading the cellular DDR is through the relocalisation of DDR proteins; a number of DDR proteins are known to be relocated to VRCs during infection including RPA32, ATR, ATRIP, TOPBP1, Rad17 and Rad9 (Stracker, Lee et al. 2005, Carson, Orazio et al. 2009). Adenovirus has also been shown to relocalise DDR proteins to PML bodies or aggresomes, such proteins include p53 and the MRN complex (Carvalho, Seeler et al. 1995, Konig, Roth et al. 1999), (Araujo, Stracker et al. 2005, Liu, Shevchenko et al. 2005).

Previous preliminary studies from our laboratory have indicated that TAB182, a protein previously shown to interact with Tankyrase 1, may be down-regulated during adenovirus infection (Seimiya and Smith 2002). Such preliminary studies included the screening of a panel of proteins that had been previously implicated in the DDR (including TAB182), to determine whether they were reduced during Ad5 infection. Amongst the

screened proteins, TAB182 was the only obvious candidate. Since more than 80% of adenoviral cellular targets are proteins involved in the DDR, it was therefore hypothesised that TAB182 could be a DDR protein targeted for proteasomal degradation during adenovirus infection in order to promote viral replication. Therefore the aim of this chapter was to examine whether TAB182 was indeed targeted for degradation during adenovirus infection and to determine the mechanistic basis for this degradation.

3.2 RESULTS

3.2.1 TAB182 is Down-Regulated following Infection with Ad5 and Ad12

To confirm the preliminary evidence obtained from our laboratory suggesting that TAB182 is degraded during adenovirus infection, HeLa cells were mock-infected or infected with Ad5 and Ad12 at an MOI of 5 and harvested at 0, 8, 24, 48, 72 and 96 hours post-infection. Cell lysates were subjected to SDS-PAGE and Western blotting using the indicated antibodies (Figure 3.1). β-actin was used as a loading control. Adenovirus early proteins E1A and E1B55K were immunoblotted along with the viral structural proteins Hexon (Ad5) and Knob (Ad12) as markers of adenovirus replication. As expected, the expression of E1A, E1B55K, Hexon (Ad5) and Knob (Ad12) was observed between 8 and 24 hours post-infection in both Ad5 and Ad12 infected cells. Mre11 and p53 were immunoblotted as positive controls since these proteins are known to be degraded during adenovirus infection (Querido, Blanchette et al. 2001, Stracker, Carson et al. 2002). As previously reported, Mre11 and p53 were degraded in both Ad5 and Ad12 infected cells by 72 and 48 hours post-

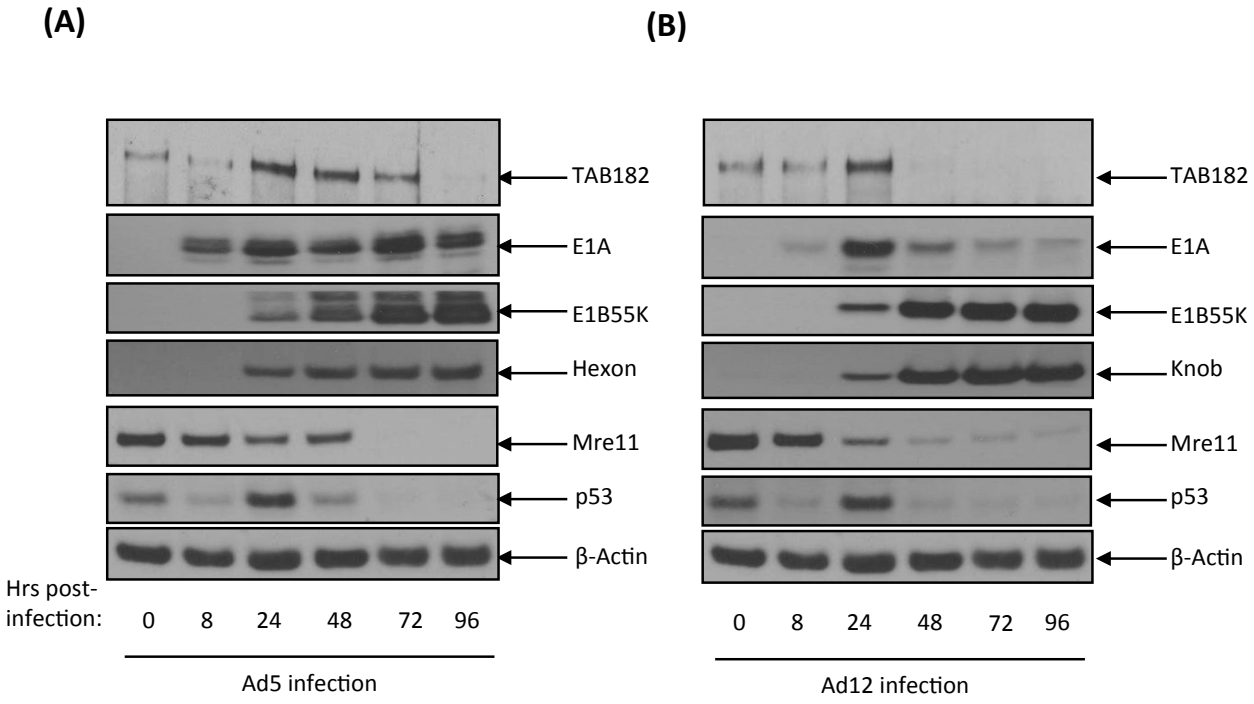

Figure 3.1: The Protein Levels of TAB182 are Reduced following Infection with Ad5 and Ad12. HeLa cells were infected with Ad5 **(A)** or Ad12 **(B)** at an MOI of 5. Cells were then harvested at various time-points (0, 8, 24, 48, 72 and 96 hours) post-infection. Cell lysates were subjected to SDS-PAGE and Western blotting using the indicated antibodies. E1A, E1B55K and Hexon/Knob were immunoblotted as markers of infection. Mre11 and p53 were immunoblotted as positive controls since these proteins are known to be degraded by Ad5 and Ad12. β-Actin was immunoblotted as a loading control. These Western blots are representative of three independent repeats.

infection, respectively. Interestingly, the expression levels of p53 increased following both Ad5 and Ad12 infection before it was degraded. This is believed to be a consequence of adenovirus infection inducing a pseudo-S phase and subsequently p53 expression is increased (Boggs and Reisman 2006, Takahashi, Polson et al. 2011). Infection of cells with Ad5 and Ad12 resulted in the reduced levels of TAB182 protein at 72 and 48 hours post-infection respectively, confirming that TAB182 is indeed a cellular target for certain adenovirus serotypes. Similarly to p53 expression levels, the expression of TAB182 increased prior to degradation, suggesting that the expression levels of TAB182 are cell cycle dependent (Figure 3.1).

3.2.2 The Down-Regulation of TAB182 during Ad5 and Ad12 Infection is Dependent on Proteasome Function

The degradation of DNA damage proteins during adenovirus infection is almost exclusively dependent on the proteasome (Querido, Blanchette et al. 2001, Stracker, Carson et al. 2002, Baker, Rohleder et al. 2007, Orazio, Naeger et al. 2011). To determine whether the down-regulation of TAB182 during adenovirus infection is also dependent on the proteasome, and therefore is a degradation target of adenovirus infection, the proteasome inhibitor bortezomib was used. HeLa cells were mock-infected or infected with Ad5 or Ad12 virus and subsequently mock-treated or treated with the proteasome inhibitor bortezomib 24 hours before each harvest time point (to limit the toxicity of bortezomib treatment). Cells were harvested at 0, 8, 24, 48 and 72 hours post-infection. Cell lysates were fractionated by SDS-PAGE and the filters were immunoblotted with the indicated antibodies (Figure 3.2). Again, E1B55K was immunoblotted as an indicator of infection, expression of E1B55K was

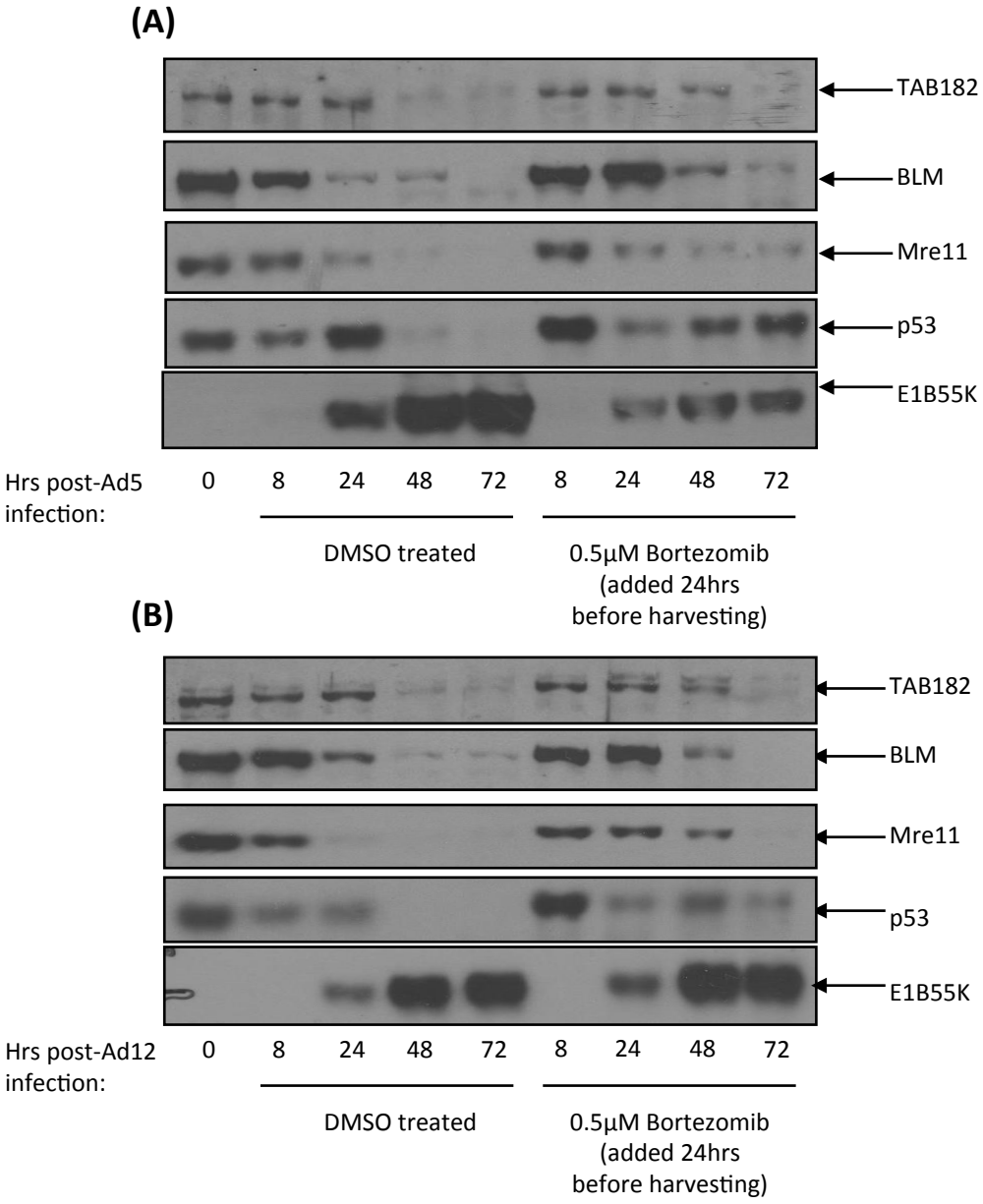

Figure 3.2: The Down-Regulation of TAB182 Protein Levels during Ad5 and Ad12 Infection can be Rescued by the Proteasomal Inhibitor Bortezomib. HeLa cells were infected with Ad5 **(A)** or Ad12 **(B)** at an MOI of 5. Cells were treated with 0.5μM of the proteasome inhibitor Bortezomib 24 hours before harvesting. Cells were harvested at various time-points (0, 8, 24, 48 and 72 hours) post-infection. Cell lysates were subjected to SDS-PAGE and Western blotting using the indicated antibodies. E1B55K was immunoblotted as a marker of infection. Mre11, BLM and p53 were immunoblotted as positive controls since these proteins are known to be degraded by Ad5 and Ad12. These Western blots are representative of three independent repeats.

observed 24 hours post-infection in DMSO, mock-treated infected cells and bortezomib treated infected cells. Ad5 infected cells treated with bortezomib showed a decrease in E1B55K expression when compared to mock-treated cells, possibly due to the toxic effects of bortezomib on the transcriptional machinery required for the virus. Mre11, p53 and BLM were immunoblotted as controls since the degradation of these proteins during Ad5 and Ad12 infection is known to be dependent on proteasome function (Querido, Blanchette et al. 2001, Stracker, Carson et al. 2002, Orazio, Naeger et al. 2011). As expected, in cells infected with Ad5 or Ad12 and mock-treated, Mre11, p53 and BLM were degraded during the course of infection (Figure 3.2A and 3.2B respectively). In cells infected with Ad5 or Ad12 and bortezomib treated, the degradation of Mre11, p53 and BLM was delayed in comparison to mock-treated control cells. Similarly, the degradation of TAB182 in infected (Ad5 or Ad12), bortezomib treated cells was delayed compared to the degradation of TAB182 in infected, mock-treated cells. These data indicate that the down-regulation of TAB182 during adenovirus infection is due to proteasomal-dependent degradation (Figure 3.2).

3.2.3 The Degradation of TAB182 during Ad5 and Ad12 Infection is Dependent on Cullin Function

It is well established that during infection, adenoviruses utilise cellular Cullin proteins in order to degrade their targets (Querido, Blanchette et al. 2001, Baker, Rohleder et al. 2007, Blackford, Patel et al. 2010, Forrester, Sedgwick et al. 2011, Orazio, Naeger et al. 2011). The small molecule inhibitor MLN4924 was used to inhibit cellular Cullin function; MLN4924 inhibits the NEDD8-activating enzyme (NAE), which in turn inhibits Cullin neddylation and therefore inhibits Cullin-RING E3 ligases (Brownell, Sintchak et al. 2010).

MLN4924 was utilised to determine whether the degradation of TAB182 during adenovirus infection is dependent on Cullin function. HeLa cells were infected with Ad12; immediately after infection, cells were also incubated with MLN4924 until harvesting. Cells were harvested 0, 8, 24, 48 and 72 hours post-infection. Cell lysates were fractionated by SDS-PAGE and the filters were probed with the indicated antibodies (Figure 3.3). Again, E1B55K was immunoblotted as a marker of infection. p53 was immunoblotted as a control since the degradation of this protein is known to be dependent on Cullin function (Querido, Blanchette et al. 2001, Stracker, Carson et al. 2002). Western blotting of Cul2 confirmed that neddylation was reduced in the presence of MLN4924. The neddylated form of Cul2 can be seen as a slower migrating band in the untreated samples; this was absent in the MLN4924 treated samples. As expected, the degradation of p53 was delayed in adenovirus infected cells treated with MLN4924 when compared to infected mock-treated cells, confirming that the degradation of this protein during adenovirus infection is dependent on Cullin function. Similarly to the degradation of p53, the protein levels of TAB182 were unaffected in adenovirus-infected cells treated with MLN4924 when compared to the degradation observed in infected, mock-treated cells, showing that the degradation of TAB182 during Ad12 infection is dependent on Nedd8 neddylation and therefore Cullin function (Figure 3.3).

To confirm that the degradation of TAB182 during adenovirus infection is indeed dependent on Cullin function, adenovirus infections were also performed in H1299 cells with knockdown of Cul2 or Cul5 protein expression and the levels of TAB182 protein were examined (Blanchette, Wimmer et al. 2013). H1299 cells lacking Cul2 or Cul5 were infected with Ad5 or Ad12 serotypes and harvested at 0, 8, 24, 48, 72 and 96 hours post-infection.

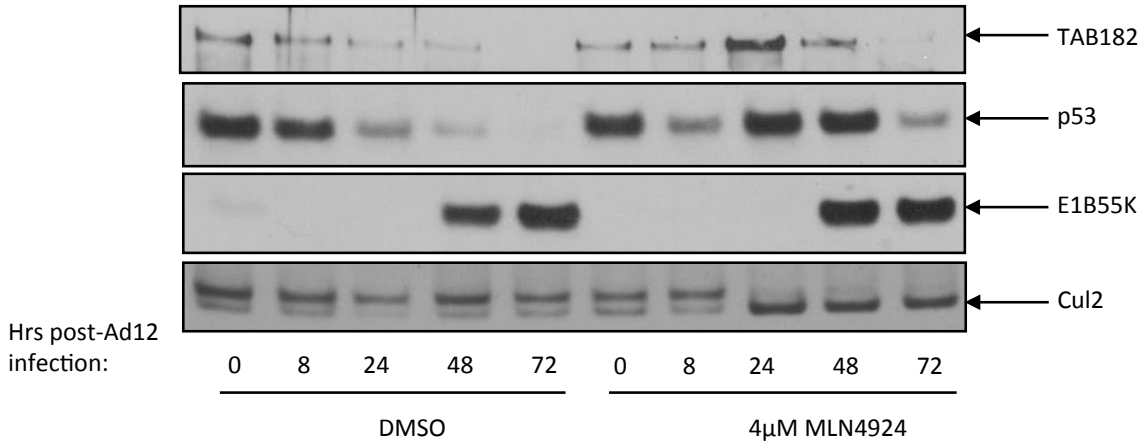

Figure 3.3: The Degradation of TAB182 during Ad12 Infection is Dependent on Cullin Function. HeLa cells were infected with Ad12 at an MOI of 5. Cells were treated with 4μM of the Nedd8 inhibitor MLN4924 immediately post-infection. Cells were harvested at various time-points (0, 8, 24, 48 and 72 hours) post-infection. Cell lysates were subjected to SDS-PAGE and Western blotting using the indicated antibodies. E1B55K was immunoblotted as a marker of infection. p53 was immunoblotted as a positive control since this protein is known to be degraded by Ad12. These Western blots are representative of three independent repeats.

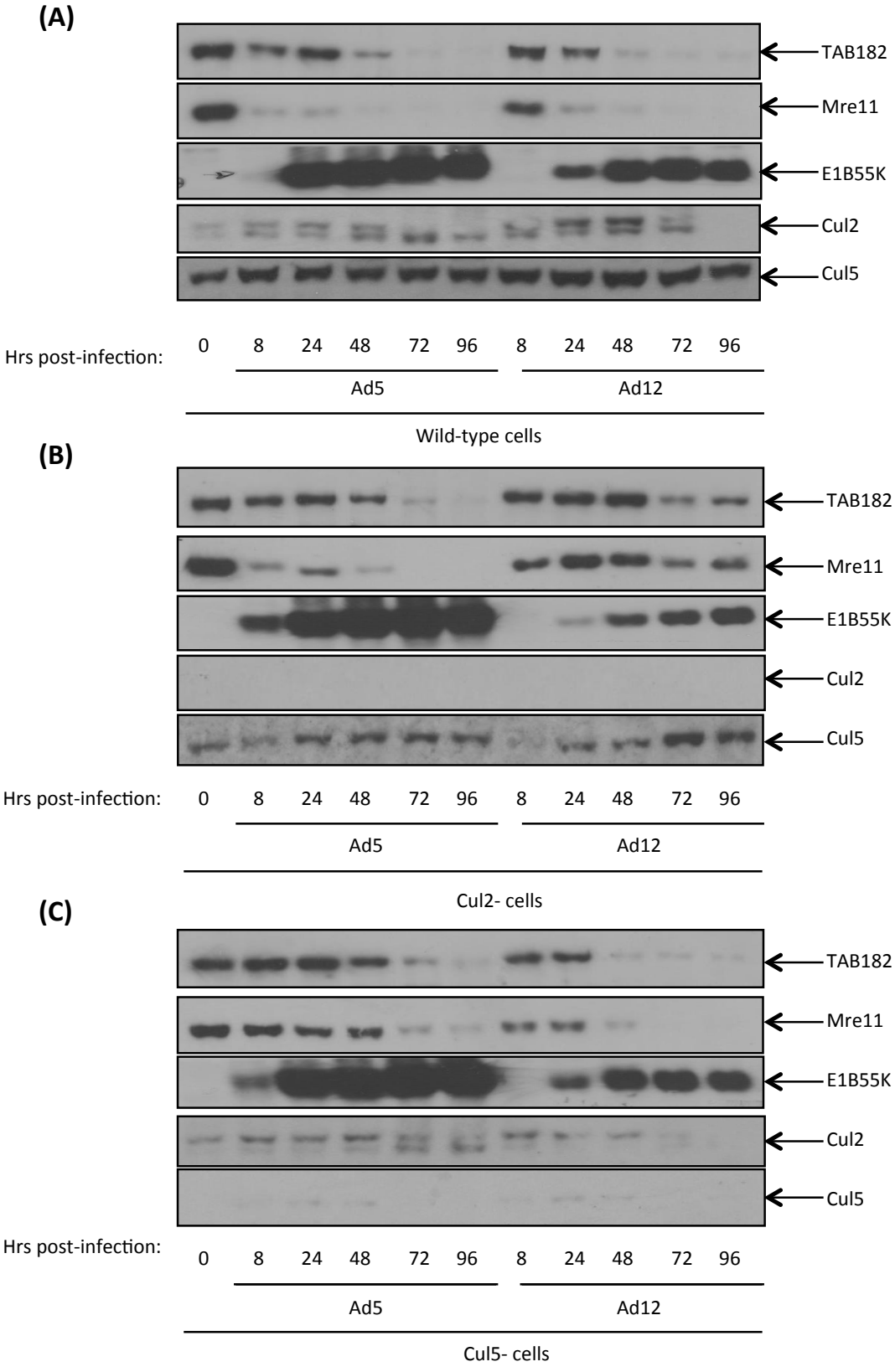

Figure 3.4: The Degradation of TAB182 during Ad5 and Ad12 Infection is Dependent on Cul5 and Cul2 Function Respectively. H1299 wildtype cells **(A)** or H1299 cells with inducible knockdown of Cul2 **(B)** or Cul5 **(C)** were infected with either Ad5 or Ad12 and harvested at 0, 8, 24, 48, 72 and 96 hours post-infection. Cell lysates were subjected to SDS-PAGE and Western blotting. Cul2 and Cul5 were immunoblotted to assess the efficiency of the inducible knockdown. E1B55K was immunoblotted as a marker of infection. Mre11 was immunoblotted since the Cullin responsible for its degradation is known. These Western blots are representative of three independent repeats.

Cell lysates were subjected to SDS-PAGE and Western blotting using the indicated antibodies (Figure 3.4). Induction of E1B55K expression confirmed successful infection. Mre11 was immunoblotted since its degradation during Ad5 infection is known to be dependent on Cul5 function, and its degradation during Ad12 infection is known to be dependent on Cul2 function (Querido, Blanchette et al. 2001, Stracker, Carson et al. 2002, Blackford, Patel et al. 2010). In infected cells lacking Cul2 protein expression, the degradation of TAB182 was unaffected during Ad5 infection, but was inhibited in Ad12 infected cells, suggesting that the degradation of TAB182 during Ad12 infection is dependent on Cul2 function. In infected cells lacking Cul5 protein expression, the degradation of TAB182 was partially inhibited in Ad5 infected cells, and unaffected in Ad12 infected cells, suggesting that the degradation of TAB182 during Ad5 infection is dependent on Cul5 function (Figure 3.4).

3.2.4 The Degradation of TAB182 following Infection with Ad5 and Ad12 is Dependent on the Adenovirus E1B55K and E4orf6 Proteins

To determine which viral proteins are responsible for the degradation of TAB182 during Ad5 and Ad12 infection, infections were performed with mutant viruses which do not express specific viral proteins. HeLa cells were mock-infected or infected with Ad5*dl*1520 (Ad5E1B55K$^-$ mutant) and Ad12*dl*620 (Ad12E1B55K$^-$ mutant) at an MOI of 5 and harvested at 0, 8, 24, 48, 72 and 96 hours post-infection. Cell lysates were fractionated by SDS-PAGE and the filters were probed with the indicated antibodies. β-actin was used as a loading control.

HeLa cells infected with Ad5*dl*1520 (Figure 3.5A) or Ad12*dl*620 (Figure 3.5B) were immunoblotted with antibodies against E1A as a positive marker for infection, E1B55K was immunoblotted as a negative control to confirm the authenticity of the virus, and Hexon

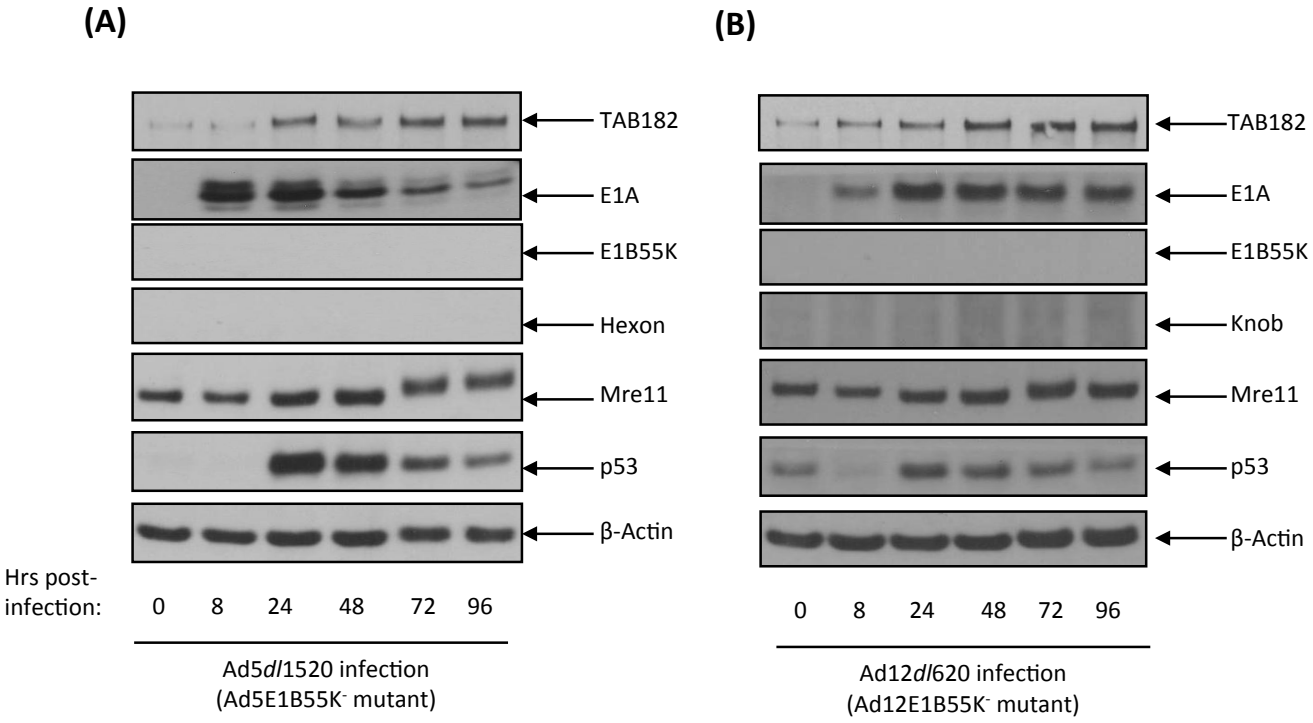

Figure 3.5: The Degradation of TAB182 following Infection with Ad5 and Ad12 is Dependent on the Adenovirus E1B55K Protein. HeLa cells were infected with Ad5*dl*1520 (Ad5E1B55K$^-$ mutant) **(A)** or Ad12*dl*620 (Ad12E1B55K$^-$ mutant) **(B)** at an MOI of 5 and were then harvested at various time-points (0, 8, 24, 48, 72 and 96 hours) post-infection. Cell lysates were subjected to SDS-PAGE and Western blotting using the indicated antibodies. E1A, E1B55K and Hexon/Knob were immunoblotted as markers of infection. Mre11 and p53 were immunoblotted as positive controls. β-Actin was used as a loading control. These Western blots are representative of three independent repeats.

(Ad5*dl*1520) and Knob (Ad12*dl*620) were immunoblotted to confirm that the loss of the E1B55K protein inhibited viral replication. As expected, expression of the E1A protein during Ad5*dl*1520 (Figure 3.5A) and Ad12*dl*620 (Figure 3.5B) infection was unaffected in the mutant viruses. Expression of E1B55K, Hexon and Knob was absent following infection with Ad5*dl*1520 (Figure 3.5A) or Ad12*dl*620 (Figure 3.5B) as expected. Mre11 and p53 were used as controls since the degradation of these proteins by Ad5 and Ad12 is known to be dependent on E1B55K protein (Querido, Blanchette et al. 2001, Stracker, Carson et al. 2002, Blackford, Patel et al. 2010). As anticipated, the protein levels of Mre11 and p53 were unaffected by infection with Ad5*dl*1520 (Figure 3.5A) and Ad12*dl*620 (Figure 3.5B), confirming that their degradation is dependent on the adenoviral E1B55K protein (Querido, Blanchette et al. 2001, Stracker, Carson et al. 2002). The levels of TAB182 protein were also unaffected by Ad5*dl*1520 (Figure 3.5A) and Ad12*dl*620 (Figure 3.5B) infection, indicating that the degradation of TAB182 during Ad5 and Ad12 infection is dependent on adenoviral E1B55K protein.

Infection of cells with Ad5*dl*155 (Ad5E4$^-$ mutant) showed that the degradation of TAB182 was dependent on one or more of the adenovirus E4 proteins (Figure 3.6). In further experiments, HeLa cells were infected with various Ad5 mutant viruses that fail to express different E4 proteins; H5*in*351 (E4orf1$^-$ mutant), H5*pm*4154 (E4orf6$^-$ mutant), H5*pm*4155 (E4orf3$^-$E4orf6$^-$ mutant), H5*pm*4166 (E4orf4$^-$ mutant), H5*dl*356 (E4orf7$^-$ mutant), H5*in*352 (E4orf2$^-$ mutant) and H5*dl*150 (E4orf3$^-$ mutant) (Figure 3.7). As expected, the expression of E1B55K protein was unaffected following infection with E4 mutant viruses. The expression of E4orf6 was confirmed but, unfortunately antibodies against other E4 proteins were unavailable, however, these viruses have been validated in Professor Thomas Dobner's

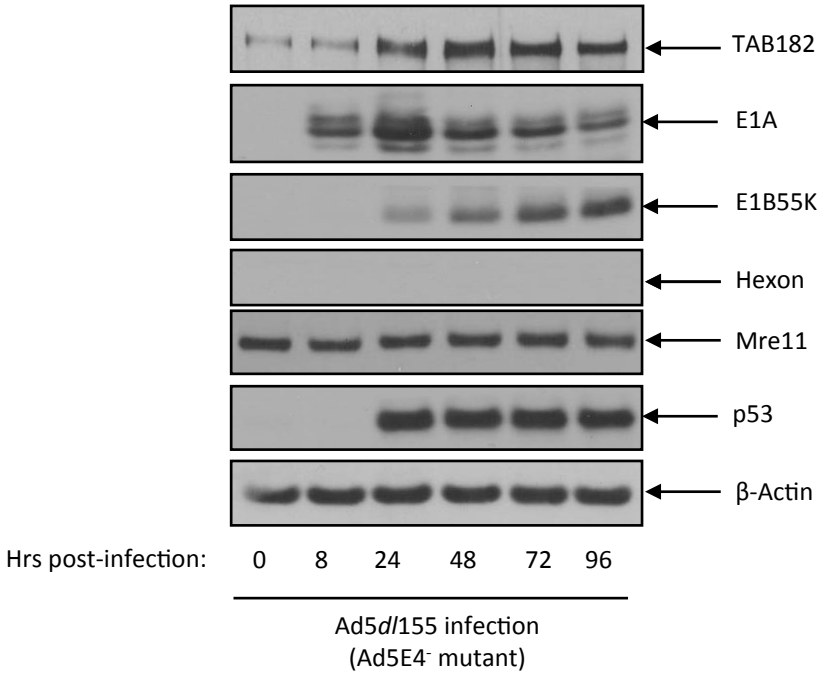

Figure 3.6: The Degradation of TAB182 following Infection with Ad5 is Dependent on the Adenovirus E4 Protein. HeLa cells were infected with Ad5*dl*155 (Ad5E4$^-$ mutant) at an MOI of 5. Cells were then harvested at various time-points (0, 8, 24, 48, 72 and 96 hours) post-infection. Cell lysates were subjected to SDS-PAGE and Western blotting using the indicated antibodies. E1A, E1B55K and Hexon/Knob were immunoblotted as markers of infection. Mre11 and p53 were immunoblotted as positive controls since these proteins are known to be degraded by Ad5. β-Actin was used as a loading control. This Western blot is representative of three independent repeats.

laboratory. The degradation of TAB182 following infection was similar to that seen with the *wt* virus in cells infected with H5*in*351 (E4orf1$^-$ mutant), H5*pm*4166 (E4orf4$^-$ mutant), H5*in*352 (E4orf2$^-$ mutant) and H5*dl*150 (E4orf3$^-$ mutant), suggesting that E4orf1, E4orf2, E4orf3 and E4orf4 are not essential for the degradation of TAB182. The degradation of TAB182 was inhibited following infection with H5*pm*4154 (E4orf6$^-$ mutant), H5*pm*4155 (E4orf3$^-$E4orf6$^-$ mutant) and unexpectedly, following infection with H5*dl*356 (E4orf7$^-$ mutant). Analysis of adenovirus protein expression in H5*dl*356 infected cells, however, showed that the expression of E4orf6 is abrogated and this may explain why the degradation of TAB182 is inhibited following infection with this mutant virus. We therefore conclude the expression of E4orf6 is essential for the degradation of TAB182 yet, further experiments are necessary to establish whether E4orf7 is also essential for the degradation of TAB182 (Figure 3.7).

To further examine whether the degradation of TAB182 indeed requires the presence of the adenovirus E1B55K and E4 proteins and to confirm that they are required for Ad12 mediated degradation, DNA transfections of Ad5, Ad12E1B55K and E4 were also performed in HeLa cells. The DNA constructs pcDNA3*Ad12E1B54K*, pcDNA3*Ad12E4orf6*, pXC15-*Ad5E1B55K*, pCMV-*Ad5E4orf6* were used to transfect the cells together with a pcDNA3 empty plasmid as a negative control. The *E4orf6* DNA constructs used for this experiment were HA-tagged. For Ad5 and Ad12 transfections, the following combinations of DNA constructs were used for the transfections, pcDNA alone; *E1B55K* alone; *E4orf6* alone; *E1B55K* and *E4orf6*. 48 hours after transfection, the cells were harvested, subjected to SDS-PAGE and immunoblotting using the indicated antibodies (Figure 3.8). Antibodies against HA confirmed successful transfection of the *E4orf6* plasmid. Antibodies against E1B55K

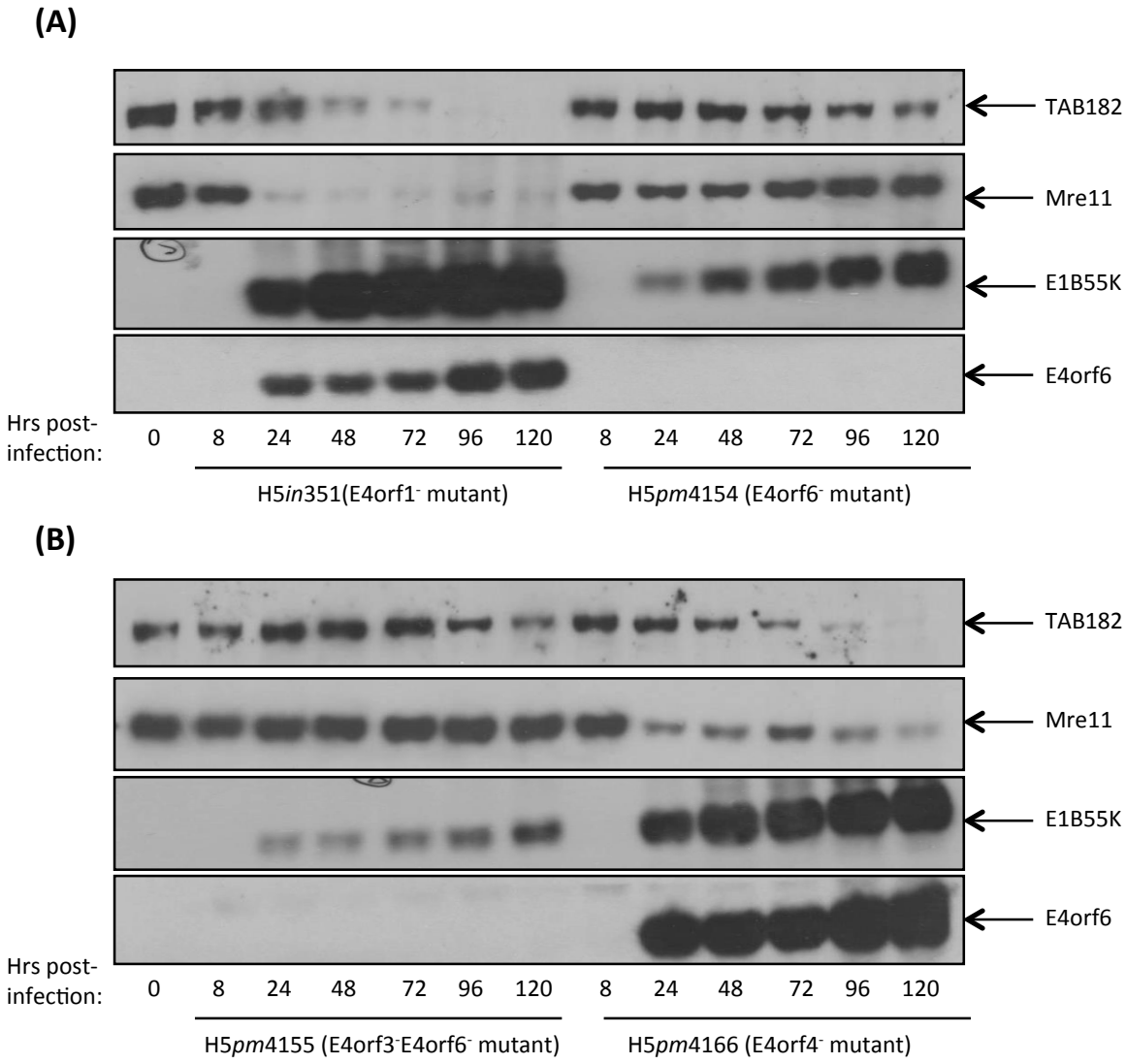

Figure 3.7: The Degradation of TAB182 following Infection with Ad5 is Dependent on the Adenovirus E4orf6 Protein. HeLa cells were infected with either the E4 mutant H5*in*351 (E4orf1$^-$ mutant) **(A)**, H5*pm*4154 (E4orf6$^-$ mutant) **(A)**, H5*pm*4155 (E4orf3$^-$E4orf6$^-$ mutant) **(B)**, H5*pm*4166 (E4orf4$^-$ mutant) **(B)**, H5*dl*356 (E4orf7$^-$ mutant) **(C)** H5*in*352 (E4orf2$^-$ mutant) **(C)** and H5*dl*150 (E4orf3$^-$ mutant) **(D)** at an MOI of 5. The cells were then harvested at various time-points (0, 8, 24, 48, 72, 96 and 120 hours) post-infection. Cell lysates were subjected to SDS-PAGE and Western blotting using the indicated antibodies. E1B55K was immunoblotted as a marker of infection. E4orf6 was immunoblotted to validate the expression of the mutant viruses. Mre11 was immunoblotted as a positive control. These Western blots are representative of three independent repeats.

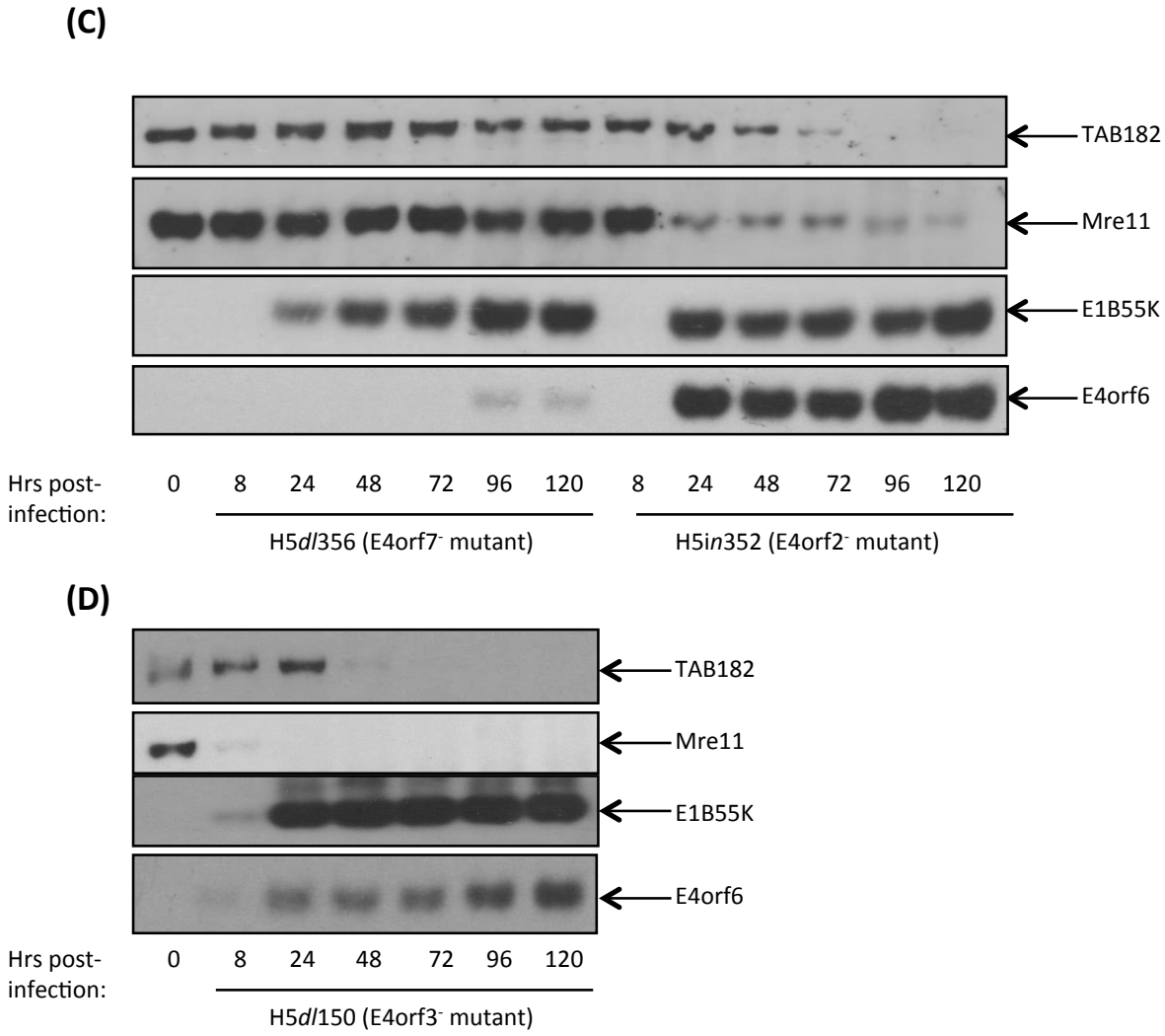

Figure 3.7 Cont'd: The Degradation of TAB182 following Infection with Ad5 is Dependent on the Adenovirus E4orf6 protein. HeLa cells were infected with E4 mutant H5*in*351 (E4orf1$^-$ mutant) **(A)**, H5*pm*4154 (E4orf6$^-$ mutant) **(A)**, H5*pm*4155 (E4orf3$^-$E4orf6$^-$ mutant) **(B)**, H5*pm*4166 (E4orf4$^-$ mutant) **(B)**, H5*dl*356 (E4orf7$^-$ mutant) **(C)**, H5*in*352 (E4orf2$^-$ mutant) **(C)** and H5*dl*150 (E4orf3$^-$ mutant) **(D)** at an MOI of 5. Cells were then harvested at various time-points (0, 8, 24, 48, 72, 96 and 120 hours) post-infection. Cell lysates were subjected to SDS-PAGE and Western blotting using the indicated antibodies. E1B55K was immunoblotted as a marker of infection. E4orf6 was immunoblotted to validate the expression of the mutant viruses. Mre11 was immunoblotted as a positive control since Mre11 is known to be degraded by Ad5. This Western blot is representative of three independent repeats.

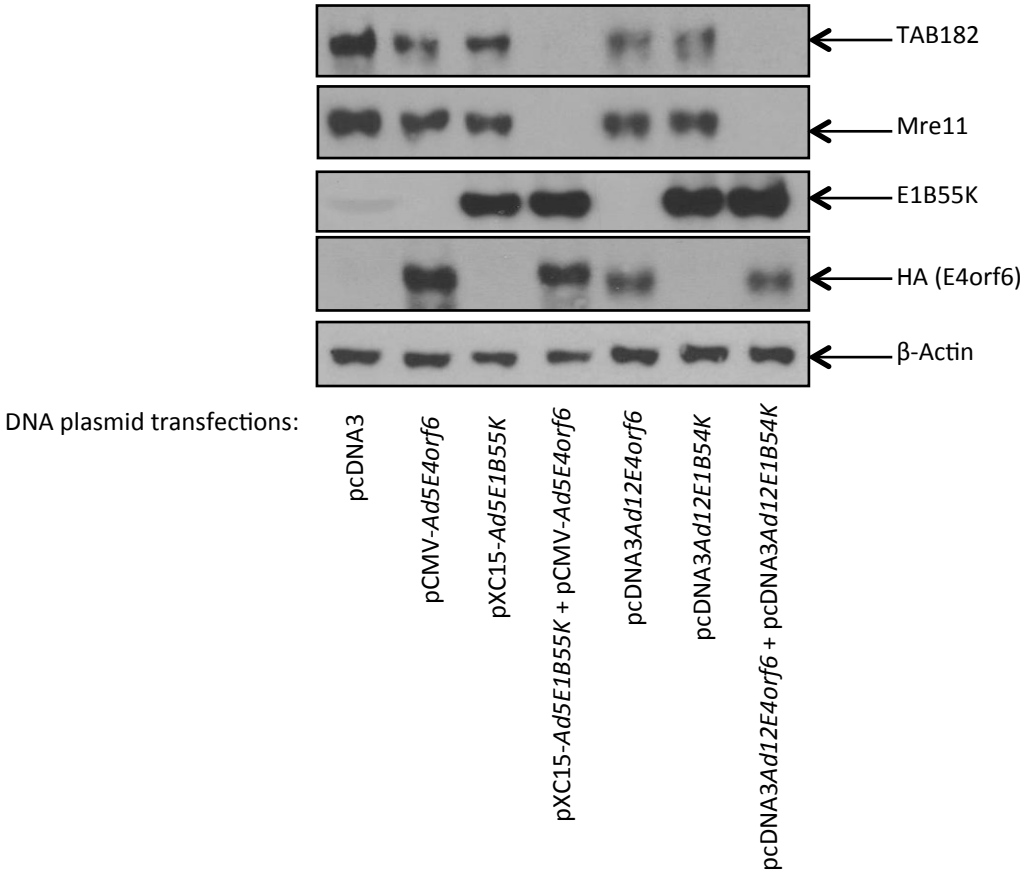

Figure 3.8: The Degradation of TAB182 during Ad5 and Ad12 Infection is Dependent on the Adenovirus E1B55K and E4orf6 Proteins. 2μg of plasmid DNA was transfected into HeLa cells and 48 hours later, the cells were harvested and the lysates subjected to SDS-PAGE and Western blotting using the indicated antibodies. E1B55K and HA (E4orf6) were immunoblotted as markers of efficient transfection. Mre11 was immunoblotted since its degradation is known to be dependent on E1B55K and E4orf6. β-Actin was immunoblotted as a loading control. This Western blot is representative of three independent repeats.

confirmed successful transfection of the *E1B55K* plasmid. TAB182 was immunoblotted to assess which combination DNA plasmid transfections affected the protein levels of TAB182; Mre11 was immunoblotted as a positive control. The results demonstrate that expression of both E1B55K and E4orf6 is necessary for the degradation of TAB182 during Ad5 or Ad12 transfections (Figure 3.8).

3.2.5 E1A Protein Expression is Elevated in Adenovirus Infected TAB182 Depleted Cells

To elucidate the relationship between TAB182 and adenovirus infection more extensively, HeLa cells were depleted of TAB182 protein using siRNA against four different TAB182 sequences (see Table 2.3). HeLa cells were transfected with a final concentration of 45nM of control (non-targeting) or TAB182 siRNA, and 48 hours later the cells were mock-infected or infected with Ad5, Ad12, Ad5*dl*1520 (Ad5E1B55K^{-} mutant), Ad12*dl*620 (Ad12E1B55K^{-} mutant) or H5pm4155 (Ad5E4^{-} mutant) at an MOI of 5. The cells were then harvested at 0, 8, 24, 48, 72 and 96 hours post-infection, cell lysates fractionated by SDS-PAGE and immunoblotted with the indicated antibodies (Figure 3.9). As before, E1A, E1B55K and Hexon/Knob were immunoblotted as markers of adenovirus infection. β-actin was immunoblotted as a loading control. Mre11 and p53 were immunoblotted as positive controls since they are known to be degraded during adenovirus infection (Querido, Blanchette et al. 2001, Stracker, Carson et al. 2002). TAB182 was immunoblotted to test whether the siRNA-mediated knockdown of TAB182 was effective. During Ad5 and Ad12 infection, the comparative levels of the degradation of Mre11 and p53 were unaffected by the depletion of TAB182 protein levels. Interestingly, the total protein levels of p53 were reduced in cells depleted of TAB182 in the absence of adenovirus infection. The protein

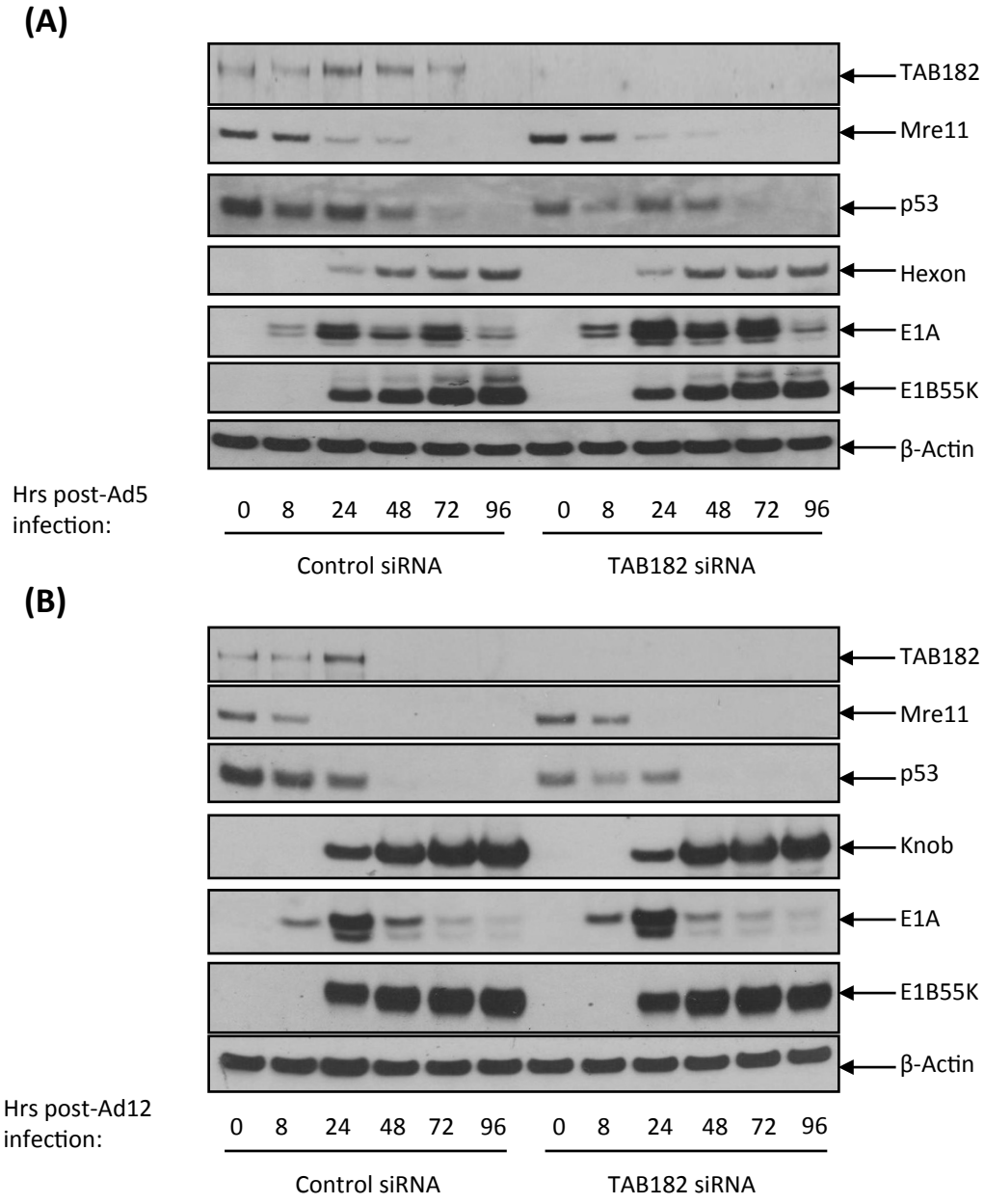

Figure 3.9: E1A Protein Expression is Elevated in Adenovirus Infected TAB182 Depleted Cells. HeLa cells were transfected with control or TAB182 siRNA. 48 hours later, the cells were infected with Ad5 **(A)**, Ad12 **(B)**, Ad5*dl*1520 (Ad5E1B55K$^-$ mutant) **(C)**, Ad12*dl*620 (Ad12E1B55K$^-$ mutant) **(D)** or Ad5*dl*4155 (Ad5E4$^-$ mutant) **(E)** at an MOI of 5. Cells were then harvested at various time-points (0, 8, 24, 48, 72 and 96 hours) post-infection. Cell lysates were subjected to SDS-PAGE and Western blotting using the indicated antibodies. E1A, E1B55K and Hexon/Knob were immunoblotted as markers of infection. Mre11 and p53 were immunoblotted as positive controls since these proteins are known to be degraded by Ad5 and Ad12. β-Actin was immunoblotted as a loading control. These Western blot are representative of three independent repeats.

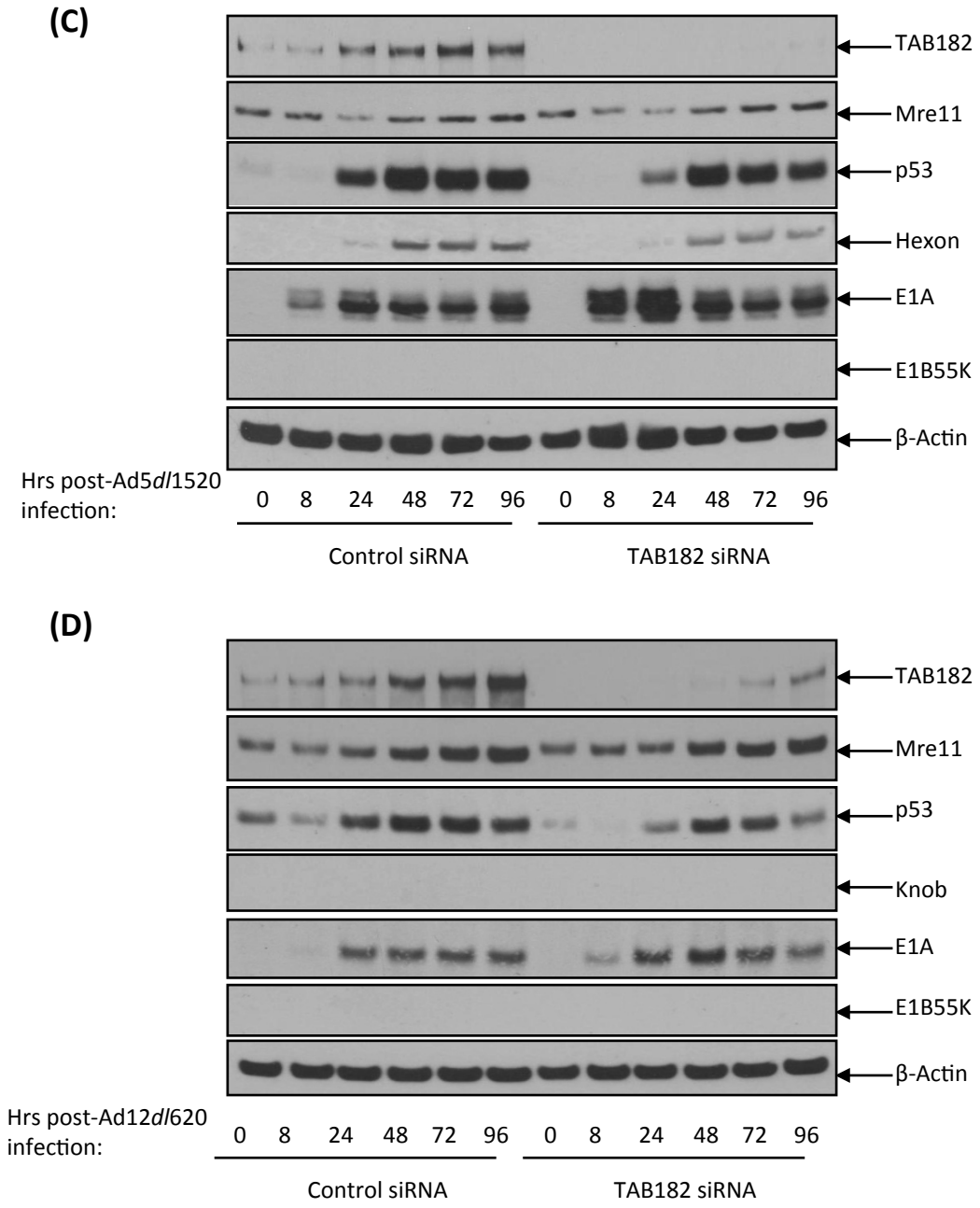

Figure 3.9 Cont'd: E1A Protein Expression is Elevated in Adenovirus Infected TAB182 Depleted Cells. HeLa cells were transfected with control or TAB182 siRNA. 48 hours later, the cells were infected with Ad5 **(A)**, Ad12 **(B)**, Ad5*dl*1520 (Ad5E1B55K$^-$ mutant) **(C)**, Ad12*dl*620 (Ad12E1B55K$^-$ mutant) **(D)** or Ad5*dl*4155 (Ad5E4$^-$ mutant) **(E)** at an MOI of 5. Cells were then harvested at various time-points (0, 8, 24, 48, 72 and 96 hours) post-infection. Cell lysates were subjected to SDS-PAGE and Western blotting using the indicated antibodies. E1A, E1B55K and Hexon/Knob were immunoblotted as markers of infection. Mre11 and p53 were immunoblotted as positive controls since these proteins are known to be degraded by Ad5 and Ad12. β-Actin was immunoblotted as a loading control. These Western blot are representative of three independent repeats.

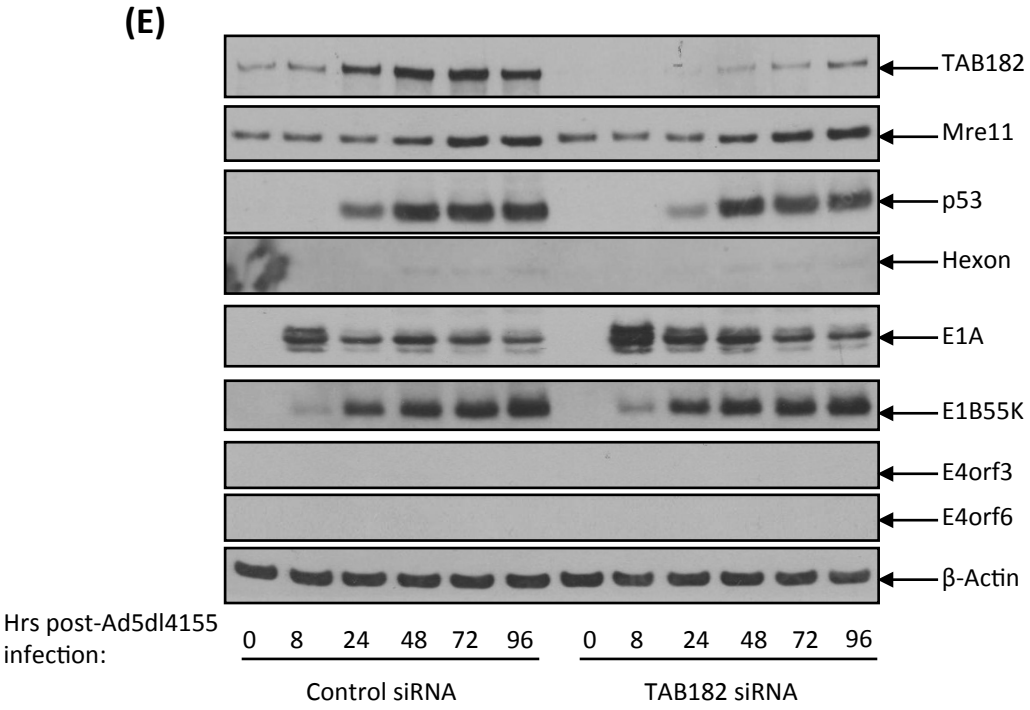

Figure 3.9 Cont'd: E1A Protein Expression is Elevated in Adenovirus Infected TAB182 Depleted Cells. HeLa cells were transfected with control or TAB182 siRNA. 48 hours later, the cells were infected with Ad5 **(A)**, Ad12 **(B)**, Ad5*dl*1520 (Ad5E1B55K$^-$ mutant) **(C)**, Ad12*dl*620 (Ad12E1B55K$^-$ mutant) **(D)** or Ad5*dl*4155 (Ad5E4$^-$ mutant) **(E)** at an MOI of 5. Cells were then harvested at various time-points (0, 8, 24, 48, 72 and 96 hours) post-infection. Cell lysates were subjected to SDS-PAGE and Western blotting using the indicated antibodies. E1A, E1B55K and Hexon/Knob were immunoblotted as markers of infection. Mre11 and p53 were immunoblotted as positive controls since these proteins are known to be degraded by Ad5 and Ad12. β-Actin was immunoblotted as a loading control. These Western blot are representative of three independent repeats.

levels of E1B55K in Ad5 and Ad12 infected cells were comparable in TAB182 depleted cells compared to control siRNA. Interestingly, during Ad5 and Ad12 infection, the protein levels of E1A appeared earlier in cells depleted of TAB182 compared to control siRNA treated cells, suggesting that the adenovirus infection appeared to go through faster in cells depleted of TAB182 compared to control siRNA treated cells (Figure 3.9).

Since the protein levels of E1A appeared earlier into the course of adenovirus infection, we next decided to determine whether infection of cells with the mutant adenoviruses Ad5*dl*1520 (Ad5E1B55K$^-$ mutant), Ad12*dl*620 (Ad12E1B55K$^-$ mutant) or H5*pm*4155 (Ad5E4$^-$ mutant) also displayed the same phenotype in the absence of TAB182 as that with the wild-type Ad5 and Ad12 viruses. HeLa cells were depleted of TAB182 protein using siRNA as previously described or were transfected with a non-silencing control siRNA. Following siRNA-mediated TAB182 depletion, control and TAB182 siRNA treated cells were mock-infected or infected with the mutant adenoviruses Ad5*dl*1520, Ad12*dl*620 or H5*pm*4155. Cells were harvested at 0, 8, 24, 48, 72 and 96 hours post-infection and resolved by SDS-PAGE and Western blotting using the required antibodies (Figure 3.9). As before, E1A, E1B55K and Hexon (Ad5) or Knob (Ad12) were immunoblotted as markers of infection, β-Actin as a loading control, TAB182 to assess the efficiency of the knockdown and Mre11 and p53 as positive controls since they are known to be degraded during the course of adenovirus infection (Querido, Blanchette et al. 2001, Stracker, Carson et al. 2002). As previously observed, the degradation of Mre11 and p53 during mutant virus infection was unaffected by the down-regulation of TAB182 levels when compared to control siRNA treated cells. Again, the total protein levels of p53 after TAB182 knockdown were decreased when compared to cells treated with control siRNA. The protein levels of E1B and Hexon

(Ad5) or Knob (Ad12) were also unaffected by TAB182 depletion when compared to cells treated with control siRNA in cells infected with mutant viruses. The protein levels of E1A were increased in cells depleted of TAB182 when infected with all mutant viruses, similarly to that observed with wild-type viruses (Figure 3.9).

3.2.6 Expression of Cyclin E is Elevated in Infected, TAB182 Depleted Cells

Since E1A expression appeared to be elevated during adenovirus infection in the absence of TAB182 protein expression, we therefore hypothesised that the cell cycle may be altered following TAB182 knockdown leading to more efficient adenovirus infection. To test this, the expression of Cyclin E was examined during the course of adenovirus infection in the presence and absence of TAB182 protein expression. HeLa cells were treated with TAB182 siRNA or with a non-targeting control siRNA. 48 hours after siRNA treatment, cells were mock-infected or infected with Ad5 or Ad12 and harvested at 0, 8, 24, 48, 72 and 96 hours post-infection. Cell lysates were subjected to SDS-PAGE and Western blotting using the indicated antibodies (Figure 3.10). There was no difference in Cyclin E expression in Ad5 infected, control siRNA treated cells when compared to Ad5 infected and TAB182 siRNA treated cells. Interestingly, elevated Cyclin E expression was observed in Ad12 infected, TAB182 siRNA treated cells when compared to Ad12 infected, control siRNA treated cells, suggesting that the cell cycle may be altered in Ad12 infected cells depleted of TAB182 (Figure 3.10).

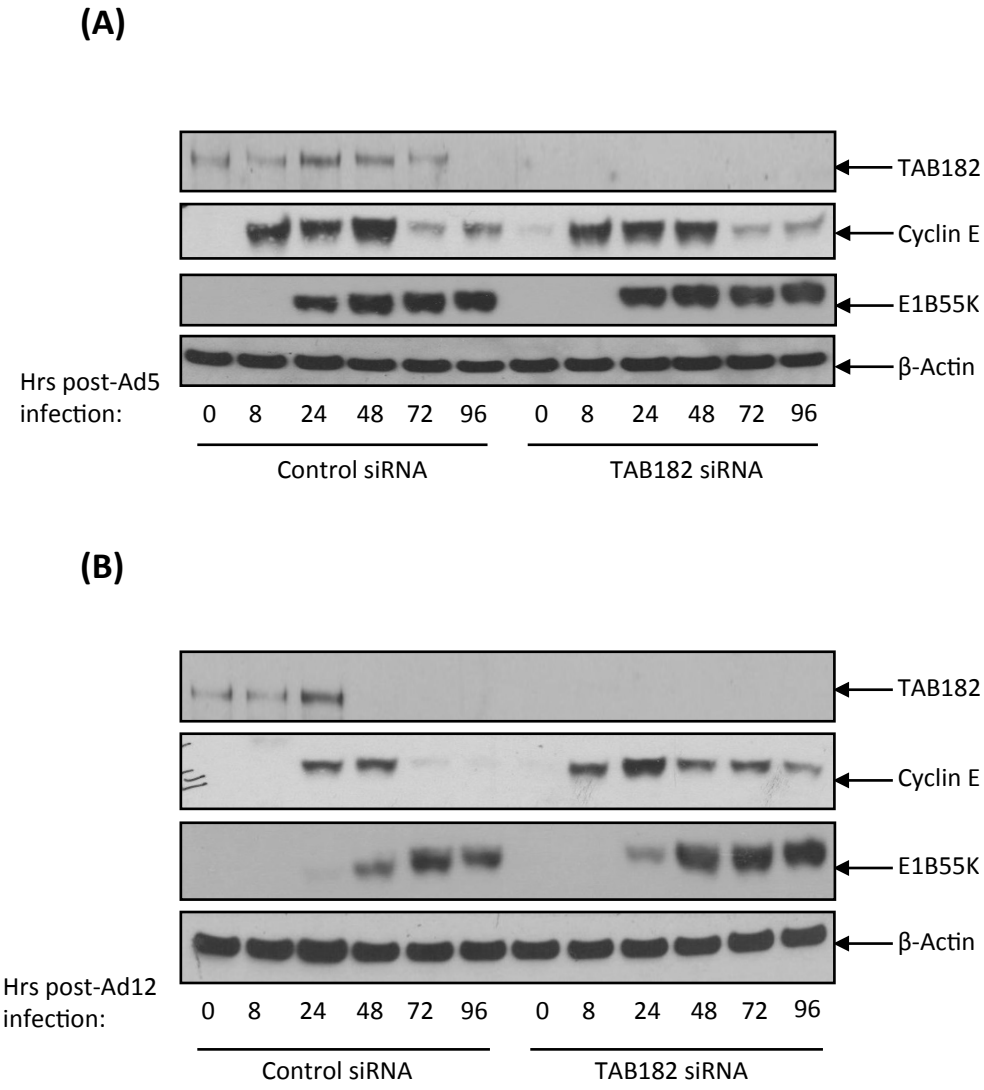

Figure 3.10: Expression of Cyclin E is Elevated in Infected, TAB182 Depleted Cells. HeLa cells were transfected with control or TAB182 siRNA. 48 hours later, the cells were also infected with adenovirus serotype 5 **(A)** or serotype 12 **(B)** at an MOI of 5. Cells were then harvested at various time-points (0, 8, 24, 48, 72 and 96 hours) post-infection. Cell lysates were subjected to SDS-PAGE and Western blotting using the indicated antibodies. E1B55K was immunoblotted as a marker of infection. TAB182 was immunoblotted to assess the efficiency of the TAB182 siRNA mediated depletion. β-Actin was immunoblotted as a loading control. These Western blots are representative of three independent repeats.

3.2.7 Adenovirus Early Region E1B55K Interacts with TAB182 *in Vitro* and *in Vivo*

To determine whether TAB182 interacts with the adenovirus early region E1B55K *in vitro*, GST pull-down assays were performed. Ad5E1HEK293 and Ad12E1HER2 cell lysates were incubated with a C-terminal fragment of TAB182 tagged to GST (referred to as GST-*TAB182C*), spanning a region of amino acids 824-867 fused to one of amino acids 1221-1729 of TAB182 (Figure 3.11)(Seimiya and Smith 2002). Cell lysates were also incubated with GST alone as a non-specific binding control, and cell lysate alone was run as a positive control. Protein complexes were captured using glutathione-agarose beads, subjected to SDS-PAGE and Western blotting (Figure 3.12A, 3.12B). Protein complexes isolated using Ad5E1HEK293 cell lysates were immunoblotted with Ad5E1B55K antibody. Analysis showed that the C-terminal fragment of TAB182 interacts with Ad5E1B55K *in vitro* (Figure 3.12A). Protein complexes isolated using Ad12E1HER2 cell lysates were immunoblotted with Ad12E1B55K antibody. Analysis showed that the C-terminal fragment of TAB182 also interacts with Ad12 E1B55K *in vitro* (Figure 3.12B).

To confirm the interaction between TAB182 and Ad5E1B55K/Ad12E1B55K, co-immunoprecipitation assays were performed. Ad5E1HEK293 and Ad12E1HER2 cell lysates were incubated with antibodies against TAB182 along with IgG alone as a non-specific binding control. Immuno-complexes were isolated using Protein-G agarose beads and subsequently resolved by SDS-PAGE and Western blotting using antibodies against Ad5/Ad12 E1B55K along with cell lysate alone as a positive control. Analysis showed that TAB182 does indeed interact with Ad5E1B55K and Ad12E1B55K *in vivo* (Figure 3.12C and Figure 3.12D). In a reciprocal experiment, Ad5E1HEK293 and Ad12E1HER2 cells were transfected with pEGFPC3-*TAB182*. After 48 hours cells were harvested and lysates

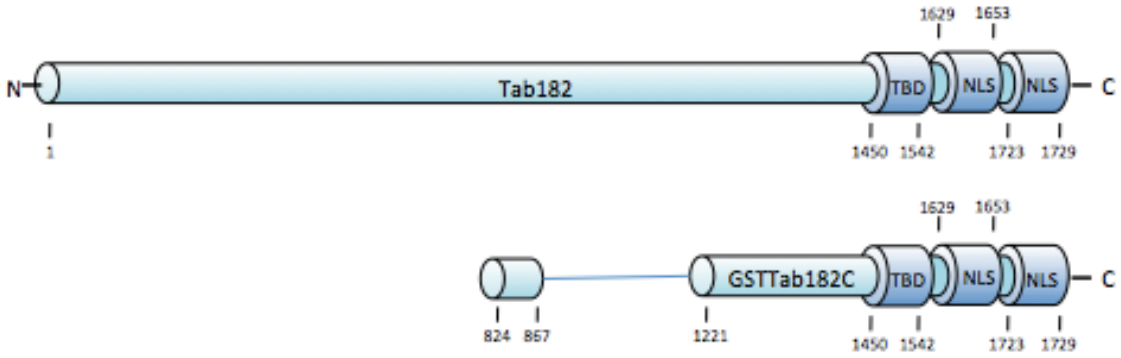

Figure 3.11: Schematic of the GST-*TAB182C* Fragment used in the GST Pull-Down Assays. (A) Schematic of full-length TAB182. Showing amino acid numbers, tankyrase binding domain (TBD) and the two nuclear localisation signals (NLS) it contains. **(B)** Schematic of the GST-*TAB182C* fragment of TAB182 provided as a kind gift from Susan Smith. GST-*TAB182C* incorporates the amino acids 824-867 fused to 1221-1729 of TAB182.

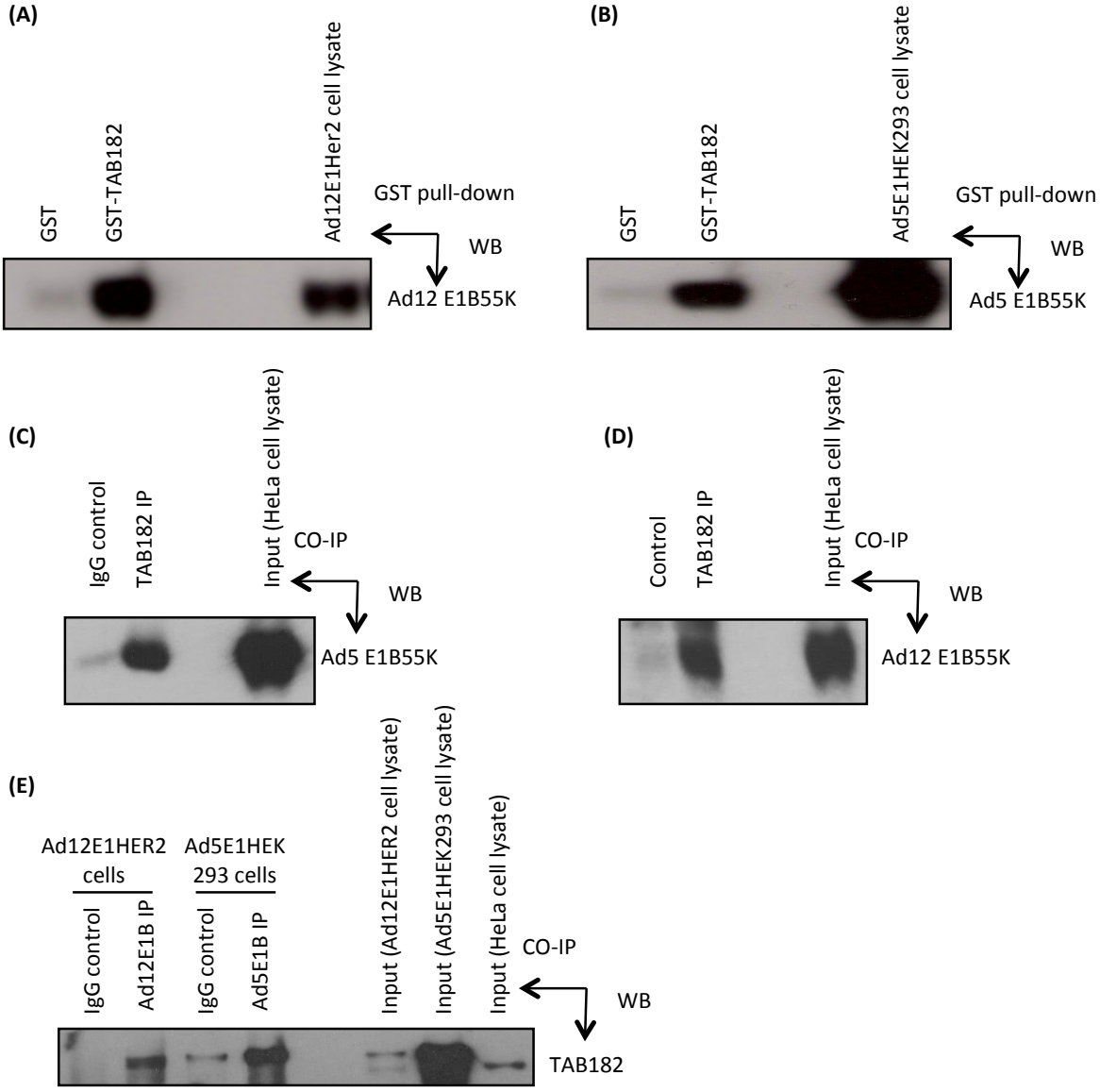

Figure 3.12: Adenovirus Early Region E1B55K Interacts with TAB182 *in Vitro* and *in Vivo*. Ad12E1HER2 **(A)** and Ad5E1HEK293 **(B)** cell lysates were incubated with either GST-*TAB182C*, or with GST alone (non-specific binding control) or cell lysate alone (positive control). Protein complexes were captured by glutathione-agarose beads, subjected to SDS-PAGE and Western blotting. Ad5E1HEK293 **(C)** and Ad12E1HER2 **(D)** cell lysates were incubated with antibodies against TAB182 together with IgG (non-specific binding control). Immuno-complexes were isolated using Protein-G agarose beads and subsequently resolved by SDS-PAGE and Western blotting using antibodies against Ad5/Ad12 E1B along with cell lysate alone as a positive control. **(E)** pEGFPC3-*TAB182* was transfected into Ad5E1HEK293 and Ad12E1HER2 cell lines and harvested. Cell lysates were incubated with Ad5 and Ad12 E1B55K antibodies together with IgG (non-specific binding control). Immuno-complexes were isolated using Protein-G agarose beads and subsequently resolved by SDS-PAGE and Western blotting using antibodies against TAB182 along with cell lysate alone as a positive control. These Western blots are representative of three independent repeats.

incubated with antibodies against Ad5E1B55K and Ad12E1B55K and the immuno-complexes formed isolated using Protein-G agarose beads. Protein complexes were resolved by SDS-PAGE and Western blotting using antibodies against TAB182. Analysis confirmed that TAB182 does indeed interact with Ad5E1B55K and Ad12E1B55K *in vivo* (Figure 3.12E).

3.2.8 TAB182 does not Localise to VRCs during Adenovirus Infection

Although a number of DNA damage proteins are degraded during adenovirus infection, it is also well established that a number are relocalised to VRCs during adenovirus infection including RPA32, ATR, ATRIP, Rad9, TOPBP1 and Rad17 (Carson, Schwartz et al. 2003, Blackford, Bruton et al. 2008, Carson, Orazio et al. 2009, Blackford, Patel et al. 2010). To determine whether TAB182 is relocalised to VRCs during the course of adenovirus infection, immunofluorescence microscopy analysis was performed (Figure 3.13).

HeLa cells were transfected with pEGFPC3-*TAB182* or an empty pEGFPC3 construct as a negative control (see Section 2.5.6 for information on the generation of the pEGFPC3-*TAB182* construct). 24 hours later, cells were re-plated onto glass cover slips and, after 24 hours, infected with wild-type Ad5 or Ad12 virus at an MOI of 5. After a further 24 hours cells were fixed, permeabilised and probed with the appropriate antibodies. Ad5 infected cells were stained for Ad5E1B55K and DBP and Ad12 infected cells stained with antibodies against Ad12E1B55K and RPA32 which has been shown previously to localise to Ad12 VRCs (Blackford, Bruton et al. 2008). There was no localisation of TAB182 to VRCs observed in neither Ad5 or Ad12 infected cells (Figure 3.13).

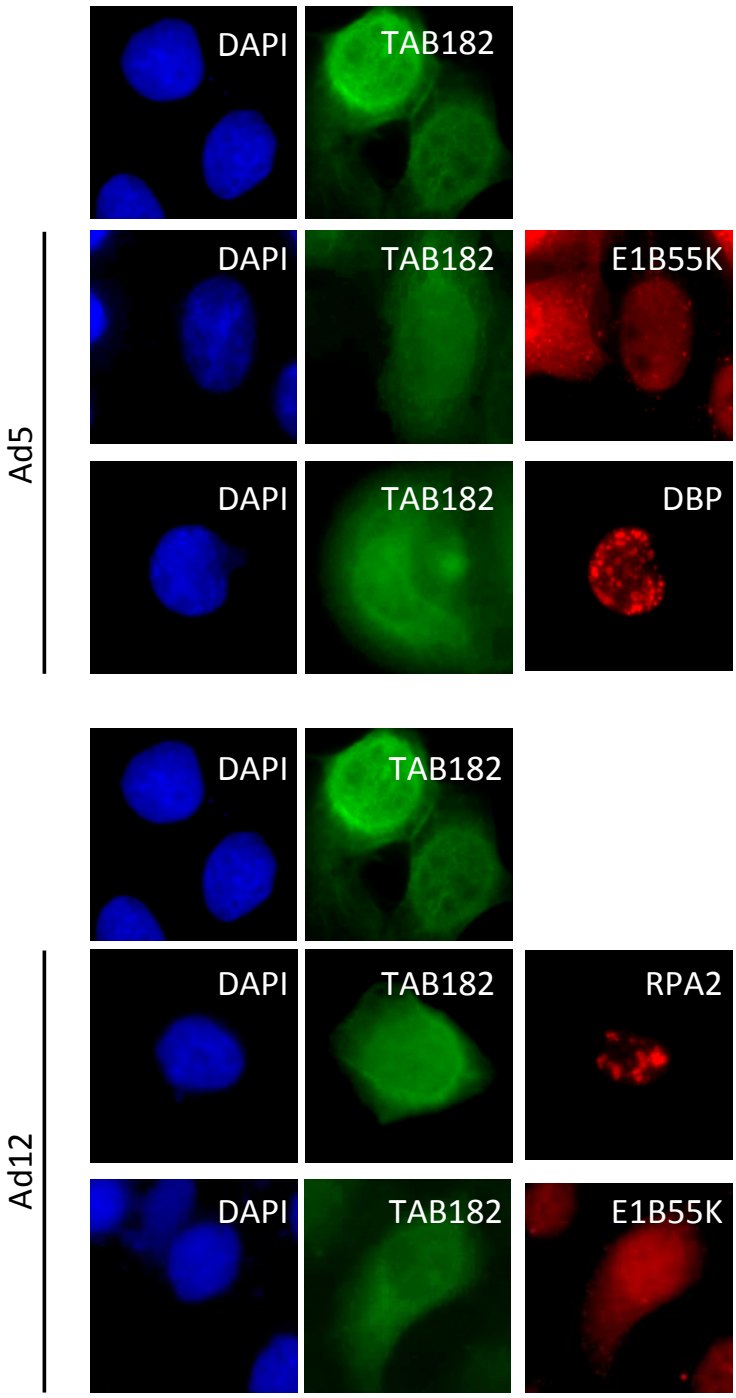

Figure 3.13: TAB182 does not Localise to VRCs during Adenovirus Infection. HeLa cells were transfected with pEGFPC3-*TAB182* and 24 hours later were infected with Ad5 or Ad12. 24 hours following infection the cells were fixed, permeabilised and probed with the appropriate antibodies. Ad5 infected cells were probed with Ad5E1B55K and DBP, whilst Ad12 infected cells were probed with Ad12E1B55K and RPA2. These immunofluorescence images are representative of three independent experiments.

3.2.9 Adenovirus Replication Centres after TAB182 Knockdown

Since TAB182 knockdown altered the expression of E1A and Cyclin E during adenovirus infection, we next wanted to examine the whether TAB182 knockdown had any effect on the formation of VRCs. To investigate this further, immunofluorescence microscopy analysis of cells deficient in TAB182 protein expression was performed. HeLa cells were treated with TAB182 siRNA along with a non-targeting control siRNA. Confirmation of TAB182 knockdown was achieved by Western blotting (data not shown). Cells were infected with wild-type Ad5 or Ad12 virus (MOI of 5) for 24 hours and were then harvested for immunofluorescence microscopy analysis. Cells were fixed, permeabilised, probed and were immunostained with Ad5/Ad12 E1B55K and DBP or Ad5/Ad12 E1B55K and RPA32 antibodies. Ad5 and Ad12 E1B55K expression was used as a marker of infection. DBP and RPA were probed as markers of VRCs. In HeLa cells treated with control siRNA, 24 hours after Ad5 and Ad12 infection, the formation of VRCs can be observed through positive DBP and RPA staining. Viral infection can also be confirmed from the appearance of Ad5E1B55K and Ad12E1B55K staining. In HeLa cells treated with TAB182 siRNA, no significant changes in the formation of VRCs were observed. In addition, there were also no significant changes in Ad5E1B55K or Ad12E1B55K staining observed (Figure 3.14). In order to further quantify this, E1B55K and RPA (Ad5 and Ad12) and E1B55K and DBP (Ad5 only) positive cells were counted as a percentage of the total number of cells. No significant difference in the percentage of E1B55K/RPA and E1B55K/DBP staining was observed between control siRNA and TAB182 siRNA treated cells (Figure 3.14D).

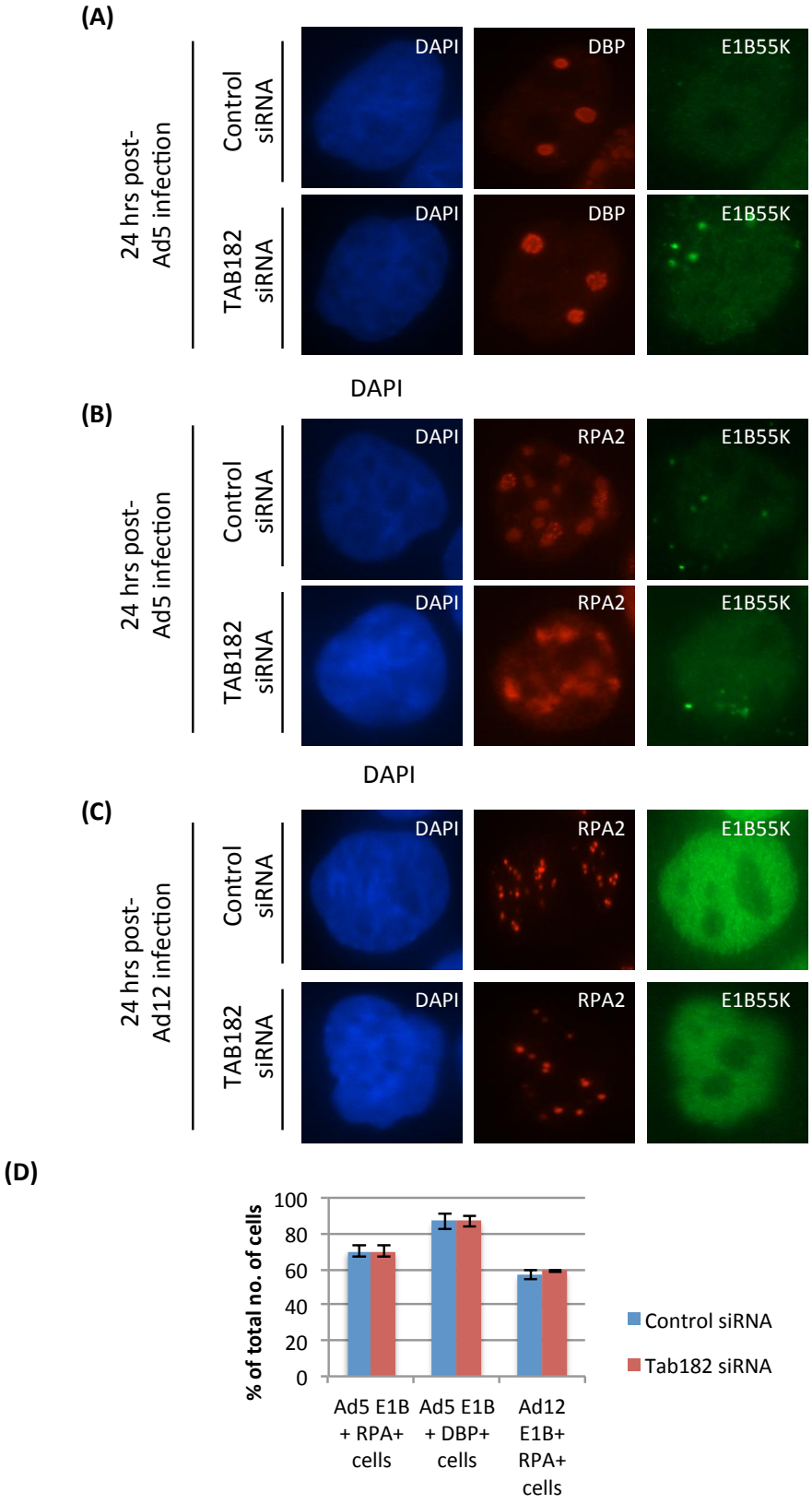

Figure 3.14: Adenovirus Replication Centres after TAB182 Knockdown. HeLa cells were transfected with control or TAB182 siRNA and 24 hours later, infected with either Ad5 or Ad12. The cells were fixed, permeabilised and probed with Ad5 E1B and DBP **(A)** or Ad5 **(B)** Ad12 **(C)** E1B and RPA32 antibodies. **(D)** Graph depicting the percentage of Ad5 E1B+ RPA+, Ad5 E1B+ DBP+ and Ad12 E1B+ RPA+ cells as a total number of cells. These immunofluorescence images are representative of three independent experiments.

3.3 DISCUSSION

It is well established that a number of cellular proteins are degraded following adenovirus infection. Most notably, a significant proportion of these proteins are involved in the DNA damage response (DDR), suggesting that adenovirus degrades these proteins in order to circumvent this pathway specifically (Querido, Blanchette et al. 2001, Stracker, Lee et al. 2005, Baker, Rohleder et al. 2007, Blackford, Patel et al. 2010, Orazio, Naeger et al. 2011, Gupta, Jha et al. 2013). The end result of blocking the DDR is the evasion of concatemerisation of viral genomes, and the replication of the virus and production of viral progeny (Weiden and Ginsberg 1994).

Results presented in this chapter implicate the Tankyrase 1 binding protein, TAB182, as a novel degradation target during adenovirus infection. TAB182 was shown to be degraded following Ad5 and Ad12 infection, in an E1B55K and E4orf6 dependent fashion (Figures 3.1, 3.5, 3.6, 3.7 and 3.8). Furthermore, using the proteasome inhibitor bortezomib, it was shown that the degradation of TAB182 was dependent on proteasome function (Figure 3.2), and through the use of the NEDD8 inhibitor MLN4924, this degradation was also found to be dependent on Cullin function (Figure 3.3). Further studies using Cul2 and Cul5 negative H1299 cell lines showed that the degradation of TAB182 during Ad5 infection is dependent on Cul5, and TAB182 degradation following Ad12 infection is dependent on Cul2 (Figure 3.4). This is consistent with other targets, such as p53, which are degraded during viral infection (Querido, Blanchette et al. 2001, Blackford, Patel et al. 2010). Using siRNA-mediated depletion of TAB182, it was shown that TAB182 suppresses E1A protein expression at early time points post-infection (Figure 3.9). From these studies it was shown that in the absence of TAB182, the expression of Cyclin E was enhanced following Ad12 infection,

suggesting that TAB182 may have a role in the regulation of the cell cycle (Figure 3.10). Co-immunoprecipitation studies showed that TAB182 interacts with both Ad5 and Ad12 E1B55K *in vitro* and *in vivo* (Figure 3.12). Finally, immunofluorescence microscopy showed that TAB182 does not appear to localise to VRCs, nor does the depletion of TAB182 expression effect the formation of VRCs (Figures 3.13 and 3.14).

In this study, TAB182 was shown to be degraded following infection with Ad5 and Ad12 serotypes (Figure 3.1). TAB182 is also known to be degraded following Ad4 infection, but not following infection with Ad3, Ad7, Ad9 and Ad11 (R Grand, personal communication). A comprehensive study from Forrester and colleagues analysing the degradation patterns of various DDR proteins following infection with a panel of Ad serotypes showed that Mre11 and p53 are degraded following infection with Ad4, Ad5 and Ad12 serotypes, but not following Ad3, Ad7, Ad9 and Ad11 infection. In agreement with this, Cheng and colleagues also showed that Mre11 is degraded with group A and C serotypes (also group F), but not degraded during infection with serotypes from group B1, B2 and D viruses (Cheng, Gilson et al. 2011). The study by Forrester and colleagues also showed that the degradation of DNA ligase IV occurs following infection with every serotype tested (i.e. Ad3, Ad4, Ad5, Ad7, Ad9, Ad11 and Ad12), which is also in agreement with the study from Cheng et al. and TOPBP1 is degraded following infection with only Ad12 (Cheng, Gilson et al. 2011, Forrester, Sedgwick et al. 2011). These data, together with the data presented in this study, suggest that the degradation of TAB182 follows the same pattern as the degradation of p53 and Mre11 suggesting that TAB182 may be degraded by the same mechanism. More recently, BLM and Tip60 were also shown to be degraded following Ad5 infection, although no other serotypes were tested for these proteins (Orazio, Naeger et al. 2011, Gupta, Jha et

al. 2013). In comparison to other proteins degraded during adenovirus infection, TAB182 is degraded relatively late. As previously discussed, there are large variations in the ways adenoviruses target DDR proteins, for example, Ad5 and Ad12 degrade p53 but Ad3 does not (Querido, Marcellus et al. 1997, Forrester, Sedgwick et al. 2011). Furthermore, some proteins are degraded later than others, for example p53 is normally degraded very early during adenovirus infection (less than 24 hours) whilst BLM is degraded in the later stages of infection (Querido, Marcellus et al. 1997, Orazio, Naeger et al. 2011). Why degradation targets are down-regulated at different times during adenovirus infection is currently unknown but presumably is linked to their function. One explanation for why TAB182 is degraded so late in the virus cycle could be that TAB182 expression is detrimental to adenovirus persistent infection. There is mounting evidence to suggest that adenovirus can persist in a latent state. Latent adenovirus has been found in lymphocytes in tonsil and intestinal tissue, as well as lung epithelial cells (Leung, Chan et al. 2005, Garnett, Talekar et al. 2009, Roy, Calcedo et al. 2011). It is currently unclear why TAB182 would be detrimental to this process but could be one explanation as to why it is degraded late in the virus cycle.

The viral proteins responsible for the degradation of adenoviral targets have been closely studied. As previously discussed, the degradation of cellular adenovirus targets is thought to be achieved through the viral proteins E1B55K and E4orf6 proteins, which recruit a Cullin-based E3 ubiquitin ligase composed of Rbx1 and Elongins B and C. In this investigation, through the use of mutant viruses and the transfection of plasmids expressing viral proteins, the viral proteins shown to be responsible for the degradation of TAB182 following Ad5 and Ad12 infection were shown to be the E1B55K and E4orf6 proteins (Figures 3.5, 3.6, 3.7 and 3.8). The degradation of p53, Mre11, DNA ligase IV, Tip60 and BLM have all

been shown to also be dependent on the E1B55K and E4orf6 proteins (Querido, Blanchette et al. 2001, Stracker, Carson et al. 2002, Baker, Rohleder et al. 2007, Blackford, Patel et al. 2010, Forrester, Sedgwick et al. 2011, Orazio, Naeger et al. 2011, Gupta, Jha et al. 2013). Whilst the degradation of DDR proteins during adenovirus infection appeared to be conserved amongst these proteins, interestingly, the degradation of TOPBP1 by Ad12 has been proposed to be dependent on the E4orf6 protein alone, together with a cellular Cullin2-based E3 ubiquitin ligase, suggesting there are different mechanisms employed for the degradation of proteins during adenovirus infection (Blackford, Patel et al. 2010). Similarly, Daxx proteasome-mediated degradation by Ad5 appears to only require the E1B55K protein and not E4orf6 (Schreiner, Wimmer et al. 2011).

Whilst different viral proteins may be employed for the degradation of proteins during adenovirus infection, the general consensus during the degradation process is that all adenoviral targets are processed by the proteasome. All DDR proteins that are degraded during adenovirus infection have been shown to be dependent on the proteasome through the use of the proteasome inhibitor MG132 (Querido, Blanchette et al. 2001, Stracker, Carson et al. 2002, Baker, Rohleder et al. 2007, Blackford, Patel et al. 2010, Orazio, Naeger et al. 2011, Gupta, Jha et al. 2013). In our hands, MG132 (following only a 24 hour incubation) was highly toxic to HeLa cells, with the majority of the cells dead (rounded cells that no longer adhered to the tissue culture dish), when compared to mock-treated, infected cells (data not shown). For this reason the proteasome inhibitor bortezomib was used; this was found to be much less toxic to the cells which allowed incubation for longer time-points. As a precaution bortezomib was added 24 hours before the harvesting of each time point in order to limit its toxic effects (Figure 3.2). Similarly to every other DDR protein degraded

during adenovirus infection, the degradation of TAB182 was shown to be dependent on the proteasome.

Since adenovirus has been shown to employ a cellular, Cullin-based E3 ubiquitin ligase to degrade its targets during infection, the NEDD8 inhibitor MLN4924, which inhibits cellular Cullins through the inhibition of neddylation, was used. The degradation of TAB182 during Ad5 and Ad12 infection was shown to be dependent on Cullin function (Figure 3.3). Furthermore, through the use of H1299 cells negative for Cul2 and Cul5 expression, the degradation of TAB182 during Ad5 infection was shown to be dependent on Cul5, and the degradation of TAB182 during Ad12 infection was shown to be dependent on Cul2 (Figure 3.4). Interestingly, the degradation of p53 during Ad5 and Ad12 infection is dependent on Cul5 and Cul2 respectively, suggesting that similar mechanisms are employed for the degradation of TAB182 as p53 (Cheng, Gilson et al. 2011, Forrester, Sedgwick et al. 2011). There are contradictory reports on the Cullins responsible for the degradation of Mre11 and DNA ligase IV. Whilst initial studies showed that Cul5 was responsible for the degradation of these proteins, more recent studies have shown that knockdown of Cul5 using siRNA has no effect on the degradation of these proteins following Ad4, Ad5 and Ad12 infection (Cul2 was also not responsible for the degradation of these proteins) (Stracker, Carson et al. 2002, Baker, Rohleder et al. 2007, Forrester, Sedgwick et al. 2011). The degradation of TOPBP1 during Ad12 infection was shown to be dependent on Cul2 function, whilst the degradation of BLM and Tip60 was shown to be dependent on Cul5 during Ad5 infection (other serotypes were not tested) (Blackford, Patel et al. 2010, Orazio, Naeger et al. 2011, Gupta, Jha et al. 2013). These data supports the idea that adenovirus adopts a mechanism similar to p53 to degrade TAB182.

From studies described in Chapter 4, there are a number of indications that suggested that TAB182 may be involved in the control of the cell cycle. It was therefore hypothesised that TAB182 may hinder the cell cycle progression which is induced by adenovirus. To test this hypothesis, the expression of a panel of viral proteins was examined in infected cells that were deficient in TAB182 expression. Interestingly, the expression of E1A was increased in infected cells (Ad5 and Ad12, along with mutant viruses) deficient in TAB182 expression when compared to non-silencing controls (Figure 3.9). These data suggest that TAB182 may be involved in the suppression of viral gene expression. The increase in E1A expression in TAB182 knockdown cells varies between virus strains (higher expression of E1A in Ad5 than Ad12 infection). Each virus strain has different properties and therefore progress differently during infection which may explain why there is a difference in expression levels. Alternatively the removal of TAB182 expression may be more beneficial during Ad5 than Ad12 infection. Interestingly, during adenovirus infection, the siRNA-mediated knockdown of Tip60 expression also has an effect on the expression of viral proteins, with an increase in the expression of all early viral genes including E1A (measured by quantitative PCR and immunoblotting) (Gupta, Jha et al. 2013). Further Tip60 studies showed that Tip60 suppresses viral early gene expression through the acetylation of Histone H4 at the E1A promoter (Gupta, Jha et al. 2013). Since TAB182 knockdown also displays a similar phenotype to Tip60 with an increase in E1A expression, it could be that TAB182 is also degraded to prevent suppression of the expression of early viral proteins.

Since the previous result suggested that TAB182 may hinder cell cycle progression during adenovirus infection, the expression of the cell cycle protein Cyclin E was examined in TAB182 deficient cells following adenovirus infection. The expression of Cyclin E in infected,

TAB182 deficient cells was increased when compared to infected cells transfected with non-silencing control siRNA, suggesting that TAB182 retards cell cycle progression (Figure 3.10). Indeed, E1A is known to target the pRB, p107 and p130 proteins in order to induce the E2F-mediated expression of Cyclin E and Cyclin A which stimulate progression of the cell cycle. Since Cyclin E expression following TAB182 depletion is increased, it therefore seems likely that TAB182 is degraded during adenovirus infection in order to relieve the TAB182-mediated suppression of cell cycle progression and therefore promote viral DNA replication (Bagchi, Raychaudhuri et al. 1990, Grand, Ibrahim et al. 1998). Further analyses of the cell cycle (by flow cytometry) during adenovirus would be required to establish whether or not this is the case. As with E1A expression, Cyclin E expression in TAB182 knockdown cells varies between Ad5 and Ad12 virus strains (higher expression in Ad12 than Ad5). Again, virus strains have different properties and this may explain the differences in expression levels. Alternatively the removal of TAB182 expression may effect Cyclin E expression to a greater extent during Ad12 than Ad5 infection as there are large variations in the ways difference adenoviruses target DDR/cell cycle proteins.

With the exception of TOPBP1, E1B55K is known to interact directly with all tested DDR proteins that it targets for degradation including p53, DNA ligase IV, BLM and Tip60 (Querido, Blanchette et al. 2001, Stracker, Lee et al. 2005, Baker, Rohleder et al. 2007, Blackford, Patel et al. 2010, Orazio, Naeger et al. 2011, Gupta, Jha et al. 2013). Following GST pull-down and co-immunoprecipitation experiments, E1B55K was shown to interact with TAB182 *in vitro* and *in vivo* respectively (Figure 3.12). These data compliment the previous results showing that TAB182 forms an E3 ubiquitin ligase composed of at least the E1B55K protein together with Cullins and presumably Elongins and Rbx1.

Following analysis by immunofluorescence microscopy, it was determined that TAB182 does not localise to VRCs during adenovirus infection (Figure 3.13). Furthermore, the composition of VRCs were analysed following siRNA-mediated TAB182 knockdown; it was found that TAB182 deficient cells displayed no problems in VRC formation determined by counting E1B55K, DBP and RPA32 positive cells as a percentage of total number of cells following infection. No significant differences were observed between control siRNA and TAB182 deficient cells (Figure 3.14). Most other DDR proteins degraded during adenovirus infection have been located at VRCs. Prior to degradation, p53 was shown to be localised to PML-containing nuclear tracks rather than VRCs during Ad4, Ad5 and Ad12 infection. p53 was also shown to be located at nuclear tracks during Ad9 infection, although there was no evidence of any p53 degradation throughout the course of infection (Forrester, Sedgwick et al. 2011). Contradictory data is available for Mre11 degradation during Ad4 infection, which was shown to localise to VRCs or PML nuclear tracks in various studies (Stracker, Lee et al. 2005, Forrester, Sedgwick et al. 2011). During Ad5 and Ad12 infection, Mre11 is found to localise to nuclear tracks and VRCs respectively (Stracker, Lee et al. 2005, Forrester, Sedgwick et al. 2011). During Ad3, Ad7 and Ad11 infection Mre11 is localised to VRCs whereas during Ad9 infection Mre11 is localised to nuclear tracks. During Ad3, Ad4, Ad5, Ad7, Ad9, Ad11 and Ad12 infection, TOPBP1 was shown to be localised to VRCs (Forrester, Sedgwick et al. 2011). BLM has been shown to be localised to VRCs during Ad5 infection (Orazio, Naeger et al. 2011). DNA ligase IV has no working immunofluorescence antibody and the location of Tip60 during adenovirus infection is currently unknown (Baker, Rohleder et al. 2007, Gupta, Jha et al. 2013). From these data it is clear that different virus serotypes adopt different localisation strategies for different DDR proteins. Although TAB182 was not

found to be located at VRCs during Ad5 or Ad12 infection, that is not to say it may not be at nuclear tracks or aggresomes. Furthermore, it is not known for certain if TAB182 localises to VRCs. The ectopic TAB182 protein was fused to GFP and its expression was forced; it is not known whether the protein is functional and to what level it is expressed compared to endogenous TAB182 protein levels. Further investigative analysis will determine whether TAB182 is located at these structures.

In conclusion, this chapter presents evidence to suggest that TAB182 is a novel protein degraded during adenovirus infection. The degradation of which is dependent on the E1B55K and E4orf6 proteins, together with a cellular Cullin E3 ubiquitin ligase complex. These data suggest that TAB182 is degraded during adenovirus infection to prevent suppression of cell cycle progression, although further studies are required to determine whether or not this is the case. Finally, TAB182 was not found to be localised to VRCs during adenovirus infection, although whether or not TAB182 is located at PML-containing nuclear tracks or aggresomes is also to be investigated further.

CHAPTER FOUR:

THE ROLE OF TAB182 IN THE DNA DAMAGE REPONSE AND REPLICATION STRESS PATHWAYS

4. THE ROLE OF TAB182 IN THE DNA DAMAGE AND REPLICATION STRESS PATHWAYS

4.1 INTRODUCTION

The DDR and repair pathways are a complex and coordinated set of networks that detect and repair DNA damage with the ultimate aim to protect the integrity of the genome. The DDR can respond to a variety of genomic insults, including SSBs, DSBs, bulky lesions and DNA mismatches. In addition, the DDR can also detect and respond to replication stress induced by unresolved DNA lesions, DNA-bound proteins and secondary structures. The two major proteins responsible for the detection of DNA damage and replication stress are the ATM and ATR kinases. Upon activation of the ATM and ATR kinases, a complex signalling network ensues that leads to the activation of the Chk2 and Chk1 kinases respectively, which act to stall the cell cycle in order to prevent replication of damaged DNA and allow time for repair. In parallel, activated ATM and ATR kinases also activate DNA repair proteins including BRCA1, 53BP1 and BLM amongst others to promote the repair of damaged DNA (see Section 1.2.1.1). If DNA damage is not repaired before DNA replication, this can lead to stalling of replication forks and perturbation of DNA synthesis. To prevent this, cells have also developed mechanisms of DNA damage tolerance that allow the by-pass of DNA lesions in order to ensure completion of genome duplication. In fact, a complex set of networks that respond to replication stress and facilitate replication restart exist but the exact mechanisms are less understood (see Section 1.2.4.2).

The function of TAB182 is currently unknown, although studies from Seiyima and colleagues have previously shown TAB182 to interact with Tanykrase 1, a protein implicated in telomere regulation, and to also associate with mitotic chromosomes (Seimiya and Smith

2002). More recently, TAB182 was identified in a mass spectrometry screen where it was identified as an ATM/ATR substrate following DNA damage (IR specifically) (Matsuoka, Ballif et al. 2007). Results from Chapter Three showed that TAB182 was degraded following infection with Ad5 and Ad12 serotypes. Since more than 80% of adenoviral targets are DDR proteins, we thus hypothesised that TAB182 could also be implicated in the DDR. Further evidence obtained from Chapter Three suggested that TAB182 was able to influence the expression of Cyclin E during adenovirus infection, suggesting that TAB182 may also be involved cell cycle progression. The aim of this chapter was therefore to elucidate a potential role of TAB182 in the DDR and/or the cell cycle.

4.2 RESULTS

4.2.1 Optimisation of TAB182 siRNA Knockdown

Since the majority of the experiments planned for this chapter involved RNA interference of TAB182, the optimal conditions for siRNA-mediated knockdown of TAB182 were established. HeLa cells were transfected with increasing concentrations of control (non-targeting) or TAB182 siRNA (20nm, 45nm, 90nm and 180nm). 48 hours following transfection, the cells were harvested, subjected to SDS-PAGE and Western blotting. TAB182 was immunoblotted to confirm siRNA-mediated knockdown of the protein along with the DNA damage proteins NBS1, Chk1, RPA and H2AX to determine whether the depletion of TAB182 affects the expression of core DNA damage proteins. β-Actin was immunoblotted as a loading control. All concentrations of TAB182 siRNA (ranging from 20nm to 180nm) significantly down-regulated TAB182 protein expression when compared to the expression

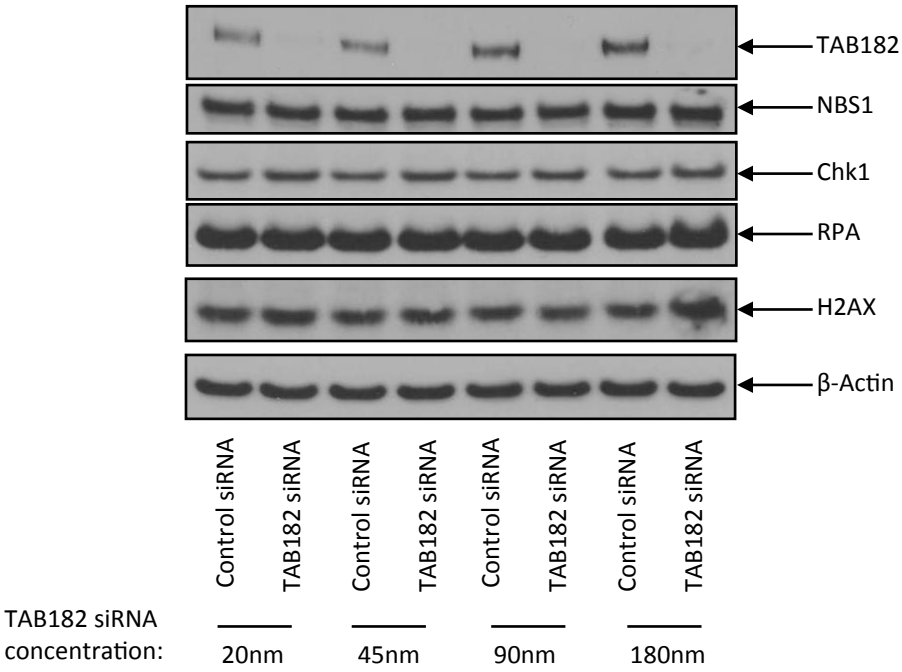

Figure 4.1: Optimisation of TAB182 siRNA Knockdown. HeLa cells were transfected with increasing concentrations of non-targeting control or TAB182 siRNA. The cells were then harvested 48 hours post-transfection. The cell lysates were subjected to SDS-PAGE and Western blotting. TAB182 was immunoblotted to assess the efficiency of the knockdown with increasing concentrations of siRNA. β-Actin was immunoblotted as a loading control. Various DDR proteins were immunoblotted to assess expression levels following TAB182 siRNA-mediated knockdown. This Western blot is representative of three independent experiments.

of TAB182 in control siRNA treated cells. Upon overexposure of the autoradiography film, some residual TAB182 protein expression was observed in cells treated with 20nm of TAB182 siRNA. It was therefore decided that the optimal concentration of TAB182 siRNA for all future experiments would be 45nm. This was to limit any toxicity and off-target effects from the use of higher concentrations of siRNA than necessary. The protein expression of the DNA damage proteins NBS1, Chk1, RPA and H2AX were unaffected by TAB182 siRNA-mediated knockdown, suggesting that the down-regulation of TAB182 protein expression has no effect on the expression of a number of DNA damage proteins (Figure 4.1).

4.2.2 Cells Depleted of TAB182 are Sensitive to Agents that Induce Replicative Stress but not IR

Since results from the Chapter Three and those from Matsuoka and colleagues suggested that TAB182 may be involved in the DDR, the cell survival of TAB182 deficient cells was assessed following exposure to various DNA damaging agents. Cells previously treated with control or TAB182 siRNA were plated at various densities and exposed to increasing concentrations of IR, UV-C irradiation or HU. Confirmation of TAB182 knockdown was achieved by Western blotting (data not shown). Following exposure, the cells were the incubated for 14 days to allow colony formation and the colonies formed were stained and counted. Colony numbers were plotted on survival graphs and analysed. Cells depleted of TAB182 were not sensitive to IR (Figure 4.2A), but were sensitive to UV-C irradiation and HU exposure when compared to the survival of cells treated with control siRNA (Figure 4.2B and 4.2C). This suggests that cells depleted of TAB182 are sensitive to agents that induce replicative stress, but not to those inducing DNA DSBs.

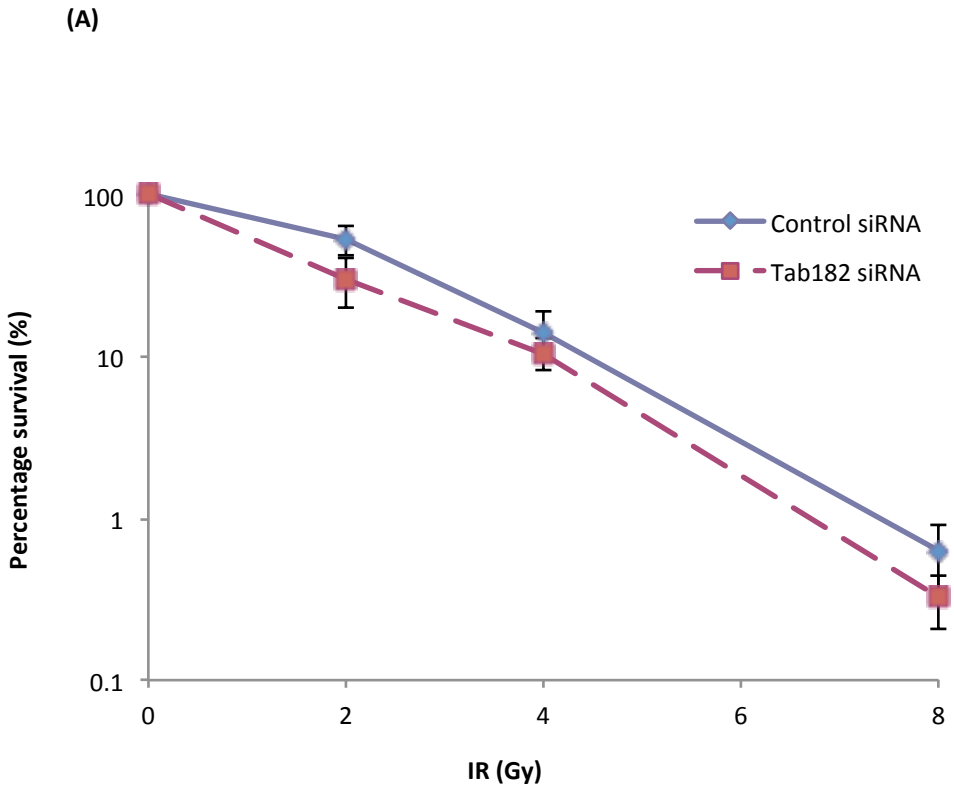

Figure 4.2: Cells Depleted of TAB182 are not Sensitive to IR, but are Sensitive to UV-C Irradiation and HU Treatment. Clonogenic survival assays were performed in cells depleted of TAB182, along with non-targeting control siRNA. Following the indicated siRNA transfections, the cells were exposed to **(A)** increasing doses of IR **(B)** increasing doses of UV-C irradiation or **(C)** increasing doses of HU treatment. Following exposure, the cells were further incubated in media for 14 days and the colonies formed were stained with 0.5% crystal violet in 20% ethanol. Colonies were counted and the data was plotted on survival graphs. Error bars represent SEM. This graph is representative of three independent experiments.

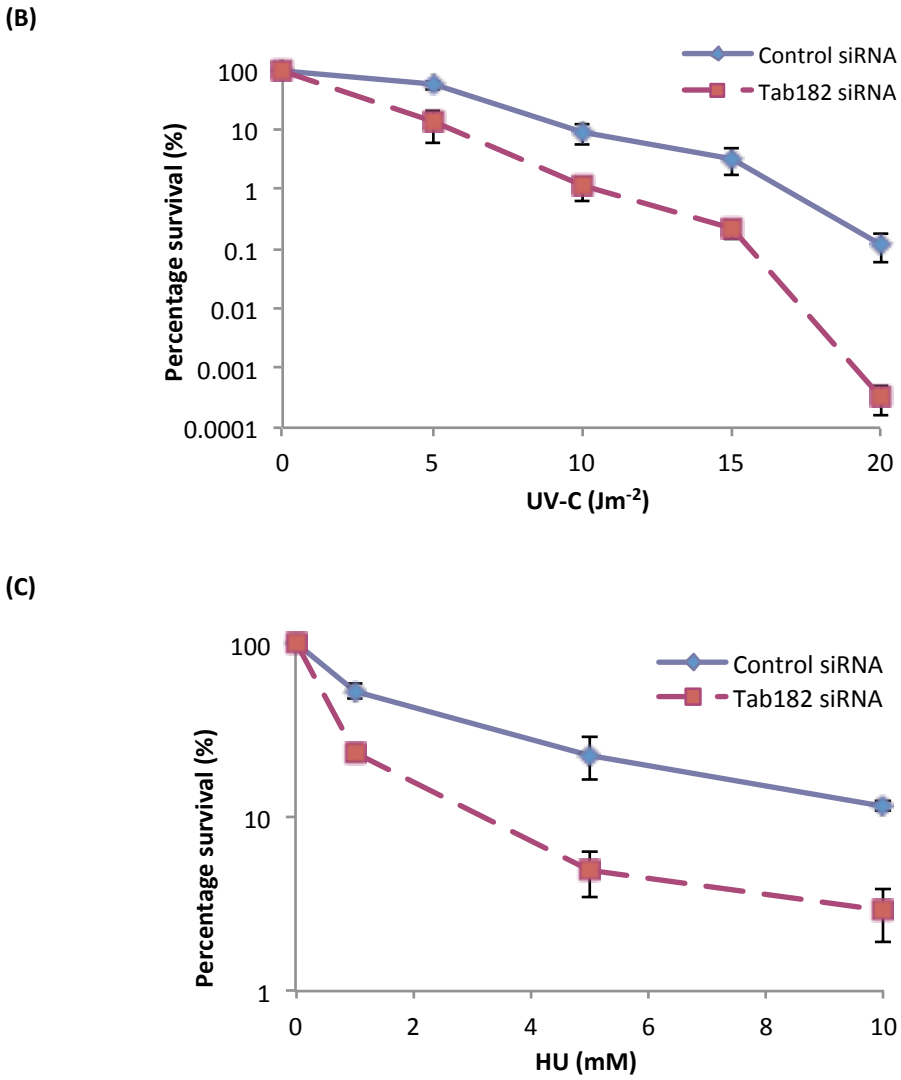

Figure 4.2 Cont'd: Cells Depleted of TAB182 are not Sensitive to IR, but are Sensitive to UV-C Irradiation and HU Treatment. Clonogenic survival assays were performed in cells depleted of TAB182, along with non-targeting control siRNA. Following the indicated siRNA transfections, the cells were exposed to **(A)** increasing doses of IR **(B)** increasing doses of UV-C irradiation or **(C)** increasing doses of HU treatment. Following exposure, the cells were further incubated in fresh media for 14 days and the colonies formed were stained with 0.5% crystal violet in 20% ethanol. Colonies were counted and the data was plotted on survival graphs. Error bars represent SEM. These graphs are representative of three independent experiments.

4.2.3 DDR Signalling is Increased in TAB182 Depleted Cells Compared to Control Cells following Exposure to IR and HU Treatment, but not after UV-C Irradiation.

HeLa cells were treated with control or TAB182 siRNA and 48 hours later mock-exposed or exposed to either 3 Gy of IR, 5 Jm^{-2} of UV-C or 2mM HU for 2 hours after which HU was removed and the cells incubated in drug-free media (denoted 'wash-out') (all further references to HU 'wash-out' refer to these conditions). Cells were harvested at 0, 1, 4, 8 and 24 hours post-exposure (an additional sample was taken at the 'wash-out' time-point which was the time of HU removal). Cells were subjected to SDS-PAGE and Western blotting using the appropriate antibodies. TAB182 was immunoblotted to assess the efficiency of TAB182 depletion after siRNA treatment. The total protein levels of NBS1, Chk1, RPA and H2AX were immunoblotted to determine whether the depletion of TAB182 affected the expression of these proteins. The levels of pNBS1 (S343), pChk1 (S317 and S345), pRPA (S4/8) and γH2AX (S139) were also assessed since the phosphorylation of these proteins indicates activation of the DDR (Figure 4.3).

In cells transfected with control or TAB182 siRNA and exposed to IR, the total protein levels of NBS1, Chk1, RPA and H2AX were unaffected in TAB182 depleted cells when compared to control cells. The protein levels of pNBS1 (S343), pChk1 (S317 and S345), pRPA (S4/8) and γH2AX (S139) increased following exposure to IR in both control and TAB182 siRNA treated cells. Interestingly, the phosphorylation of pNBS1 (S343), pChk1 (S317 and S345), pRPA (S4/8) and γH2AX (S139) was elevated in TAB182 depleted cells above that of control siRNA treated cells (Figure 4.3A). This suggests that depletion of TAB182 enhances certain phosphorylation events during the DDR signalling following IR exposure despite the lack of difference in cell survival.

In cells transfected with control or TAB182 siRNA and exposed to UV-C irradiation, the total protein levels of NBS1, Chk1, RPA and H2AX were unaffected by TAB182 depletion when compared to cells treated with control siRNA. The levels of pNBS1 (S343), pChk1 (S317 and S345), pRPA (S4/8) and γH2AX (S139) increased following UV-C irradiation confirming activation of the DDR. However, there was little observable difference in the levels of phosphorylated DNA damage proteins between control and TAB182 siRNA treated cells apart from the levels of pChk1 (S317), which appeared to be slightly elevated in TAB182 depleted cells compared to control cells (Figure 4.3B). Therefore, the siRNA-mediated depletion of TAB182 does not impact on DNA damage signalling after UV-C irradiation, at least with respect to the phosphorylation events examined here.

In cells transfected with control or TAB182 siRNA and exposed to 2mM HU (wash-out), the total protein levels of NBS1, Chk1, RPA and H2AX were unaffected in TAB182 depleted cells compared to cells treated with control siRNA. The levels of pNBS1 (S343), pChk1 (S317 and S345), pRPA (S4/8) and γH2AX (S139) increased following exposure to 2mM HU (wash-out), confirming activation of DDR signalling. There was no observable difference in the phosphorylation of pNBS1 (S343) in TAB182 deficient cells compared to control cells exposed to 2mM HU (wash-out). However, the expression of pChk1 (S317 and S345), pRPA (S4/8) and γH2AX (S139) was elevated in TAB182 depleted cells compared to control cells following 2mM HU (Figure 4.3C). This suggests that depletion of TAB182 enhances DDR signalling following release from HU exposure.

Taken together, these data suggest that the DNA damage signalling in TAB182 depleted cells is elevated upon exposure to certain damaging agents such as IR and HU, but

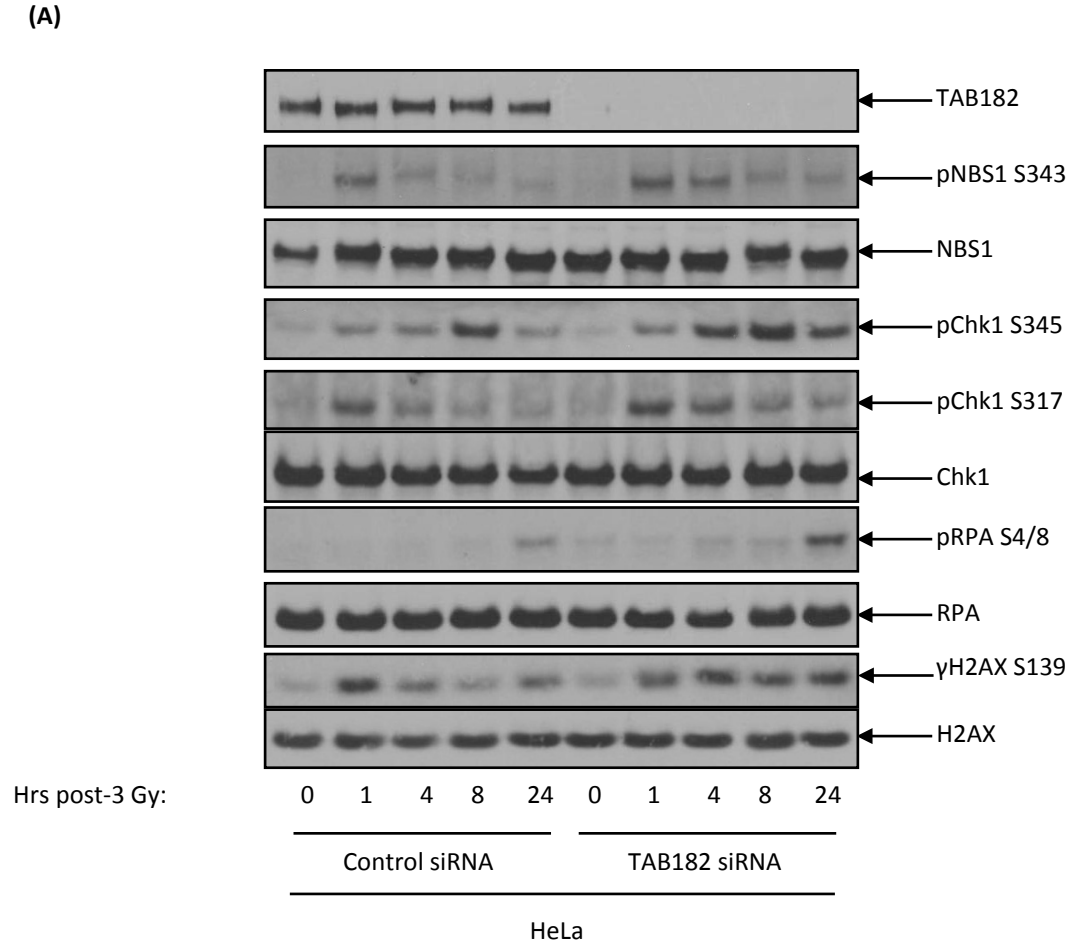

Figure 4.3: DDR Signalling is Increased in TAB182 Depleted Cells Compared to Control Cells following Exposure to IR and HU Treatment, but not after UV-C Irradiation. 50μg of TAB182 depleted or control siRNA treated HeLa cell extracts were immunoblotted for proteins involved in DDR signalling in response to **(A)** 3 Gy IR exposure, **(B)** 5 Jm^{-2} UV-C irradiation or **(C)** 2 hour treatment with 2mM HU, followed by 3 washes in HU-free media and incubation in fresh media for the indicated time-points. TAB182 expression was analysed to assess the efficiency of TAB182 depletion following siRNA treatment. This Western blot is representative of three independent repeats. Wash-out (WO) corresponds to the time-point at which cells were harvested immediately after HU treatment.

(B)

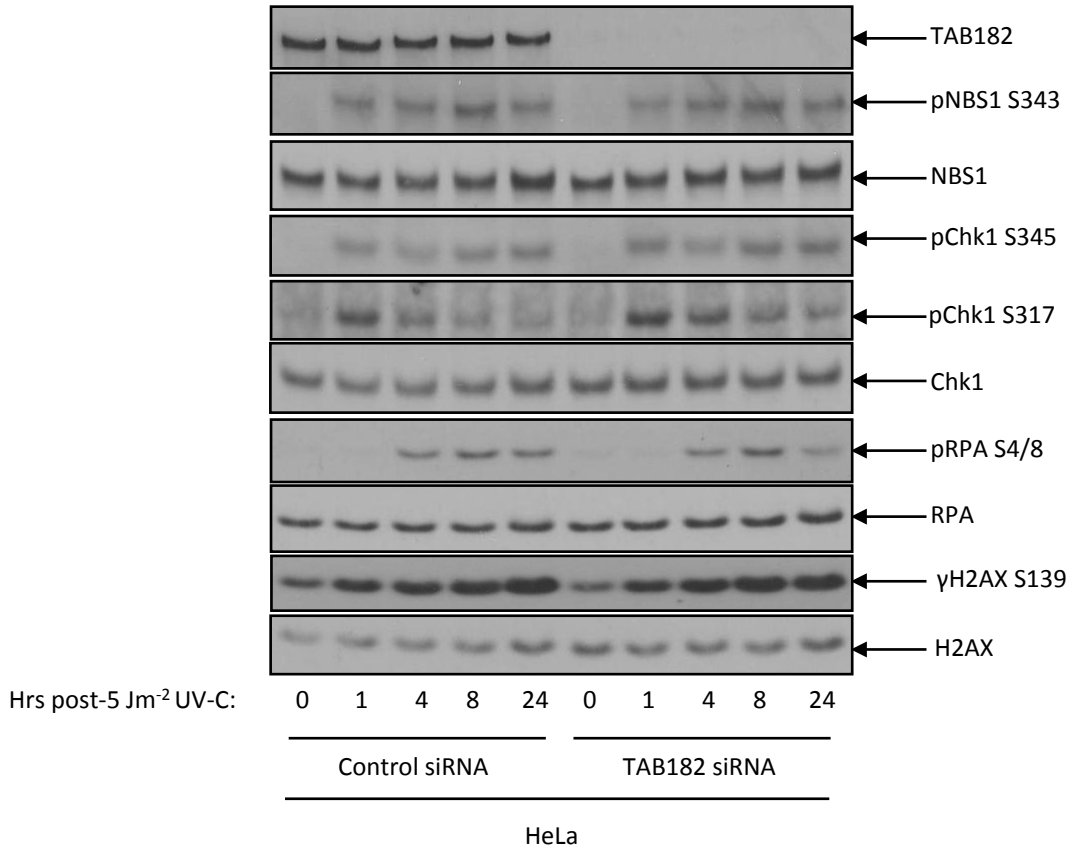

Figure 4.3 Cont'd: DDR Signalling is Increased in TAB182 Depleted Cells Compared to Control Cells following Exposure to IR and HU Treatment, but not after UV-C Irradiation. 50µg of TAB182 depleted or control siRNA treated HeLa cell extracts were immunoblotted for proteins involved in DDR signalling in response to **(A)** 3 Gy IR exposure, **(B)** 5 Jm^{-2} UV-C irradiation or **(C)** 2 hour treatment with 2mM HU, followed by 3 washes in HU-free media and incubation in fresh media for the indicated time-points. TAB182 expression was analysed to assess the efficiency of TAB182 depletion following siRNA treatment. This Western blot is representative of three independent repeats. Wash-out (WO) corresponds to the time-point at which cells were harvested immediately after HU treatment.

(C)

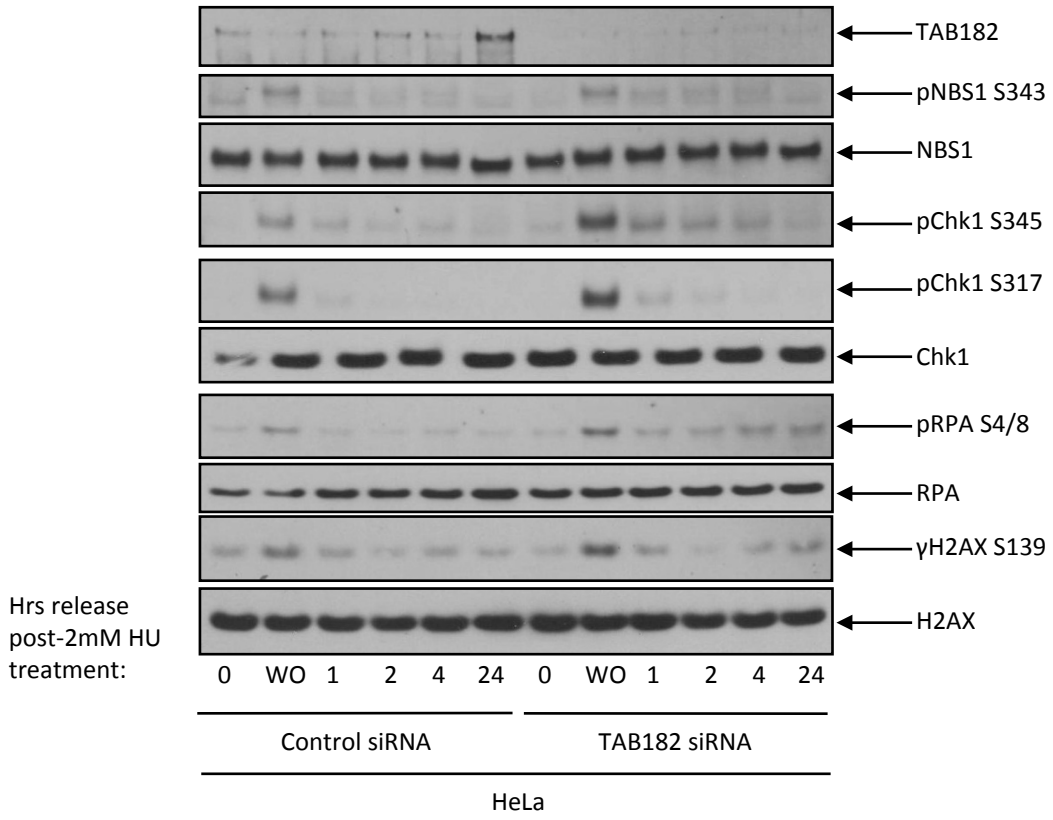

Figure 4.3 Cont'd: DDR Signalling is Increased in TAB182 Depleted Cells Compared to Control Cells following Exposure to IR and HU Treatment, but not after UV-C Irradiation. 50µg of TAB182 depleted or control siRNA treated HeLa cell extracts were immunoblotted for proteins involved in DDR signalling in response to **(A)** 3 Gy IR exposure, **(B)** 5 Jm^{-2} UV-C irradiation or **(C)** 2 hour treatment with 2mM HU, followed by 3 washes in HU-free media and incubation in fresh media for the indicated time-points. TAB182 expression was analysed to assess the efficiency of TAB182 depletion following siRNA treatment. This Western blot is representative of three independent repeats. Wash-out (WO) corresponds to the time-point at which cells were harvested immediately after HU treatment.

not following UV-C irradiation, despite the fact that TAB182 depleted cells are sensitive to UV-C irradiation as shown by previous cell survival assays (Figure 4.2).

4.2.4 Depletion of TAB182 has no Effect on Cell Cycle Progression in HeLa Cells

Activation of the DDR can result in cell cycle arrest and therefore, a number of DDR proteins can directly affect the cell cycle following their activation. To assess whether the depletion of TAB182 had any effect on cell cycle progression in HeLa cells, flow cytometry analysis was performed. To begin with, HeLa cells were transfected with control or TAB182 siRNA and harvested at 0, 24, 48 and 72 hours post siRNA-mediated knockdown in order to ascertain whether knockdown of TAB182 has any effect on cell cycle progression in the absence of DNA damage. Confirmation of TAB182 knockdown was achieved by Western blotting (data not shown). Cells were stained with the DNA stain PI and the cell cycle profile analysed by flow cytometry. There was no observable difference in the cell cycle profiles between control siRNA and TAB182 depleted cells (Figure 4.4A). The data are represented in a graphical format, where the average cell cycle was plotted from three independent experiments (Figure 4.4B).

4.2.5 Cells Depleted of TAB182 Exhibit Delayed Cell Cycle Progression following Exposure to Various DNA Damaging Agents.

Since there was no effect of TAB182 depletion on the cell cycle progression in the absence of DNA damage, we next performed the same experiment but following exposure

(A)

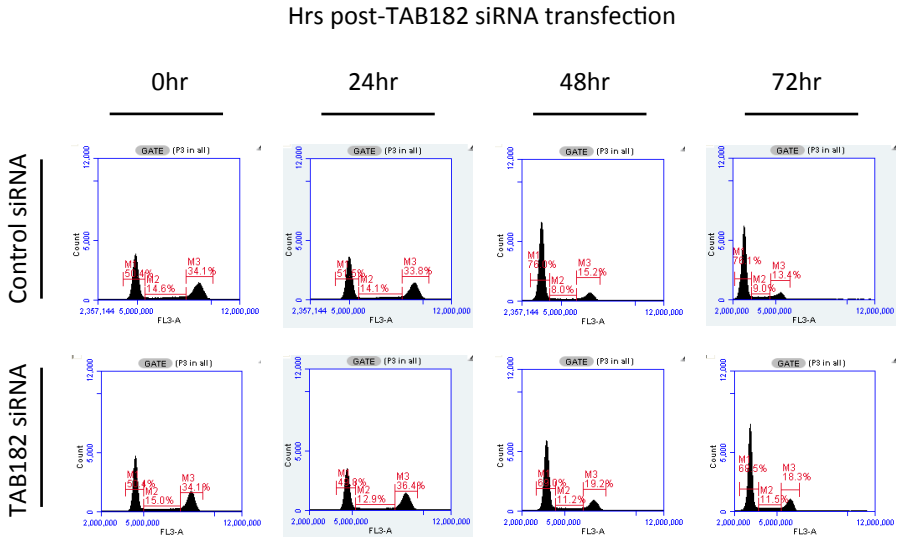

(B)

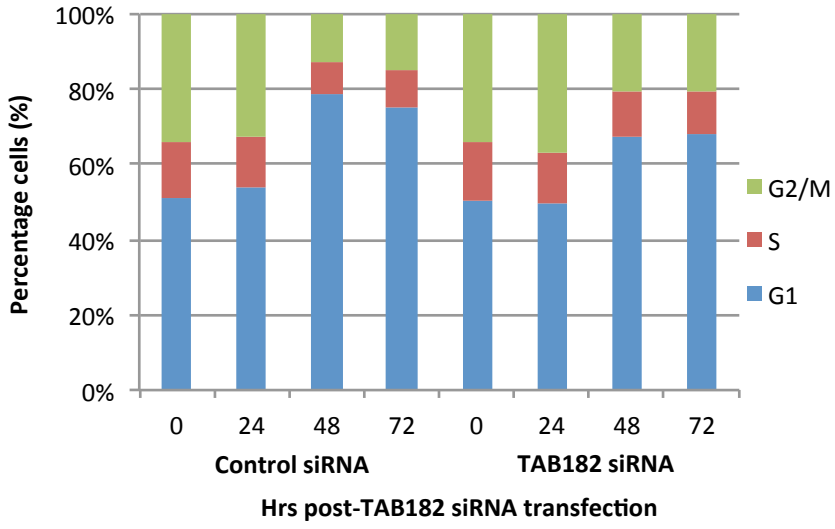

Figure 4.4: Depletion of TAB182 has no Effect on Cell Cycle Progression in HeLa Cells. HeLa cells were transfected with either non-targeting control or TAB182 siRNA, stained with PI and the cell cycle profile was analysed by flow cytometry at various time-points post-transfection. **(A)** is representative of a typical flow cytometry plot observed **(B)** Graph depicts the average cell cycle profile observed in three independent experiments.

to various DNA damaging agents. HeLa cells were transfected with control or TAB182 siRNA, and 48 hours later were exposed to either 3 Gy of IR, 5 Jm^{-2} of UV-C or 2mM HU washed out following 2 hours exposure (wash-out). Samples were harvested and fixed with ethanol at various time-points post-exposure depending on the DNA damaging agent used. Cells were stained with PI and the cell cycle profile analysed by flow cytometry (Figure 4.5). Confirmation of TAB182 knockdown was achieved by Western blotting (data not shown).

Ordinarily, exposure to IR delays the progression through the cell cycle through the activation of cell cycle checkpoints (namely the G1 checkpoint, the S checkpoint and the G2/M checkpoint). Delay in the progression through the cell cycle after exposure to IR occurs in all phases of the cell cycle; however, the delay during the G2 phase of the cell cycle is most noticeable (Lucke-Huhle, Blakely et al. 1979). In control cells, exposure to IR induced a notable delay in G2 phase progression (caused by the activation of the G2/M checkpoint). 24 hours post-IR, the cell cycle arrest induced by IR was attenuated and the cell cycle resumed, 36 hours post-IR exposure the cell cycle profile of control cells was similar to pre-IR exposure levels. Cells transfected with TAB182 siRNA appeared to accumulate at the G2/M phase of the cell cycle to a greater extent than control cells exposed to IR (most notable at 8hrs post-IR). Similarly to control cells, the G2/M arrest seen in TAB182 siRNA transfected cells was also alleviated 24 hours after the initial IR exposure, and the cell cycle profile of TAB182 siRNA treated cells returned to a pre-IR exposure profile 36 hours following IR exposure (Figure 4.5A).

Exposure to UV-C irradiation induced cell cycle arrest in control cells which, however, was most notable as a delay in S phase progression (Figure 4.5B) (Domon and Rauth 1968). This delay in S phase progression was visible by cell cycle profile analysis 8 hours following

UV-C irradiation. 24 hours post-UV-C irradiation, a release from the cell cycle arrest was observed which, in turn, led to the progression through S phase, and then into the G2/M phase of the cell cycle. 48 hours post initial UV-C irradiation, the cell cycle profile of control cells began to return to that of a pre-exposure profile. In TAB182 defective cells, cell cycle arrest following UV-C irradiation exposure was also observed. Interestingly, the percentage of cells in S phase appeared to be two-fold higher in TAB182 knockdown cells than in control cells 4 hours post-UV-C irradiation. A greater percentage of cells in G2/M following TAB182 depletion was also noticeable 24 hrs after UV-C irradiation, compared to control cells. 48 hours after exposure to UV-C irradiation the cell cycle profile of cells treated with TAB182 siRNA had returned to that of a pre-exposure profile (Figure 4.5B).

Control and TAB182 siRNA transfected cells exposed 2mM HU for two hours (wash-out) were harvested at 0, the point of HU removal, 1, 4, 8 and 24 hours post-exposure. Cells were harvested, fixed and stained with PI and the cell cycle profile of the cells was analysed by flow cytometry. In cells treated with 2mM HU for two hours, a cell cycle arrest which was most noticeable as a delay in the G2 phase of the cell cycle was observed. 24 hours post-initial HU exposure, cell cycle arrest induced by HU was alleviated and the cells continued to go through the cell cycle. Interestingly, cells transfected with TAB182 siRNA exhibited an increase in the percentage of cells in G2/M phase when compared to control cells and this was observed at both 8 hours and 24 hours post-2mM HU release (Figure 4.5C).

Taken together, these results show that following exposure to IR, UV-C and 2mM HU (wash-out), TAB182 deficient cells exhibit a delay in cell cycle progression (namely G2/M phase following IR and HU exposure, and S phase following UV-C irradiation). Delays in cell cycle progression in TAB182 deficient cells could indicate a cell cycle checkpoint defect.

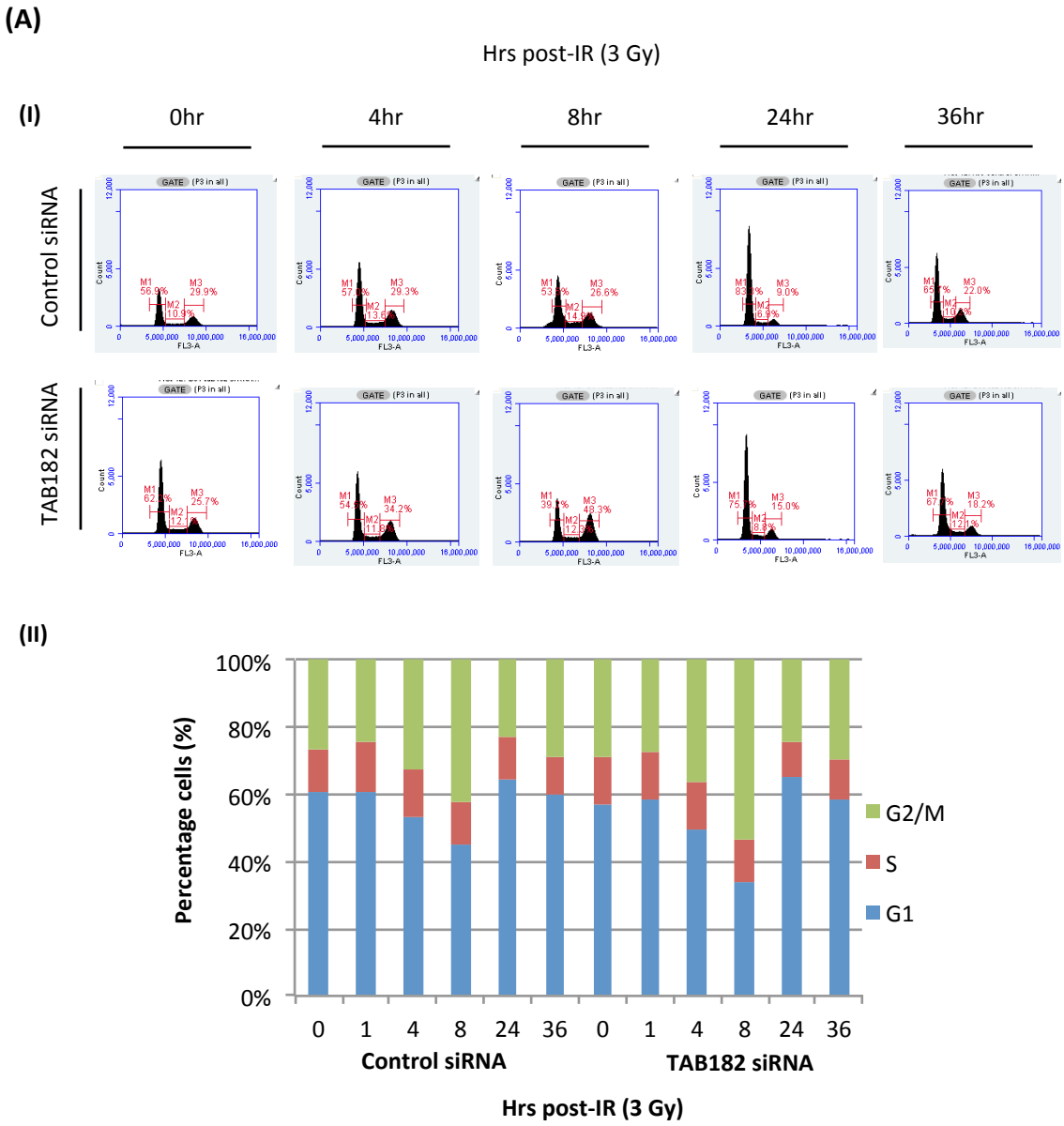

Figure 4.5: Cells Depleted of TAB182 Exhibit Delayed Cell Cycle Progression following Exposure to Various DNA Damaging Agents. HeLa cells were transfected with either non-targeting control or TAB182 siRNA, and 48 hours later mock-exposed or exposed to **(A)** 3 Gy of IR, **(B)** 5 Jm^{-2} UV-C irradiation or **(C)** 2 hour treatment with 2mM HU for 2 hours, followed by 3 washes in HU-free media and incubation in fresh media for the indicated time-points. Cells were harvested for analysis at various time-points post-exposure, stained with PI and the cell cycle profile analysed by flow cytometry. **(I)** Representative images of the flow cytometry plot obtained **(II)** Graph depicting the average cell cycle profile obtained from three independent experiments.

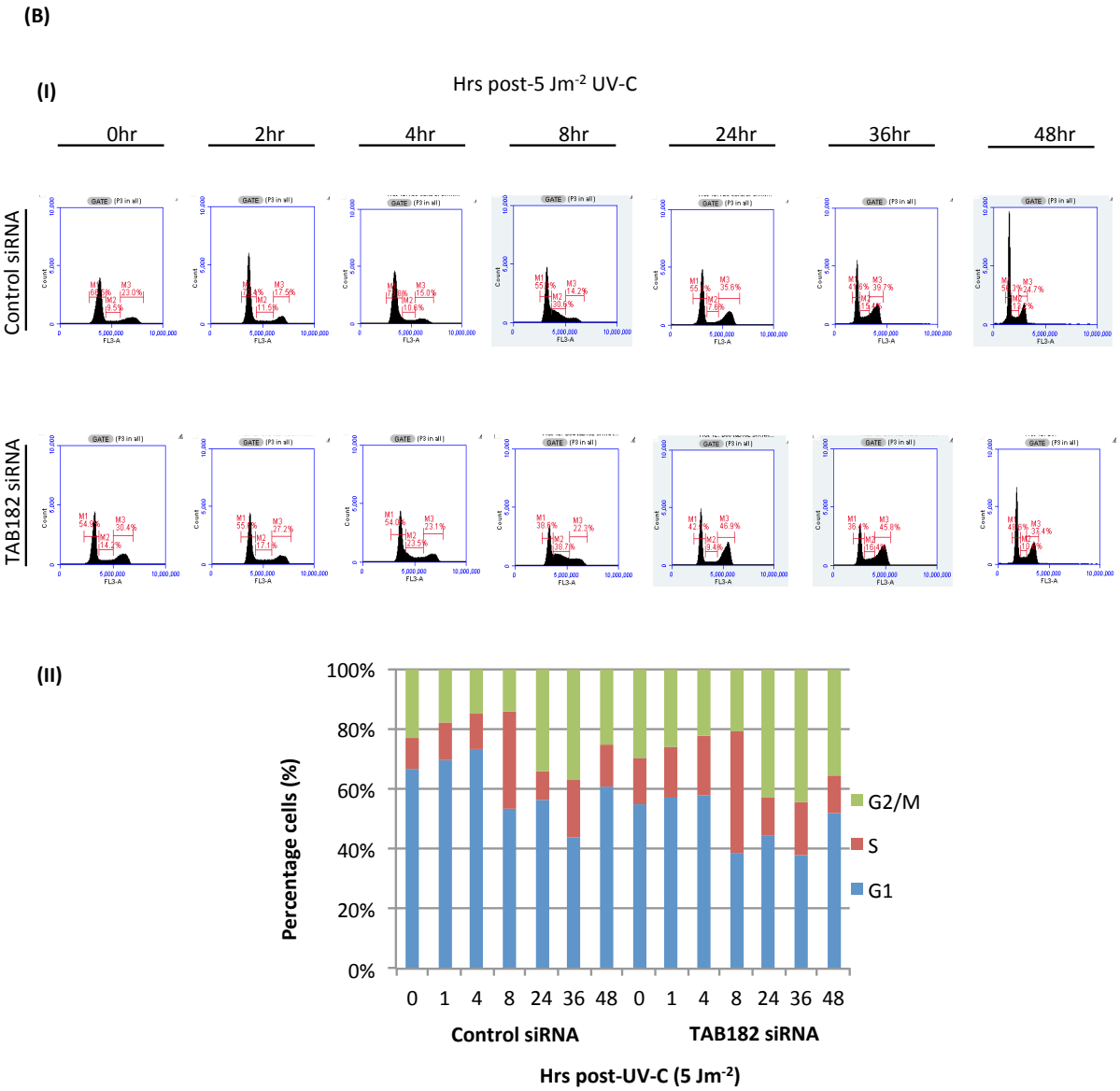

Figure 4.5 Cont'd: Cells Depleted of TAB182 Exhibit Delayed Cell Cycle Progression following Exposure to Various DNA Damaging Agents. HeLa cells were transfected with either non-targeting control or TAB182 siRNA, and 48 hours later mock-exposed or exposed to **(A)** 3 Gy of IR, **(B)** 5 Jm^{-2} UV-C irradiation or **(C)** 2 hour treatment with 2mM HU for 2 hours, followed by 3 washes in HU-free media and incubation in fresh media for the indicated time-points. Cells were harvested for analysis at various time-points post-exposure, stained with PI and the cell cycle profile analysed by flow cytometry. **(I)** Representative images of the flow cytometry plot obtained **(II)** Graph depicting the average cell cycle profile obtained from three independent experiments.

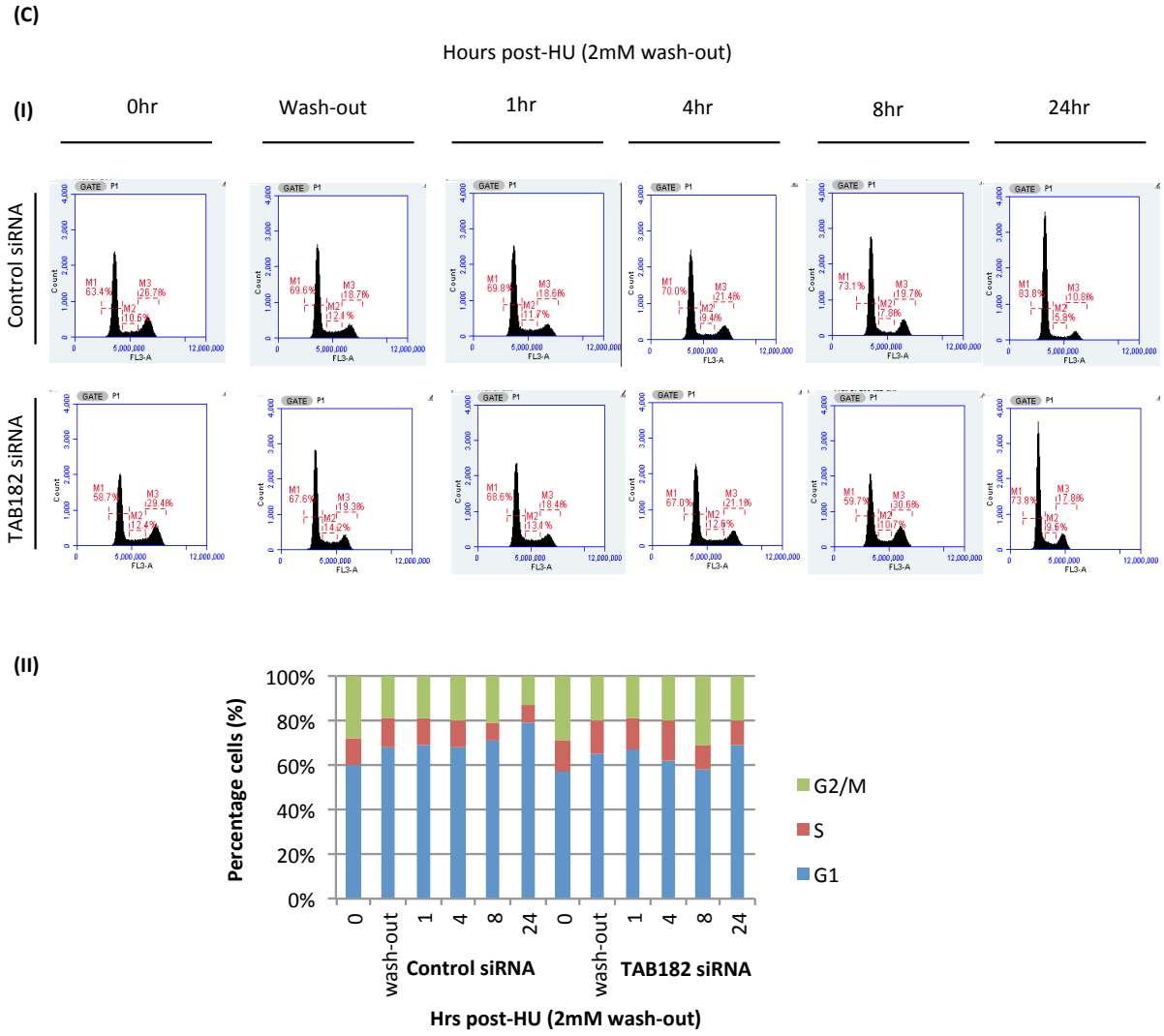

Figure 4.5 Cont'd: Cells Depleted of TAB182 Exhibit Delayed Cell Cycle Progression following Exposure to Various DNA Damaging Agents. HeLa cells were transfected with either non-targeting control or TAB182 siRNA, and 48 hours later mock-exposed or exposed to **(A)** 3 Gy of IR, **(B)** 5 Jm^{-2} UV-C irradiation or **(C)** 2 hour treatment with 2mM HU for 2 hours, followed by 3 washes in HU-free media and incubation in fresh media for the indicated time-points. Cells were harvested for analysis at various time-points post-exposure, stained with PI and the cell cycle profile analysed by flow cytometry. **(I)** Representative images of the flow cytometry plot obtained **(II)** Graph depicting the average cell cycle profile obtained from three independent experiments.

4.2.6 The G2/M Checkpoint is Proficient in TAB182 Depleted Cells following Exposure to Various DNA Damaging Agents.

Since the cell cycle profile of cells deficient in TAB182 expression revealed some accumulation in G2/M phase of the cell cycle following exposure to various types of DNA damaging agents, we also wanted to examine whether the G2/M checkpoint was intact. HeLa cells were treated with either control or TAB182 siRNA, and 48 hours later exposed to either 3 Gy of IR, 5 Jm^{-2} of UV-C or 2mM HU (wash-out). Samples were harvested and fixed at various time-points post-exposure depending on the DNA damaging agent used. Cells were stained with an antibody recognising Histone H3 phosphorylated on Serine 10 (phospho-H3 Ser10) as a marker of cells entering mitosis. The cell cycle profiles of the samples were then analysed by flow cytometry (Figure 4.6). Confirmation of TAB182 knockdown was achieved by Western blotting (data not shown).

1-4 hours following IR, the percentage of control cells entering mitosis (shown by phospho-H3 (Ser10) staining) was steadily reduced as the G2/M checkpoint became activated. 24 hours after the initial IR exposure, the percentage of cells in mitosis began to increase and 36 hours later it reached pre-exposure levels. Importantly, there was no significant difference in the percentage of cells in mitosis between TAB182 deficient and control cells at any of the time-points examined (Figure 4.6A).

Within 4-8 after UV-C irradiation at 5 Jm^{-2}, the percentage of cells in mitosis decreased as a consequence of the activation of the G2/M checkpoint, with a gradual release from the checkpoint becoming evident 24 to 48 hours after UV-C irradiation. In TAB182 siRNA treated cells, there was a slight increase in the percentage of cells in mitosis throughout the time-course following UV-C irradiation when compared to control siRNA

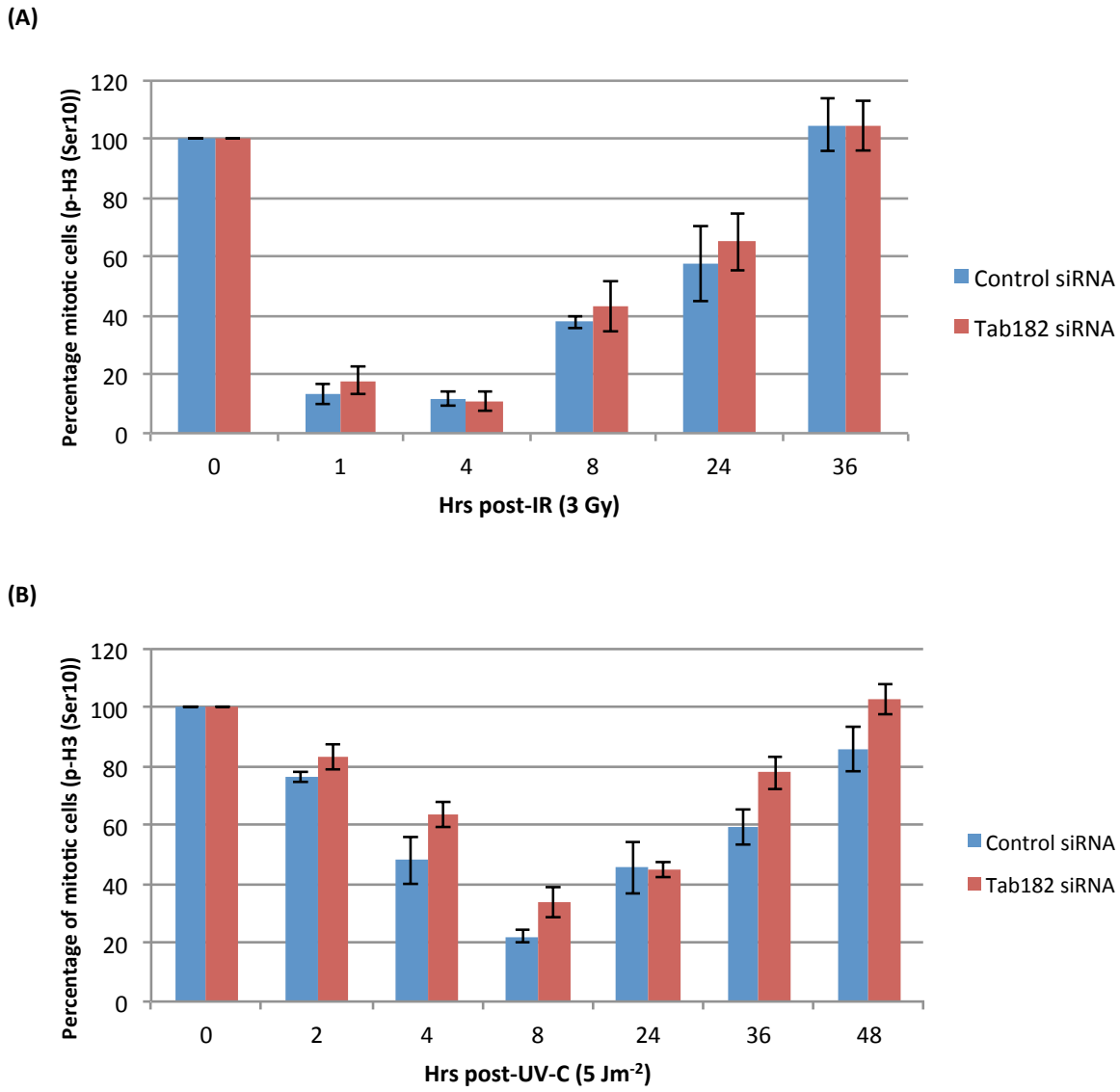

Figure 4.6: The G2/M Checkpoint is Proficient in TAB182 Depleted Cells following Exposure to Various DNA Damaging Agents. HeLa cells were transfected with either control or TAB182 siRNA and 48 hours post-transfection exposed to either **(A)** 3 Gy of IR, **(B)** 5 Jm^{-2} of UV-C or **(C)** 2mM HU wash-out (washed out after 2 hours of incubation). Following treatment, the cells were harvested for analysis at various time-points post exposure, stained with phospho-H3 (Ser10) antibody as a marker of cells entering mitosis and analysed by flow cytometry. Graphs are representative of three independent experiments, error bars represent SEM.

(C)

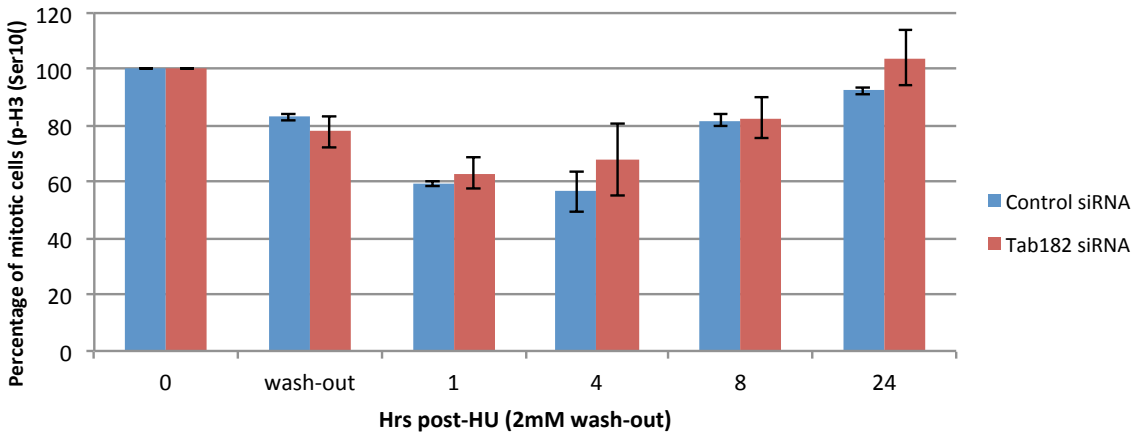

Figure 4.6 Cont'd: The G2/M Checkpoint is Proficient in TAB182 Depleted Cells following Exposure to Various DNA Damaging Agents. HeLa cells were transfected with either control or TAB182 siRNA and 48 hours post-transfection exposed to either **(A)** 3 Gy of IR, **(B)** 5 Jm^{-2} of UV-C or **(C)** 2mM HU wash-out (washed out after 2 hours of incubation). Following treatment, the cells were harvested for analysis at various time-points post exposure, stained with phospho-H3 (Ser10) antibody as a marker of cells entering mitosis and analysed by flow cytometry. Graphs are representative of three independent experiments, error bars represent SEM.

treated cells. Since this difference was mild it was concluded that the G2/M checkpoint following UV-C irradiation was intact (Figure 4.6B).

In control siRNA treated cells exposed to 2mM HU (wash-out), the percentage of cells in mitosis decreased following initial exposure and continued to decrease up to 4 hours post-exposure (Figure 4.6C). This was expected and was indicative of the activation of the G2/M checkpoint following acute, high-dose HU exposure. 8 hours after HU exposure and release, the percentage of cells in mitosis increased and by 24 hours, the percentage of cells in mitosis had reached pre-exposure levels. In cells depleted of TAB182 and exposed to 2mM HU, the same reduction in the percentage of cells in mitosis up to 4 hours post-exposure was observed, followed by a comparable increase in the percentage of cells in mitosis after 8 hours initial HU exposure, recovering to pre-exposure levels following 24 hours (Figure 4.6C).

Taken together, these results show that the G2/M checkpoint in TAB182 depleted cells is proficient following IR, UV-C irradiation and HU treatment. Since cells depleted of TAB182 appeared to accumulate in G2/M phase of the cell cycle following exposure to various types of DNA damaging agents, it could also be that there is a problem with the G1 checkpoint in these cells.

4.2.7 TAB182 Depletion has no Effect on Replication Fork Progression in the Absence of Replication Stress or following Release from HU.

Since the previous results showed potential cell cycle progression abnormalities in TAB182 deficient cells in response to DNA damage without any G2/M checkpoint defects, these could reflect problems during S phase/DNA replication. To assess DNA replication speed in TAB182 depleted cells, DNA fibre analysis was performed by the immunolabelling

of DNA using the DNA analogues CldU and IdU. HeLa cells were transfected with control or TAB182 siRNA and 48 hours later, CldU was added to the cells to label the DNA during replication. CldU was removed from the cells and the cells were subsequently mock-treated or treated with 2mM HU to induce replication stress. Following 2 hours of HU treatment, HU was removed from the cells and IdU was added in HU-free media to label nascent DNA synthesis. DNA replication speed was calculated by measuring the lengths of the CldU and IdU tracks using Image J software. The lengths obtained in Image J were converted into micrometers using the scale bars on the microscope (Figure 4.7). Confirmation of TAB182 knockdown was achieved by Western blotting (data not shown).

In control cells the average fork speed before exposure to HU was 1.45kb per minute (CldU staining). In TAB182 depleted cells, there was little significant difference in average fork speed (1.22kb per minute) compared to control cells before exposure to HU (CldU staining), showing that knockdown of TAB182 alone does not affect replication fork kinetics. In control siRNA treated cells the average fork speed following exposure to HU was reduced to 0.54 kb per minute (IdU staining), showing that treatment with HU followed by a 45 minute incubation in HU-free media induces replication stress and therefore slows DNA replication. Similarly, in TAB182 deficient cells, the average fork speed following HU treatment was reduced to 0.47 kb per minute (measured by IdU staining), showing that there was no significant difference in the replication fork kinetics in these cells compared to control siRNA cells after HU treatment (Figure 4.7).

From this experiment we concluded that TAB182 defective cells replicate their DNA as efficiently as control cells both in the absence and presence of replication stress induced by HU.

(A)

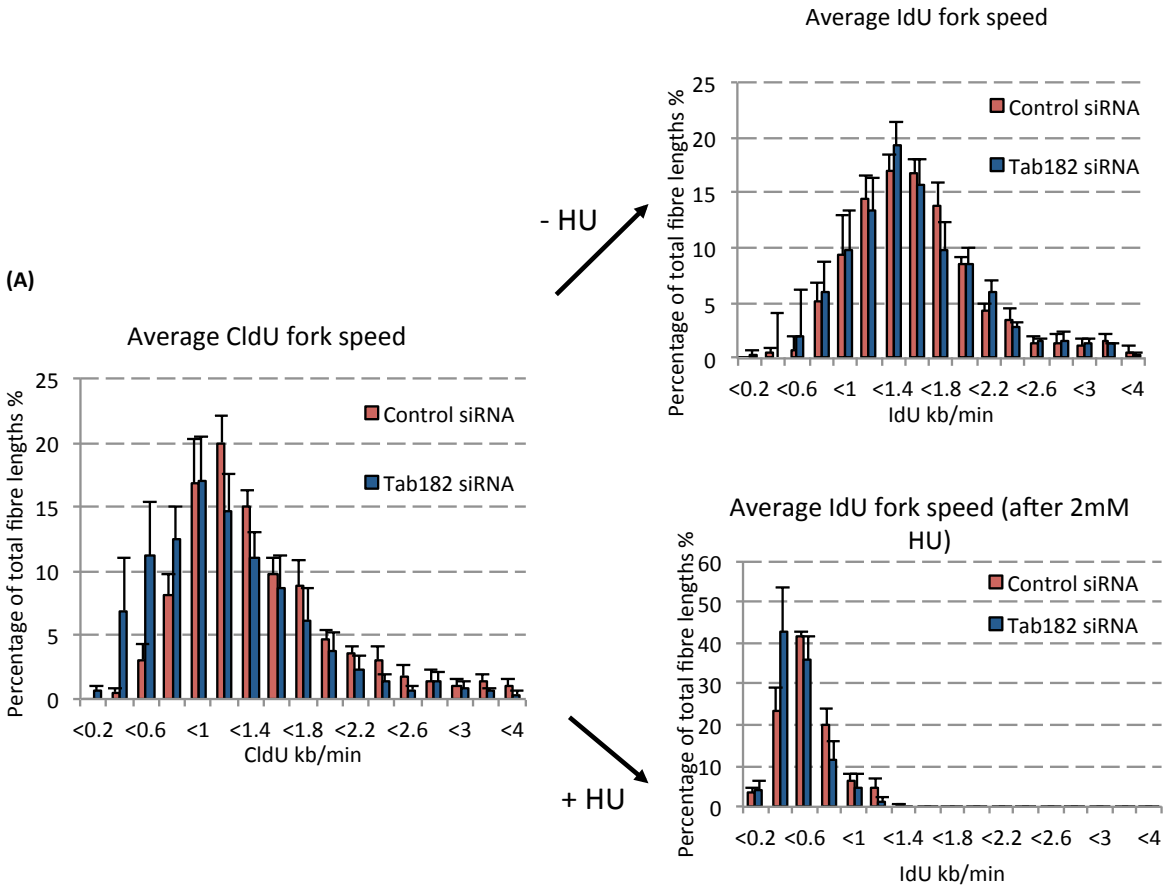

(B)

Control siRNA Untreated		TAB182 siRNA Untreated		Control siRNA 2mM HU		TAB182 siRNA 2mM HU	
CldU kb/min average	IdU kb/min average	CldU kb/min average	IdU kb/min average	CldU kb/min average	IdU kb/min average	CldU kb/min average	IdU kb/min average
1.45	1.60	1.22	1.48	1.45	0.54	1.16	0.47

Figure 4.7: TAB182 Depletion has no Effect on Replication Fork Progression in the Absence of Replication Stress or following Release from HU. HeLa cells were transfected with control or TAB182 siRNA. 48 hours post-tranfection, cells were incubated with CldU for 20 minutes, followed by mock-treatment or treatment with 2mM HU for 2 hours. Following HU treatment, cells were incubated with IdU for 45 minutes. DNA was spread onto slides, probed with the appropriate antibodies and visualised by fluorescence microscopy. DNA fibre speed was calculated by measuring the lengths of the CldU and IdU tracks using Image J software. **(A)** Graphs represent the average CldU fork speed (before HU exposure) and average IdU fork speed (HU exposure). **(B)** Table shows the average CldU and IdU fork speeds in control siRNA and TAB182 siRNA treated cells mock-exposed or exposed to HU. These data are representative of three independent experiments. Error bars represent SEM.

4.2.8 Cells Depleted of TAB182 Display Excessive New Origin Firing and Increased Fork Restart following Release from HU

To further investigate whether TAB182 deficient cells exhibit any irregularities during DNA replication, DNA fibre analysis was performed by analysing the structures of DNA fibres following replication stress. HeLa cells were transfected with control or TAB182 siRNA and 48 hours later were incubated with media containing the DNA analogue CldU. Following CldU incorporation, the cells were mock-treated or treated with 2mM HU for 2 hours, the HU was then removed and the cells were further incubated with HU-free media containing IdU for 45 minutes. Cells were fixed, spread onto slides and incubated with antibodies against CldU and IdU. DNA was viewed under the microscope and the observed DNA structures recorded (Figure 4.8). Confirmation of TAB182 knockdown was achieved by Western blotting (data not shown).

DNA tracks were analysed and categorised into the following structures. Ongoing forks represent forks that have continued to replicate following the removal of HU and are denoted by a CldU (red) together with IdU (green) tracks. 1st label origins represent an origin of replication that occurred during the first label and which continued to replicate following the removal of HU in both directions, these are denoted by a CldU (red) track with IdU (green) tracks on either side. 2nd label origins represent new origins of replication that occurred during the second label and are denoted by an IdU (green) track alone. 1st label terminations represent forks that collapsed during the first label and did not restart during the second label. They are denoted by a CldU (red) track alone. 2nd label terminations represent two forks that were ongoing and replicating during the first label and have converged and terminated during the second label. They are denoted by an IdU track (green)

with two CldU (red) tracks on either side. The different fibre structures are further represented in Figure 4.8A. DNA fibre structures were calculated as a percentage of total number of CldU positive structures counted.

In control, undamaged HeLa cells subjected to DNA fibre structure analysis, the following distribution of structures were obtained; 70-80% of DNA fibre structures were 'ongoing forks', approximately 5% of forks were '1st label origins', 10% of forks were '2nd label origins', 10% of forks were '1st label terminations' and 5% of forks were '2nd label terminations' (78%, 5%, 8%, 8% and 5% respectively (Figure 4.8B)). Following treatment with HU, these cells generally displayed the following DNA structure changes. 'Ongoing forks' decreased to approximately 65% due to an increase in the percentages of other DNA structures in response to HU treatment (63% in Figure 4.8B). '1st label origins' remained unchanged at approximately 5% of DNA structures (5% in Figure 4.8B). '2nd label origins' decreased to 3% of forks (3% in Figure 4.8B), this is because the induction of new origins following replicative stress is normally prevented by the S phase checkpoint to prevent deleterious DNA replication. '1st label terminations', i.e. stalled ongoing forks, increased to approximately 30% (27% in Figure 4.8B), due to the replication stress exhibited during the HU treatment stalling ongoing forks in order to prevent deleterious DNA replication. Finally, '2nd label terminations' were reduced from approximately 5% to 3% (3% in Figure 4.8B), due to ongoing DNA replication decreasing and, therefore, the termination of DNA replication also decreasing as a consequence.

In undamaged, TAB182 deficient cells, the distribution of DNA fibre structures was comparable to undamaged, control cells, the percentage of ongoing forks was 79%, 1st label origins were 5%, 2nd label origins and 1st label terminations were 9% and 8% respectively,

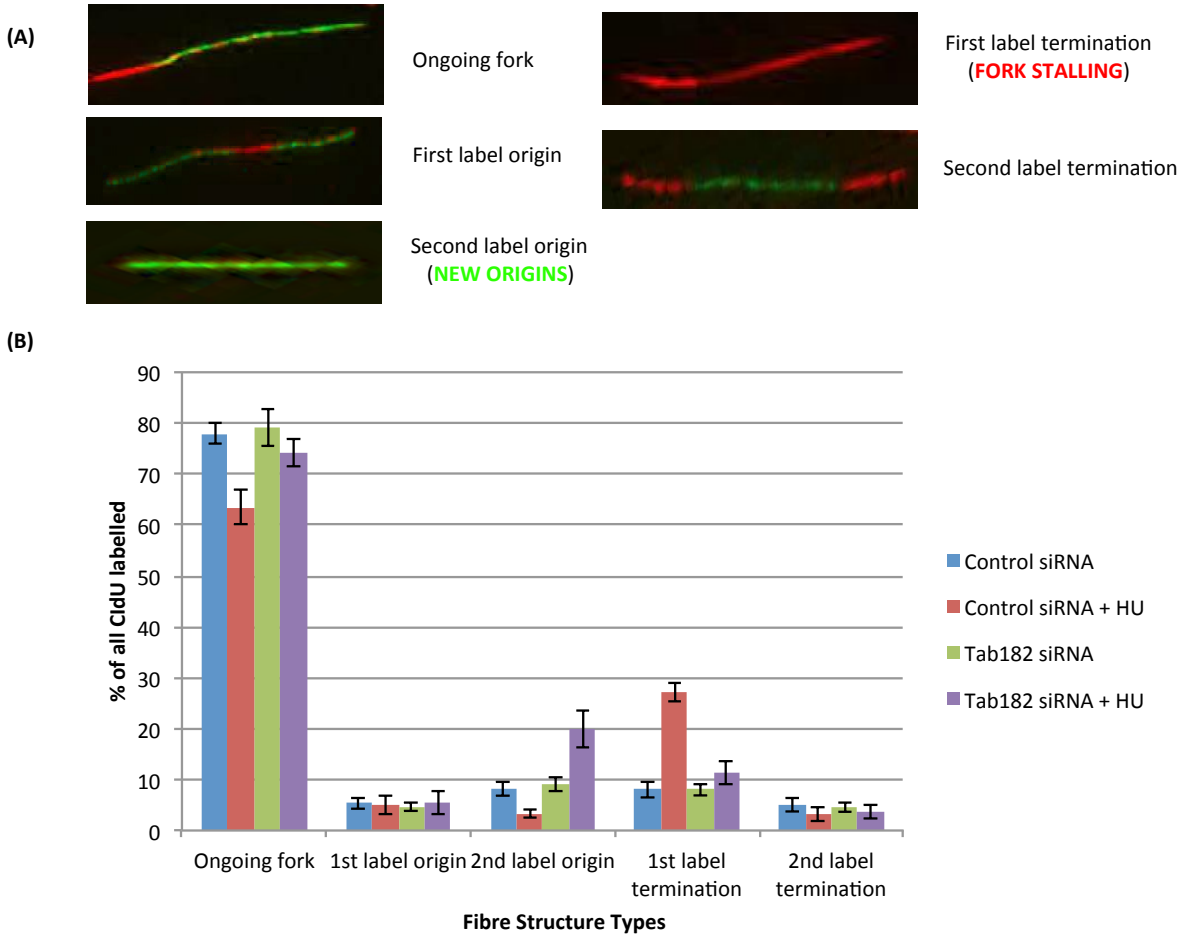

Figure 4.8: Cells Depleted of TAB182 Display Excessive New Origin Firing and Increased Fork Restart following Release from HU. HeLa cells were transfected with control or TAB182 siRNA. 48 hours post-transfection, the cells were incubated with CldU for 20 minutes, followed by mock-treatment or treatment with 2mM HU for 2 hours. Following HU treatment, cells were incubated with HU-free media containing IdU for 45 minutes. DNA was spread onto slides, probed with the appropriate antibodies and visualised by fluorescence microscopy. **(A)** Diagram illustrates the various types of replication structures scored. **(B)** Graph shows the fibre structures as a percentage of all CldU labelled structures. Error bars represent SEM. These data are representative of three independent experiments.

and 2nd label terminations were 4% (Figure 4.8B). These data suggest that the knockdown of TAB182 has no effect on DNA replication in the absence of replicative stress. In TAB182 depleted cells treated with HU, the percentage of ongoing forks decreased from 79% in undamaged cells to only 74%, which was not comparable to control cells where the reduction was more significant (78% to 63%). The percentage of 1st label origins in TAB182 deficient cells was 5% and was similar to control HU exposed cells. Interestingly, the percentage of 2nd label origins following HU treatment in TAB182 deficient cells increased to 20%, in contrast to control cells in which it was 3%, suggesting that TAB182 deficient cells excessively fire new origins. Furthermore, TAB182 defective cells displayed no significant increase in the percentage of 1st label terminations following HU (11% in TAB182 depleted cells vs 27% in control cells), suggesting that these cells may be defective at fork stalling/collapse in response to HU, the reason for this being currently unknown. Finally, the percentage of 2nd label terminations observed in TAB182 deficient cells was 3%, which was comparable to the percentage of 2nd label terminations observed in control cells (Figure 4.8).

Taken together, these results demonstrate that TAB182 depleted cells exhibit excessive new origin firing as well as increased fork recovery following release from HU, suggesting that TAB182 suppresses new origin firing and prevents fork restart following replication stress.

4.2.9 DNA Fibre Structures in TAB182 Deficient Cells following Replication Stress in the Absence of Chk1 and ATR

Since TAB182 deficient cells exhibit irregularities during DNA replication in the presence of replication stress, the next aim was to understand how these defects occurred.

As there had already been an indication that they may be attributed to defects in the cell cycle checkpoint regulation, DNA fibre analysis was performed as before, but this time we also made use of the checkpoint Chk1 and ATR inhibitors.

To this end, HeLa cells were transfected with either control or TAB182 siRNA and 48 hours later, were incubated in media containing CldU and subsequently mock-treated or treated with HU or both HU and 1µM Chk1 inhibitor for 2 hours. Following HU or both HU and Chk1 inhibitor treatment, the cells were then incubated with HU-free media containing IdU. After this incubation the cells were then fixed, spread onto slides and incubated with antibodies against CldU and IdU. DNA was viewed under the microscope and DNA structures observed recorded (Figures 4.9 and 4.10). Confirmation of TAB182 knockdown was achieved by Western blotting (data not shown).

Since we were mainly interested in '2nd label origins' and '1st label terminations' at this stage none of the other structures will be referred to in this section (see Figure 4.9 for more detailed results). In undamaged control cells, as previously observed, the percentage of 2nd label origins decreased following HU treatment from 11% to 3% due to the activation of the S phase checkpoint that suppresses new origin firing (Maya-Mendoza, Petermann et al. 2007, Petermann, Woodcock et al. 2010). In the same cells treated with both HU and Chk1 inhibitor, the percentage of 2nd label origins increased from 3% to 41%, as expected, since Chk1 activation, known to suppress new origin firing, was inhibited. The percentage of 1st label terminations in control cells increased with HU treatment from approximately 9% to 31% and up to 55% when the cells were also incubated with the Chk1 inhibitor. This suggested that Chk1 inhibition following HU treatment compromises replication fork restart

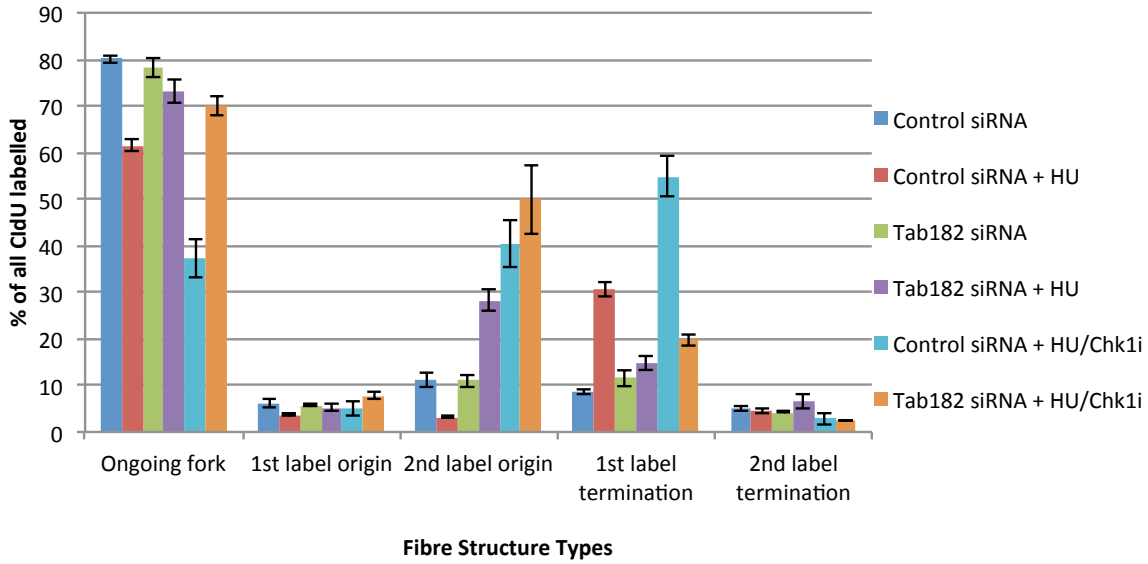

Figure 4.9: DNA Fibre Structures in TAB182 Deficient Cells following Replication Stress in the Absence of Chk1. HeLa cells were transfected with control or TAB182 siRNA. 48 hours post-transfection, the cells were incubated with CldU for 20 minutes, followed by mock-treatment or treatment with 2mM HU for 2 hours together with 1µM of Chk1 inhibitor. Following HU treatment, the cells were incubated in HU-free media containing IdU for 45 minutes. DNA was spread onto slides and staining processed as in Figure 4.8. The graph shows the DNA fibre structures as a percentage of all CldU labelled structures. Error bars represent SEM. These data are representative of three independent experiments.

in control cells in agreement with previous reports (Figure 4.9) (Feijoo, Hall-Jackson et al. 2001, Petermann, Orta et al. 2010).

Similarly to the previous results obtained in Section 4.2.8, the percentage of 2nd label origins in TAB182 deficient cells was higher than that in control cells following HU treatment (3% in control vs 28% in TAB182 deficient cells). Furthermore, inhibition of Chk1 during exposure to HU led to a further increase in the percentage of 2nd label origins in both control and TAB182 deficient cells, but more importantly, the difference was marginal (40% in control cells vs 50% in TAB182 depleted cells). This suggested that 1) inhibiting Chk1 activity attenuated the difference observed in new origin firing between control and TAB182 deficient cells following release from HU and 2) that Chk1 is important for suppressing new origin firing in response to HU in both control and TAB182 depleted cells (Figure 4.9).

Addition of the Chk1 inhibitor during HU treatment led to a marked increase in the percentage of 1st label terminations in control cells compared to those treated with HU alone (31% to approximately 55%). Strikingly, the percentage of 1st label terminations in TAB182 deficient cells treated with both HU and Chk1 inhibitor was no different than those treated with HU alone (from 20% to 15%, respectively). Thus, inhibition of Chk1 in TAB182 depleted cells had neither any significant effect on 1st label terminations nor any impact on the ability of these cells to promote replication fork restart. This suggests that TAB182 is required for fork stalling/collapse following release from fork blocking and prevents replication fork restart even in the absence of Chk1 activity (Figure 4.9).

To examine the effects of ATR inhibition on TAB182 deficient cells, HeLa cells were treated with either control or TAB182 siRNA and 48 hours later, mock-treated or treated with HU or HU and 5μM ATR inhibitor. Following HU or both HU and ATR inhibitor

treatment, the cells were incubated with HU-free media containing IdU. Cells were fixed, spread onto slides and incubated with antibodies against CldU and IdU. DNA was viewed under the microscope and DNA structures observed recorded (Figure 4.10).

Since, in this experiment, we are mainly interested in '2nd label origins' and '1st label terminations' at this stage none of the other structures will be referred to in this section (see Figure 4.10 for more detailed results). As previously observed, the percentage of 2nd label origins in control cells decreased following HU treatment. Treatment with both HU and ATR inhibitor led to an increase in 2nd label origins compared to those exposed to HU alone from 3% to 46% as expected since ATR is known to suppress new origin firing via Chk1 (Tercero and Diffley 2001, Heffernan, Unsal-Kacmaz et al. 2007). Regarding the percentage of 1st label terminations in control cells, HU treatment led to an increase from 9% to 31% with a further increase in the percentage of fork stalling to up to 49% upon ATR inhibition as ATR is known to stabilise replication forks (see Section 1.2.4.2.2)(Figure 4.10).

We previously observed that the percentage of 2nd label origins increased following HU treatment in TAB182 deficient cells compared to control cells following release from HU (3% in control cells vs 28% in TAB182 depleted cells). Notably, control and TAB182 depleted cells exposed to both HU and ATR inhibitor displayed a similar percentage of 2nd label origins (46% and 47%, respectively). Similarly to Chk1, ATR inhibition in response to HU treatment completely abrogated the difference between the two cell lines by increasing the percentage of new origin firing to approximately 45% in both cell lines. This was also the case for the decreased amount of 1st label terminations observed in TAB182 deficient cells in response to HU (15%) compared to control cells (12%) as addition of the ATR inhibitor resulted in an

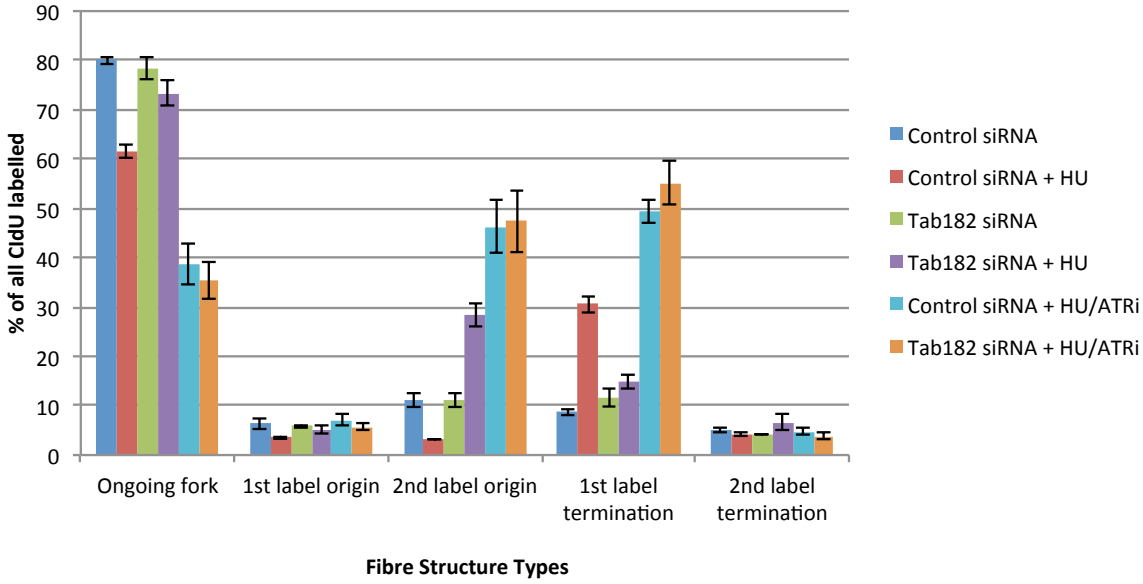

Figure 4.10: DNA Fibre Structures in TAB182 Deficient Cells following Replication Stress in the Absence of ATR. HeLa cells were transfected with control or TAB182 siRNA. 48 hours post-transfection, the cells were incubated with CldU for 20 minutes, followed by mock-treatment or treatment with 2mM HU for 2 hours together with 5µM of ATR inhibitor. Following HU treatment, the cells were incubated in HU-free media containing IdU for 45 minutes. DNA was spread onto slides and staining processed as in Figure 4.8. The graph shows the DNA fibre structures as a percentage of all CldU labelled structures. Error bars represent SEM. These data are representative of three independent experiments.

increase in replication fork stalling/collapse of approximately 50% in both cell lines (Figure 4.10).

Taken together, these results show that Chk1 and ATR activity is important for suppressing new origin firing in both control and TAB182 defective cells. In addition, TAB182 is important for fork stalling/collapse even in the absence of Chk1 activity but not upon inhibition of ATR.

4.2.10 DNA Fibre Structures in TAB182 Deficient Cells following Replication Stress in the Absence of CDK

Based on the DNA fibre data from Figure 4.8, we wondered whether the elevated new origin firing observed in TAB182 deficient cells compared to control cells following release from HU (20% vs 3%), was occurring in order to rescue DNA replication in TAB182 depleted cells in response to replication stress. For this reason the same experiments were performed but this time in the presence of a CDK 1/2 inhibitor that suppresses new origin firing. HeLa cells were treated with control or TAB182 siRNA and 48 hours later, stained with CldU and mock-treated or treated with HU or treated with both HU and 25µM CDK 1/2 inhibitor III. The cells were then incubated with HU-free media containing IdU, harvested, fixed, spread onto slides and incubated with antibodies against CldU and IdU (Figure 4.11). Confirmation of TAB182 knockdown was achieved by Western blotting (data not shown).

We focused on '2nd label origins' and '1st label terminations' (see Figure 4.11 for more detailed results). As before, control cells exhibited a decrease in the percentage of 2nd label origins following exposure to HU when compared to mock-treated cells (10% to 2%). Incubation of these cells with the CDK inhibitor during HU treatment led to a further a decrease in the percentage of 2nd label origins by 1% since CDKs are required for new origin

firing (Petermann, Woodcock et al. 2010). In TAB182 deficient cells, HU treatment led to an increase in 2nd label origins from 2% to 21% but this was completely suppressed following incubation with the CDK inhibitor that led to a marked reduction down to control levels. Thus, inhibition of CDK during replication stress almost completely suppressed new origin firing in both control and TAB182 depleted cells as expected. This showed that CDK inhibition is able to suppress excessive new origin firing observed in TAB182 deficient cells following release from HU and that the defect in new origin firing suppression is therefore dependent on CDK function.

The 1st label termination percentage in untreated control cells was 11% and increased to 34% following HU treatment and remained unaltered following CDK inhibition (Figure 4.11). This was not unexpected since CDK inhibition has no documented effect on replication restart (Petermann, Orta et al. 2010). More importantly, since the percentage of 1st label terminations in TAB182 deficient cells exposed to both HU and CDK inhibitor was comparable to TAB182 deficient cells treated with HU alone (15%), it can be concluded that the defect in terminations observed in TAB182 deficient cells is not dependent on CDK function (Figure 4.11).

Taken together, these data show that the excessive new origin firing defect observed in TAB182 deficient cells is dependent on CDK function but that the elevated fork recovery in TAB182 depleted cells is not due to increased new origin firing.

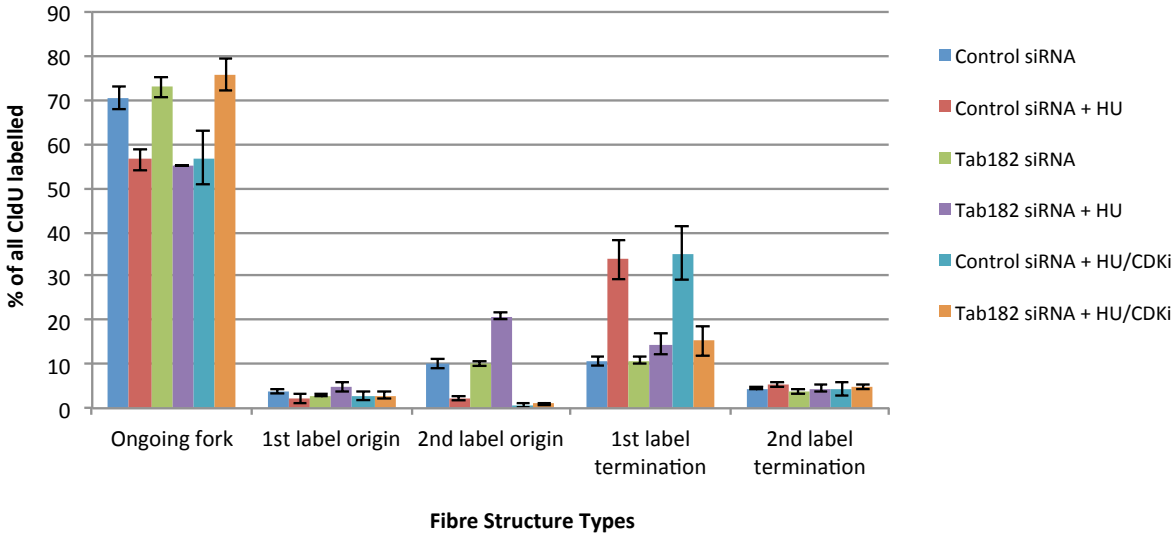

Figure 4.11: DNA Fibre Structures in TAB182 Deficient Cells following Replication Stress in the Absence of CDK. HeLa cells were transfected with control or TAB182 siRNA. 48 hours post-transfection, the cells were incubated with CldU for 20 minutes, followed by mock-treatment or treatment with 2mM HU for 2 hours together with 25µM of CDK 1/2 inhibitor III. Following HU treatment, the cells were incubated in HU-free media containing IdU for 45 minutes. DNA was spread onto slides and staining processed as in Figure 4.8. The graph shows the fibre structures as a percentage of all CldU labelled structures. Error bars represent SEM. These data are representative of three independent experiments.

4.2.11 The C-Terminal Fragment of TAB182 Interacts with Tankyrase 1, Chk1 and Aurora Kinase *in Vitro.*

To gain further insight into the role of TAB182, a series of GST pull-down assays were performed with a panel of DDR and cell cycle proteins using antibodies that were already available in the lab. HeLa cell lysates were incubated with a C-terminal fragment of TAB182 tagged to GST (referred to as GST-TAB182C), spanning amino acids 824-867 fused to amino acids 1221-1729 of TAB182 (Figure 1.16) (Seimiya and Smith 2002). Cell lysates were also incubated with GST alone as a non-specific binding control, and cell lysate alone was run as a positive control. Protein complexes were captured using glutathione-agarose beads, subjected to SDS-PAGE and Western blotting (Figure 4.12). Protein complexes isolated using HeLa cell lysates were immunoblotted with a panel of antibodies involved in the DDR and cell cycle control. The analysis showed that the C-terminal fragment of TAB182 interacts with Tankyrase 1, Chk1 and Aurora kinase *in vitro* (Figure 4.12). Table 4.1 shows the proteins that were found to not be associated with TAB182C *in vitro.*

4.2.12 TAB182 does not Localise to DNA Damage Foci following HU or IR Exposure

It is well established that DNA damage can be indirectly observed through the detection of the accumulation of proteins at regions of DNA damage which form distinct sites known as foci. To determine whether TAB182 is relocalised to DNA damage foci following DNA damage, immunofluorescence analysis was performed. A TAB182 DNA construct (eGFPC3-*TAB182*) was made by performing a PCR reaction from cDNA encompassing the genomic sequence of TAB182 (Section 2.5.6). The PCR product was ligated into a construct containing GFP. eGFPC3-*TAB182* was transfected, along with an empty

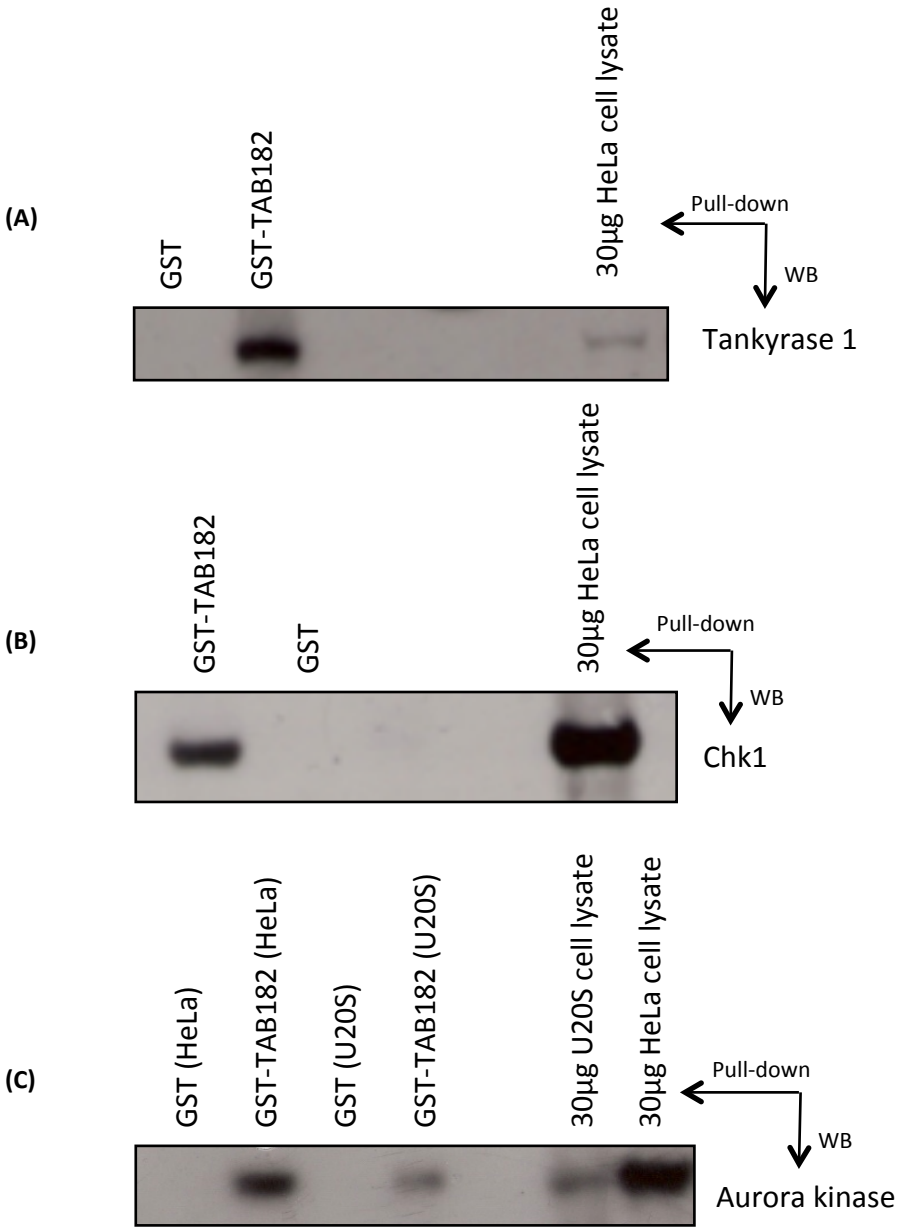

Figure 4.12: The C-Terminal Fragment of TAB182 Interacts with Tankyrase 1, Chk1 and Aurora Kinase *in Vitro.* HeLa and U20S cell lysates were incubated with GST-TAB182C, together with GST alone (non-specific binding control) or cell lysate alone (positive control). Protein complexes were captured by glutathione-agarose beads, subjected to SDS-PAGE and Western blotting with antibodies against **(A)** Tankyrase 1 **(B)** Chk1 and **(C)** Aurora kinase. These Western blots are representative of three independent repeats.

GST-TAB182C Non-Interacting Proteins
53BP1
ATR
BLM
Chk2
CtIP
DNA-PK
hnRNPUL1
Ku80
MDC1
Mre11
NBS1
p53
PCNA
Rad9
Rad18
Rad50
Rad51
TOPBP1

Table 4.1: GST-TAB182C Non-Interacting Proteins. Table to illustrate the proteins that do not interact with the C-terminal part of TAB182 following GST pull-down assays using GST-TAB182C.

eGFPC3 construct as a negative control, into HeLa cells and left for 48 hours. 48 hours post-transfection, the cells were exposed to 2mM HU (left-in throughout the course of the experiment) or 3 Gy of IR. 2 hours post-exposure, the cells were then fixed, permeabilised and probed with antibodies against γH2AX (Figure 4.13).

Mock-exposed, GFP-TAB182 transfected cells exhibited a pan-cellular staining pattern that appeared to be concentrated around the nucleus. It can be seen from the γH2AX staining that DNA damage foci are formed in both HU and IR exposed cells. Following exposure to either IR or HU, the staining pattern of GFP-TAB182 did not change, suggesting that TAB182 does not localise to DNA damage foci following DNA damage at least at the time-points examined (Figure 4.13).

4.2.13 γH2AX and 53BP1 Foci after HU Exposure are Reduced in TAB182 Knockdown Cells

Since TAB182 depleted cells displayed elevated levels of replication fork recovery, we wanted to monitor the levels of DNA damage as these cells were released from a two hour HU exposure, a treatment that was also employed during our fibre analysis. HeLa cells were treated with control or TAB182 siRNA and 48 hours later either mock-exposed or exposed to 2mM HU for two hours. Cells were fixed and extracted at 0, the point of HU removal, 1, 2, 4 and 24 hours post-HU release. Fixed cells were then probed with antibodies against γH2AX to monitor the formation of DNA damage and 53BP1 that represents sites of DNA DSBs. Cells were analysed by fluorescence microscopy, γH2AX and 53BP1 foci positive cells were counted and are denoted as those that had more than 7 foci per cell (Figure 4.14). Confirmation of TAB182 knockdown was achieved by Western blotting (data not shown).

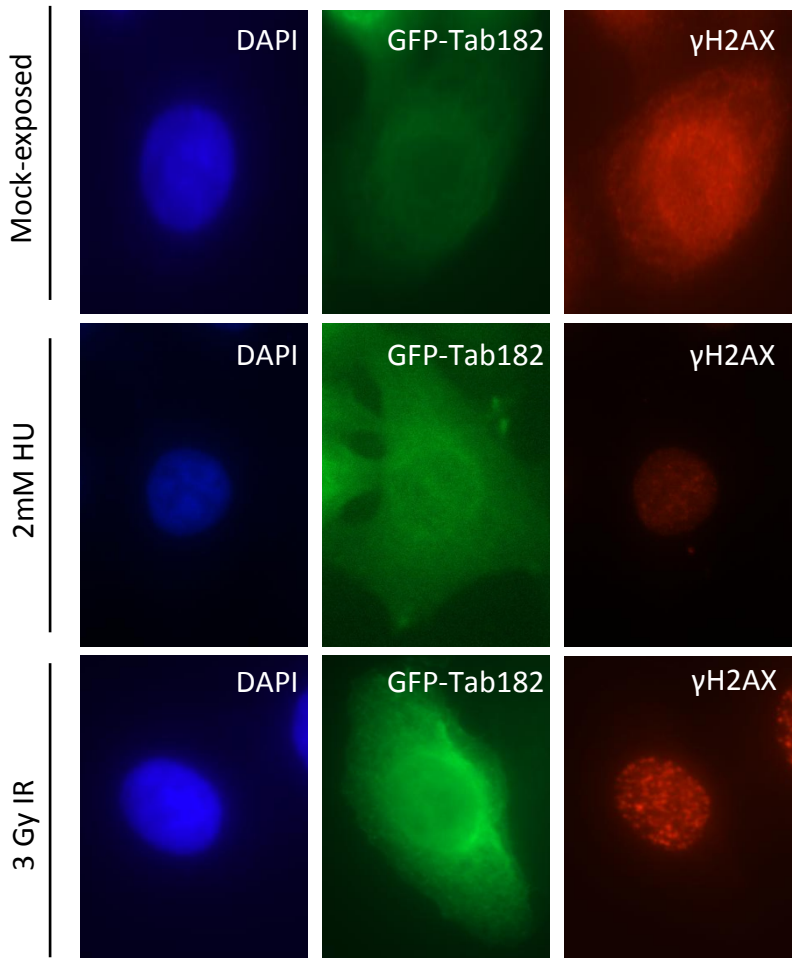

Figure 4.13: TAB182 does not Localise to DNA Damage Foci following HU Treatment or IR Exposure. HeLa cells were transfected with eGFPC3-*TAB182* and 48 hours later, mock-exposed or exposed to 2mM HU (left-in throughout the duration of the experiment) or irradiated at 3 Gy IR. 2 hours post-treatment the cells were then fixed, permeabilised and probed with antibodies against γH2AX. These immunofluorescence images are representative of three independent experiments.

In the absence of any DNA damage, there was a basal level of γH2AX foci positive control cells (approximately 12%). Following 2 hours incubation with 2mM HU, the percentage of γH2AX foci positive cells increased to approximately 20%, this is indicative of the initiation of formation of DNA damage following the addition of HU. 1 hour after release from HU, the percentage of γH2AX foci positive cells was approximately 49%, representing the highest percentage of γH2AX foci positive cells throughout the course of the experiment. 2 to 24 hours post-release from HU, the percentage of γH2AX foci positive cells was reduced to around 21 to 30%, indicating that there was dissolution of γH2AX foci and possibly clearance of DNA damage. Upon TAB182 depletion, the basal levels of γH2AX foci positive cells were similar to control siRNA treated cells (approximately 10%). The percentage of γH2AX foci positive cells at the point of HU removal in the absence of TAB182 was also equivalent to control siRNA treated cells (approximately 20%). This was not the case 1 hour post-HU release where only 14% of TAB182 depleted cells displayed γH2AX foci when compared to 50% of control cells. This reduction in the percentage of cells with γH2AX positive foci was evident in all the other time-points examined (Figure 4.14A). This suggested that there is either less DNA damage/faster clearance of damage or fork recovery following release from HU in TAB182 deficient cells in agreement with the observation that there is less fork stalling, or that the phosphorylation/dephosphorylation equilibrium of γH2AX in TAB182 defective cells is compromised (Figure 4.14A).

To ascertain whether there is less DNA damage in the form of DSBs in TAB182 cells, we also examined the levels of 53BP1 foci positive cells. The percentage of cells with constitutive 53BP1 positive foci was approximately 3% but following 2 hours incubation of 2mM HU treatment, the percentage of cells with 53BP1 positive foci increased to 20%,

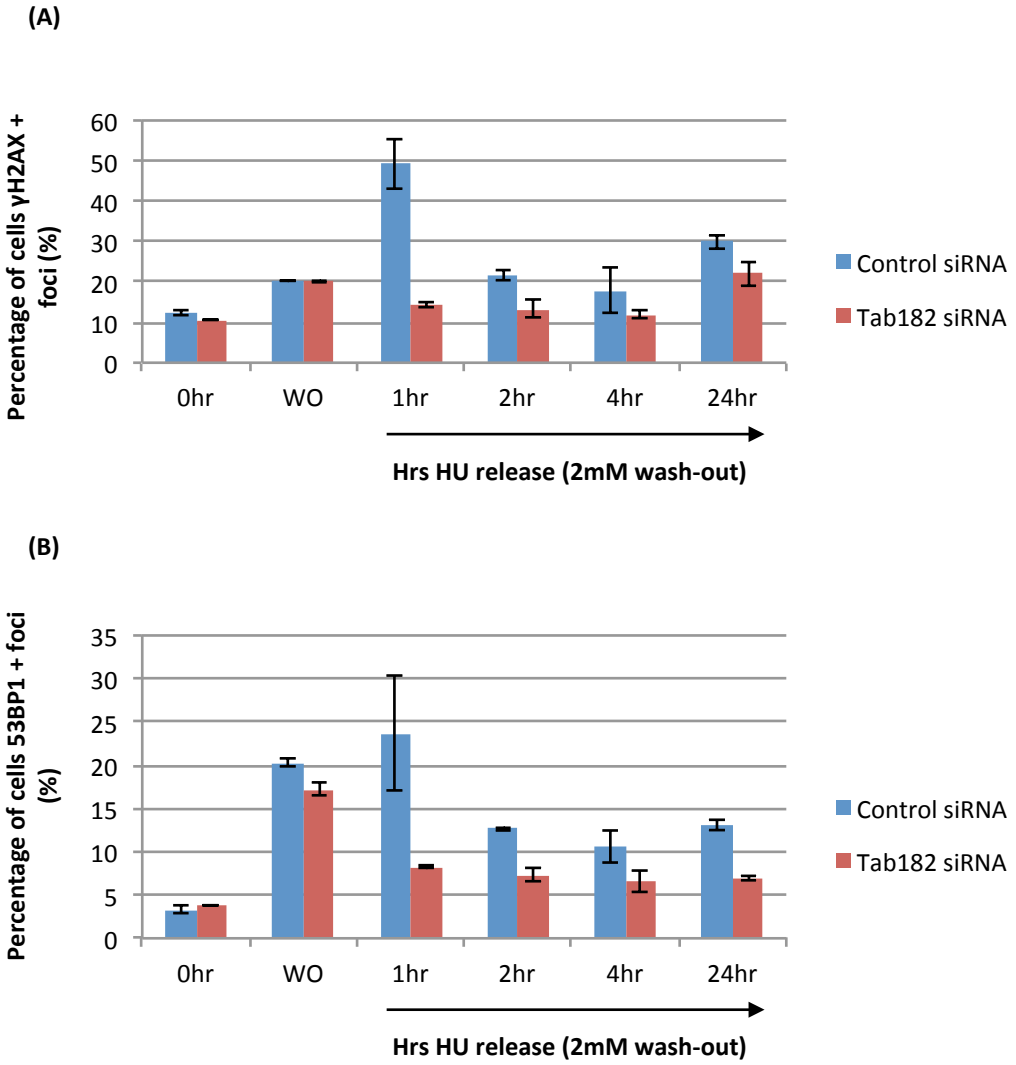

Figure 4.14: γH2AX and 53BP1 Foci after HU Exposure are Reduced in TAB182 Knockdown Cells. HeLa cells were treated with control or TAB182 siRNA and 48 hours later, were mock-exposed or exposed to 2mM HU for 2 hours. The cells were then fixed and permeabilised at 0, point of release, 1, 2, 4 and 24 hours post-HU treatment. Fixed cells were probed with antibodies against YH2AX or 53BP1. Cells were analysed by fluorescence microscopy and YH2AX+ or 53BP1+ cells scored as those having more than 7 foci per cell. **(A)** Graph shows the percentage of cells with γH2AX+ foci across various time-points after 2mM HU exposure. **(B)** Graph depicts the percentage of cells with 53BP1+ foci across various time-points following 2mM HU exposure. Error bars represent SEM. These data are representative of three independent experiments.

representing induction of DNA breaks and/or collapsed forks. 1 hour after release from HU the percentage of cells with 53BP1 positive foci was approximately 24%, representing the maximal percentage of 53BP1 positive cells throughout the course of the experiment. At later time-points the levels of 53BP1 positive cells reduced suggesting that the DNA DSBs were resolved/repaired. In TAB182 depleted cells the percentage of cells displaying constitutive 53BP1 positive foci was equivalent to control cells. At the point of HU removal, the percentage of cells with 53BP1 positive foci was approximately 17% and slightly decreased compared to control cells (20%). Strikingly, 1 hour after HU release the percentage of TAB182 depleted cells with 53BP1 positive foci was approximately 8%, which was significantly lower than the percentage of control cells with 53BP1 positive foci (approximately 24%). The levels of 53BP1 foci remained relatively constant thereafter but were always reduced compared to control cells. These data suggest that DNA DSBs or collapsed forks marked by 53BP1 formed with HU treatment are resolved faster in TAB182 depleted cells in agreement with the reduction in 1st label terminations we previously observed compared to control cells in our fibre analysis (Figure 4.14B).

4.2.14 TAB182 Depleted Cells Exhibit Elevated Levels of 53BP1 Bodies in G1 following Release from HU

Unresolved replication intermediates or under-replicated DNA transmitted to daughter cells in G1 phase, is sequestered in nuclear compartments that are marked by 53BP1 (Harrigan, Belotserkovskaya et al. 2011, Lukas, Savic et al. 2011). These 53BP1 positive bodies protect chromosomal fragile sites in these compartments against erosion. Despite the faster replication fork recovery upon release from HU blocking, TAB182 deficient

cells are sensitive to replication stress, and so we wondered whether there is more under-replicated DNA in these cells transmitted into the ensuing G1 phase than in control cells. For this reason, we quantified the percentage of G1 cells with 53BP1 bodies as well as the number of 53BP1 bodies following exposure of cells to HU. HeLa cells were transfected with control or TAB182 siRNA and 48 hours later were mock-exposed or exposed to 2mM HU for 2 hours. Cells were fixed, permeabilised and stained with antibodies against Cyclin A (Cyclin A negative cells were scored as G1 cells) and 53BP1 at 4 and 24 hours post-HU release. Cells were visualised by fluorescence microscopy and G1 cells (Cyclin A negative) were scored into the following categories; 1-2 53BP1 bodies per cell, 3-4 53BP1 bodies per cell, 5-6 53BP1 bodies per cell, 7-8 53BP1 bodies per cell or 9+ 53BP1 bodies per cell (Figure 4.15). Confirmation of TAB182 knockdown was achieved by Western blotting (data not shown).

In the HeLa cells that were utilised for this experiment, there was a high level of background 53BP1 bodies in G1 in both control and TAB182 depleted, untreated cells (Figure 4.15A). 4 hours post-HU release there was a mild induction of 1-2 53BP1 bodies in both control cells and TAB182 depleted cells. 24 hours following release from HU there was an increase in the percentage of cells containing 1-2 53BP1 bodies that were deficient in TAB182 compared to controls (37% of TAB182 knockdown cells vs 27% of control cells). This suggested that after release from replication blocking with HU, in particular 24 hours after release, there is an increase in the levels of under-replicated DNA or regions of replication stress in TAB182 cells (Figure 4.15).

(A)

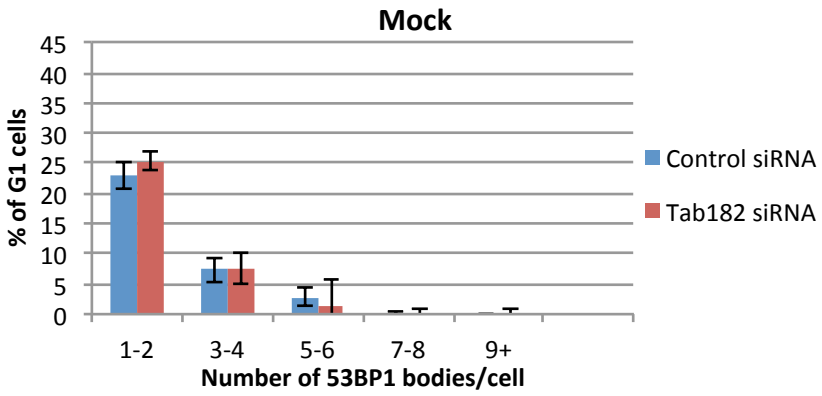

(B)

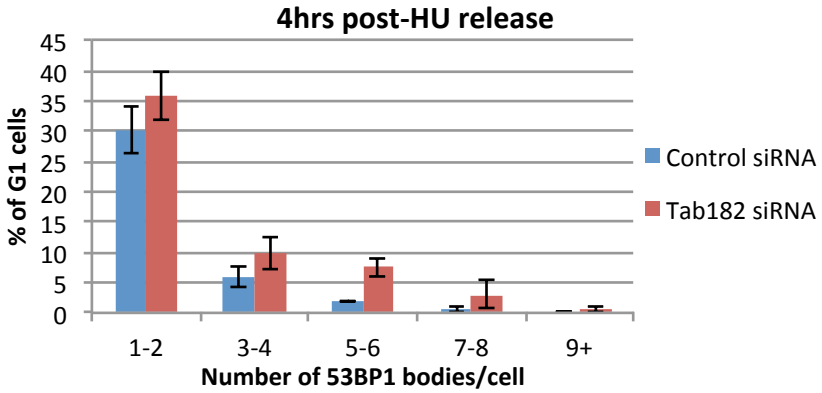

(C)

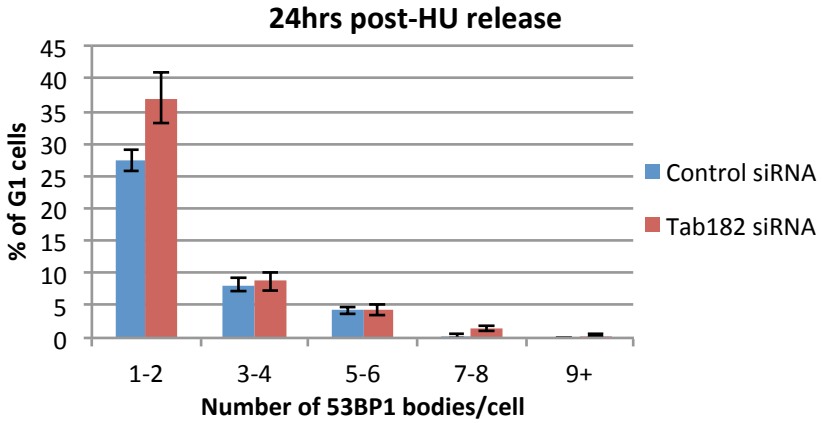

Figure 4.15: TAB182 Depleted Cells Exhibit Elevated Levels of 53BP1 Bodies in G1 following Release from HU. HeLa cells were treated with control or TAB182 siRNA and 48 hrs later, were mock-exposed **(A)** or exposed to 2mM HU for 2 hrs. Cells were fixed and permeabilised at 4 **(B)** and 24 hrs (C) post-HU treatment. Fixed cells were probed with antibodies against Cyclin A and 53BP1. The cells were analysed by fluorescence microscopy and the number of 53BP1 bodies in G1 counted. Graphs illustrate the percentage of G1 cells with 53BP1+ bodies across various time-points following 2mM HU treatment. Error bars represent SEM. These data are representative of three independent experiments.

4.2.15 TAB182 Depleted Cells Exhibit Increased Micronuclei after HU Treatment

Micronuclei are parts of, or whole, chromosomes that have been separated from the nucleus during mitosis and are markers of genome instability. To determine whether TAB182 deficient cells are genetically unstable, micronuclei analysis of TAB182 depleted cells after HU treatment was performed. HeLa cells were transfected with control or TAB182 siRNA and 48 hours later, either exposed or mock-exposed to 2mM HU for 2 hours. The cells were then fixed, permeabilised and stained with DAPI. Cells with no micronuclei, 1 micronucleus, 2-5 micronuclei or 5+ micronuclei associated with each cell were quantified. Mitotic catastrophe and anaphase bridging were also determined (Figure 4.16). Confirmation of TAB182 knockdown was achieved by Western blotting (data not shown).

Prior to HU exposure, less than 1% of control cells had any associated micronuclei as expected (data not shown). Similarly, the percentage of cells with micronuclei in undamaged TAB182 deficient cells was also less than 1%. 48 hours following release from HU treatment 2.2% of cells had 1 micronucleus, 0.4% of cells had 2-5 micronuclei, no cells had 5+ micronuclei and 0.2% of cells exhibited mitotic catastrophe but there were no observed anaphase bridges. In TAB182 depleted cells 48 hours after HU release, the percentage of cells with micronuclei was slightly higher than that of control cells; 4.9% of cells had 1 micronucleus, 1.0% of cells had 2-5 micronuclei and 0.3% of cells had 5+ micronuclei. In addition, 0.7% of cells exhibited mitotic catastrophes and 0.1% of cells showed anaphase bridging. These data show that cells depleted of TAB182 have an increased number of associated micronuclei following treatment with HU, a marker of genomic instability (Figure 4.16).

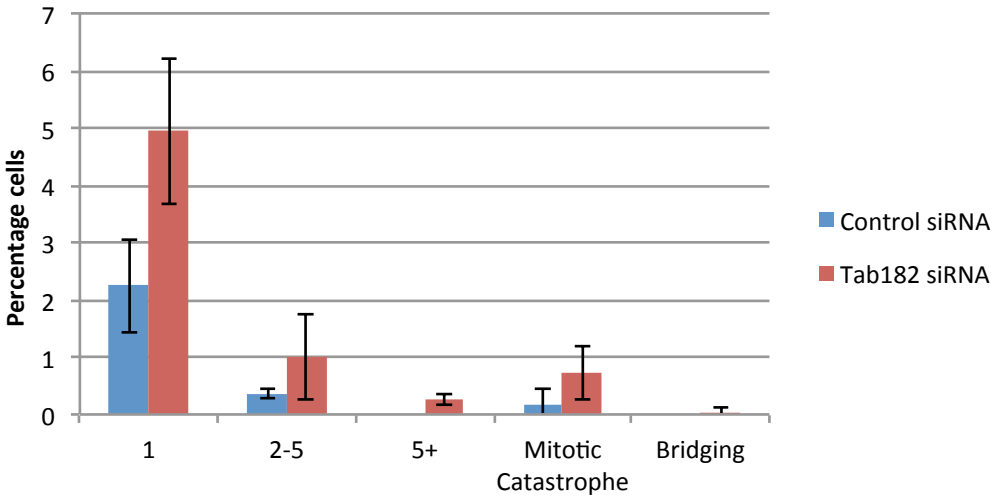

Figure 4.16: TAB182 Depleted Cells Exhibit Increased Micronuclei after HU Exposure. HeLa cells were transfected with control or TAB182 siRNA and 48 hours later, were mock-exposed or exposed to 2mM HU for 2 hours. After removal of HU, the cells were further incubated for 48 hours before being fixed, permeabilised and stained with DAPI. The cells were analysed by fluorescence microscopy and scored into various categories (see above). Error bars represent SEM. These data are representative of three independent experiments.

4.2.16 TAB182 Deficient Cells Display Less DNA Gaps/Breaks following Exposure to HU

Since TAB182 deficient cells displayed elevated numbers of micronuclei and 53BP1 bodies in response to replication stress, metaphase spread analysis was also performed in order to analyse chromosomal damage of metaphase chromosomes. HeLa cells were transfected with control or TAB182 siRNA and 48 hours later were either mock-exposed or incubated in media containing 2mM HU for 2 hours. 48 hours after HU release, the cells were treated with colcemid to block cells in mitosis. The cells were then fixed and dropped onto slides, followed by Giemsa staining to allow visualisation of chromosomal damage of metaphase chromosomes. The total number of chromatid gaps/breaks was scored in a total of 50 metaphase spreads in both control and TAB182 depleted cells. Confirmation of TAB182 knockdown was achieved by Western blotting (data not shown). In control siRNA treated cells, the total number of chromatid gaps/breaks was 0.67 per metaphase, in contrast to TAB182 deficient cells where the total number of chromatid gaps/breaks following HU treatment was 0.32 per metaphase (Figure 4.17). These data show that TAB182 depleted cells have less DNA gaps/breaks compared to control cells following exposure to HU.

4.2.17 TAB182 is Down-Regulated during G1 Phase of the Cell Cycle

Given that TAB182 depletion in response to replication stress leads to a defective S phase checkpoint but reduced 1st label terminations compared to control cells, we wished to examine the levels of TAB182 protein throughout the cell cycle. To this end, we made use of the mitotic spindle formation inhibitor nocodazole, which blocks cells in prometaphase. HeLa cells were mock-treated or treated with nocodazole for 18 hours then released from

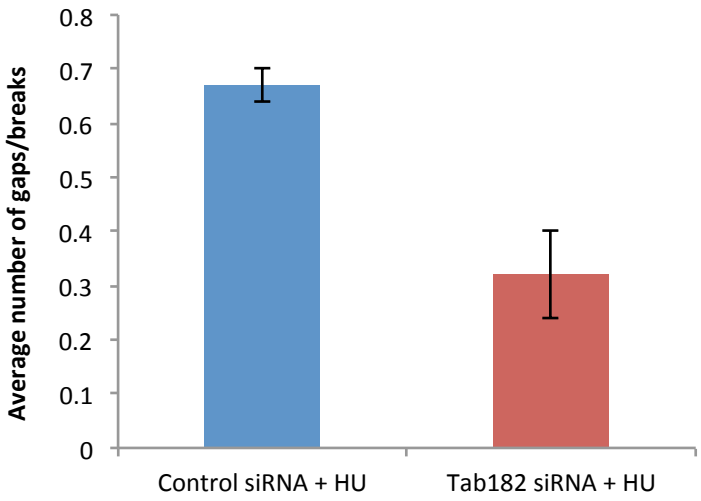

Figure 4.17: TAB182 Deficient Cells Display Less DNA Gaps/Breaks following Exposure to HU. HeLa cells were transfected with control siRNA or TAB182 siRNA and 48 hours later, were exposed to 2mM HU for 2 hours and then incubated in HU-free media. 48 hours later, the cells were treated with colcemid to block cells in mitosis. Cells were fixed, dropped onto slides and stained with Giemsa ready for analysis. Metaphase spreads were visualised by light microscopy and counted for the number of chromatid gaps/breaks. Error bars represent SEM. These data are representative of two independent experiments. Experiment performed by Dr John Reynolds.

the G2/M block into fresh media and samples were harvested at 0, 1, 2, 4, 6, 8, 10 and 24 hours later. Budding uninhibited by benzimidazoles-related 1 (BubR1) and Cdc27 were immunoblotted since they are highly phosphorylated in mitosis but become gradually dephosphorylated as the cells exit M phase and proceed into G1. Claspin and Cyclin A levels are high during S phase but are largely diminished during mitosis and G1. Cyclin B and H3 phosphorylated on Ser10 are markers of mitosis with their levels being greatly reduced during entry into G1 phase. All proteins were present in the asynchronous population apart from phospho-H3 (Ser10) which is specifically phosphorylated during mitosis and therefore, only displays a very weak band in the asynchronous cell lysate sample. Interestingly, TAB182 appeared to migrate more slowly in the nocodazole treated population, suggesting that it is modified during mitosis. During the release from nocodazole block (between 1 and 24 hours), the phosphorylation (denoted by retarded migration on the gel) of BubR1 and Cdc27 was diminished as the cells progress through G1 and into S phase. The protein expression levels of Claspin and Cyclin A (between 1 and 24 hours) started to increase at approximately 6-8 hours after nocodazole release as the cells were going from G1 into S phase. Finally, the protein expression levels of Cyclin B and phospho-H3 (Ser10) decreased during the nocodazole release as the cells exited mitosis and enter G1 phase. Interestingly, the intensity of the TAB182 band decreased during nocodazole release and exit into G1 and increased as the cells entered S phase. This result suggests that TAB182 in down-regulated during G1 but the protein levels increase during S phase (Figure 4.18).

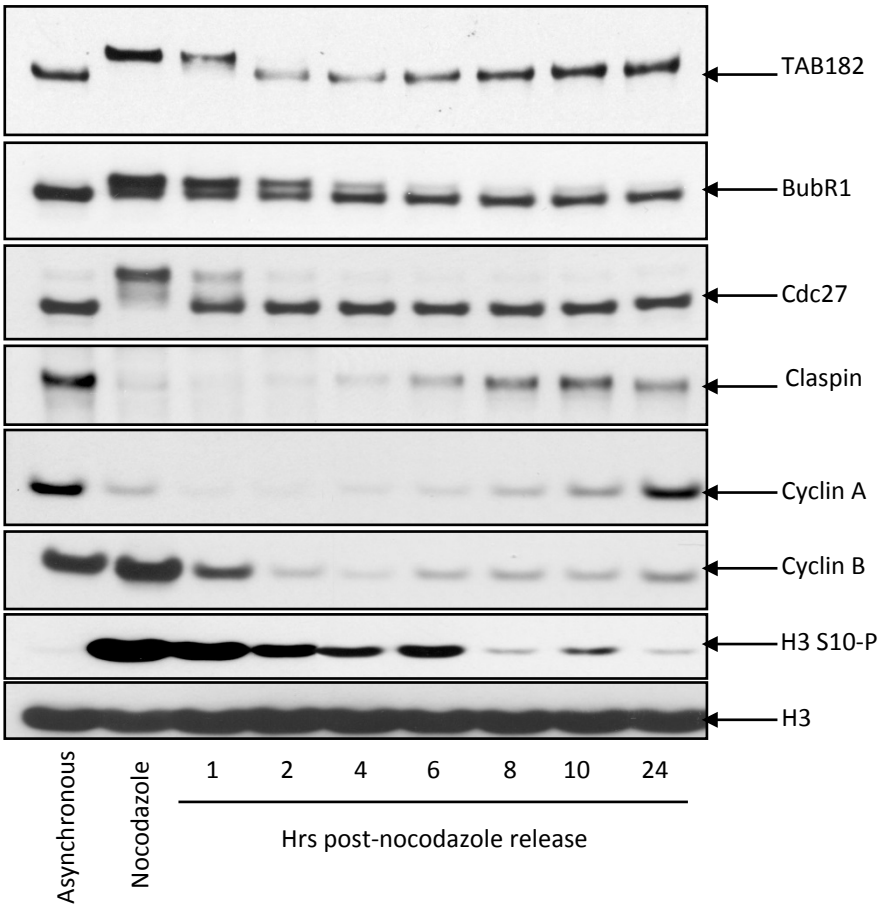

Figure 4.18: TAB182 is Down-Regulated during G1 Phase of the Cell Cycle. HeLa cells were mock-treated or treated with nocodazole for 18 hours. Cells were harvested at 1, 2, 4, 6, 8, 10 and 24 hours post-nocodazole release, along with a mock-treated sample and a nocodazole treated but not released control. Cells lysates were subjected to SDS-PAGE and Western blotting with the indicated antibodies. This Western blot is representative of three independent experiments.

4.3 DISCUSSION

To date, very little is known about the function of TAB182. It has been previously established that it interacts with Tankyrase 1, and that Tankyrase 1 is able to ribosylate TAB182 *in vitro* (Seimiya and Smith 2002). In addition to this interaction, it has been suggested that TAB182 may be involved in the DDR pathways, since it is thought to be a substrate of ATM/ATR phosphorylation (Matsuoka, Ballif et al. 2007). Work presented in this chapter has implicated TAB182 in the DDR for several reasons. Firstly, cells deficient in TAB182 are sensitive to agents that induce replicative stress (UV-C irradiation and HU), but not IR (Figure 4.2). Secondly, following exposure to various DNA damaging agents such as IR and HU, TAB182 deficient cells exhibited an increase in DDR signalling measured by the elevated levels of phosphorylated DDR proteins such a pChk1 (S317 and S345), pRPA (S4/8) and γH2AX (Figure 4.3). Furthermore, a minor delay in the progression through G2/M after IR or HU treatment, or in the progression through S phase after UV-C irradiation was observed in TAB182 depleted cells (Figure 4.5). Further analysis of the G2/M checkpoint by flow cytometry, measuring the content of pHistone H3 (Ser 10), a marker of mitosis, revealed that the G2/M checkpoint in TAB182 depleted cells after all types of DNA damage tested was intact (Figure 4.6).

Work presented in this chapter has also shown that TAB182 depletion does not affect replication fork speeds before or after replication stress (Figure 4.7). Interestingly, TAB182 depleted cells exhibit elevated levels of new origin firing and reduced fork stalling following release from HU (Figure 4.8). Furthermore, the new origin firing defect observed in TAB182 deficient cells was abrogated upon inhibition of CDK activity (Figure 4.11). The reduced fork stalling observed in TAB182 deficient cells following HU treatment was shown to be

dependent on ATR but not on Chk1 or CDK function, suggesting that in the absence of TAB182, ATR is important for replication resumption (Figures 4.10, 4.9 and 4.11, respectively).

It was shown that TAB182 does not localise to DNA damage foci following exposure to HU (Figure 4.13). Further analyses revealed that TAB182 depletion leads to a reduction in the numbers of γH2AX and 53BP1 foci positive cells following 1hr release from 2mM HU exposure, suggesting that TAB182 defective cells resolve DNA damage and DSBs, respectively more than control cells (alternatively recruitment of these proteins to foci may be deficient) (Figure 4.14). Furthermore, TAB182 depletion resulted in a mild increase in the percentage of cells having 1-2 53BP1 bodies in G1, indicative of increased replication stress and elevated levels of under-replicated DNA (Figure 4.15). We also detected higher levels of associated micronuclei following exposure to HU in TAB182 deficient cells (Figure 4.16). Interestingly, metaphase spread analysis showed that TAB182 depleted cells have less chromatid gaps/breaks following exposure to HU, the reason for this result is unclear at present (Figure 4.17). Finally, using nocodazole release assays, TAB182 was shown to be down-regulated during G1 and its expression increased as the cells progressed through the cell cycle, further suggesting that TAB182 may be important during S phase (Figure 4.18). Similarly, it was observed that as adenovirus infection progressed there was an increase in TAB182 expression before its degradation. This is probably due to infected cells entering pseudo-S phase (Figure 3.1).

Clonogenic Survival, DNA Damage Response Signalling and Cell Cycle Control in TAB182 Deficient Cells

Clonogenic survival assays demonstrated that TAB182 depleted cells are sensitive to UV-C and HU treatment, but not to IR (Figure 4.2). These data suggest that TAB182 is important for cellular survival in response to replication stress and bulky lesions induced by HU and UV-C exposure, but it is dispensable for survival in response to lesions induced by IR such as DSBs. These data are the first evidence to suggest that TAB182 may be important for cell viability following replication stress. For this reason, the DNA damage signalling response to various DNA damaging agents in TAB182 deficient cells was also examined. The levels of pNBS1 S343, pChk1 S317/S345, pRPA S4/8 and γH2AX S139 were determined. ATM is responsible for the phosphorylation of NBS1 on S343, which is indicative of the activation of the S phase checkpoint (Lim, Kim et al. 2000). ATM and ATR have been shown to phosphorylate Chk1 on S317 or S345 (Zhao and Piwnica-Worms 2001, Gatei, Sloper et al. 2003). Phosphorylation of Chk1 at S317 is required for cell cycle re-entry after stalled replication (Martin and Ouchi 2008). Phosphorylation of Chk1 on S345 is required for Chk1 localisation to the nucleus following activation of the checkpoint (Jiang, Pereira et al. 2003). Phosphorylation on S4/8 of RPA is indicative of RPA-bound ssDNA formed as a result of replication stress, or following resection of DSBs during HR repair (Shi, Feng et al. 2010). Finally, phosphorylation of H2AX on S139 (termed γH2AX) is indicative of an activated DDR and can be phosphorylated by both ATM, ATR and DNA-PK (Rogakou, Pilch et al. 1998, Ward and Chen 2001). Following exposure to IR, TAB182 depleted cells displayed slightly elevated levels of pNBS1 (S343), pChk1 (S317 and S345), pRPA (S4/8) and γH2AX (S139). This does not necessarily indicate that the cells should be sensitive to IR as the differences observed are

mild and there may be compensatory pathways to promote cellular survival in these cells following exposure to IR. Following exposure to 2mM HU, TAB182 defective cells displayed slightly elevated levels of pRPA (S4/8) and γH2AX (S139) and elevated levels of pChk1 (S317 and S345), suggesting that there is a higher checkpoint activation immediately after treatment with HU. How and whether this may be connected to the cellular hypersensitivity observed in these cells is unknown. Following UV-C irradiation, a mild hyperphosphorylation of Chk1 (S317) was observed in TAB182 knockdown cells but again, as before, whether this can account for the UV-C hypersensitivity observed is unclear. Significantly, however, TAB182 depleted cells appeared to progress through S phase slower than control cells after UV-C irradiation, indicating that there may be a role for TAB182 in replication progression. Progression through S phase in the presence of other types of DNA damage/stress under conditions of down-regulation of TAB182 expression, appeared to be intact, but with a bigger fraction of cells accumulating in G2/M compared to control cells.

Using nocodazole release assays, it was shown that TAB182 was down-regulated during G1 phase of the cell cycle (Figure 4.18). The reason for this down-regulation is unclear at present. Interestingly, during mitosis TAB182 appeared to migrate more slowly by SDS-PAGE, suggesting that TAB182 may undergo post-translational modifications such as phosphorylation or ribosylation during mitosis. Indeed, studies from Matsuoka and colleagues have identified ATM/ATR phosphorylation sites within TAB182, although these have not been confirmed in this study (Matsuoka, Ballif et al. 2007).

DNA Fibre Analysis

The sensitivity of TAB182 knockdown cells to HU suggested that it may play a role in S phase. DNA fibre analysis is a robust technique facilitating the visualisation of single DNA molecules during DNA replication following release from replication stress (Jackson and Pombo 1998). This technique was therefore employed to analyse the replication dynamics in TAB182 deficient cells. In both unperturbed cells as well as cells released from 2mM HU treatment, the speed of replication fork progression in TAB182 depleted cells was comparable to control siRNA cells, suggesting that TAB182 depletion has no effect on the progression of actively replicating forks (Figure 4.7). Interestingly, TAB182 depleted cells exhibited excessive new origin firing (measured by the elevated percentage of 2^{nd} label origins compared to control siRNA treated cells), as well as an increase in fork restart events (measured by decreased fork stalling compared to control siRNA treated cells), following release from HU (Figure 4.8). This suggested that TAB182 deficient cells may fire new origins to facilitate replication progression, thus ensuring replication completion. In this scenario, the elevated fork restart observed in TAB182 deficient cells could be an indirect effect, or at least in part, of elevated origin firing observed in these cells. To determine whether or not replication fork recovery was dependent on elevated new origin firing, a CDK inhibitor was employed to ablate new origin firing and the effect on fork restart was assessed (Figure 4.11). The CDK I/II inhibitor abolished new origin firing as expected, but strikingly, this did not impact on the percentage of fork restart events in TAB182 knockdown cells, showing that the increased fork restart observed in these cells is not a result of elevated new origin firing. Interestingly, DT40 cells lines that do not express the FANCM helicase, a protein which has previously been implicated in fork restart, display both increased new origin firing and

elevated fork restart following release from replication blocks (Schwab, Blackford et al. 2010). However, the increased fork restart observed in FANCM negative cells is a result of new origin firing, as upon CDK inhibition, increased fork restart reaches control levels. Furthermore, in contrast to TAB182 depleted cells that replicate their DNA at similar rates to control cells, FANCM deficient HeLa cells show increased fork replication speeds in both unperturbed and replication stressed cells (Luke-Glaser, Luke et al. 2010). This suggests that FANCM is able to slow down replication fork progression. Nethertheless, in this study, FANCM defective cells displayed decreased fork restart (as opposed to increased fork restart) following release from replication blocks, suggesting that there is some discrepancy between DT40 and HeLa cells (Luke-Glaser, Luke et al. 2010).

Our results show that TAB182 is important for the suppression of new origin firing in the absence of both Chk1 and ATR function. In addition, TAB182 is important for fork stalling or collapse even in the absence of Chk1 activity but not upon inhibition of ATR. Whether the elevated levels of new origin firing in TAB182 defective cells reflect a checkpoint function for TAB182 is unclear. Moreover, it has been shown in this study that the C-terminal fragment of TAB182 interacts with Chk1 *in vitro* (Figure 4.12). However, cells with defective ATR/Chk1 signalling display increased new origin firing even in the absence of replication stress and this is also accompanied by a decrease in the speed of replication fork progression. Examples of such proteins include ATR, Chk1, CLASPIN and TIMELESS (Petermann, Maya-Mendoza et al. 2006, Maya-Mendoza, Petermann et al. 2007, Wilsker, Petermann et al. 2008). These two phenotypes are not observed in TAB182 deficient cells suggesting that 1) either TAB182 has checkpoint roles outside the ATR/Chk1 pathways or 2) that it does not have a role in checkpoint function.

Taken together, we hypothesise that TAB182 may be involved in promoting fork stalling or collapse in response to replication stress. In this scenario, in the absence of TAB182, forks do not stall but continue to replicate in a manner that is dependent on ATR. Meanwhile, new origins are fired independently as part of the response to replication stress, in a CDK dependent manner.

Localisation of TAB182 in the Cell

Immunofluorescence analysis showed that TAB182 does not localise to nuclear DNA damage foci following replication stress induced by HU (Figure 4.13). A lack of accumulation into nuclear foci upon DNA damage does not necessarily indicate that TAB182 may not have a role in the DDR or a role following replication stress. For example, the Ku heterodimer as well as other established components of the cellular DDR fail to form DNA damage-induced foci (Britton, Coates et al. 2013). Furthermore, due to the fact that there were no available specific antibodies against TAB182 that could be utilised to allow the visualisation of the localisation of the endogenous protein within the cell, we made use of a pEGFPC3-*TAB182* construct to perform this analysis. GFP-TAB182 exhibited pan-cellular localisation that remained unaltered upon the induction of replication stress. However, due to the fact that the ectopic protein is fused to GFP and that its expression was forced, we cannot rule out that some of it, if not all, is not functional in the cell.

Formation of γH2AX and 53BP1 foci following Release from HU

The examination of γH2AX and 53BP1 positive foci following release from HU can be used to assess the kinetics of DNA damage and DSBs, respectively. We observed a reduction

in cells exhibiting γH2AX and 53BP1 foci upon TAB182 depletion, suggesting that TAB182 may be promoting the stalling/collapsing of forks into DSBs (Figure 4.14). We do not know if TAB182 acts directly at the fork but since *in silico* analysis has not revealed any nuclease domains in TAB182, it is unlikely that it may be nucleolytically processing forks. Yet, we cannot exclude the possibility that TAB182 binds to factors that remodel forks or promote the collapse of forks in response to replication stress.

Genome Instability Induced by Unresolved Replication Stress

Stalling of replication forks can lead to regions of DNA being left under replicated or replication intermediates, which if left unresolved may be detrimental to genomic instability. Unresolved replication stress can be visualised in the cell in a number of different ways. One example is the presence of nuclear compartments that are positive for 53BP1 (termed 53BP1 bodies) in G1 following replication stress (Harrigan, Belotserkovskaya et al. 2011, Lukas, Savic et al. 2011). Knockdown of TAB182 slightly increased the levels of 53BP1 bodies above those observed in control cells indicative of elevated levels of under-replicated DNA or replication stress (Figure 4.15). Another example of unresolved replication stress leading to genomic instability is the presence of chromatid gaps and breaks that can be visualised by chromosomal metaphase spreads following replication stress. Our analysis showed that knockdown of TAB182 lead to a reduction in the average number of gaps and breaks following release from HU. Nevertheless, an increase in micronuclei was observed in TAB182 defective cells upon replication stress.

Taken together, in the absence of TAB182, cells are sensitive to replication stress, with more replication forks restarting following release from HU. Finally, TAB182 depleted

cells display elevated levels of under-replicated DNA and a higher number of micronuclei indicative of elevated genomic instability.

CHAPTER FIVE:

THE ROLE OF TAB182 AND THE CNOT COMPLEX IN THE DNA DAMAGE RESPONSE AND REPLICATION STRESS PATHWAYS

5. THE ROLE OF TAB182 AND THE CNOT COMPLEX IN THE DNA DAMAGE RESPONSE AND REPLICATION STRESS PATHWAYS

5.1 INTRODUCTION

Work presented in the previous chapters has implicated TAB182 in the DDR. The first indication that TAB182 may be involved in the DDR comes from work presented in Chapter Three, where TAB182 was shown to be degraded following infection with a number of adenovirus serotypes. More than 80% of proteins known to be degraded by adenovirus are involved in the DDR, therefore adenoviral targets are likely to be DDR proteins (Querido, Blanchette et al. 2001, Stracker, Carson et al. 2002, Baker, Rohleder et al. 2007, Orazio, Naeger et al. 2011, Gupta, Jha et al. 2013). Furthermore, work presented in Chapter Three showed that TAB182 depletion enhanced the expression of the cell cycle protein, Cyclin E, and elevated the expression of the adenoviral E1A protein (Figures 3.10 and 3.9, respectively). This suggested that, firstly, TAB182 may be involved in cell cycle control or the regulation of replication, and secondly, that the degradation of TAB182 during adenovirus infection is beneficial for both viral replication and the production of viral progeny.

A potential role for TAB182 in the DDR was further indicated in Chapter Four. Using cell survival assays, TAB182 depleted cells appeared to be sensitive to agents that induce replication stress (Figure 4.2). Moreover, TAB182 deficient cells displayed increased DDR signalling following exposure to various DNA damaging agents (Figure 4.3). Cell cycle analyses revealed that TAB182 deficient cells exhibit a delay in cell cycle progression following exposure to DNA damaging agents (especially after UV-C irradiation), which was not due to a defective G2/M checkpoint (Figures 4.5 and 4.6, respectively).

Using DNA fibre assays, the replication checkpoint in TAB182 deficient cells both in the absence of stress and following HU release was shown to be proficient, since replication elongation speeds were comparable to control cells (also shown by proficient Chk1 phosphorylation) (Figures 4.7 and 4.3, respectively). However, DNA fibre structures following replication stress demonstrated that TAB182 deficient cells displayed excessive new origin firing and increased fork restart following release from replication blocks induced by HU (Figure 4.8). A CDK I/II inhibitor was used to inhibit new origin firing in order to determine whether the elevated new origin firing and increased fork restart observed in TAB182 depleted cells following replication stress were dependent upon each other (Figure 4.11). Since elevated new origin firing was shown to be independent of the increased fork restart in TAB182 deficient cells after HU release, TAB182 was thought to have direct involvement in fork stalling following replication stress (see Chapter Four). The fact that there are less cells with γH2AX and 53BP1 foci and less chromatid gaps/breaks are formed after replication stress upon TAB182 depletion, suggests that less replication forks stall in TAB182 deficient cells and therefore less DSBs may be accumulating (Figures 4.14 and 4.17, respectively). However, TAB182 deficient cells displayed increased levels of micronuclei as well as increased numbers of cells with 1-2 53BP1 bodies in G1, suggesting that TAB182 deficient cells may also exhibit phenotypes of genomic instability (Figures 4.16 and 4.15, respectively).

Taken together, the work presented in Chapters Three and Four indicates that TAB182 may be involved in the response to replication stress as well as in the maintenance of genome stability. However, no precise mechanism for the involvement of TAB182 in the DDR has been elucidated thus far. The aim of this chapter was therefore to try to identify

putative novel TAB182 binding partners, in an attempt to elucidate the role that TAB182 plays in the DDR.

5.2 RESULTS

5.2.1 TAB182 Interacts with the CNOT Complex *in Vivo*

GST pull-down assays previously performed in Chapter Four revealed that TAB182 interacted with Tankyrase 1, Chk1 and Aurora kinase (Figure 4.12). To gain further insight into the function of TAB182, co-immunoprecipitation experiments were performed in HeLa cell lysates, along with Ad5 and Ad12 infected HeLas and the resulting TAB182-protein complexes were analysed by mass spectrometry. After immunoprecipitation, proteins were digested with trypsin as described in Section 2.3.5. The resulting peptides were separated using a Bruker amaZon ion trap mass spectrometer and processed and analysed by using the ProteinScape central bioinformatic platform (Bruker). Protein names, peptide number, percentage coverage and Mascot score were all determined (Table 5.1).

TAB182 co-immunoprecipitations performed in uninfected HeLa cells revealed a number of components of the CNOT complex to interact with TAB182 including CNOT1, CNOT2, CNOT3, CNOT6L, CNOT8, CNOT9, CNOT10 and CNOT11. In addition, protein arginine N-methyltransferase 3 (PRMT3) and four and a half LIM domain 2 (FHL2) proteins were also consistently found to interact with TAB182 in this screen (Table 5.1A). Similarly, the TAB182 immunoprecipitations performed in Ad5 and Ad12 infected HeLa cells also identified a number of components of the CNOT complex including CNOT1, CNOT2, CNOT3, CNOT6L

(A) Uninfected HeLas:

Protein	Peptide number	Percentage coverage	Mascot Score
TAB182	68	49.4	3491
CNOT1	38	17.4	1472
CNOT3	7	10.2	237
CNOT7	6	28.8	211
CNOT2	5	12.2	245
CNOT6L	1	1.8	21
CNOT10	1	1.3	29
CNOT11	1	2.4	56
CNOT9	6	20.4	224
PRMT3	9	18.5	377
FHL2	12	52.3	470

(B) Ad5 Infected HeLas (24hr):

Protein	Peptide number	Percentage coverage	Mascot Score
TAB182	70	47.2	4302
CNOT1	51	22.6	2423
CNOT3	15	19.1	607
CNOT2	7	15.4	343
CNOT10	5	10.2	219
CNOT6L	2	4.1	90
CNOT8	1	4.8	45
CNOT11	3	8	122
CNOT9	10	36.5	470
PRMT3	8	17.3	356
FHL2	18	60.6	707

(C) Ad12 Infected HeLas (24hr):

Protein	Peptide number	Percentage coverage	Mascot Score
TAB182	68	49.4	3491
CNOT1	38	17.4	1472
CNOT2	5	12.2	245
CNOT3	7	10.2	237
CNOT7	6	28.8	211
CNOT10	1	1.3	29
CNOT6L	1	1.8	21
CNOT11	1	2.4	56
CNOT9	6	20.4	234
PRMT3	9	18.5	376.8
FHL2	12	52.3	470

Table 5.1: TAB182 Interacts with the CNOT Complex *in Vivo*. TAB182 was immunoprecipitated from **(A)** uninfected, **(B)** Ad5 or **(C)** Ad12 infected HeLa cell lysates and the resulting associated proteins identified by mass spectrometry. Proteins identified are shown in the above table, together with peptide number, percentage coverage and Mascot scores.

CNOT7 (Ad12 only), CNOT8 (Ad5 only), CNOT9, CNOT10 and CNOT11. Again, PRMT3 and FHL2 proteins were found to interact with TAB182 in this screen (Table 5.1B and Table 5.1C).

These results are representative of 10 independent mass spectrometry screens performed throughout the duration of this study. Taken together these data show that TAB182 is likely to interact with various components of the CNOT complex, as well as the proteins PRMT3 and FHL2. Interestingly, CNOT4 was never identified in any of the co-immunoprecipitations. It is assumed that the peptides identified as deriving from CNOT6L could have also been components of CNOT6 due to the high similarity between the two proteins. When the TAB182 immunoprecipitation was performed in the presence of Ad5 and Ad12 infected lysates, no additional interactions were observed. This suggests that adenoviral infection did not affect TAB182 interactions with other proteins detected in this screen. A representation of the interactions of TAB182, identified by mass spectrometry, is shown in Table 5.1.

5.2.2 Adenovirus Down-Regulates Components of the CNOT complex during Ad5 and Ad12 Infection

Since the previous mass spectrometry data (Table 5.1) showed a potential interaction between TAB182 and various components of the CNOT complex (namely CNOT1, CNOT2, CNOT3, CNOT6L, CNOT7, CNOT9, CNOT10 and CNOT11), we aimed to determine whether components of the CNOT complex were also down-regulated during adenovirus infection as TAB182 is. To test this hypothesis, HeLa cells were infected with Ad5 and Ad12 serotypes at an MOI of 5. Cells were harvested at 0, 8, 24, 48, 72 and 96 hours post-infection and

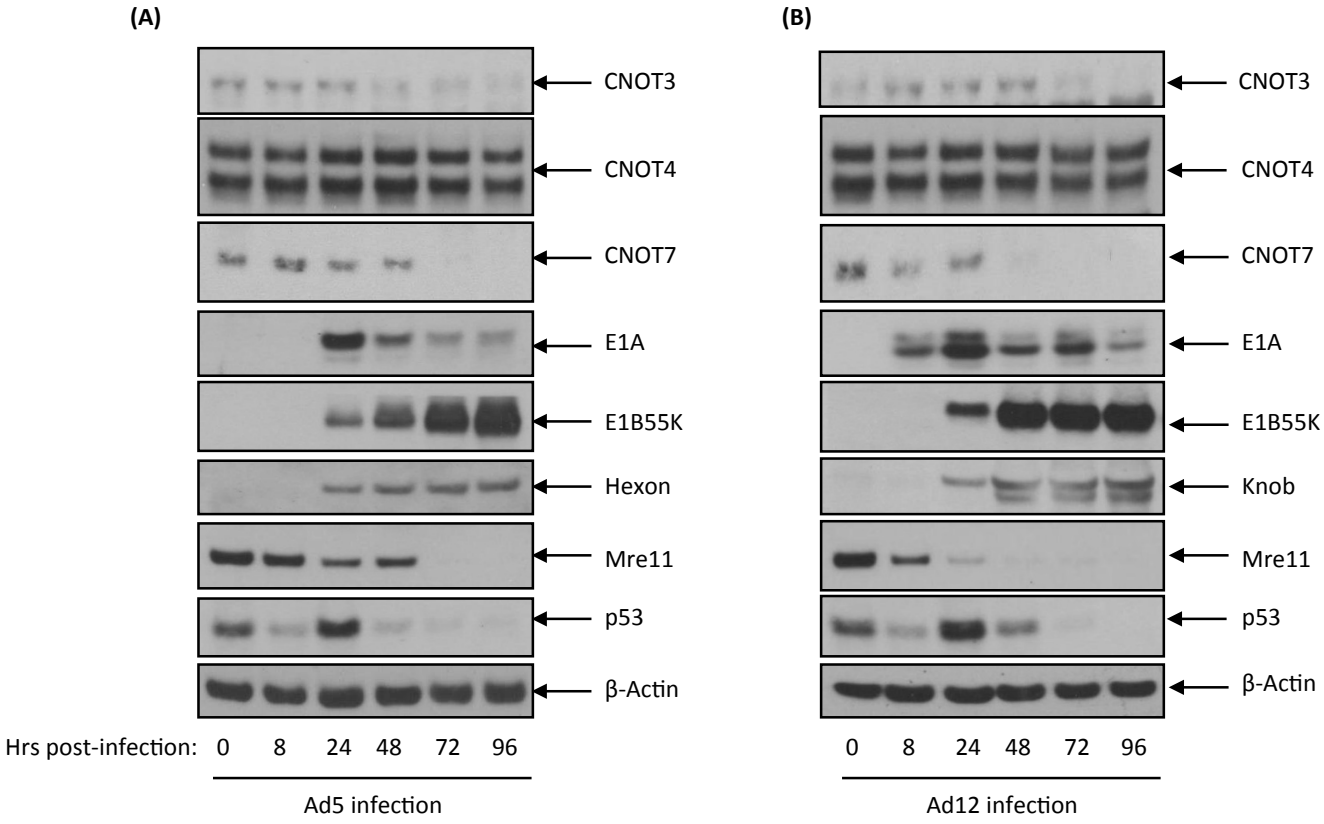

Figure 5.1: Adenovirus Down-Regulates Components of the CNOT Complex during Ad5 and Ad12 Infection. HeLa cells were infected with **(A)** Ad5 or **(B)** Ad12 at an MOI of 5. Cells were harvested at 0, 8, 24, 48, 72 and 96 hours post-infection, subjected to SDS-PAGE and Western blotting using the indicated antibodies. These Western blots are representative of three independent experiments.

subjected to SDS-PAGE and Western blotting with the required antibodies. β-actin was immunoblotted as a loading control. Adenovirus early proteins E1A and E1B55K were immunoblotted along with the viral structural proteins Hexon (Ad5) and Knob (Ad12) as markers of adenovirus infection. As expected, the expression of E1A, E1B55K, Hexon (Ad5) and Knob (Ad12) was observed between 8 and 24 hours post-infection in both Ad5 and Ad12 infected cells confirming infection with these serotypes. Mre11 and p53 were immunoblotted as positive controls since these proteins are known to be degraded during adenovirus infection (Querido, Blanchette et al. 2001, Stracker, Carson et al. 2002). As anticipated, Mre11 and p53 were degraded in both Ad5 and Ad12 infected cells by 72 hours post-infection. CNOT4 expression was unaffected during the course of both Ad5 and Ad12 infection. CNOT3 and CNOT7 were down-regulated 72 hours post-Ad5 and Ad12 infection (Figure 5.1). Other members of the CNOT complex were not examined. These data show that adenovirus is able to down-regulate components of the CNOT complex.

5.2.3 Optimisation of CNOT4 and CNOT6 siRNA Knockdown in HeLa Cells

Two of the major enzyme activities associated with the CCR4-NOT complex are deadenylation and E3 ubiquitin ligase activity, which have been attributed to CNOT6 and CNOT4 respectively (Albert, Hanzawa et al. 2002, Chen, Chiang et al. 2002). Since CNOT4 and CNOT6 are the two most characterised CNOT subunits, we decided to focus on these two proteins for the following experiments. To examine to what extent these proteins impacted on the DDR and adenovirus infection, siRNA knockdown experiments were undertaken. Therefore optimal conditions for siRNA-mediated knockdown of these protein were established. HeLa cells were transfected with increasing concentrations of control (non-

targeting), CNOT4 or CNOT6 siRNA (20nm, 45nm and 90nm). 48 hours post-transfection, cells were harvested, subjected to SDS-PAGE and Western blotting. CNOT4 was immunoblotted to confirm siRNA-mediated knockdown of these proteins. TAB182 was immunoblotted to determine if the siRNA-mediated knockdown of CNOT4 and CNOT6 had any effect on TAB182 protein levels. β-Actin was immunoblotted as a loading control (Figure 5.2A).

The expression of CNOT4 was significantly down-regulated in all CNOT4 siRNA concentrations used (20nm, 45nm and 90nm) when compared to control siRNA treated samples. Upon overexposure of autoradiography film, there was some residual CNOT4 expression in the cell lysate treated with 20nm of CNOT4 siRNA. It was therefore decided that the 45nm CNOT4 siRNA concentration would be used for all future experiments. A number of known commercial CNOT6 antibodies were tested but in each case the expression of CNOT6 was seen to be unaffected in all CNOT6 siRNA concentrations used (data not shown) (Figure 5.2A). The reason for this could be either that none of the commercial antibodies detected CNOT6 or the CNOT6 siRNA does not work.

TAB182 was also immunoblotted in cells transfected with control, CNOT4 or CNOT6 siRNA to determine whether the knockdown of these proteins had any effect on the expression of TAB182. siRNA mediated knockdown of CNOT6 had no effect on the expression of TAB182 when compared to control cells. Interestingly, the depletion of CNOT4 appeared to slightly down-regulate the levels of TAB182 when compared to control siRNA treated cells. This suggests that CNOT4 may play a role in the regulation of TAB182 levels (Figure 5.2A).

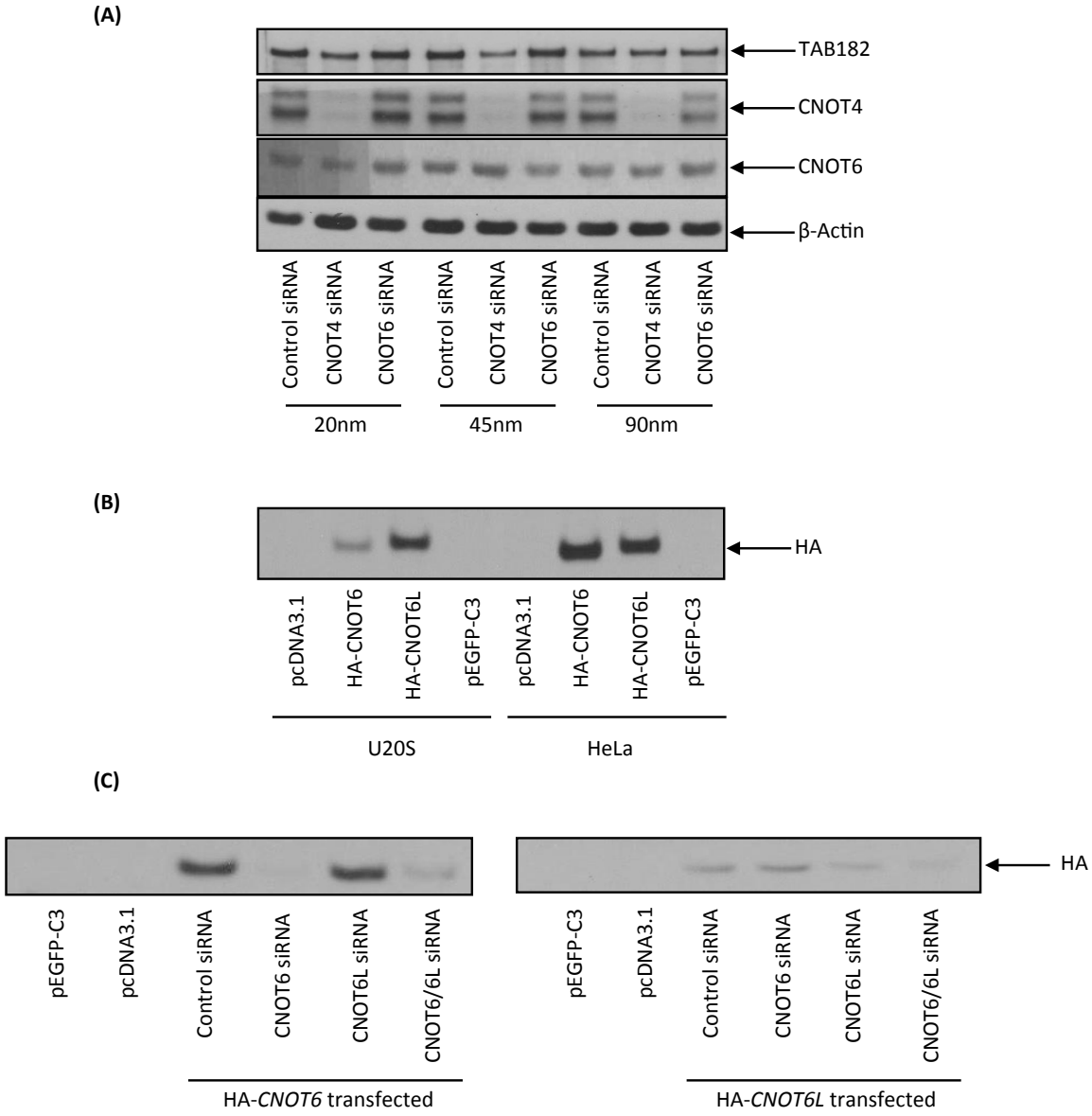

Figure 5.2: Optimisation of CNOT4 and CNOT6 siRNA Knockdown. (A) HeLa cells were transfected with control, CNOT4 or CNOT6 siRNA at the indicated concentrations. 48 hours post-transfection, cells were harvested, subjected to SDS-PAGE and Western blotting using the indicated antibodies. **(B)** Optimisation of HA-*NOT6* and HA-*NOT6L* transfections. HeLa or U20S cells were transfected with 2µg of either HA-*CNOT6* or HA-*CNOT6L* or pcDNA3.1 or pEGFP-C3 only as negative controls. 48 hours later, the cells were harvested, fractionated by SDS-PAGE and subjected to Western blotting. HA was immunoblotted to assess the efficiency of the transfection. **(C)** CNOT6 siRNA optimisation. HeLa or U20S cells were transfected with control, CNOT6, CNOT6L or CNOT6/CNOT6L siRNA and 48 hours later transfected with 2µg of either HA-*CNOT6*, HA-*CNOT6L*, both HA-*CNOT6* and HA-*CNOT6L* or pcDNA3.1 or pEGFP-C3 only as negative controls. 48 hours post-transfection cells were harvested and the cell lysates subjected to SDS-PAGE and Western blotting using HA antibodies.

Since it had not been determined whether the lack of down-regulation of CNOT6 expression after the use of increasing concentrations of CNOT6 siRNA was due to a non-specific antibody or a failure of the CNOT6 siRNA to effectively knockdown the expression of the protein, the following experiment was carried out. Figure 5.3B shows validation of HA-*CNOT6* and HA-*CNOT6L* plasmids received from Dr Sebastian Winkler (University of Nottingham). U20S and HeLa cells were transfected with HA-*CNOT6* and HA-*CNOT6L* along with pEGFP-C3 and pcDNA3.1 as controls. 48 hours later the cells were harvested, fractionated by SDS-PAGE and subjected to Western blotting using a HA antibody to assess the efficiency of the transfection (Figure 5.2B). Following confirmation of successful transfection, the experiment was repeated but this time in the presence of siRNA. HeLa cells were transfected with control siRNA, CNOT6, CNOT6L or CNOT6/CNOT6L siRNA and 48 hours later, were further transfected with HA-*CNOT6* or HA-*CNOT6L* along with the empty vectors pEGFP-C3 and pcDNA3.1. 48 hours later cells were harvested, subjected to SDS-PAGE and Western blotting with the required antibodies. Western blot analysis showed that CNOT6 siRNA does indeed reduce the levels of ectopically expressed CNOT6 (Figure 5.2C). Furthermore, knockdown of CNOT6L has no effect on CNOT6 expression and vice versa (Figure 5.2C).

5.2.4 CNOT4 or CNOT6 Knockdown has no Effect on Adenoviral Protein Expression

To further investigate if the CNOT complex has any role during adenovirus infection, the effect of CNOT4 or CNOT6 knockdown on the expression of various adenoviral proteins was also analysed. HeLa cells were transfected with control, CNOT4 or CNOT6 siRNA and 48 hours later, either mock-infected or infected with Ad5 or Ad12 at an MOI of 5. Cells were

harvested at 0, 8, 24, 48 and 72 hours post-infection, subjected to SDS-PAGE and Western blotting using the appropriate antibodies. CNOT4 was immunoblotted to assess the efficiency of the CNOT4 siRNA, CNOT6 was not immunoblotted since no known commercial antibodies are specific for this protein (see Section 5.2.3). E1A, E1B55K, Hexon (Ad5) and Knob (Ad12) were immunoblotted as markers of adenovirus infection, Mre11 as a protein known to be degraded during Ad5 and Ad12 infection and β-Actin was used as a loading control (Figure 5.3) (Stracker, Carson et al. 2002).

In control siRNA treated cells infected with Ad5, the expression of the adenovirus early protein E1A appeared 8 hours post-infection, whilst the expression of the adenovirus early protein E1B55K and the adenovirus structural protein Hexon was seen 24 hours post-infection. Mre11 had begun to be degraded by 24 hours post-infection. In both CNOT4 and CNOT6 siRNA treated cells infected with Ad5, the protein expression of the adenoviral proteins was comparable to control siRNA treated, infected cells. The expression of E1A also appeared 8 hours post-infection in cells treated with both CNOT4 and CNOT6 siRNA, whilst the expression of E1B55K and Hexon appeared 24 hours post-infection in both CNOT4 and CNOT6 siRNA treated cells. Finally, the degradation of Mre11 during Ad5 infection in CNOT4 and CNOT6 siRNA treated cells was also comparable to control siRNA treated cells, where it began to be degraded 24 hours post-infection (Figure 5.3A).

In control siRNA treated cells infected with Ad12, the expression of the adenovirus early protein E1A appeared 8 hours post-infection, whilst the expression of the adenovirus early protein E1B55K and the viral structural protein Knob appeared 24 hours post-infection. Mre11 was degraded 24 hours post-infection in control siRNA treated infected cells. In CNOT4 and CNOT6 siRNA treated cells infected with Ad12, the protein expression of both

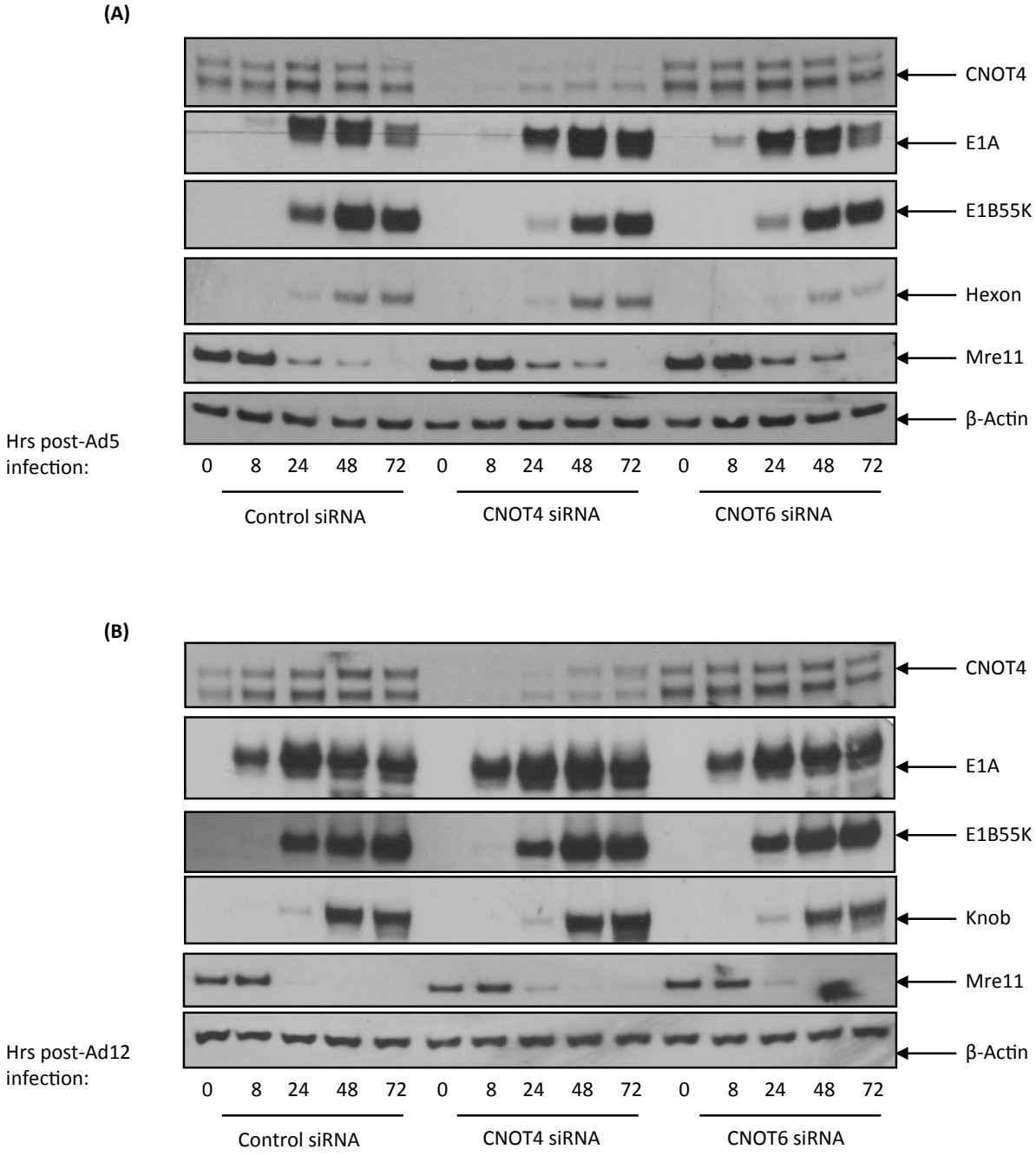

Figure 5.3: CNOT4 or CNOT6 Knockdown has no Effect on Adenoviral Protein Expression. HeLa cells were transfected with control, CNOT4 or CNOT6 siRNA and 48 hours later mock-infected or infected with **(A)** Ad5 or **(B)** Ad12 at an MOI of 5. Cells were harvested at 0, 8, 24, 48 and 72 hours post-infection, subjected to SDS-PAGE and Western blotting using the indicated antibodies. These Western blots are representative of three independent experiments.

adenoviral early and structural proteins was comparable to control siRNA treated cells. The expression of E1A also appeared 8 hours post-infection, whilst the expression of E1B55K and Knob also appeared 24 hours post-infection. The degradation of Mre11 in CNOT4 and CNOT6 siRNA treated cells was also comparable to control siRNA treated cells, where it was degraded 24 hours post-infection (Figure 5.3B).

Taken together these data show that the knockdown of CNOT4 or CNOT6 has no effect on the expression of adenovirus proteins during Ad5 or Ad12 infection.

5.2.5 CNOT4 Depleted Cells Display Normal DNA Fibre Structures following HU Release, Whilst CNOT6 Depleted Cells Display Excessive New Origin Firing

Studies in budding yeast have shown that CCR4-NOT complex may have a role in the response to replication stress, since a number of yeast mutant strains of various components of the CCR4-NOT complex are sensitive to agents that induce replication stress (Bennett, Lewis et al. 2001, Westmoreland, Marks et al. 2004, Mulder, Winkler et al. 2005, Traven, Hammet et al. 2005, Woolstencroft, Beilharz et al. 2006, Deshpande, Hayles et al. 2009). To investigate this further, DNA fibre structure analysis was performed in cells depleted of CNOT4 and CNOT6. HeLa cells were transfected with control, CNOT4 or CNOT6 siRNA and 48 hours later, labelled with the DNA analogue CldU. Following CldU labelling, cells were mock-treated or treated with 2mM HU for 2 hours, and subsequently incubated with IdU in HU-free media. Cells were fixed, spread onto slides and incubated with antibodies against CldU and IdU. DNA was viewed under the microscope and DNA structures observed recorded (Figure 5.4). DNA tracks were analysed and categorised into the

(A)

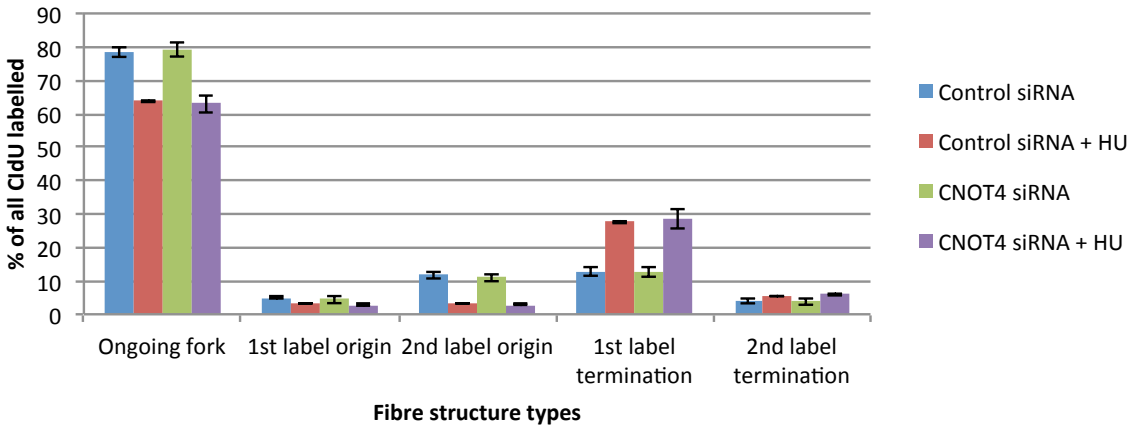

(B)

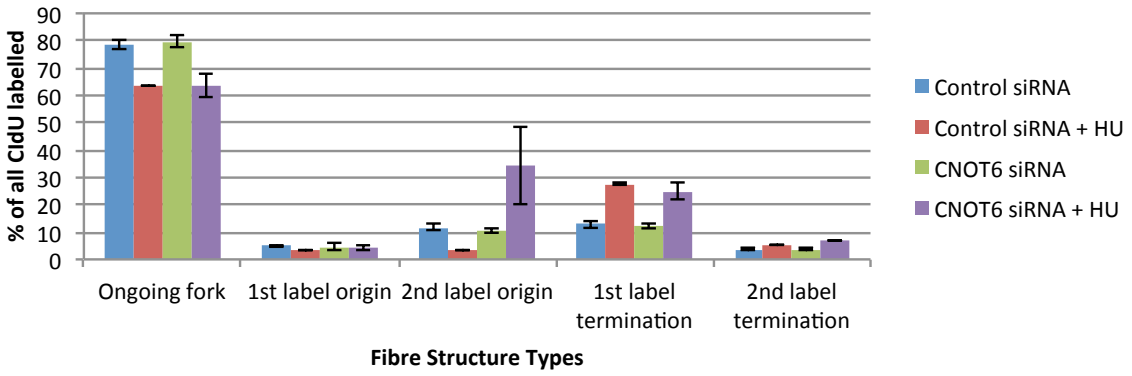

Figure 5.4: CNOT4 Depleted Cells Display Normal DNA Fibre Structures following HU Release, Whilst CNOT6 Depleted Cells Display Excessive New Origin Firing. HeLa cells were transfected with control, CNOT4 or CNOT6 siRNA. 48 hours post-transfection, the cells were incubated with CldU for 20 minutes and then were mock-treated or treated with 2mM HU for 2 hours. Following HU treatment, the cells were incubated with IdU in HU-free media for 45 minutes. DNA was spread onto slides, probed with the appropriate antibodies and visualised by fluorescence microscopy. Graphs show the fibre structures as a percentage of all CldU labelled structures. **(A)** DNA fibre structures after CNOT4 knockdown. **(B)** DNA fibre structures after CNOT6 knockdown. Error bars represent SEM. These data are representative of three independent experiments.

structures as described previously (Section 4.2.8). Confirmation of CNOT4 knockdown was achieved by Western blotting (data not shown).

In CNOT4 siRNA treated, undamaged cells, the percentage of 'ongoing forks' was comparable to control siRNA treated, undamaged cells at 79%. The percentage of '1st label origins' was 4% and '2nd label origins' were 11%. '1st label terminations' were 13% and finally '2nd label terminations' were 4%. In CNOT4 siRNA cells exposed to 2mM HU for 2 hours, the percentages of the different DNA structures were all similar to control, HU exposed cells. Again, in CNOT6 transfected, undamaged cells, the percentages of DNA fibre structures were all similar to control, undamaged cells. However, even though 'ongoing forks', '1st label origins', '1st label terminations' and '2nd label terminations were similar in CNOT6 and control siRNA transfected cells after release from HU block, this was not the case for '2nd label origins' that were significantly increased in CNOT6 siRNA treated cells by 34% compared to control cells (Figure 5.4).

Taken together, these results showed that CNOT4 knockdown has no effect on DNA replication progression following HU treatment. However, the depletion of CNOT6 in cells exposed to HU caused a similar effect on '2nd label origins' as the one previously observed following TAB182 knockdown. This suggested that TAB182 and CNOT6 may be acting in a common pathway in response to replication stress.

5.2.6 Fibres Structure Analysis after Double Knockdown of TAB182 and either CNOT4 or CNOT6

Double knockdowns with TAB182 and either CNOT4 or CNOT6 were also performed and the DNA fibre structures determined. HeLa cells were transfected with the following

combinations; control; TAB182; CNOT4; CNOT6; TAB182 and CNOT4; or TAB182 and CNOT6. 48 hours later, cells were labelled with the DNA analogue CldU. Following CldU labelling, cells were mock-treated or treated with 2mM HU for 2 hours, and subsequently incubated with IdU in HU-free media. Cells were then processed for DNA fibre analysis as before. Double knockdowns were validated by Western blotting, note there was no specific CNOT6 antibody available in this study and therefore CNOT6 knockdown could not be validated (Figures 5.2 and 5.5C).

Since we are purely interested in '2nd label origins' and '1st label terminations' at this stage none of the other structures will be referred to in this section (see Figure 5.5A for more detailed results). As previously discussed, the percentage of '2nd label origins' in control siRNA treated undamaged cells was approximately 11%, decreasing to 3% upon the addition of HU treatment. As previously seen in Figure 4.8, the percentage of '2nd label origins' in TAB182 siRNA treated undamaged cells was also approximately 10%, but upon the addition of HU treatment was increased to approximately 18%. The percentage of '2nd label origins' in CNOT4 siRNA treated, undamaged cells was approximately 11%, decreasing to approximately 3% upon the addition of HU, which was similar to control siRNA treated cells (Figure 5.5A). In TAB182/CNOT4 double knockdown cells this percentage was approximately 11% in undamaged cells and upon the addition of HU, remains similar, suggesting that CNOT4 may be able to partially rescue elevated new origin firing observed in TAB182 deficient cells alone (Figure 5.5A). In contrast to CNOT4, the percentage of '2nd label origins' after CNOT6 siRNA treatment was approximately 9% and following release from HU treatment, increased to approximately 19%. In TAB182/CNOT6 double knockdown cells, this percentage increased from 8% in undamaged cells, to 17%, similar to TAB182 or CNOT6

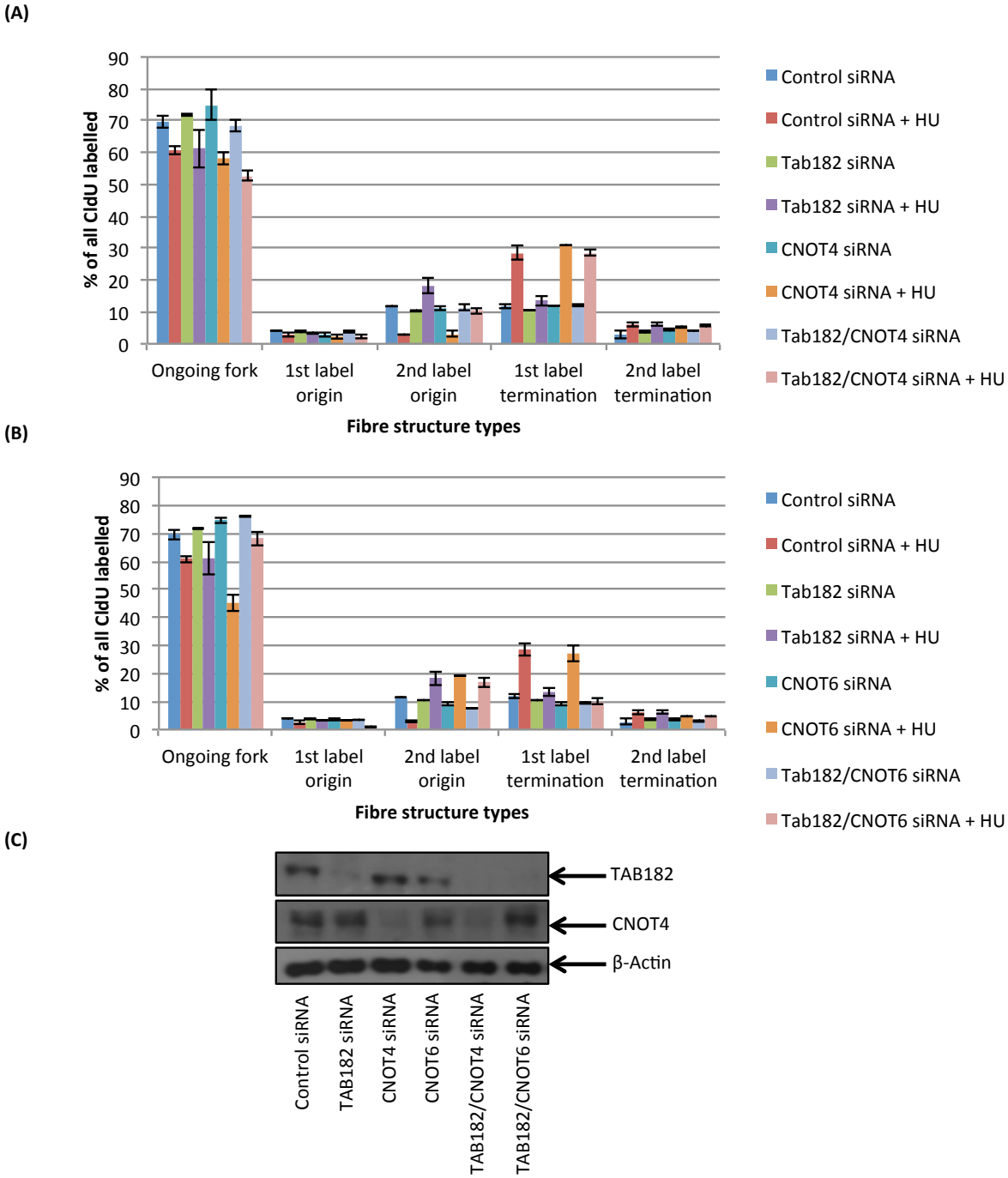

Figure 5.5: DNA Fibre Structures After Double Knockdowns of TAB182 with either CNOT4 or CNOT6. HeLa cells were transfected with control, TAB182, CNOT4, CNOT6, TAB182/CNOT4 or TAB182/CNOT6 siRNA and were then treated as in Figure 5.4. Graphs show the fibre structures as a percentage of all CldU structures. **(A)** DNA fibre structures after TAB182/CNOT4 double knockdown. **(B)** DNA fibre structures after TAB182/CNOT6 double knockdown. Error bars represent SEM. **(C)** Western blot shows validation of TAB182, CNOT4, CNOT6, TAB182/CNOT4 and TAB182/CNOT6 knockdowns. These data are representative of three independent experiments.

siRNA transfected cells alone. This suggests that firstly, upon deletion of TAB182 or CNOT6 a similar defect in new origin firing is observed in response to replication stress and secondly, that this defect is not further enhanced in cells deficient in both TAB182 and CNOT6 (Figure 5.5B).

The percentage of '1st label terminations' in control siRNA undamaged cells was 12% and increased to 28% upon the addition of HU. In TAB182 defective, undamaged cells, the percentage of '1st label terminations' was approximately 10% increasing up to 14% upon the addition of HU. In CNOT4 depleted, undamaged cells the percentage of '1st label terminations' was approximately 12% and increased up to 31% upon the addition of HU similarly to control cells. In TAB182/CNOT4 double knockdown undamaged cells the percentage of '1st label terminations' was approximately 12% and following HU release increased up to 29%. This suggests that CNOT4 depletion can restore the '1st label termination' defect observed in TAB182 deficient cells to control levels following HU treatment (Figure 5.5A).

In CNOT6 deficient, undamaged cells the percentage of '1st label terminations' was 9%, increasing to approximately 27% after HU release, as in control cells. In TAB182/CNOT6 double knockdown undamaged cells this percentage was approximately 9% and remained the same after release from HU. This indicates that CNOT6 knockdown cannot rescue the '1st label termination' defect observed in TAB182 deficient cells.

5.2.7 Depletion of CNOT4 or CNOT6 Results in Hypersensitivity to HU which is Additive Upon Co-Depletion of TAB182.

Since TAB182 was shown to associate with components of the CNOT complex, we also aimed to examine how CNOT4 and CNOT6 impacts on cellular survival in response to replication stress. To this end, HeLa cells were transfected with the following siRNA combinations; control; TAB182; CNOT4; CNOT6; TAB182 and CNOT4; or TAB182 and CNOT6. 48 hours later, the cells were plated at various densities and were exposed to increasing concentrations of HU (0-10mM HU). Following exposure, the cells were incubated for 14 days and the colonies formed were stained and counted. Colony numbers were plotted on survival graphs and analysed (Figure 5.6). Confirmation of TAB182 and CNOT4 knockdown was achieved by Western blotting (Figure 5.5C).

As previously shown (Figure 4.2), TAB182 deficient cells are sensitive to HU. Interestingly, CNOT4 and CNOT6 are also similarly sensitive to HU as TAB182. When double knockdowns of TAB182 and CNOT4, or TAB182 and CNOT6 were performed, the HU sensitivity was additive in all cases compared to single knockdowns of these proteins, suggesting that TAB182 and CNOT4/CNOT6 are not epistatic in the survival following replication stress (Figure 5.6).

5.2.8 TAB182 Depletion has no Effect on RNR Expression

Previous studies in the literature suggested that components of the yeast CCR4-NOT complex were able to affect the expression of components of the RNR complex (Mulder, Winkler et al. 2005, Takahashi, Kontani et al. 2007). To determine whether some components of the CNOT complex have a similar function in mammalian cells, the

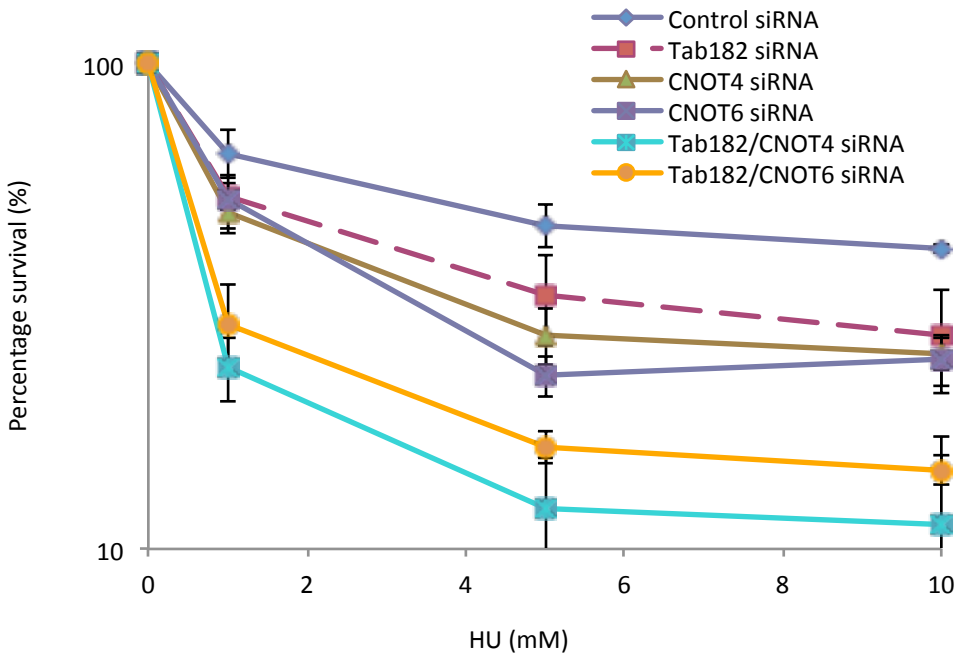

Figure 5.6: Depletion of CNOT4 or CNOT6 Results in Hypersensitivity to HU which is Additive Upon Co-Depletion of TAB182. HeLa cells were transfected with one of the following combinations; TAB182; CNOT4; CNOT6; TAB182 and CNOT4; TAB182 and CNOT6 TAB182, along with non-targeting control siRNA. 48 hours later, the cells were then exposed to increasing doses of HU. Following exposure, the cells were replated in fresh media and further incubated for 14 days. The colonies formed were stained with 0.5% crystal violet in 20% ethanol. Colonies were counted and the data plotted on survival graphs. This graph is representative of three independent experiments.

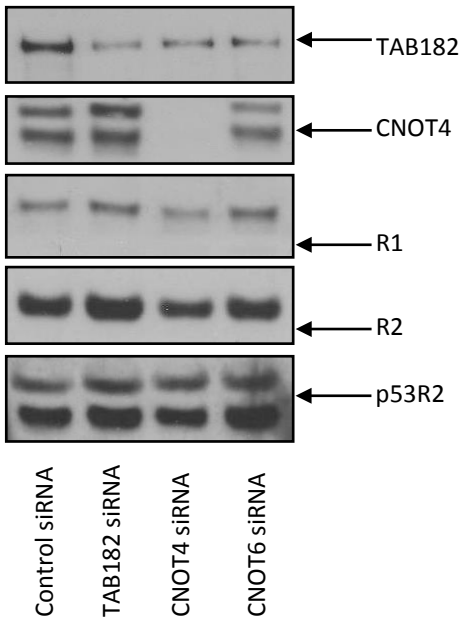

Figure 5.7: TAB182 Depletion has no Effect on RNR Expression. HeLa cells were transfected with control, TAB182, CNOT4 or CNOT6 siRNA. 48 hours post-transfection cells were harvested, and the resulting cell lysates subjected to SDS-PAGE and Western blotting using the indicated antibodies.

expression levels of components of the RNR complex were assessed after TAB182, CNOT4 and CNOT6 depletion. HeLa cells were transfected with control, TAB182, CNOT4 or CNOT6 siRNA and harvested 48 hours later. Cells were subjected to SDS-PAGE and Western blotting using antibodies against R1, R2 and p53R2 (Figure 5.7).

Knockdown of TAB182 expression appeared to have no effect on the expression of R1, R2 or p53R2. Slightly reduced levels of R1 and R2 expression were observed in CNOT4 deficient cells, whilst the expression of p53R2 remained unaltered following CNOT4 knockdown. Similarly to TAB182 depleted cells, in CNOT6 deficient cells, no differences in the expression of R1, R2 or p53R2 were observed. Interestingly, knockdown of both CNOT4 and CNOT6 appeared to reduce the expression of TAB182, suggesting that the expression of these proteins may be important for TAB182 levels (Figure 5.7).

5.2.9 TAB182 is Associated with Deadenylase Activity

To ascertain whether TAB182 is associated with an enzymatically active CNOT complex, simple deadenylation assays were carried out. TAB182 was immunoprecipitated from a HeLa cell extract and then the washed protein G-agarose/antibody/antigen pellet was incubated with an adenylated ribonucleotide (see Section 2.3.7). After an hour, an aliquot of the assay mixture was fractionated on an acrylamide gel run in the presence of 8M urea. Figure 5.8A shows that the TAB182 immunoprecipitate has deadenylase activity with the deadenylated ribonucleotide migrating faster (as it has a lower molecular weight due to the loss of adenyl moieties) and the concentration of the full-length ribonucleotide being markedly reduced (Figure 5.8A). Interestingly, Ad5 and Ad12 E1B immunoprecipitates were also shown to have deadenylase activity. Furthermore, Figure 5.8B shows that deadenylase

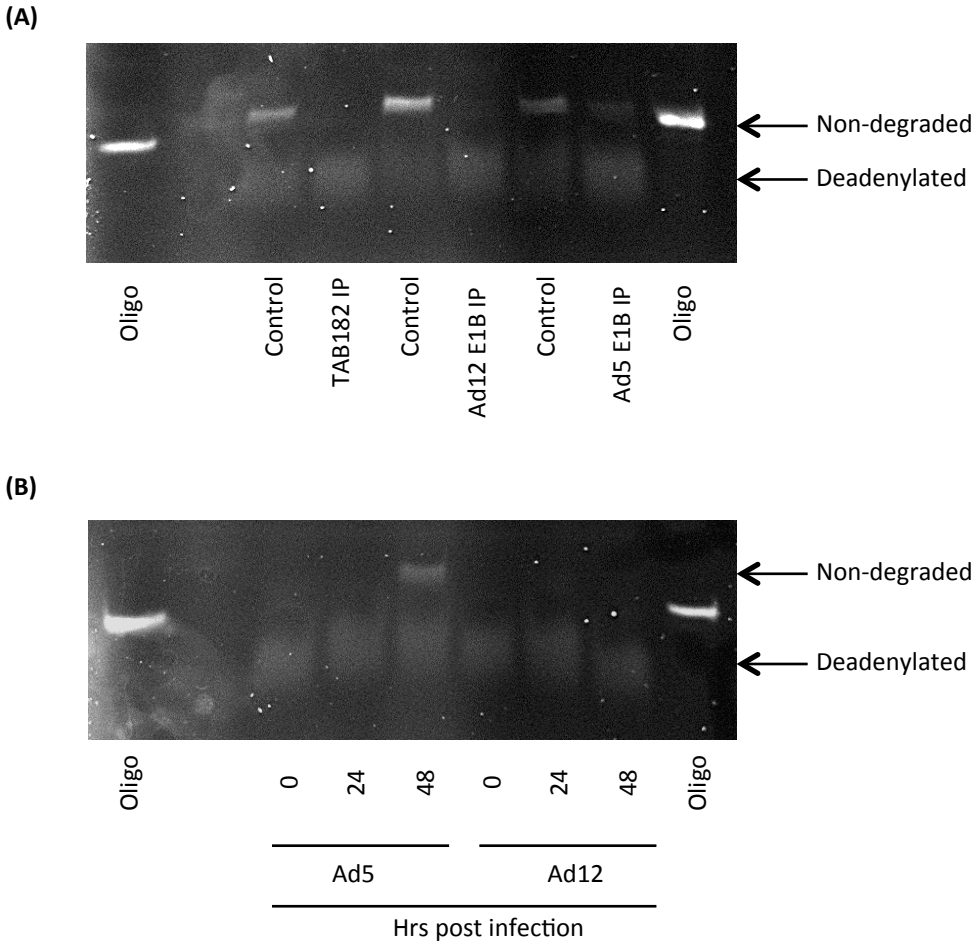

Figure 5.8: TAB182 is Associated with Deadenylase Activity. (A) TAB182 and adenovirus E1B55K proteins were immunoprecipitated from HeLa and adenovirus E1 transformed cells, respectively. Antibody/antigen complexes were incubated at 37°C in appropriate buffer containing a target fluorescein-labelled ribonucleotide as described in Section 2.3.7. After 1 hour the reaction supernatant was mixed with RNA loading buffer, heated at 85°C and subjected to electrophoresis on a 20% acrylamide gel run in the presence of 8M urea/TBE. Fluoroscein-labelled ribonucleotide was visualised using a Fusion SL chemiluminescence imaging system. 'Control' lane represents untreated ribonucleotide. **(B)** Cell lysates from Ad5 and Ad12 infected HeLa cells were incubated with fluorescein-labelled ribonucleotide as described above. After 1 hour an aliquot was subjected to electrophoresis and the gel visualised using the Fusion SL chemiluminescence imaging system.

activity is present in the cell lysates from adenovirus infected cells. As CNOT components are degraded during viral infection we considered that this might result in loss of deadenylase activity; however the data presented suggested that this is not the case.

5.3 DISCUSSION

Mass spectrometry experiments described in this chapter indicated that TAB182 was associated with a number of subunits of the CNOT complex including CNOT1, CNOT2, CNOT3, CNOT6L, CNOT7, CNOT8, CNOT9, CNOT10 and CNOT11 in both uninfected HeLa cells and Ad5 and Ad12 infected cells (Table 5.1). CNOT3 and CNOT7 were shown to be down-regulated following both Ad5 and Ad12 infection, suggesting that components of the CNOT complex may also be targeted by adenovirus for degradation (Figure 5.1). DNA fibre analysis revealed that CNOT4 depleted cells exhibited replication dynamics similar to control cells, but interestingly, CNOT4 knockdown in TAB182 deficient cells was able to partially rescue the new origin firing defect observed and to completely rescue the increased fork restart observed in TAB182 deficient cells following release from replication block (Figures 5.4 and 5.5). CNOT6 depleted cells showed firstly, an increase in new origin firing after release from HU that was comparable to that observed in TAB182 depleted cells, and secondly, a mild increase in fork restart (Figure 5.4). Interestingly, CNOT6 and TAB182 were epistatic in the new origin defect observed following release from HU. However, CNOT6 knockdown in TAB182 deficient cells had no effect on the increased fork restart observed in these cells (Figure 5.5). Interestingly, colony survival assays of single or double knockdowns showed that CNOT4 or CNOT6 were not epistatic with TAB182 (Figure 5.6). Defects observed in TAB182, CNOT4 and CNOT6 proteins were shown to not be a product of affecting RNR

expression, although depletion of CNOT4 was shown to mildly affect the expression of R1 and R2 (Figure 5.7). Finally, TAB182 was shown to have associated deadenylase activity *in vivo* (Figure 5.8).

There is limited information about the function of TAB182, but some reports in the literature have suggested that TAB182 interacts with a large, multi-subunit complex known as the CCR4-NOT complex in yeast, and the CNOT complex in mammalian cells (Morita, Suzuki et al. 2007, Lau, Kolkman et al. 2009). Our mass spectrometry data have confirmed that TAB182 interacts with a number of subunits of the CNOT complex including CNOT1, CNOT2, CNOT3, CNOT6L, CNOT7, CNOT8, CNOT9, CNOT10 and CNOT11 in both uninfected HeLa cells and Ad5 and Ad12 infected cells (Table 5.1). Regarding adenovirus infection, this suggests that infection has no effect on the interaction between TAB182 and components of the CNOT complex. Interestingly, neither CNOT4 nor CNOT6 were detected in TAB182 co-immunoprecipitates. The explanation for the lack of detection of CNOT6 may be due to the high amino acid sequence similarity (79%) between CNOT6 and CNOT6L, and so CNOT6 may be identified as CNOT6L. The CNOT complex is a highly conserved, multi-subunit complex with roles in the regulation of gene expression. It has been implicated in mRNA regulation, transcription elongation, chromatin modifications and interestingly, the DDR (Liu, Badarinarayana et al. 1998, Bennett, Lewis et al. 2001, Tucker, Valencia-Sanchez et al. 2001, Westmoreland, Marks et al. 2004, Mulder, Winkler et al. 2005, Traven, Hammet et al. 2005, Woolstencroft, Beilharz et al. 2006, Deshpande, Hayles et al. 2009). Although the majority of studies on the CCR4-NOT complex have been performed in mutant yeast strains, a study by Lau and colleagues in HeLa cells has helped to elucidate the composition of the CNOT complex and its interacting proteins in human cells. Also using mass spectrometry, this

group found the core components of the CNOT complex to be CNOT1, CNOT2, CNOT3, CNOT9, CNOT10 and the two previously unidentified CNOT complex components CNOT11 and TAB182. Interestingly, the deadenylases CNOT6, CNOT6L, CNOT7 and CNOT8 were found to be variable subunits of the CNOT complex. CNOT7 was not found in CNOT8 purifications, nor CNOT8 found in CNOT7 purifications, suggesting that CNOT7 and CNOT8 exist in separate complexes. Furthermore, both CNOT6/CNOT6L were identified in CNOT7, but not CNOT8 purifications, suggesting that CNOT6/CNOT6L does not stably interact with CNOT8 (Figure 1.15) (Lau, Kolkman et al. 2009). In the TAB182 purifications presented in this chapter, no co-purification between TAB182 and CNOT4 was observed, confirming that CNOT4 is not a core component of the CNOT complex. In this regard, the lack of TAB182 co-purification with CNOT6 may also be due to CNOT6 not being a core component of the CNOT complex. In addition, CNOT7 and CNOT8 were identified in our co-purifications even though these subunits are not thought to stably interact with the core CNOT complex, suggesting that either CNOT7/CNOT8 transiently associate with TAB182 and/or TAB182 may be in a complex with CNOT7/CNOT8 (Table 5.1). PRMT3 and FHL2 were also identified in the TAB182 mass spectrometry screen. PRMT3 is a type I arginine methyltransferase which catalyses the methylation of guanidine nitrogens of arginine residues of proteins. Protein arginine methylation has a role in a number of cellular functions including protein-protein interactions, protein localisation and DNA repair (Tang, Gary et al. 1998). FHL2 belongs to the FHL family of transcription co-repressors and has been shown to interact with a number of transcription factors linked to tumour development (Kleiber, Strebhardt et al. 2007). FHL2 has also been shown to interact with BRCA1 and enhances the transactivation of FHL2 (Yan, Zhu et al. 2003). As yet the function of the potential interaction between PRMT3 and FHL2

with TAB182 is unknown (Table 5.1). The TAB182 interacting proteins Tankyrase 1, Chk1 and Aurora kinase that were identified in the GST pull-downs performed in this study (Figure 4.12), were not identified in the mass spectrometry screen. There are a number of explanations for the different interacting proteins identified between experiments. Firstly, the mass spectrometry screen was performed following co-immunoprecipitation assays and not GST pull-downs, and so could yield different results. Secondly, the GST pull-downs were performed using a C-terminal fragment (Figure 3.11) of TAB182 only and may not be representative of the entire TAB182 protein as in the mass spectrometry experiment. Finally, the mass spectrometry experiment was performed in whole cell lysates and thus a large pool of TAB182 interacting proteins were identified, whereas the GST pull-downs were only an examination of TAB182 interaction with one protein. For this reason less abundant interactions, for example, Tankyrase 1, Chk1 and Aurora kinase, may be masked by larger protein pools, for example, such as those with the CNOT complex.

Results from Table 5.1 showed that adenovirus infection had no effect on the interaction between TAB182 and components of the CNOT complex. Since TAB182 appeared to be a stable core component of the CNOT complex, and TAB182 is degraded during infection with a number of different adenovirus serotypes, it was next hypothesised that components of the CNOT complex may also be targeted for degradation during adenovirus infection (Figure 5.1). CNOT4 was not down-regulated following infection with adenovirus serotypes 5 or 12. Interestingly, CNOT3 and CNOT7 were down-regulated during Ad5 and Ad12 infection, indicating that adenovirus may also target at least two other CNOT components for degradation. Unfortunately, of the panel of CNOT6 antibodies tested, none were shown to be specific (using CNOT6 siRNA) and therefore, analysis of CNOT6 levels after

adenovirus infection was not performed. Since depletion of TAB182 was shown to affect the levels of the early adenoviral protein E1A during adenovirus infection, it was next determined whether depletion of CNOT4 and CNOT6 had the same effect on viral protein expression. Depletion of CNOT4 and CNOT6 had no effect on the expression of any of the viral proteins detected, suggesting that the depletion of TAB182 may be directly responsible for the changes in E1A protein expression observed in TAB182 deficient cells in Chapter Three (Figures 3.9 and 5.3).

DNA fibre analysis revealed that cells depleted of CNOT4 exhibit replication structures similar to control cells following release from HU. Interestingly, cells deficient in CNOT6 exhibit a similar replication structure profile to that of TAB182 depleted cells (Figure 5.4). Following release from HU, CNOT6 knockdown cells showed an increase in new origin firing similar to TAB182 depleted cells. Although CNOT4 depletion alone displayed a normal replication profile following release from HU, CNOT4/TAB182 depleted cells partially rescued the new origin firing defect and completely rescued the increased fork restart present in TAB182 deficient cells alone (Figure 5.5). This suggests that the new origin firing defect observed in TAB182 depleted cells following release from HU is partially dependent on the activity of the CNOT4 protein, and the increased fork restart observed in these cells is completely dependent on CNOT4 activity. This leads to the question of whether the defects in new origin firing and fork restart are dependent on the E3 ubiquitin ligase activity of CNOT4. To date, only two substrates of NOT4 have been identified in yeast. Nascent associated polypeptide complex (NAC), a chaperone protein which has been shown to bind nascent peptides associated with the ribosome (Panasenko, Landrieux et al. 2006). Although the role for the ubiquitination of NAC by NOT4 is currently unknown, it has been suggested

that the ubiquitination of NAC stimulates its association with the ribosome and proteasome and acts as a surveillance protein for transcriptionally-damaged proteins (Panasenko, David et al. 2009). In both yeast and human cells, NOT4/hCNOT4 has been shown to ubiquitinate and subsequently target the yeast histone 3 Lys 4 (H3K4) demethylase Jhd2/human jumonji and AT-rich interaction domain 1C (JARID1C) protein for degradation. This function is thought to achieve a balance between histone demethylase and histone methyltransferases and therefore H3K4 methylation and transcription (Mersman, Du et al. 2009). Since only two NOT4/hCNOT4 substrates have been identified to date, it is difficult to speculate why knockdown of CNOT4 is able to rescue the defects observed in TAB182 depleted cells following release from HU. Since CNOT4 has been shown to exist in a complex distinct from the core CNOT complex, it is likely that CNOT4 interacts with other proteins that are yet to be identified. Identification of such proteins may help to elucidate the role of CNOT4 and TAB182 in response to replication stress.

Double knockdown of CNOT6/TAB182 revealed that the excessive new origin firing observed following release from HU in these cells was epistatic (Figure 5.5). However, the double knockdown of CNOT6/TAB182 had no effect on the increased fork restart observed in TAB182 deficient cells alone, suggesting that CNOT6 cannot rescue this defect. Reports in the literature have suggested that sensitivity to DNA damaging agents in CCR4 (hCNOT6) mutant yeast strains is due to the loss of deadenylation activity (Traven, Hammet et al. 2005, Woolstencroft, Beilharz et al. 2006). Indeed, CCR4 has been shown to regulate compromised recognition of TCV 1 (CRT1) mRNA poly(A) tail length, a transcriptional repressor of a number of DNA damage related genes (Woolstencroft, Beilharz et al. 2006). We have also identified TAB182 to be associated with a deadenylase activity (Figure 5.8), suggesting that

together TAB182 and CNOT6, together with other proteins, may deadenylate various DNA damage and/or replication stress genes, and in their absence, a number of these genes are not deadenylated, thus explaining why these cells display elevated new origin firing following release from HU.

Since the CNOT complex component TAB182 was shown to be sensitive to agents that induced replication stress, and studies in yeast mutant strains had shown a number of components of the CCR4-NOT complex to be sensitive to almost all DNA damaging agents tested, it was hypothesised that cells depleted of CNOT4 and CNOT6 in mammalian cells may also be sensitive to DNA damaging agents, particularly those that induced replicative stress (Bennett, Lewis et al. 2001, Westmoreland, Marks et al. 2004, Mulder, Winkler et al. 2005, Traven, Hammet et al. 2005, Woolstencroft, Beilharz et al. 2006, Deshpande, Hayles et al. 2009). In this study, both CNOT4 and CNOT6 depleted cells were shown to be sensitive to HU to a similar extent to the observed sensitivity of TAB182 depleted cells. However, double knockdown of TAB182/CNOT4 or TAB182/CNOT6 revealed that TAB182 and CNOT4/CNOT6 act independently of one another (Figure 5.6). These data suggest the mechanisms of promoting survival in TAB182 depleted cells and CNOT4/CNOT6 depleted cells are distinct. Thorough studies have been performed in yeast mutant strains to address the mechanism behind the sensitivity observed in CNOT4/CNOT6 deficient cells. As previously discussed, CCR4 (hCNOT6/hCNOT6L) yeast mutant strains have been shown to be sensitive to IR, UV-C, HU, 4-NQO and camptothecin (Bennett, Lewis et al. 2001, Westmoreland, Marks et al. 2004, Mulder, Winkler et al. 2005, Traven, Hammet et al. 2005, Woolstencroft, Beilharz et al. 2006, Deshpande, Hayles et al. 2009). Caf1 (CNOT7/CNOT8) yeast mutant strains have been shown to be sensitive to IR, HU, 4-NQO, camptothecin, MMS (Mulder, Winkler et al. 2005,

Woolstencroft, Beilharz et al. 2006, Deshpande, Hayles et al. 2009). NOT1, NOT2, NOT3, NOT4 and NOT5 mutant yeast strains have been shown to be sensitive to HU (Mulder, Winkler et al. 2005). A number of mechanisms of sensitivity have been postulated. Interestingly, Woolstencroft and colleagues demonstrated that CCR4 (hCNOT6/hCNOT6L) yeast strains with mutations in the region responsible for deadenylase activity also displayed sensitivity to HU, but not to the same extent as the CCR4 deletion yeast strain, suggesting that the sensitivity to HU observed in CCR4 mutants operates via both deadenylation-dependent and independent mechanisms. Studies from Traven and colleagues also suggested that the deadenylase activity of the CCR4-NOT complex is required for the DDR (Traven, Hammet et al. 2005, Woolstencroft, Beilharz et al. 2006). Further studies from these groups revealed that CCR4 and Chk1 cooperate in the same pathway in response to replication stress induced by HU. CCR4 was later found to regulate CRT1 mRNA poly(A) tail length, CRT is a transcriptional repressor of a number of DNA damage-related genes and therefore the sensitivity of CCR4 yeast mutants was attributed to deregulated CRT mRNA poly(A) tail length (Woolstencroft, Beilharz et al. 2006). Another study by Mulder and colleagues suggested that defective RNR mRNA accumulation in CCR4-NOT mutants was responsible for the HU sensitivity observed in these strains (Mulder, Winkler et al. 2005). In contrast, Traven and colleagues showed that sensitivity to HU is not due to defective RNR expression (Traven, Hammet et al. 2005). Takahashi and colleagues suggested that the Caf1 (hCNOT7/hCNOT8) component of the CNOT complex is responsible for Spd1 degradation and Suc22 translocation (Spd1 is the RNR inhibitory protein that holds Suc22, the RNR regulatory subunit in the nucleoplasm), and therefore is sensitive to HU (Takahashi, Kontani et al. 2007). It therefore remains unclear what the exact mechanism for the sensitivity to

various DNA damaging agents is in cells depleted of various CCR4-NOT components, although data presented here suggests that the mechanism of sensitivity of TAB182 depleted cells is distinct from CNOT4/CNOT6 depleted cells. It should be borne in mind that mutation/deletion of one CNOT component could affect the complex as a whole and might impinge on other necessary activities.

Numerous reports have suggested that RNR activity is related to the sensitivities to DNA agents observed in CCR4-NOT mutant yeast strains (Mulder, Winkler et al. 2005, Traven, Hammet et al. 2005, Takahashi, Kontani et al. 2007). RNR catalyses the conversion of NDPs into dNDPs, which is the rate limiting step in the production of dNTPs which are necessary for DNA replication (Jordan and Reichard 1998). RNR activity is also important during DNA damage and replication stress, RNR genes become transcriptionally active in response to these conditions. In yeast, four RNR subunits exist (RNR1-4) which are activated in response to DNA damage and/or replication stress in a Mec1p/Rad53p/Dun1p dependent manner (Chabes, Georgieva et al. 2003). Interestingly, RNR 1, 2, and 4 yeast mutant strains display sensitivities to DNA damaging agents (Elledge and Davis 1989, Wang, Chabes et al. 1997). In mammalian cells, three RNR subunits exist, R1 and R2, which become transcriptionally activated during S phase in order to allow dNTP production during DNA replication (Chabes, Bjorklund et al. 2004, Hakansson, Hofer et al. 2006). The third mammalian RNR subunit, known as p53R2, becomes transcriptionally activated by p53 following DNA damage (Tanaka, Arakawa et al. 2000). Since the sensitivity to DNA damaging agents observed in CCR4-NOT complex mutants has been linked to RNR expression, it was thought that TAB182 depletion may have an effect on mammalian RNR expression. However, no differences in the expression of the RNR subunits were observed in TAB182

depleted cells, suggesting that the sensitivity to HU observed in these cells is not due to the direct effect of TAB182 on RNR subunits expression (Figure 5.7).

In mammalian cells, the deadenylase activity of the CNOT complex is achieved through the CNOT6, CNOT6L, CNOT7 and CNOT8 components, which are thought to transiently associate with the CNOT complex (Figure 1.14)(Lau, Kolkman et al. 2009). In this study it was shown that TAB182 containing complexes have deadenylase activity (Figure 5.8). Interestingly, it had previously been assumed that the deadenylase components of the CNOT complex only associated with the complex transiently. On the other hand, it could be that TAB182 is not a core component of the complex as previously thought. Indeed, in our hands we have only performed the co-immunoprecipitations followed by mass spectrometry using TAB182 as bait and not vice versa. Perhaps, if components of the CNOT complex were used as bait, TAB182 would not always be identified in the purifications, suggesting that TAB182 is not a core component of the CNOT complex, however, this would be contradictory to the results obtained from Lau and colleagues (Lau, Kolkman et al. 2009). Furthermore, deadenylation activity (or lack of) was thought to be responsible for the observed sensitivities of CCR4, NOT4 and Caf1 to DNA damaging agents in the yeast studies (Mulder, Winkler et al. 2005, Woolstencroft, Beilharz et al. 2006, Takahashi, Kontani et al. 2007). If defective deadenylation activity was responsible for the sensitivity of TAB182 depleted cells following HU, it would be expected that TAB182 and CNOT6 would appear to be epistatic, that is of course assuming both sensitivities seen in TAB182 and CNOT6 were due to defective deadenylation. Of course the diversity of mechanisms that have been postulated for the sensitivities to DNA damaging agents of CCR4-NOT components show that a definitive mechanism for the observed sensitivities is currently unclear.

CHAPTER SIX

FINAL DISCUSSION AND FUTURE WORK

6. FINAL DISCUSSION AND FUTURE WORK

6.1 ADENOVIRUS, TAB182 AND THE CNOT COMPLEX

Previous to this study, little was known about the function of TAB182. Preliminary evidence from our laboratory suggested that TAB182 may be degraded following adenovirus infection. Furthermore, TAB182 was thought to be a potential substrate of ATM/ATR phosphorylation (Matsuoka, Ballif et al. 2007). Taken together these observations pointed towards a role for TAB182 in the DNA damage response (DDR).

In this study, it was found that TAB182 was degraded following Ad5 and Ad12 infection, in a manner that was dependent on the adenoviral E1B55K and E4orf6 proteins. Furthermore, the degradation of TAB182 following Ad5 and Ad12 infection was shown to be dependent on Cul5 and Cul2, respectively. In addition, knockdown of TAB182 elevated E1A expression to a limited extent following Ad5 and Ad12 infection, suggesting that its expression has an inhibitory effect on viral infection. This is also the case for Cyclin E expression following Ad12 infection in TAB182 depleted cells, where its expression was increased, but whether this is directly regulated by TAB182, or via transcriptional hyperactivation mediated by the upregulation of E1A levels is unclear. TAB182 did not localise to VRCs following Ad infection, but may localise to nuclear tracks or aggresomes, something that is yet to be examined.

TAB182 is a component of the CNOT complex, which in yeast, has roles in mRNA regulation, transcriptional elongation, chromatin modification and the DDR (Liu, Badarinarayana et al. 1998, Bennett, Lewis et al. 2001, Tucker, Valencia-Sanchez et al. 2001, Westmoreland, Marks et al. 2004, Mulder, Winkler et al. 2005, Traven, Hammet et al. 2005,

Woolstencroft, Beilharz et al. 2006, Deshpande, Hayles et al. 2009). In mammalian cells, the role of the CNOT complex is unknown. In this study, similarly to TAB182, subunits of the core CNOT complex (CNOT3 and CNOT7) were shown to be down-regulated following adenovirus infection. However, in contrast to TAB182, depletion of subunits of the CNOT complex had no effect on E1A expression following infection, although the CNOT subunits used for this experiment were not part of the core CNOT complex. Whether targeting both TAB182 as well as components of the CNOT complex provides an additional advantage for adenovirus infection, is unclear at present.

The use of adenovirus to study the function of TAB182 has suggested a role for the protein in the DDR, and more specifically, a potential role in the regulation of the cell cycle. We can envisage a number of reasons why adenovirus may degrade TAB182. Firstly, if TAB182 is indeed a cell cycle regulatory protein, its degradation will be advantageous to promote viral infection. Removal of cell cycle regulatory proteins (such as p53) allows the cell cycle to proceed thus allowing viral DNA replication. If TAB182 is also a cell cycle regulatory protein this could be the reason for its degradation during adenovirus infection. Secondly, it is also plausible that the effects on the cell cycle observed upon TAB182 depletion are indirectly linked to a potential role of TAB182 in the DDR. To further examine whether adenovirus degrades TAB182 to promote viral infection, cell cycle analysis could be performed following infection in the presence and absence of TAB182. Furthermore, quantification of E1A expression by quantitative PCR in TAB182 deficient, infected cells will confirm the elevated E1A expression observed by Western blotting. Indeed, depletion of the DDR protein Tip60 also leads to the same elevation in E1A expression following adenovirus

infection, which in this case, relieves the Tip60 transcriptional repression on the adenovirus E1A promoter (Gupta, Jha et al. 2013).

Adenovirus is known to relocalise some components of the DDR to VRCs, nuclear tracks and aggresomes, which, at least in the case of VRCs, is thought to inhibit the function of the DDR proteins to promote viral DNA replication (Stracker, Lee et al. 2005, Carson, Orazio et al. 2009). In this study, TAB182 was not found to localise to VRCs. Further analysis of TAB182 localisation to nuclear tracks and aggresomes will establish whether it is advantageous for adenovirus to sequester TAB182 within these structures.

Components of the core CNOT complex are also down-regulated during adenovirus infection (CNOT3 and CNOT7), but it is unknown whether the down-regulation of these proteins has any effect on the efficiency of adenovirus infection. If similar phenotypes were observed for TAB182 and the CNOT complex, this would suggest that adenovirus may degrade these proteins to compromise a common pathway in order to promote viral infection. However, CNOT4 and CNOT6 depletion had no effect on E1A expression during adenovirus infection, but at the same time these proteins were not shown to associate with TAB182 in the mass spectrometry screen performed in this study. Therefore, further analysis of the kinetics of adenovirus infection following depletion of other components of the CNOT complex may elucidate the relationship between TAB182 and the CNOT complex during adenovirus infection.

6.2 THE POTENTIAL ROLE OF TAB182 IN THE DDR AND REPLICATION STRESS PATHWAYS

One of the most striking phenotypes observed in TAB182 depleted cells is increased fork restart with a concomitant increase in new origin firing following release from HU. This suggests that TAB182 prevents fork restart and suppresses new origin firing following release from replication stress even though the mechanism through which this occurs is unknown. *In silico* analysis did not reveal any predicted functional domains in TAB182. Therefore, the question arises as to how does TAB182 regulate fork recovery and origin firing upon release from replication blocking. One possibility could be that it is present at stalled forks where it associates with proteins involved in the response to replication stress. In support of this, TAB182 was found to directly interact with Chk1 (Figure 4.12), which is necessary for checkpoint activation and suppression of new origin firing during replication stress (Maya-Mendoza, Petermann et al. 2007, Petermann, Woodcock et al. 2010). Furthermore, TAB182 may be associated with fork remodelling complexes at the fork. In this respect, FANCM, a helicase mutated in the Fanconi anaemia M group, displays a very similar phenotype to TAB182. In fact, amongst the helicases implicated in the regulation of replication fork restart, such as BLM, WRN, SMARCAL1 and FBH1, it is only FANCM depletion that leads to elevated fork restart, something we also observed in TAB182 deficient cells (Schwab, Blackford et al. 2010). However, FANCM deficient cells exhibit an increase in DSB formation, something that was not observed in TAB182 deficient cells (Blackford, Schwab et al. 2012). Another possibility is that TAB182 may be required for fork collapse in order to facilitate an alternative pathway of replication intermediate resolution at sites of stalled replication. If TAB182 is necessary for fork collapse, it may act in concert with structure-specific endonucleases at the fork. Interestingly, similarly to TAB182 deficient cells,

depletion of the structure-specific endonuclease MUS81 leads to a minor increase in micronuclei formation as well as a reduction in gaps and breaks following replication stress (Ying, Minocherhomji et al. 2013, Pepe and West 2014, Sarbajna, Davies et al. 2014). Moreover, MUS81 depleted cells show reduced DSB formation following replication stress as measured by pulse-field gel electrophoresis (PFGE), a phenotype also present in TAB182 deficient cells as indicated by the reduction of 53BP1 foci positive cells following release from HU (Pepe and West 2014). Similarly to TAB182, MUS81 depleted cells show no differences in fork speed both during unperturbed replication as well as following replication stress, but display elevated new origin firing following release from HU (Fu, Martin et al. 2015). However, in contrast to TAB182 deficient cells, MUS81 depleted cells exhibit a decrease in replication fork restart following release from replication stress (Naim, Wilhelm et al. 2013, Ying, Minocherhomji et al. 2013). Finally, the possibility cannot be excluded that TAB182 down-regulation may impact on the expression levels of factors that are important for replication fork recovery and new origin firing, following replication stress.

DNA fibre analysis revealed that the elevated fork restart observed in TAB182 depleted cells following release from HU was unaffected by CDK or Chk1 inhibition but was dependent on ATR. This suggests that 1) excessive new origin firing does not account for the elevated fork restart in TAB182 deficient cells, 2) inhibition of Chk1 does not suppress fork recovery or increase fork stalling/collapse in TAB182 depleted cells but 3) ATR is essential for fork stability and restart in TAB182 knockdown cells. A number of different experiments described below will allow us to understand more about the role of TAB182 during replication stress.

Firstly, to address the question of whether TAB182 is associated with the replication fork, iPOND followed by mass spectrometry could be performed. iPOND involves the labelling of nascent DNA using the nucleoside analogue 5-ethynyl-2'-deoxyuridine (EdU). Biotin can be conjugated to EdU-labelled DNA using click chemistry and allows a one-step purification of nascent DNA-bound proteins. Using this technique, it can be determined whether TAB182 is associated with active, stalled or collapsed replication forks (Sirbu, McDonald et al. 2013). Furthermore, performing TAB182 immunoprecipitation experiments in human cells before and after replication stress would give insight about the proteins that TAB182 associates with. DNA damage signalling in TAB182 deficient cells can be further examined by monitoring the activation of additional factors activated upon replication stress. To better characterise the phenotypes observed after release from HU, we could examine the ability of cells to form Rad51 foci to see whether homologous recombination is the pathway that facilitates replication fork restart in the absence of TAB182. To confirm whether the decreased γH2AX and 53BP1 foci observed in TAB182 deficient cells following release from HU are a consequence of fork collapse into DSBs, we could perform PFGE and/or comet assays to measure the amount of DNA breaks resulting from collapsed forks. Whether structure-specific endonucleases and/or helicases are important for fork restart after HU in TAB182 deficient cells is also an important question that could be investigated through the use of DNA fibre analysis in TAB182 and helicase/nuclease co-depleted cells following release from replication stress.

6.3 A POTENTIAL ROLE FOR THE CNOT COMPLEX IN THE DDR AND REPLICATION STRESS PATHWAYS

Together with a previous publication, mass spectrometry performed in this study has confirmed TAB182 to interact with the CNOT complex (Lau, Kolkman et al. 2009). Using fibre analysis, it was shown that cells depleted of the E3 ubiquitin ligase, CNOT4, displayed normal replication fork dynamics, but cells depleted of the CNOT deadenylation subunit, CNOT6, exhibited elevated new origin firing following release from replication stress. Interestingly, co-depletion of CNOT4 and TAB182 was able to partially rescue the new origin firing defect and completely restore the increased fork restart observed in TAB182 depleted cells alone to control levels following release from replication stress. Furthermore, co-depletion of CNOT6 and TAB182 showed that the new origin firing defect observed in CNOT6 or TAB182 deficient cells alone was epistatic, suggesting that they may be acting in a common pathway that regulates new origin firing. However, CNOT6 and TAB182 depletion had no effect on the increased fork restart observed following replication stress in TAB182 cells alone. This leads to the question as to whether the phenotypes observed in TAB182 deficient cells is dependent on the E3 ubiquitin ligase and deadenylation activity of the CNOT complex. In our hands, TAB182 was shown to have associated deadenylase activity. Interestingly, the sensitivity to HU observed in TAB182 and CNOT4/6 deficient cells was shown to be independent of one another, perhaps suggesting that the sensitivity and replication fork dynamics of TAB182 deficient cells operate by independent mechanisms. To address these questions, co-depletions of TAB182 together with CNOT4 or CNOT6 could be performed to see whether the replication functions of TAB182 are linked to the CNOT complex. For example, the formation of γH2AX and 53BP1 foci, levels of 53BP1 bodies in G1 and

micronuclei could be assessed following replication stress in cells depleted of both TAB182 and CNOT4/CNOT6. It may also be important to study other components of the CNOT complex, such as those that were also shown to be degraded following adenovirus infection, to determine which components of the complex, together with TAB182 are involved in the response to replication stress.

The identification of novel proteins involved in the DDR and replication stress pathways has important implications for the understanding of genomic instability, a hallmark of cancer (Hanahan and Weinberg 2011). Work presented in this thesis has demonstrated TAB182 to be degraded during adenovirus infection, implicating a role for this protein in the DDR. In this study we show TAB182 prevented replication fork restart and suppressed new origin firing following replication stress. Furthermore, TAB182 deficient cells displayed markers of genome instability. To date, the precise role of TAB182 in the DDR and replication stress pathways is currently unknown. Further studies such as those discussed in this chapter, will elucidate a role for TAB182, either alone or together in a complex with CNOT, in these pathways.

CHAPTER SEVEN

REFERENCES

7. REFERENCES

Acharya, S., T. Wilson, S. Gradia, M. F. Kane, S. Guerrette, G. T. Marsischky, R. Kolodner and R. Fishel (1996). "hMSH2 forms specific mispair-binding complexes with hMSH3 and hMSH6." Proceedings of the National Academy of Sciences of the United States of America **93**(24): 13629-13634.

Adams, M. D., M. McVey and J. J. Sekelsky (2003). "Drosophila BLM in double-strand break repair by synthesis-dependent strand annealing." Science **299**(5604): 265-267.

Ahnesorg, P., P. Smith and S. P. Jackson (2006). "XLF interacts with the XRCC4-DNA ligase IV complex to promote DNA nonhomologous end-joining." Cell **124**(2): 301-313.

Albert, T. K., H. Hanzawa, Y. I. Legtenberg, M. J. de Ruwe, F. A. van den Heuvel, M. A. Collart, R. Boelens and H. T. Timmers (2002). "Identification of a ubiquitin-protein ligase subunit within the CCR4-NOT transcription repressor complex." EMBO J **21**(3): 355-364.

Alexander, P. and K. A. Stacey (1958). "Comparison of the changes produced by ionizing radiations and by the alkylating agents; evidence for a similar mechanism at the molecular level." Ann N Y Acad Sci **68**(3): 1225-1237.

Alkhatib, H. M., D. F. Chen, B. Cherney, K. Bhatia, V. Notario, C. Giri, G. Stein, E. Slattery, R. G. Roeder and M. E. Smulson (1987). "Cloning and expression of cDNA for human poly(ADP-ribose) polymerase." Proc Natl Acad Sci U S A **84**(5): 1224-1228.

Altmeyer, M., S. Messner, P. O. Hassa, M. Fey and M. O. Hottiger (2009). "Molecular mechanism of poly(ADP-ribosyl)ation by PARP1 and identification of lysine residues as ADP-ribose acceptor sites." Nucleic Acids Res **37**(11): 3723-3738.

Alzu, A., R. Bermejo, M. Begnis, C. Lucca, D. Piccini, W. Carotenuto, M. Saponaro, A. Brambati, A. Cocito, M. Foiani and G. Liberi (2012). "Senataxin Associates with Replication Forks to Protect Fork Integrity across RNA-Polymerase-II-Transcribed Genes." Cell **151**(4): 835-846.

Anderson, C. W. (1990). "The proteinase polypeptide of adenovirus serotype 2 virions." Virology **177**(1): 259-272.

Anglana, M., F. Apiou, A. Bensimon and M. Debatisse (2003). "Dynamics of DNA replication in mammalian somatic cells: Nucleotide pool modulates origin choice and interorigin spacing." Cell **114**(3): 385-394.

Aparicio, O. M., A. M. Stout and S. P. Bell (1999). "Differential assembly of Cdc45p and DNA polymerases at early and late origins of DNA replication." Proc Natl Acad Sci U S A **96**(16): 9130-9135.

Araki, M., C. Masutani, M. Takemura, A. Uchida, K. Sugasawa, J. Kondoh, Y. Ohkuma and F. Hanaoka (2001). "Centrosome protein centrin 2/caltractin 1 is part of the xeroderma pigmentosum group C complex that initiates global genome nucleotide excision repair." Journal of Biological Chemistry **276**(22): 18665-18672.

Arany, Z., D. Newsome, E. Oldread, D. M. Livingston and R. Eckner (1995). "A family of transcriptional adaptor proteins targeted by the E1A oncoprotein." Nature **374**(6517): 81-84.

Araujo, F. D., T. H. Stracker, C. T. Carson, D. V. Lee and M. D. Weitzman (2005). "Adenovirus type 5 E4orf3 protein targets the Mre11 complex to cytoplasmic aggresomes." Journal of Virology **79**(17): 11382-11391.

Athappilly, F. K., R. Murali, J. J. Rux, Z. Cai and R. M. Burnett (1994). "The refined crystal structure of hexon, the major coat protein of adenovirus type 2, at 2.9 A resolution." J Mol Biol **242**(4): 430-455.
Avvakumov, N., M. Sahbegovic, Z. Zhang, M. Shuen and J. S. Mymryk (2002). "Analysis of DNA binding by the adenovirus type 5 E1A oncoprotein." J Gen Virol **83**(Pt 3): 517-524.
Babiss, L. E. and H. S. Ginsberg (1984). "Adenovirus type 5 early region 1b gene product is required for efficient shutoff of host protein synthesis." J Virol **50**(1): 202-212.
Babiss, L. E., H. S. Ginsberg and J. E. Darnell, Jr. (1985). "Adenovirus E1B proteins are required for accumulation of late viral mRNA and for effects on cellular mRNA translation and transport." Mol Cell Biol **5**(10): 2552-2558.
Bagchi, S., P. Raychaudhuri and J. R. Nevins (1990). "Adenovirus E1A proteins can dissociate heteromeric complexes involving the E2F transcription factor: a novel mechanism for E1A trans-activation." Cell **62**(4): 659-669.
Bahassi, E. L. M., R. F. Hennigan, D. L. Myer and P. J. Stambrook (2004). "Cdc25C phosphorylation on serine 191 by Plk3 promotes its nuclear translocation." Oncogene **23**(15): 2658-2663.
Baker, A., K. J. Rohleder, L. A. Hanakahi and G. Ketner (2007). "Adenovirus E4 34k and E1b 55k oncoproteins target host DNA ligase IV for proteasomal degradation." J Virol **81**(13): 7034-7040.
Bakkenist, C. J. and M. B. Kastan (2003). "DNA damage activates ATM through intermolecular autophosphorylation and dimer dissociation." Nature **421**(6922): 499-506.
Banin, S., L. Moyal, S. Shieh, Y. Taya, C. W. Anderson, L. Chessa, N. I. Smorodinsky, C. Prives, Y. Reiss, Y. Shiloh and Y. Ziv (1998). "Enhanced phosphorylation of p53 by ATM in response to DNA damage." Science **281**(5383): 1674-1677.
Banin, S., L. Moyal, S. Y. Shieh, Y. Taya, C. W. Anderson, L. Chessa, N. I. Smorodinsky, C. Prives, Y. Reiss, Y. Shiloh and Y. Ziv (1998). "Enhanced phosphorylation of p53 by ATN in response to DNA damage." Science **281**(5383): 1674-1677.
Bansbach, C. E., R. Betous, C. A. Lovejoy, G. G. Glick and D. Cortez (2009). "The annealing helicase SMARCAL1 maintains genome integrity at stalled replication forks." Genes & Development **23**(20): 2405-2414.
Barlow, J. H., R. B. Faryabi, E. Callen, N. Wong, A. Malhowski, H. T. Chen, G. Gutierrez-Cruz, H. W. Sun, P. McKinnon, G. Wright, R. Casellas, D. F. Robbiani, L. Staudt, O. Fernandez-Capetillo and A. Nussenzweig (2013). "Identification of early replicating fragile sites that contribute to genome instability." Cell **152**(3): 620-632.
Baumann, P., F. E. Benson and S. C. West (1996). "Human Rad51 protein promotes ATP-dependent homologous pairing and strand transfer reactions in vitro." Cell **87**(4): 757-766.
Beijersbergen, R. L., L. Carlee, R. M. Kerkhoven and R. Bernards (1995). "Regulation of the retinoblastoma protein-related p107 by G1 cyclin complexes." Genes Dev **9**(11): 1340-1353.
Bell, S. P. and B. Stillman (1992). "Atp-Dependent Recognition of Eukaryotic Origins of DNA-Replication by a Multiprotein Complex." Nature **357**(6374): 128-134.
Beltz, G. A. and S. J. Flint (1979). "Inhibition of HeLa cell protein synthesis during adenovirus infection. Restriction of cellular messenger RNA sequences to the nucleus." J Mol Biol **131**(2): 353-373.

Benjamin, R. C. and D. M. Gill (1980). "Poly(ADP-ribose) synthesis in vitro programmed by damaged DNA. A comparison of DNA molecules containing different types of strand breaks." J Biol Chem **255**(21): 10502-10508.
Bennett, C. B., L. K. Lewis, G. Karthikeyan, K. S. Lobachev, Y. H. Jin, J. F. Sterling, J. R. Snipe and M. A. Resnick (2001). "Genes required for ionizing radiation resistance in yeast." Nat Genet **29**(4): 426-434.
Bennett, F. M., W. Hamilton, B. B. Law and A. Macdonald (1957). "Adenovirus eye infections in Aberdeen." Lancet **273**(6997): 670-673.
Bergelson, J. M., J. A. Cunningham, G. Droguett, E. A. Kurt-Jones, A. Krithivas, J. S. Hong, M. S. Horwitz, R. L. Crowell and R. W. Finberg (1997). "Isolation of a common receptor for Coxsackie B viruses and adenoviruses 2 and 5." Science **275**(5304): 1320-1323.
Berk, A. J. (2005). "Recent lessons in gene expression, cell cycle control, and cell biology from adenovirus." Oncogene **24**(52): 7673-7685.
Bermejo, R., T. Capra, V. Gonzalez-Huici, D. Fachinetti, A. Cocito, G. Natoli, Y. Katou, H. Mori, K. Kurokawa, K. Shirahige and M. Foiani (2009). "Genome-Organizing Factors Top2 and Hmo1 Prevent Chromosome Fragility at Sites of S phase Transcription." Cell **138**(5): 870-884.
Bermudez, V. P., L. A. Lindsey-Boltz, A. J. Cesare, Y. Maniwa, J. D. Griffith, J. Hurwitz and A. Sancar (2003). "Loading of the human 9-1-1 checkpoint complex onto DNA by the checkpoint clamp loader hRad17-replication factor C complex in vitro." Proc Natl Acad Sci U S A **100**(4): 1633-1638.
Berti, M., A. R. Chaudhuri, S. Thangavel, S. Gomathinayagam, S. Kenig, M. Vujanovic, F. Odreman, T. Glatter, S. Graziano, R. Mendoza-Maldonado, F. Marino, B. Lucic, V. Biasin, M. Gstaiger, R. Aebersold, J. M. Sidorova, R. J. Monnat, M. Lopes and A. Vindigni (2013). "Human RECQ1 promotes restart of replication forks reversed by DNA topoisomerase I inhibition." Nature Structural & Molecular Biology **20**(3): 347-354.
Bezzubova, O., A. Silbergleit, Y. Yamaguchi-Iwai, S. Takeda and J. M. Buerstedde (1997). "Reduced X-ray resistance and homologous recombination frequencies in a RAD54-/- mutant of the chicken DT40 cell line." Cell **89**(2): 185-193.
Bianchi, V., E. Pontis and P. Reichard (1986). "Changes of deoxyribonucleoside triphosphate pools induced by hydroxyurea and their relation to DNA synthesis." J Biol Chem **261**(34): 16037-16042.
Bin, W. and S. J. Elledge (2007). "Ubc13/Rnf8 ubiquitin ligases control foci formation of the Rap80/Abraxas/Brca1/Brcc36 complex in response to DNA damage." Proceedings of the National Academy of Sciences of the United States of America **104**(52): 20759-20763.
Bishop, D. K., U. Ear, A. Bhattacharyya, C. Calderone, M. Beckett, R. R. Weichselbaum and A. Shinohara (1998). "Xrcc3 is required for assembly of Rad51 complexes in vivo." Journal of Biological Chemistry **273**(34): 21482-21488.
Blackford, A. N., R. K. Bruton, O. Dirlik, G. S. Stewart, A. M. R. Taylor, T. Dobner, R. J. A. Grand and A. S. Turnell (2008). "Role for E1B-AP5 in ATR signaling pathways during adenovirus infection." Journal of Virology **82**(15): 7640-7652.
Blackford, A. N., R. N. Patel, N. A. Forrester, K. Theil, P. Groitl, G. S. Stewart, A. M. Taylor, I. M. Morgan, T. Dobner, R. J. Grand and A. S. Turnell (2010). "Adenovirus 12 E4orf6 inhibits ATR activation by promoting TOPBP1 degradation." Proc Natl Acad Sci U S A **107**(27): 12251-12256.

Blackford, A. N., R. N. Patel, N. A. Forrester, K. Theil, P. Groitl, G. S. Stewart, A. M. R. Taylor, I. M. Morgan, T. Dobner, R. J. A. Grand and A. S. Turnell (2010). "Adenovirus 12 E4orf6 inhibits ATR activation by promoting TOPBP1 degradation." Proceedings of the National Academy of Sciences of the United States of America **107**(27): 12251-12256.
Blackford, A. N., R. A. Schwab, J. Nieminuszczy, A. J. Deans, S. C. West and W. Niedzwiedz (2012). "The DNA translocase activity of FANCM protects stalled replication forks." Hum Mol Genet **21**(9): 2005-2016.
Blanchette, P., C. Y. Cheng, Q. Yan, G. Ketner, D. A. Ornelles, T. Dobner, R. C. Conaway, J. W. Conaway and P. E. Branton (2004). "Both BC-Box motifs of adenovirus protein E4orf6 are required to efficiently assemble an E3 ligase complex that degrades p53." Molecular and Cellular Biology **24**(21): 9619-9629.
Blanchette, P., P. Wimmer, F. Dallaire, C. Y. Cheng and P. E. Branton (2013). "Aggresome Formation by the Adenoviral Protein E1B55K Is Not Conserved among Adenovirus Species and Is Not Required for Efficient Degradation of Nuclear Substrates." Journal of Virology **87**(9): 4872-4881.
Blier, P. R., A. J. Griffith, J. Craft and J. A. Hardin (1993). "Binding of Ku protein to DNA. Measurement of affinity for ends and demonstration of binding to nicks." J Biol Chem **268**(10): 7594-7601.
Boddy, M. N., P. H. L. Gaillard, W. H. McDonald, P. Shanahan, J. R. Yates and P. Russell (2001). "Mus81-Eme1 are essential components of a Holliday junction resolvase." Cell **107**(4): 537-548.
Boggs, K. and D. Reisman (2006). "Increased p53 transcription prior to DNA synthesis is regulated through a novel regulatory element within the p53 promoter." Oncogene **25**(4): 555-565.
Bondesson, M., K. Ohman, M. Manervik, S. Fan and G. Akusjarvi (1996). "Adenovirus E4 open reading frame 4 protein autoregulates E4 transcription by inhibiting E1A transactivation of the E4 promoter." J Virol **70**(6): 3844-3851.
Boyer, J., K. Rohleder and G. Ketner (1999). "Adenovirus E4 34k and E4 11k inhibit double strand break repair and are physically associated with the cellular DNA-dependent protein kinase." Virology **263**(2): 307-312.
Brandt, C. D., H. W. Kim, A. J. Vargosko, B. C. Jeffries, J. O. Arrobio, B. Rindge, R. H. Parrott and R. M. Chanock (1969). "Infections in 18,000 infants and children in a controlled study of respiratory tract disease. I. Adenovirus pathogenicity in relation to serologic type and illness syndrome." Am J Epidemiol **90**(6): 484-500.
Bridge, E. and G. Ketner (1989). "Redundant control of adenovirus late gene expression by early region 4." J Virol **63**(2): 631-638.
Britton, S., J. Coates and S. P. Jackson (2013). "A new method for high-resolution imaging of Ku foci to decipher mechanisms of DNA double-strand break repair." J Cell Biol **202**(3): 579-595.
Brookman, K. W., R. S. Tebbs, S. A. Allen, J. D. Tucker, R. R. Swiger, J. E. Lamerdin, A. V. Carrano and L. H. Thompson (1994). "Isolation and characterization of mouse Xrcc-1, a DNA repair gene affecting ligation." Genomics **22**(1): 180-188.
Brownell, J. E., M. D. Sintchak, J. M. Gavin, H. Liao, F. J. Bruzzese, N. J. Bump, T. A. Soucy, M. A. Milhollen, X. F. Yang, A. L. Burkhardt, J. Y. Ma, H. K. Loke, T. Lingaraj, D. Y. Wu, K. B. Hamman, J. J. Spelman, C. A. Cullis, S. P. Langston, S. Vyskocil, T. B. Sells, W. D. Mallender, I.

Visiers, P. Li, C. F. Claiborne, M. Rolfe, J. B. Bolen and L. R. Dick (2010). "Substrate-Assisted Inhibition of Ubiquitin-like Protein-Activating Enzymes: The NEDD8 E1 Inhibitor MLN4924 Forms a NEDD8-AMP Mimetic In Situ." Molecular Cell **37**(1): 102-111.
Bryant, H. E., E. Petermann, N. Schultz, A. S. Jemth, O. Loseva, N. Issaeva, F. Johansson, S. Fernandez, P. McGlynn and T. Helleday (2009). "PARP is activated at stalled forks to mediate Mre11-dependent replication restart and recombination." Embo Journal **28**(17): 2601-2615.
Bulavin, D. V., Y. Higashimoto, I. J. Popoff, W. A. Gaarde, V. Basrur, O. Potapova, E. Appella and A. J. Fornace (2001). "Initiation of a G2/M checkpoint after ultraviolet radiation requires p38 kinase." Nature **411**(6833): 102-107.
Byun, T. S., M. Pacek, M. C. Yee, J. C. Walter and K. A. Cimprich (2005). "Functional uncoupling of MCM helicase and DNA polymerase activities activates the ATR-dependent checkpoint." Genes Dev **19**(9): 1040-1052.
Caldecott, K. W., S. Aoufouchi, P. Johnson and S. Shall (1996). "XRCC1 polypeptide interacts with DNA polymerase beta and possibly poly(ADP-ribose) polymerase, and DNA ligase III is a novel molecular 'nick-sensor' in vitro." Nucleic Acids Research **24**(22): 4387-4394.
Caldecott, K. W., C. K. McKeown, J. D. Tucker, S. Ljungquist and L. H. Thompson (1994). "An interaction between the mammalian DNA repair protein XRCC1 and DNA ligase III." Mol Cell Biol **14**(1): 68-76.
Caldecott, K. W., J. D. Tucker, L. H. Stanker and L. H. Thompson (1995). "Characterization of the XRCC1-DNA ligase III complex in vitro and its absence from mutant hamster cells." Nucleic Acids Res **23**(23): 4836-4843.
Calsou, P., C. Delteil, P. Frit, J. Droulet and B. Salles (2003). "Coordinated assembly of Ku and p460 subunits of the DNA-dependent protein kinase on DNA ends is necessary for XRCC4-ligase IV recruitment." Journal of Molecular Biology **326**(1): 93-103.
Canman, C. E. and M. B. Kastan (1998). "Small contribution of G1 checkpoint control manipulation to modulation of p53-mediated apoptosis." Oncogene **16**(8): 957-966.
Canman, C. E., D. S. Lim, K. A. Cimprich, Y. Taya, K. Tamai, K. Sakaguchi, E. Appella, M. B. Kastan and J. D. Siliciano (1998). "Activation of the ATM kinase by ionizing radiation and phosphorylation of p53." Science **281**(5383): 1677-1679.
Cao, L., B. Faha, M. Dembski, L. H. Tsai, E. Harlow and N. Dyson (1992). "Independent binding of the retinoblastoma protein and p107 to the transcription factor E2F." Nature **355**(6356): 176-179.
Carrigan, D. R. (1997). "Adenovirus infections in immunocompromised patients." Am J Med **102**(3A): 71-74.
Carson, C. T., N. I. Orazio, D. V. Lee, J. Suh, S. Bekker-Jensen, F. D. Araujo, S. S. Lakdawala, C. E. Lilley, J. Bartek, J. Lukas and M. D. Weitzman (2009). "Mislocalization of the MRN complex prevents ATR signaling during adenovirus infection." EMBO J **28**(6): 652-662.
Carson, C. T., N. I. Orazio, D. V. Lee, J. H. Suh, S. Bekker-Jensen, F. D. Araujo, S. S. Lakdawala, C. E. Lilley, J. Bartek, J. Lukas and M. D. Weitzman (2009). "Mislocalization of the MRN complex prevents ATR signaling during adenovirus infection." Embo Journal **28**(6): 652-662.
Carson, C. T., R. A. Schwartz, T. H. Stracker, C. E. Lilley, D. V. Lee and M. D. Weitzman (2003). "The Mre11 complex is required for ATM activation and the G2/M checkpoint." EMBO J **22**(24): 6610-6620.

Carvalho, T., J. S. Seeler, K. Ohman, P. Jordan, U. Pettersson, G. Akusjarvi, M. Carmofonseca and A. Dejean (1995). "Targeting of Adenovirus E1a and E4-Orf3 Proteins to Nuclear Matrix-Associated Pml Bodies." Journal of Cell Biology **131**(1): 45-56.
Celeste, A., S. Petersen, P. J. Romanienko, O. Fernandez-Capetillo, H. T. Chen, O. A. Sedelnikova, B. Reina-San-Martin, V. Coppola, E. Meffre, M. J. Difilippantonio, C. Redon, D. R. Pilch, A. Olaru, M. Eckhaus, R. D. Camerini-Otero, L. Tessarollo, F. Livak, K. Manova, W. M. Bonner, M. C. Nussenzweig and A. Nussenzweig (2002). "Genomic instability in mice lacking histone H2AX." Science **296**(5569): 922-927.
Chabes, A., B. Georgieva, V. Domkin, X. Zhao, R. Rothstein and L. Thelander (2003). "Survival of DNA damage in yeast directly depends on increased dNTP levels allowed by relaxed feedback inhibition of ribonucleotide reductase." Cell **112**(3): 391-401.
Chabes, A. L., S. Bjorklund and L. Thelander (2004). "S Phase-specific transcription of the mouse ribonucleotide reductase R2 gene requires both a proximal repressive E2F-binding site and an upstream promoter activating region." J Biol Chem **279**(11): 10796-10807.
Chan, D. W. and S. P. Lees-Miller (1996). "The DNA-dependent protein kinase is inactivated by autophosphorylation of the catalytic subunit." J Biol Chem **271**(15): 8936-8941.
Chatterjee, P. K., M. E. Vayda and S. J. Flint (1985). "Interactions among the three adenovirus core proteins." J Virol **55**(2): 379-386.
Chatton, B., J. L. Bocco, M. Gaire, C. Hauss, B. Reimund, J. Goetz and C. Kedinger (1993). "Transcriptional activation by the adenovirus larger E1a product is mediated by members of the cellular transcription factor ATF family which can directly associate with E1a." Mol Cell Biol **13**(1): 561-570.
Chaudhuri, A. R., Y. Hashimoto, R. Herrador, K. J. Neelsen, D. Fachinetti, R. Bermejo, A. Cocito, V. Costanzo and M. Lopes (2012). "Topoisomerase I poisoning results in PARP-mediated replication fork reversal." Nature Structural & Molecular Biology **19**(4): 417-423.
Chellappan, S. P., S. Hiebert, M. Mudryj, J. M. Horowitz and J. R. Nevins (1991). "The E2F transcription factor is a cellular target for the RB protein." Cell **65**(6): 1053-1061.
Chen, J., Y. C. Chiang and C. L. Denis (2002). "CCR4, a 3'-5' poly(A) RNA and ssDNA exonuclease, is the catalytic component of the cytoplasmic deadenylase." EMBO J **21**(6): 1414-1426.
Cheng, C. Y., T. Gilson, F. Dallaire, G. Ketner, P. E. Branton and P. Blanchette (2011). "The E4orf6/E1B55K E3 ubiquitin ligase complexes of human adenoviruses exhibit heterogeneity in composition and substrate specificity." J Virol **85**(2): 765-775.
Chiou, S. K., C. C. Tseng, L. Rao and E. White (1994). "Functional complementation of the adenovirus E1B 19-kilodalton protein with Bcl-2 in the inhibition of apoptosis in infected cells." J Virol **68**(10): 6553-6566.
Ciccia, A., A. L. Bredemeyer, M. E. Sowa, M. E. Terret, P. V. Jallepalli, J. W. Harper and S. J. Elledge (2009). "The SIOD disorder protein SMARCAL1 is an RPA-interacting protein involved in replication fork restart." Genes & Development **23**(20): 2415-2425.
Ciccia, A., C. Ling, R. Coulthard, Z. Yan, Y. Xue, A. R. Meetei, H. Laghmani el, H. Joenje, N. McDonald, J. P. de Winter, W. Wang and S. C. West (2007). "Identification of FAAP24, a Fanconi anemia core complex protein that interacts with FANCM." Mol Cell **25**(3): 331-343.
Coombs, D. H., A. J. Robinson, J. W. Bodnar, C. J. Jones and G. D. Pearson (1979). "Detection of covalent DNA-protein complexes: the adenovirus DNA-terminal protein complex and HeLa DNA-protein complexes." Cold Spring Harb Symp Quant Biol **43 Pt 2**: 741-753.

Cordeiro-Stone, M., L. S. Zaritskaya, L. K. Price and W. K. Kaufmann (1997). "Replication fork bypass of a pyrimidine dimer blocking leading strand DNA synthesis." J Biol Chem **272**(21): 13945-13954.
Cortes-Ledesma, F. and A. Aguilera (2006). "Double-strand breaks arising by replication through a nick are repaired by cohesin-dependent sister-chromatid exchange." Embo Reports **7**(9): 919-926.
Costanzo, V., K. Robertson, M. Bibikova, E. Kim, D. Grieco, M. Gottesman, D. Carroll and J. Gautier (2001). "Mre11 protein complex prevents double-strand break accumulation during chromosomal DNA replication." Mol Cell **8**(1): 137-147.
Couch, F. B., C. E. Bansbach, R. Driscoll, J. W. Luzwick, G. G. Glick, R. Betous, C. M. Carroll, S. Y. Jung, J. Qin, K. A. Cimprich and D. Cortez (2013). "ATR phosphorylates SMARCAL1 to prevent replication fork collapse." Genes Dev **27**(14): 1610-1623.
Dallaire, F., P. Blanchette, P. Groitl, T. Dobner and P. E. Branton (2009). "Identification of Integrin alpha 3 as a New Substrate of the Adenovirus E4orf6/E1B 55-Kilodalton E3 Ubiquitin Ligase Complex." Journal of Virology **83**(11): 5329-5338.
Daugeron, M. C., F. Mauxion and B. Seraphin (2001). "The yeast POP2 gene encodes a nuclease involved in mRNA deadenylation." Nucleic Acids Res **29**(12): 2448-2455.
Davies, S. L., P. S. North, A. Dart, N. D. Lakin and I. D. Hickson (2004). "Phosphorylation of the Bloom's syndrome helicase and its role in recovery from S-phase arrest." Mol Cell Biol **24**(3): 1279-1291.
Davies, S. L., P. S. North and I. D. Hickson (2007). "Role for BLM in replication-fork restart and suppression of origin firing after replicative stress." Nature Structural & Molecular Biology **14**(7): 677-679.
De Falco, M., E. Ferrari, M. De Felice, M. Rossi, U. Hubscher and F. M. Pisani (2007). "The human GINS complex binds to and specifically stimulates human DNA polymerase alpha-primase." EMBO Rep **8**(1): 99-103.
De Piccoli, G., Y. Katou, T. Itoh, R. Nakato, K. Shirahige and K. Labib (2012). "Replisome stability at defective DNA replication forks is independent of S phase checkpoint kinases." Mol Cell **45**(5): 696-704.
Deans, A. J. and S. C. West (2011). "DNA interstrand crosslink repair and cancer." Nat Rev Cancer **11**(7): 467-480.
Debbas, M. and E. White (1993). "Wild-type p53 mediates apoptosis by E1A, which is inhibited by E1B." Genes Dev **7**(4): 546-554.
Dellaire, G. and D. P. Bazett-Jones (2004). "PML nuclear bodies: dynamic sensors of DNA damage and cellular stress." Bioessays **26**(9): 963-977.
Demple, B., T. Herman and D. S. Chen (1991). "Cloning and expression of APE, the cDNA encoding the major human apurinic endonuclease: definition of a family of DNA repair enzymes." Proc Natl Acad Sci U S A **88**(24): 11450-11454.
Deshpande, G. P., J. Hayles, K. L. Hoe, D. U. Kim, H. O. Park and E. Hartsuiker (2009). "Screening a genome-wide S. pombe deletion library identifies novel genes and pathways involved in genome stability maintenance." DNA Repair (Amst) **8**(5): 672-679.
Dianov, G., A. Price and T. Lindahl (1992). "Generation of single-nucleotide repair patches following excision of uracil residues from DNA." Mol Cell Biol **12**(4): 1605-1612.

Dimitrova, D. S. and D. M. Gilbert (2000). "Temporally coordinated assembly and disassembly of replication factories in the absence of DNA synthesis." Nature Cell Biology **2**(10): 686-694.
Ding, Q., Y. V. Reddy, W. Wang, T. Woods, P. Douglas, D. A. Ramsden, S. P. Lees-Miller and K. Meek (2003). "Autophosphorylation of the catalytic subunit of the DNA-dependent protein kinase is required for efficient end processing during DNA double-strand break repair." Mol Cell Biol **23**(16): 5836-5848.
Dix, I. and K. N. Leppard (1995). "Expression of adenovirus type 5 E4 Orf2 protein during lytic infection." J Gen Virol **76 (Pt 4)**: 1051-1055.
Dobbelstein, M., J. Roth, W. T. Kimberly, A. J. Levine and T. Shenk (1997). "Nuclear export of the E1B 55-kDa and E4 34-kDa adenoviral oncoproteins mediated by a rev-like signal sequence." EMBO J **16**(14): 4276-4284.
Dobner, T., N. Horikoshi, S. Rubenwolf and T. Shenk (1996). "Blockage by adenovirus E4orf6 of transcriptional activation by the p53 tumor suppressor." Science **272**(5267): 1470-1473.
Doil, C., N. Mailand, S. Bekker-Jensen, P. Menard, D. H. Larsen, R. Pepperkok, J. Ellenberg, S. Panier, D. Durocher, J. Bartek, J. Lukas and C. Lukas (2009). "RNF168 Binds and Amplifies Ubiquitin Conjugates on Damaged Chromosomes to Allow Accumulation of Repair Proteins." Cell **136**(3): 435-446.
Domon, M. and A. M. Rauth (1968). "Ultraviolet irradiation of mouse L cells: effects on DNA synthesis and progression through the cell cycle." Radiat Res **35**(2): 350-368.
Donahue, B. A., S. Yin, J. S. Taylor, D. Reines and P. C. Hanawalt (1994). "Transcript Cleavage by Rna-Polymerase-Ii Arrested by a Cyclobutane Pyrimidine Dimer in the DNA-Template." Proceedings of the National Academy of Sciences of the United States of America **91**(18): 8502-8506.
Dosch, T., F. Horn, G. Schneider, F. Kratzer, T. Dobner, J. Hauber and R. H. Stauber (2001). "The adenovirus type 5 E1B-55K oncoprotein actively shuttles in virus-infected cells, whereas transport of E4orf6 is mediated by a CRM1-independent mechanism." J Virol **75**(12): 5677-5683.
Douki, T. and J. Cadet (2001). "Individual determination of the yield of the main UV-induced dimeric pyrimidine photoproducts in DNA suggests a high mutagenicity of CC photolesions." Biochemistry **40**(8): 2495-2501.
Drummond, J. T., G. M. Li, M. J. Longley and P. Modrich (1995). "Isolation of an Hmsh2-P160 Heterodimer That Restores DNA Mismatch Repair to Tumor-Cells." Science **268**(5219): 1909-1912.
Dumaz, N. and D. W. Meek (1999). "Serine15 phosphorylation stimulates p53 transactivation but does not directly influence interaction with HDM2." Embo Journal **18**(24): 7002-7010.
Dunsworth-Browne, M., R. E. Schell and A. J. Berk (1980). "Adenovirus terminal protein protects single stranded DNA from digestion by a cellular exonuclease." Nucleic Acids Res **8**(3): 543-554.
Eckner, R., M. E. Ewen, D. Newsome, M. Gerdes, J. A. DeCaprio, J. B. Lawrence and D. M. Livingston (1994). "Molecular cloning and functional analysis of the adenovirus E1A-associated 300-kD protein (p300) reveals a protein with properties of a transcriptional adaptor." Genes Dev **8**(8): 869-884.

El-Khamisy, S. F., M. Masutani, H. Suzuki and K. W. Caldecott (2003). "A requirement for PARP-1 for the assembly or stability of XRCC1 nuclear foci at sites of oxidative DNA damage." Nucleic Acids Research **31**(19): 5526-5533.
Elledge, S. J. and R. W. Davis (1989). "DNA damage induction of ribonucleotide reductase." Mol Cell Biol **9**(11): 4932-4940.
Evans, J. D. and P. Hearing (2005). "Relocalization of the Mre11-Rad50-Nbs1 complex by the adenovirus E4 ORF3 protein is required for viral replication." Journal of Virology **79**(10): 6207-6215.
Everett, R. D. (2001). "DNA viruses and viral proteins that interact with PML nuclear bodies." Oncogene **20**(49): 7266-7273.
Evrin, C., P. Clarke, J. Zech, R. Lurz, J. C. Sun, S. Uhle, H. L. Li, B. Stillman and C. Speck (2009). "A double-hexameric MCM2-7 complex is loaded onto origin DNA during licensing of eukaryotic DNA replication." Proceedings of the National Academy of Sciences of the United States of America **106**(48): 20240-20245.
Ewen, M. E., H. K. Sluss, C. J. Sherr, H. Matsushime, J. Kato and D. M. Livingston (1993). "Functional interactions of the retinoblastoma protein with mammalian D-type cyclins." Cell **73**(3): 487-497.
Ezhevsky, S. A., H. Nagahara, A. M. Vocero-Akbani, D. R. Gius, M. C. Wei and S. F. Dowdy (1997). "Hypo-phosphorylation of the retinoblastoma protein (pRb) by cyclin D:Cdk4/6 complexes results in active pRb." Proc Natl Acad Sci U S A **94**(20): 10699-10704.
Falck, J., J. Coates and S. P. Jackson (2005). "Conserved modes of recruitment of ATM, ATR and DNA-PKcs to sites of DNA damage." Nature **434**(7033): 605-611.
Falck, J., N. Mailand, R. G. Syljuasen, J. Bartek and J. Lukas (2001). "The ATM-Chk2-Cdc25A checkpoint pathway guards against radioresistant DNA synthesis." Nature **410**(6830): 842-847.
Feijoo, C., C. Hall-Jackson, R. Wu, D. Jenkins, J. Leitch, D. M. Gilbert and C. Smythe (2001). "Activation of mammalian Chk1 during DNA replication arrest: a role for Chk1 in the intra-S phase checkpoint monitoring replication origin firing." Journal of Cell Biology **154**(5): 913-923.
Fekairi, S., S. Scaglione, C. Chahwan, E. R. Taylor, A. Tissier, S. Coulon, M. Q. Dong, C. Ruse, J. R. Yates, P. Russell, R. P. Fuchs, C. H. McGowan and P. H. L. Gaillard (2009). "Human SLX4 Is a Holliday Junction Resolvase Subunit that Binds Multiple DNA Repair/Recombination Endonucleases." Cell **138**(1): 78-89.
Forrester, N. A., G. G. Sedgwick, A. Thomas, A. N. Blackford, T. Speiseder, T. Dobner, P. J. Byrd, G. S. Stewart, A. S. Turnell and R. J. A. Grand (2011). "Serotype-Specific Inactivation of the Cellular DNA Damage Response during Adenovirus Infection." Journal of Virology **85**(5): 2201-2211.
Franchitto, A. and P. Pichierri (2002). "Bloom's syndrome protein is required for correct relocalization of RAD50/MRE11/NBS1 complex after replication fork arrest." Journal of Cell Biology **157**(1): 19-30.
Fry, M. and L. A. Loeb (1999). "Human Werner syndrome DNA helicase unwinds tetrahelical structures of the fragile X syndrome repeat sequence d(CGG)(n)." Journal of Biological Chemistry **274**(18): 12797-12802.

Fu, H., M. M. Martin, M. Regairaz, L. Huang, Y. You, C. M. Lin, M. Ryan, R. Kim, T. Shimura, Y. Pommier and M. I. Aladjem (2015). "The DNA repair endonuclease Mus81 facilitates fast DNA replication in the absence of exogenous damage." Nat Commun **6**: 6746.
Gacy, A. M., G. Goellner, N. Juranic, S. Macura and C. T. McMurray (1995). "Trinucleotide repeats that expand in human disease form hairpin structures in vitro." Cell **81**(4): 533-540.
Gallimore, P. H. and A. S. Turnell (2001). "Adenovirus E1A: remodelling the host cell, a life or death experience." Oncogene **20**(54): 7824-7835.
Garnett, C. T., G. Talekar, J. A. Mahr, W. Huang, Y. Zhang, D. A. Ornelles and L. R. Gooding (2009). "Latent species C adenoviruses in human tonsil tissues." J Virol **83**(6): 2417-2428.
Gatei, M., K. Sloper, C. Sorensen, R. Syljuasen, J. Falck, K. Hobson, K. Savage, J. Lukas, B. B. Zhou, J. Bartek and K. K. Khanna (2003). "Ataxia-telangiectasia-mutated (ATM) and NBS1-dependent phosphorylation of Chk1 on Ser-317 in response to ionizing radiation." J Biol Chem **278**(17): 14806-14811.
Gavin, K. A., M. Hidaka and B. Stillman (1995). "Conserved Initiator Proteins in Eukaryotes." Science **270**(5242): 1667-1671.
Ge, X. Q., D. A. Jackson and J. J. Blow (2007). "Dormant origins licensed by excess Mcm2-7 are required for human cells to survive replicative stress." Genes & Development **21**(24): 3331-3341.
Geisberg, J. V., W. S. Lee, A. J. Berk and R. P. Ricciardi (1994). "The zinc finger region of the adenovirus E1A transactivating domain complexes with the TATA box binding protein." Proc Natl Acad Sci U S A **91**(7): 2488-2492.
Genschel, J., L. R. Bazemore and P. Modrich (2002). "Human exonuclease I is required for 5 ' and 3 ' mismatch repair." Journal of Biological Chemistry **277**(15): 13302-13311.
Gerlach, V. L., L. Aravind, G. Gotway, R. A. Schultz, E. V. Koonin and E. C. Friedberg (1999). "Human and mouse homologs of Escherichia coli DinB (DNA polymerase IV), members of the UmuC/DinB superfamily." Proc Natl Acad Sci U S A **96**(21): 11922-11927.
Ghosal, G. and K. Muniyappa (2005). "Saccharomyces cerevisiae Mre11 is a high-affinity G4 DNA-binding protein and a G-rich DNA-specific endonuclease: implications for replication of telomeric DNA." Nucleic Acids Research **33**(15): 4692-4703.
Gibbs, P. E., W. G. McGregor, V. M. Maher, P. Nisson and C. W. Lawrence (1998). "A human homolog of the Saccharomyces cerevisiae REV3 gene, which encodes the catalytic subunit of DNA polymerase zeta." Proc Natl Acad Sci U S A **95**(12): 6876-6880.
Ginsberg, H. S., E. Gold, W. S. Jordan, Jr., S. Katz, G. F. Badger and J. H. Dingle (1955). "Relation of the new respiratory agents to acute respiratory diseases." Am J Public Health Nations Health **45**(7): 915-922.
Goldberg, M., M. Stucki, J. Falck, D. D'Amours, D. Rahman, D. Pappin, J. Bartek and S. P. Jackson (2003). "MDC1 is required for the intra-S-phase DNA damage checkpoint." Nature **421**(6926): 952-956.
Gonzalez, R., W. Huang, R. Finnen, C. Bragg and S. J. Flint (2006). "Adenovirus E1B 55-kilodalton protein is required for both regulation of mRNA export and efficient entry into the late phase of infection in normal human fibroblasts." J Virol **80**(2): 964-974.
Goodarzi, A. A., Y. Yu, E. Riballo, P. Douglas, S. A. Walker, R. Ye, C. Harer, C. Marchetti, N. Morrice, P. A. Jeggo and S. P. Lees-Miller (2006). "DNA-PK autophosphorylation facilitates Artemis endonuclease activity." EMBO J **25**(16): 3880-3889.

Gradia, S., S. Acharya and R. Fishel (1997). "The human mismatch recognition complex hMSH2-hMSH6 functions as a novel molecular switch." Cell **91**(7): 995-1005.
Gradwohl, G., J. M. Menissier de Murcia, M. Molinete, F. Simonin, M. Koken, J. H. Hoeijmakers and G. de Murcia (1990). "The second zinc-finger domain of poly(ADP-ribose) polymerase determines specificity for single-stranded breaks in DNA." Proc Natl Acad Sci U S A **87**(8): 2990-2994.
Graham, F. L., A. J. van der Eb and H. L. Heijneker (1974). "Size and location of the transforming region in human adenovirus type 5 DNA." Nature **251**(5477): 687-691.
Grand, R. J., M. L. Grant and P. H. Gallimore (1994). "Enhanced expression of p53 in human cells infected with mutant adenoviruses." Virology **203**(2): 229-240.
Grand, R. J., A. P. Ibrahim, A. M. Taylor, A. E. Milner, C. D. Gregory, P. H. Gallimore and A. S. Turnell (1998). "Human cells arrest in S phase in response to adenovirus 12 E1A." Virology **244**(2): 330-342.
Greber, U. F., P. Webster, J. Weber and A. Helenius (1996). "The role of the adenovirus protease on virus entry into cells." EMBO J **15**(8): 1766-1777.
Groth, A., A. Corpet, A. J. Cook, D. Roche, J. Bartek, J. Lukas and G. Almouzni (2007). "Regulation of replication fork progression through histone supply and demand." Science **318**(5858): 1928-1931.
Gu, L. Y., Y. Hong, S. McCulloch, H. Watanabe and G. M. Li (1998). "ATP-dependent interaction of human mismatch repair proteins and dual role of PCNA in mismatch repair." Nucleic Acids Research **26**(5): 1173-1178.
Gupta, A., S. Jha, D. A. Engel, D. A. Ornelles and A. Dutta (2013). "Tip60 degradation by adenovirus relieves transcriptional repression of viral transcriptional activator EIA." Oncogene **32**(42): 5017-5025.
Hakansson, P., A. Hofer and L. Thelander (2006). "Regulation of mammalian ribonucleotide reduction and dNTP pools after DNA damage and in resting cells." J Biol Chem **281**(12): 7834-7841.
Halazonetis, T. D., V. G. Gorgoulis and J. Bartek (2008). "An oncogene-induced DNA damage model for cancer development." Science **319**(5868): 1352-1355.
Halbert, D. N., J. R. Cutt and T. Shenk (1985). "Adenovirus early region 4 encodes functions required for efficient DNA replication, late gene expression, and host cell shutoff." J Virol **56**(1): 250-257.
Hanada, K., M. Budzowska, S. L. Davies, E. van Drunen, H. Onizawa, H. B. Beverloo, A. Maas, J. Essers, I. D. Hickson and R. Kanaar (2007). "The structure-specific endonuclease Mus81 contributes to replication restart by generating double-strand DNA breaks." Nature Structural & Molecular Biology **14**(11): 1096-1104.
Hanahan, D. and R. A. Weinberg (2011). "Hallmarks of cancer: the next generation." Cell **144**(5): 646-674.
Harbour, J. W., R. X. Luo, A. D. Santi, A. A. Postigo and D. C. Dean (1999). "Cdk phosphorylation triggers sequential intramolecular interactions that progressively block Rb functions as cells move through G1." Cell **98**(6): 859-869.
Harrigan, J. A., R. Belotserkovskaya, J. Coates, D. S. Dimitrova, S. E. Polo, C. R. Bradshaw, P. Fraser and S. P. Jackson (2011). "Replication stress induces 53BP1-containing OPT domains in G1 cells." J Cell Biol **193**(1): 97-108.

Hart, L. S., D. Ornelles and C. Koumenis (2007). "The adenoviral E4orf6 protein induces atypical apoptosis in response to DNA damage." Journal of Biological Chemistry **282**(9): 6061-6067.
Hart, L. S., S. M. Yannone, C. Naczki, J. S. Orlando, S. B. Waters, S. A. Akman, D. J. Chen, D. Ornelles and C. Koumenis (2005). "The adenovirus E4orf6 protein inhibits DNA double strand break repair and radiosensitizes human tumor cells in an E1B-55K-independent manner." Journal of Biological Chemistry **280**(2): 1474-1481.
Hashimoto, Y., A. R. Chaudhuri, M. Lopes and V. Costanzo (2010). "Rad51 protects nascent DNA from Mre11-dependent degradation and promotes continuous DNA synthesis." Nature Structural & Molecular Biology **17**(11): 1305-U1268.
Hateboer, G., H. T. Timmers, A. K. Rustgi, M. Billaud, L. J. van 't Veer and R. Bernards (1993). "TATA-binding protein and the retinoblastoma gene product bind to overlapping epitopes on c-Myc and adenovirus E1A protein." Proc Natl Acad Sci U S A **90**(18): 8489-8493.
He, G. G., Z. H. Siddik, Z. F. Huang, R. N. Wang, J. Koomen, R. Kobayashi, A. R. Khokhar and J. Kuang (2005). "Induction of p21 by p53 following DNA damage inhibits both Cdk4 and Cdk2 activities." Oncogene **24**(18): 2929-2943.
Heffernan, T. P., K. Unsal-Kacmaz, A. N. Heinloth, D. A. Simpson, R. S. Paules, A. Sancar, M. Cordeiro-Stone and W. K. Kaufmann (2007). "Cdc7-Dbf4 and the human S checkpoint response to UVC." J Biol Chem **282**(13): 9458-9468.
Heidenreich, E., R. Novotny, B. Kneidinger, V. Holzmann and U. Wintersberger (2003). "Non-homologous end joining as an important mutagenic process in cell cycle-arrested cells." EMBO J **22**(9): 2274-2283.
Heller, R. C., S. Kang, W. M. Lam, S. Chen, C. S. Chan and S. P. Bell (2011). "Eukaryotic Origin-Dependent DNA Replication In Vitro Reveals Sequential Action of DDK and S-CDK Kinases." Cell **146**(1): 80-91.
Helmrich, A., M. Ballarino and L. Tora (2011). "Collisions between Replication and Transcription Complexes Cause Common Fragile Site Instability at the Longest Human Genes." Molecular Cell **44**(6): 966-977.
Hentges, P., P. Ahnesorg, R. S. Pitcher, C. K. Bruce, B. Kysela, A. J. Green, J. Bianchi, T. E. Wilson, S. P. Jackson and A. J. Doherty (2006). "Evolutionary and functional conservation of the DNA non-homologous end-joining protein, XLF/Cernunnos." J Biol Chem **281**(49): 37517-37526.
Hermeking, H., C. Lengauer, K. Polyak, T. C. He, L. Zhang, S. Thiagalingam, K. W. Kinzler and B. Vogelstein (1997). "14-3-3 sigma is a p53-regulated inhibitor of G2/M progression." Molecular Cell **1**(1): 3-11.
Higgins, N. P., K. Kato and B. Strauss (1976). "Model for Replication Repair in Mammalian-Cells." Journal of Molecular Biology **101**(3): 417-425.
Hilleman, M. R. and J. H. Werner (1954). "Recovery of new agent from patients with acute respiratory illness." Proc Soc Exp Biol Med **85**(1): 183-188.
Hoege, C., B. Pfander, G. L. Moldovan, G. Pyrowolakis and S. Jentsch (2002). "RAD6-dependent DNA repair is linked to modification of PCNA by ubiquitin and SUMO." Nature **419**(6903): 135-141.
Holmes, J., Jr., S. Clark and P. Modrich (1990). "Strand-specific mismatch correction in nuclear extracts of human and Drosophila melanogaster cell lines." Proc Natl Acad Sci U S A **87**(15): 5837-5841.

Hoppe, A., S. J. Beech, J. Dimmock and K. N. Leppard (2006). "Interaction of the adenovirus type 5 E4 Orf3 protein with promyelocytic leukemia protein isoform II is required for ND10 disruption." Journal of Virology **80**(6): 3042-3049.
Horne, R. W., S. Brenner, A. P. Waterson and P. Wildy (1959). "The icosahedral form of an adenovirus." Journal of Molecular Biology **1**(1): 84-IN15.
Houweling, A., P. J. van den Elsen and A. J. van der Eb (1980). "Partial transformation of primary rat cells by the leftmost 4.5% fragment of adenovirus 5 DNA." Virology **105**(2): 537-550.
Huang, M. M. and P. Hearing (1989). "The adenovirus early region 4 open reading frame 6/7 protein regulates the DNA binding activity of the cellular transcription factor, E2F, through a direct complex." Genes Dev **3**(11): 1699-1710.
Huen, M. S., R. Grant, I. Manke, K. Minn, X. Yu, M. B. Yaffe and J. Chen (2007). "RNF8 transduces the DNA-damage signal via histone ubiquitylation and checkpoint protein assembly." Cell **131**(5): 901-914.
Huertas, P. and A. Aguilera (2003). "Cotranscriptionally formed DNA : RNA hybrids mediate transcription elongation impairment and transcription-associated recombination." Molecular Cell **12**(3): 711-721.
Huertas, P. and S. P. Jackson (2009). "Human CtIP Mediates Cell Cycle Control of DNA End Resection and Double Strand Break Repair." Journal of Biological Chemistry **284**(14): 9558-9565.
Hwang, B. J., S. Toering, U. Francke and G. Chu (1998). "p48 activates a UV-damaged-DNA binding factor and is defective in xeroderma pigmentosum group E cells that lack binding activity." Molecular and Cellular Biology **18**(7): 4391-4399.
Ilves, I., T. Petojevic, J. J. Pesavento and M. R. Botchan (2010). "Activation of the MCM2-7 Helicase by Association with Cdc45 and GINS Proteins." Molecular Cell **37**(2): 247-258.
Ip, S. C. Y., U. Rass, M. G. Blanco, H. R. Flynn, J. M. Skehel and S. C. West (2008). "Identification of Holliday junction resolvases from humans and yeast." Nature **456**(7220): 357-U339.
Ira, G., D. Satory and J. E. Haber (2006). "Conservative inheritance of newly synthesized DNA in double-strand break-induced gene conversion." Mol Cell Biol **26**(24): 9424-9429.
Izumi, T. and J. L. Maller (1993). "Elimination of Cdc2 Phosphorylation Sites in the Cdc25 Phosphatase Blocks Initiation of M-Phase." Molecular Biology of the Cell **4**(12): 1337-1350.
Jackson, D. A. and A. Pombo (1998). "Replicon clusters are stable units of chromosome structure: evidence that nuclear organization contributes to the efficient activation and propagation of S phase in human cells." J Cell Biol **140**(6): 1285-1295.
Jackson, S. P. and J. Bartek (2009). "The DNA-damage response in human biology and disease." Nature **461**(7267): 1071-1078.
Javier, R., K. Raska, Jr. and T. Shenk (1992). "Requirement for the adenovirus type 9 E4 region in production of mammary tumors." Science **257**(5074): 1267-1271.
Javier, R. T. (1994). "Adenovirus type 9 E4 open reading frame 1 encodes a transforming protein required for the production of mammary tumors in rats." J Virol **68**(6): 3917-3924.
Jazayeri, A., J. Falck, C. Lukas, J. Bartek, G. C. Smith, J. Lukas and S. P. Jackson (2006). "ATM- and cell cycle-dependent regulation of ATR in response to DNA double-strand breaks." Nat Cell Biol **8**(1): 37-45.

Jiang, K., E. Pereira, M. Maxfield, B. Russell, D. M. Goudelock and Y. Sanchez (2003). "Regulation of Chk1 includes chromatin association and 14-3-3 binding following phosphorylation on Ser-345." J Biol Chem **278**(27): 25207-25217.
Jilani, A., D. Ramotar, C. Slack, C. Ong, X. M. Yang, S. W. Scherer and D. D. Lasko (1999). "Molecular cloning of the human gene, PNKP, encoding a polynucleotide kinase 3 '-phosphatase and evidence for its role in repair of DNA strand breaks caused by oxidative damage." Journal of Biological Chemistry **274**(34): 24176-24186.
Jones, R. M., O. Mortusewicz, I. Afzal, M. Lorvellec, P. Garcia, T. Helleday and E. Petermann (2013). "Increased replication initiation and conflicts with transcription underlie Cyclin E-induced replication stress." Oncogene **32**(32): 3744-3753.
Jones, R. M. and E. Petermann (2012). "Replication fork dynamics and the DNA damage response." Biochem J **443**(1): 13-26.
Jordan, A. and P. Reichard (1998). "Ribonucleotide reductases." Annu Rev Biochem **67**: 71-98.
Kadyrov, F. A., L. Dzantiev, N. Constantin and P. Modrich (2006). "Endonucleolytic function of MutL alpha in human mismatch repair." Cell **126**(2): 297-308.
Kanai, M., M. Miwa, Y. Kuchino and T. Sugimura (1982). "Presence of branched portion in poly(adenosine diphosphate ribose) in vivo." J Biol Chem **257**(11): 6217-6223.
Kannouche, P. L., J. Wing and A. R. Lehmann (2004). "Interaction of human DNA polymerase eta with monoubiquitinated PCNA: a possible mechanism for the polymerase switch in response to DNA damage." Mol Cell **14**(4): 491-500.
Kato, J., H. Matsushime, S. W. Hiebert, M. E. Ewen and C. J. Sherr (1993). "Direct binding of cyclin D to the retinoblastoma gene product (pRb) and pRb phosphorylation by the cyclin D-dependent kinase CDK4." Genes Dev **7**(3): 331-342.
Khanna, K. K., K. E. Keating, S. Kozlov, S. Scott, M. Gatei, K. Hobson, Y. Taya, B. Gabrielli, D. Chan, S. P. Lees-Miller and M. F. Lavin (1998). "ATM associates with and phosphorylates p53: mapping the region of interaction." Nat Genet **20**(4): 398-400.
Kindsmuller, K., P. Groitl, B. Hartl, P. Blanchette, J. Hauber and T. Dobner (2007). "Intranuclear targeting and nuclear export of the adenovirus E1B-55K protein are regulated by SUMO1 conjugation." Proc Natl Acad Sci U S A **104**(16): 6684-6689.
Kleiber, K., K. Strebhardt and B. T. Martin (2007). "The biological relevance of FHL2 in tumour cells and its role as a putative cancer target." Anticancer Res **27**(1A): 55-61.
Kleinberger, T. and T. Shenk (1993). "Adenovirus E4orf4 protein binds to protein phosphatase 2A, and the complex down regulates E1A-enhanced junB transcription." J Virol **67**(12): 7556-7560.
Klungland, A. and T. Lindahl (1997). "Second pathway for completion of human DNA base excision-repair: reconstitution with purified proteins and requirement for DNase IV (FEN1)." EMBO J **16**(11): 3341-3348.
Kolas, N. K., J. R. Chapman, S. Nakada, J. Ylanko, R. Chahwan, F. D. Sweeney, S. Panier, M. Mendez, J. Wildenhain, T. M. Thomson, L. Pelletier, S. P. Jackson and D. Durocher (2007). "Orchestration of the DNA-damage response by the RNF8 ubiquitin ligase." Science **318**(5856): 1637-1640.
Konig, C., J. Roth and M. Dobbelstein (1999). "Adenovirus type 5 E4orf3 protein relieves p53 inhibition by E1B-55-kilodalton protein." Journal of Virology **73**(3): 2253-2262.

Krokan, H., E. Wist and R. H. Krokan (1981). "Aphidicolin inhibits DNA synthesis by DNA polymerase alpha and isolated nuclei by a similar mechanism." Nucleic Acids Res **9**(18): 4709-4719.
Kumagai, A. and W. G. Dunphy (1999). "Binding of 14-3-3 proteins and nuclear export control the intracellular localization of the mitotic inducer Cdc25." Genes & Development **13**(9): 1067-1072.
Kumagai, A., J. Lee, H. Y. Yoo and W. G. Dunphy (2006). "TopBP1 activates the ATR-ATRIP complex." Cell **124**(5): 943-955.
Kumagai, A., A. Shevchenko, A. Shevchenko and W. G. Dunphy (2010). "Treslin Collaborates with TopBP1 in Triggering the Initiation of DNA Replication." Cell **140**(3): 349-U359.
Kuzminov, A. (2001). "Single-strand interruptions in replicating chromosomes cause double-strand breaks." Proc Natl Acad Sci U S A **98**(15): 8241-8246.
Lacks, S. A., J. J. Dunn and B. Greenberg (1982). "Identification of base mismatches recognized by the heteroduplex-DNA-repair system of Streptococcus pneumoniae." Cell **31**(2 Pt 1): 327-336.
Lakdawala, S. S., R. A. Schwartz, K. Ferenchak, C. T. Carson, B. P. McSharry, G. W. Wilkinson and M. D. Weitzman (2008). "Differential requirements of the C terminus of Nbs1 in suppressing adenovirus DNA replication and promoting concatemer formation." J Virol **82**(17): 8362-8372.
Lakin, N. D., B. C. Hann and S. P. Jackson (1999). "The ataxia-telangiectasia related protein ATR mediates DNA-dependent phosphorylation of p53." Oncogene **18**(27): 3989-3995.
Lau, N. C., A. Kolkman, F. M. van Schaik, K. W. Mulder, W. W. Pijnappel, A. J. Heck and H. T. Timmers (2009). "Human Ccr4-Not complexes contain variable deadenylase subunits." Biochem J **422**(3): 443-453.
Lazzaro, F., D. Novarina, F. Amara, D. L. Watt, J. E. Stone, V. Costanzo, P. M. Burgers, T. A. Kunkel, P. Plevani and M. Muzi-Falconil (2012). "RNase H and Postreplication Repair Protect Cells from Ribonucleotides Incorporated in DNA." Molecular Cell **45**(1): 99-110.
Leber, R., T. W. Wise, R. Mizuta and K. Meek (1998). "The XRCC4 gene product is a target for and interacts with the DNA-dependent protein kinase." Journal of Biological Chemistry **273**(3): 1794-1801.
Lee, J. H. and T. T. Paull (2005). "ATM activation by DNA double-strand breaks through the Mre11-Rad50-Nbs1 complex." Science **308**(5721): 551-554.
Lees-Miller, S. P., Y. R. Chen and C. W. Anderson (1990). "Human cells contain a DNA-activated protein kinase that phosphorylates simian virus 40 T antigen, mouse p53, and the human Ku autoantigen." Mol Cell Biol **10**(12): 6472-6481.
Leppard, K. N. and R. D. Everett (1999). "The adenovirus type 5 E1b 55K and E4 Orf3 proteins associate in infected cells and affect ND10 components." Journal of General Virology **80**: 997-1008.
Leung, A. Y., M. Chan, V. C. Cheng, K. Y. Yuen and Y. L. Kwong (2005). "Quantification of adenovirus in the lower respiratory tract of patients without clinical adenovirus-related respiratory disease." Clin Infect Dis **40**(10): 1541-1544.
Li, H., C. Leo, J. Zhu, X. Y. Wu, J. O'Neil, E. J. Park and J. D. Chen (2000). "Sequestration and inhibition of Daxx-mediated transcriptional repression by PML." Molecular and Cellular Biology **20**(5): 1784-1796.

Li, L., S. J. Elledge, C. A. Peterson, E. S. Bales and R. J. Legerski (1994). "Specific Association between the Human DNA-Repair Proteins Xpa and Ercc1." Proceedings of the National Academy of Sciences of the United States of America **91**(11): 5012-5016.
Liang, F., M. Han, P. J. Romanienko and M. Jasin (1998). "Homology-directed repair is a major double-strand break repair pathway in mammalian cells." Proc Natl Acad Sci U S A **95**(9): 5172-5177.
Lieber, M. R. (2010). "The Mechanism of Double-Strand DNA Break Repair by the Nonhomologous DNA End-Joining Pathway." Annual Review of Biochemistry, Vol 79 **79**: 181-211.
Lill, N. L., S. R. Grossman, D. Ginsberg, J. DeCaprio and D. M. Livingston (1997). "Binding and modulation of p53 by p300/CBP coactivators." Nature **387**(6635): 823-827.
Lim, D. S., S. T. Kim, B. Xu, R. S. Maser, J. Lin, J. H. Petrini and M. B. Kastan (2000). "ATM phosphorylates p95/nbs1 in an S-phase checkpoint pathway." Nature **404**(6778): 613-617.
Lindahl, T. (1974). "An N-glycosidase from Escherichia coli that releases free uracil from DNA containing deaminated cytosine residues." Proc Natl Acad Sci U S A **71**(9): 3649-3653.
Lindahl, T. (1993). "Instability and decay of the primary structure of DNA." Nature **362**(6422): 709-715.
Liu, F., J. J. Stanton, Z. Wu and H. Piwnica-Worms (1997). "The human Myt1 kinase preferentially phosphorylates Cdc2 on threonine 14 and localizes to the endoplasmic reticulum and Golgi complex." Faseb Journal **11**(9): A1391-A1391.
Liu, H., S. Takeda, R. Kumar, T. D. Westergard, E. J. Brown, T. K. Pandita, E. H. Y. Cheng and J. J. D. Hsieh (2010). "Phosphorylation of MLL by ATR is required for execution of mammalian S-phase checkpoint." Nature **467**(7313): 343-U126.
Liu, H. Y., V. Badarinarayana, D. C. Audino, J. Rappsilber, M. Mann and C. L. Denis (1998). "The NOT proteins are part of the CCR4 transcriptional complex and affect gene expression both positively and negatively." EMBO J **17**(4): 1096-1106.
Liu, L. F., C. C. Liu and B. M. Alberts (1980). "Type II DNA topoisomerases: enzymes that can unknot a topologically knotted DNA molecule via a reversible double-strand break." Cell **19**(3): 697-707.
Liu, P. J., L. R. Barkley, T. Day, X. H. Bi, D. M. Slater, M. G. Alexandrow, H. P. Nasheuer and C. Vaziri (2006). "The Chk1-mediated S-phase checkpoint targets initiation factor Cdc45 via a Cdc25A/Cdk2-independent mechanism." Journal of Biological Chemistry **281**(41): 30631-30644.
Liu, Q., S. Guntuku, X. S. Cui, S. Matsuoka, D. Cortez, K. Tamai, G. Luo, S. Carattini-Rivera, F. DeMayo, A. Bradley, L. A. Donehower and S. J. Elledge (2000). "Chk1 is an essential kinase that is regulated by Atr and required for the G(2)/M DNA damage checkpoint." Genes Dev **14**(12): 1448-1459.
Liu, Y., A. Shevchenko, A. Shevchenko and A. J. Berk (2005). "Adenovirus exploits the cellular aggresome response to accelerate inactivation of the MRN complex." Journal of Virology **79**(22): 14004-14016.
Lomonosov, M., S. Anand, M. Sangrithi, R. Davies and A. R. Venkitaraman (2003). "Stabilization of stalled DNA replication forks by the BRCA2 breast cancer susceptibility protein." Genes Dev **17**(24): 3017-3022.
Longley, M. J., A. J. Pierce and P. Modrich (1997). "DNA polymerase delta is required for human mismatch repair in vitro." Journal of Biological Chemistry **272**(16): 10917-10921.

Lopez-Girona, A., B. Furnari, O. Mondesert and P. Russell (1999). "Nuclear localization of Cdc25 is regulated by DNA damage and a 14-3-3 protein." Nature **397**(6715): 172-175.
Lou, Z., K. Minter-Dykhouse, S. Franco, M. Gostissa, M. A. Rivera, A. Celeste, J. P. Manis, J. van Deursen, A. Nussenzweig, T. T. Paull, F. W. Alt and J. Chen (2006). "MDC1 maintains genomic stability by participating in the amplification of ATM-dependent DNA damage signals." Mol Cell **21**(2): 187-200.
Lucke-Huhle, C., E. A. Blakely, P. Y. Chang and C. A. Tobias (1979). "Drastic G2 arrest in mammalian cells after irradiation with heavy-ion beams." Radiat Res **79**(1): 97-112.
Lukas, C., V. Savic, S. Bekker-Jensen, C. Doil, B. Neumann, R. S. Pedersen, M. Grofte, K. L. Chan, I. D. Hickson, J. Bartek and J. Lukas (2011). "53BP1 nuclear bodies form around DNA lesions generated by mitotic transmission of chromosomes under replication stress." Nat Cell Biol **13**(3): 243-253.
Luke-Glaser, S., B. Luke, S. Grossi and A. Constantinou (2010). "FANCM regulates DNA chain elongation and is stabilized by S-phase checkpoint signalling." Embo Journal **29**(4): 795-805.
Lundberg, A. S. and R. A. Weinberg (1998). "Functional inactivation of the retinoblastoma protein requires sequential modification by at least two distinct cyclin-cdk complexes." Molecular and Cellular Biology **18**(2): 753-761.
Ma, Y. M., U. Pannicke, K. Schwarz and M. R. Lieber (2002). "Hairpin opening and overhang processing by an Artemis/DNA-dependent protein kinase complex in nonhomologous end joining and V(D)J recombination." Cell **108**(6): 781-794.
Machida, Y. J., Y. Machida, Y. Chen, A. M. Gurtan, G. M. Kupfer, A. D. D'Andrea and A. Dutta (2006). "UBE2T is the E2 in the Fanconi anemia pathway and undergoes negative autoregulation." Mol Cell **23**(4): 589-596.
Machwe, A., L. R. Xiao, J. Groden and D. K. Orren (2006). "The Werner and Bloom syndrome proteins catalyze regression of a model replication fork." Biochemistry **45**(47): 13939-13946.
MacKay, C., A. C. Declais, C. Lundin, A. Agostinho, A. J. Deans, T. J. MacArtney, K. Hofmann, A. Gartner, S. C. West, T. Helleday, D. M. Lilley and J. Rouse (2010). "Identification of KIAA1018/FAN1, a DNA repair nuclease recruited to DNA damage by monoubiquitinated FANCD2." Cell **142**(1): 65-76.
Maguire, K., X. P. Shi, N. Horikoshi, J. Rappaport, M. Rosenberg and R. Weinmann (1991). "Interactions between adenovirus E1A and members of the AP-1 family of cellular transcription factors." Oncogene **6**(8): 1417-1422.
Mailand, N., S. Bekker-Jensen, H. Faustrup, F. Melander, J. Bartek, C. Lukas and J. Lukas (2007). "RNF8 ubiquitylates histones at DNA double-strand breaks and promotes assembly of repair proteins." Cell **131**(5): 887-900.
Malumbres, M. and M. Barbacid (2009). "Cell cycle, CDKs and cancer: a changing paradigm." Nature Reviews Cancer **9**(3): 153-166.
Mannervik, M., S. Fan, A. C. Strom, K. Helin and G. Akusjarvi (1999). "Adenovirus E4 open reading frame 4-induced dephosphorylation inhibits E1A activation of the E2 promoter and E2F-1-mediated transactivation independently of the retinoblastoma tumor suppressor protein." Virology **256**(2): 313-321.
Marcellus, R. C., J. N. Lavoie, D. Boivin, G. C. Shore, G. Ketner and P. E. Branton (1998). "The early region 4 orf4 protein of human adenovirus type 5 induces p53-independent cell death by apoptosis." J Virol **72**(9): 7144-7153.

Martin, S. A. and T. Ouchi (2008). "Cellular commitment to reentry into the cell cycle after stalled DNA is determined by site-specific phosphorylation of Chk1 and PTEN." Mol Cancer Ther **7**(8): 2509-2516.
Masson, M., C. Niedergang, V. Schreiber, S. Muller, J. Menissier-de Murcia and G. de Murcia (1998). "XRCC1 is specifically associated with poly(ADP-ribose) polymerase and negatively regulates its activity following DNA damage." Molecular and Cellular Biology **18**(6): 3563-3571.
Masuda-Sasa, T., P. Polaczek, X. P. Peng, L. Chen and J. L. Campbell (2008). "Processing of G4 DNA by Dna2 helicase/nuclease and replication protein a (RPA) provides insights into the mechanism of Dna2/RPA substrate recognition." Journal of Biological Chemistry **283**(36): 24359-24373.
Matsumoto, Y., N. Suzuki, N. Namba, N. Umeda, X. J. Ma, A. Morita, M. Tomita, A. Enomoto, S. Serizawa, K. Hirano, K. Sakai, H. Yasuda and Y. Hosoi (2000). "Cleavage and phosphorylation of XRCC4 protein induced by X-irradiation." Febs Letters **478**(1-2): 67-71.
Matsuoka, S., B. A. Ballif, A. Smogorzewska, E. R. McDonald, K. E. Hurov, J. Luo, C. E. Bakalarski, Z. M. Zhao, N. Solimini, Y. Lerenthal, Y. Shiloh, S. P. Gygi and S. J. Elledge (2007). "ATM and ATR substrate analysis reveals extensive protein networks responsive to DNA damage." Science **316**(5828): 1160-1166.
Matsuoka, S., M. Huang and S. J. Elledge (1998). "Linkage of ATM to cell cycle regulation by the Chk2 protein kinase." Science **282**(5395): 1893-1897.
Matsuoka, S., G. Rotman, A. Ogawa, Y. Shiloh, K. Tamai and S. J. Elledge (2000). "Ataxia telangiectasia-mutated phosphorylates Chk2 in vivo and in vitro." Proc Natl Acad Sci U S A **97**(19): 10389-10394.
Matsushime, H., D. E. Quelle, S. A. Shurtleff, M. Shibuya, C. J. Sherr and J. Y. Kato (1994). "D-type cyclin-dependent kinase activity in mammalian cells." Mol Cell Biol **14**(3): 2066-2076.
Matthews, D. A. and W. C. Russell (1998). "Adenovirus core protein V interacts with p32--a protein which is associated with both the mitochondria and the nucleus." J Gen Virol **79 (Pt 7)**: 1677-1685.
Matthews, D. A. and W. C. Russell (1998). "Adenovirus core protein V is delivered by the invading virus to the nucleus of the infected cell and later in infection is associated with nucleoli." J Gen Virol **79 (Pt 7)**: 1671-1675.
Mattiroli, F., J. H. A. Vissers, W. J. van Dijk, P. Ikpa, E. Citterio, W. Vermeulen, J. A. Marteijn and T. K. Sixma (2012). "RNF168 Ubiquitinates K13-15 on H2A/H2AX to Drive DNA Damage Signaling." Cell **150**(6): 1182-1195.
Maya-Mendoza, A., E. Petermann, D. A. F. Gillespie, K. W. Caldecott and D. A. Jackson (2007). "Chk1 regulates the density of active replication origins during the vertebrate S phase." Embo Journal **26**(11): 2719-2731.
Mayol, X., J. Garriga and X. Grana (1995). "Cell cycle-dependent phosphorylation of the retinoblastoma-related protein p130." Oncogene **11**(4): 801-808.
Mazzarelli, J. M., G. B. Atkins, J. V. Geisberg and R. P. Ricciardi (1995). "The viral oncoproteins Ad5 E1A, HPV16 E7 and SV40 TAg bind a common region of the TBP-associated factor-110." Oncogene **11**(9): 1859-1864.
McBride, W. D. and A. Wiener (1964). "In Vitro Transformation of Hamster Kidney Cells by Human Adenovirus Type 12." Proc Soc Exp Biol Med **115**: 870-874.

McCulloch, S. D., L. Y. Gu and G. M. Li (2003). "Nick-dependent and -independent processing of large DNA loops in human cells." Journal of Biological Chemistry **278**(50): 50803-50809.
Mcdougal.Jk (1970). "Effects of Adenoviruses on Chromosomes of Normal Human Cells and Cells Trisomic for an E-Chromosome." Nature **225**(5231): 456-&.
Mcdougal.Jk (1971). "Adenovirus-Induced Chromosome Aberrations in Human Cells." Journal of General Virology **12**(Jul): 43-&.
McElhinny, S. A. N., B. E. Watts, D. Kumar, D. L. Watt, E. B. Lundstrom, P. M. J. Burgers, E. Johansson, A. Chabes and T. A. Kunkel (2010). "Abundant ribonucleotide incorporation into DNA by yeast replicative polymerases." Proceedings of the National Academy of Sciences of the United States of America **107**(11): 4949-4954.
Mejlvang, J., Y. Feng, C. Alabert, K. J. Neelsen, Z. Jasencakova, X. Zhao, M. Lees, A. Sandelin, P. Pasero, M. Lopes and A. Groth (2014). "New histone supply regulates replication fork speed and PCNA unloading." J Cell Biol **204**(1): 29-43.
Mellon, I., G. Spivak and P. C. Hanawalt (1987). "Selective removal of transcription-blocking DNA damage from the transcribed strand of the mammalian DHFR gene." Cell **51**(2): 241-249.
Mendoza-Alvarez, H. and R. Alvarez-Gonzalez (1993). "Poly(ADP-ribose) polymerase is a catalytic dimer and the automodification reaction is intermolecular." J Biol Chem **268**(30): 22575-22580.
Mersman, D. P., H. N. Du, I. M. Fingerman, P. F. South and S. D. Briggs (2009). "Polyubiquitination of the demethylase Jhd2 controls histone methylation and gene expression." Genes Dev **23**(8): 951-962.
Messner, S., M. Altmeyer, H. T. Zhao, A. Pozivil, B. Roschitzki, P. Gehrig, D. Rutishauser, D. Z. Huang, A. Caflisch and M. O. Hottiger (2010). "PARP1 ADP-ribosylates lysine residues of the core histone tails." Nucleic Acids Research **38**(19): 6350-6362.
Meyerson, M. and E. Harlow (1994). "Identification of G1 kinase activity for cdk6, a novel cyclin D partner." Mol Cell Biol **14**(3): 2077-2086.
Michel, B., S. D. Ehrlich and M. Uzest (1997). "DNA double-strand breaks caused by replication arrest." EMBO J **16**(2): 430-438.
Minocherhomji, S., S. Ying, V. A. Bjerregaard, S. Bursomanno, A. Aleliunaite, W. Wu, H. W. Mankouri, H. Shen, Y. Liu and I. D. Hickson (2015). "Replication stress activates DNA repair synthesis in mitosis." Nature **528**(7581): 286-290.
Mirzoeva, O. K. and J. H. J. Petrini (2003). "DNA replication-dependent nuclear dynamics of the Mre11 complex." Molecular Cancer Research **1**(3): 207-218.
Mittal, S., A. Aslam, R. Doidge, R. Medica and G. S. Winkler (2011). "The Ccr4a (CNOT6) and Ccr4b (CNOT6L) deadenylase subunits of the human Ccr4-Not complex contribute to the prevention of cell death and senescence." Mol Biol Cell **22**(6): 748-758.
Moldovan, G. L., M. V. Madhavan, K. D. Mirchandani, R. M. McCaffrey, P. Vinciguerra and A. D. D'Andrea (2010). "DNA polymerase POLN participates in cross-link repair and homologous recombination." Mol Cell Biol **30**(4): 1088-1096.
Moldovan, G. L., B. Pfander and S. Jentsch (2007). "PCNA, the maestro of the replication fork." Cell **129**(4): 665-679.
Mordes, D. A., G. G. Glick, R. Zhao and D. Cortez (2008). "TopBP1 activates ATR through ATRIP and a PIKK regulatory domain." Genes Dev **22**(11): 1478-1489.

Morita, M., T. Suzuki, T. Nakamura, K. Yokoyama, T. Miyasaka and T. Yamamoto (2007). "Depletion of mammalian CCR4b deadenylase triggers elevation of the p27Kip1 mRNA level and impairs cell growth." Mol Cell Biol **27**(13): 4980-4990.
Moser, J., H. Kool, I. Giakzidis, K. Caldecott, L. H. F. Mullenders and M. I. Fousteri (2007). "Sealing of chromosomal DNA nicks during nucleotide excision repair requires XRCC1 and DNA ligase III alpha in a cell-cycle-specific manner." Molecular Cell **27**(2): 311-323.
Mulder, K. W., G. S. Winkler and H. T. Timmers (2005). "DNA damage and replication stress induced transcription of RNR genes is dependent on the Ccr4-Not complex." Nucleic Acids Res **33**(19): 6384-6392.
Muller, S. and T. Dobner (2008). "The adenovirus E1B-55K oncoprotein induces SUMO modification of p53." Cell Cycle **7**(6): 754-758.
Muller, U., T. Kleinberger and T. Shenk (1992). "Adenovirus E4orf4 protein reduces phosphorylation of c-Fos and E1A proteins while simultaneously reducing the level of AP-1." J Virol **66**(10): 5867-5878.
Nagata, K., R. A. Guggenheimer, T. Enomoto, J. H. Lichy and J. Hurwitz (1982). "Adenovirus DNA replication in vitro: identification of a host factor that stimulates synthesis of the preterminal protein-dCMP complex." Proc Natl Acad Sci U S A **79**(21): 6438-6442.
Nagata, K., R. A. Guggenheimer and J. Hurwitz (1983). "Specific binding of a cellular DNA replication protein to the origin of replication of adenovirus DNA." Proc Natl Acad Sci U S A **80**(20): 6177-6181.
Naim, V., T. Wilhelm, M. Debatisse and F. Rosselli (2013). "ERCC1 and MUS81-EME1 promote sister chromatid separation by processing late replication intermediates at common fragile sites during mitosis." Nature Cell Biology **15**(8): 1008-U1270.
Nakayama, K. I. and K. Nakayama (2006). "Ubiquitin ligases: cell-cycle control and cancer." Nat Rev Cancer **6**(5): 369-381.
Nimonkar, A. V., J. Genschel, E. Kinoshita, P. Polaczek, J. L. Campbell, C. Wyman, P. Modrich and S. C. Kowalczykowski (2011). "BLM-DNA2-RPA-MRN and EXO1-BLM-RPA-MRN constitute two DNA end resection machineries for human DNA break repair." Genes & Development **25**(4): 350-362.
Nishitani, H., Z. Lygerou, T. Nishimoto and P. Nurse (2000). "The Cdt1 protein is required to license DNA for replication in fission yeast." Nature **404**(6778): 625-+.
Nordqvist, K., K. Ohman and G. Akusjarvi (1994). "Human Adenovirus Encodes 2 Proteins Which Have Opposite Effects on Accumulation of Alternatively Spliced Messenger-Rnas." Molecular and Cellular Biology **14**(1): 437-445.
O'Connor, R. J. and P. Hearing (2000). "The E4-6/7 protein functionally compensates for the loss of E1A expression in adenovirus infection." J Virol **74**(13): 5819-5824.
O'Connor, T. R. and J. Laval (1989). "Physical association of the 2,6-diamino-4-hydroxy-5N-formamidopyrimidine-DNA glycosylase of Escherichia coli and an activity nicking DNA at apurinic/apyrimidinic sites." Proc Natl Acad Sci U S A **86**(14): 5222-5226.
Obert, S., R. J. O'Connor, S. Schmid and P. Hearing (1994). "The adenovirus E4-6/7 protein transactivates the E2 promoter by inducing dimerization of a heteromeric E2F complex." Mol Cell Biol **14**(2): 1333-1346.
Odonovan, A., A. A. Davies, J. G. Moggs, S. C. West and R. D. Wood (1994). "Xpg Endonuclease Makes the 3' Incision in Human DNA Nucleotide Excision-Repair." Nature **371**(6496): 432-435.

Ogryzko, V. V., R. L. Schiltz, V. Russanova, B. H. Howard and Y. Nakatani (1996). "The transcriptional coactivators p300 and CBP are histone acetyltransferases." Cell **87**(5): 953-959.
Ohtani, K., J. DeGregori and J. R. Nevins (1995). "Regulation of the cyclin E gene by transcription factor E2F1." Proc Natl Acad Sci U S A **92**(26): 12146-12150.
Orazio, N. I., C. M. Naeger, J. Karlseder and M. D. Weitzman (2011). "The Adenovirus E1b55K/E4orf6 Complex Induces Degradation of the Bloom Helicase during Infection." Journal of Virology **85**(4): 1887-1892.
Orazio, N. I., C. M. Naeger, J. Karlseder and M. D. Weitzman (2011). "The adenovirus E1b55K/E4orf6 complex induces degradation of the Bloom helicase during infection." J Virol **85**(4): 1887-1892.
Ornelles, D. A. and T. Shenk (1991). "Localization of the adenovirus early region 1B 55-kilodalton protein during lytic infection: association with nuclear viral inclusions requires the early region 4 34-kilodalton protein." J Virol **65**(1): 424-429.
Pacek, M. and J. C. Walter (2004). "A requirement for MCM7 and Cdc45 in chromosome unwinding during eukaryotic DNA replication." EMBO J **23**(18): 3667-3676.
Paeschke, K., M. L. Bochman, P. D. Garcia, P. Cejka, K. L. Friedman, S. C. Kowalczykowski and V. A. Zakian (2013). "Pif1 family helicases suppress genome instability at G-quadruplex motifs." Nature **497**(7450): 458-462.
Palombo, F., I. Iaccarino, E. Nakajima, M. Ikejima, T. Shimada and J. Jiricny (1996). "hMutS beta, a heterodimer of hMSH2 and hMSH3, binds to insertion/deletion leaps in DNA." Current Biology **6**(9): 1181-1184.
Panasenko, O., E. Landrieux, M. Feuermann, A. Finka, N. Paquet and M. A. Collart (2006). "The yeast Ccr4-Not complex controls ubiquitination of the nascent-associated polypeptide (NAC-EGD) complex." J Biol Chem **281**(42): 31389-31398.
Panasenko, O. O. and M. A. Collart (2011). "Not4 E3 ligase contributes to proteasome assembly and functional integrity in part through Ecm29." Mol Cell Biol **31**(8): 1610-1623.
Panasenko, O. O., F. P. David and M. A. Collart (2009). "Ribosome association and stability of the nascent polypeptide-associated complex is dependent upon its own ubiquitination." Genetics **181**(2): 447-460.
Park, C. H. and A. Sancar (1994). "Formation of a Ternary Complex by Human Xpa, Ercc1, and Ercc4(Xpf) Excision-Repair Proteins." Proceedings of the National Academy of Sciences of the United States of America **91**(11): 5017-5021.
Parker, L. L. and H. Piwnicaworms (1992). "Inactivation of the P34(Cdc2)-Cyclin-B Complex by the Human Wee1 Tyrosine Kinase." Science **257**(5078): 1955-1957.
Parrilla-Castellar, E. R., S. J. Arlander and L. Karnitz (2004). "Dial 9-1-1 for DNA damage: the Rad9-Hus1-Rad1 (9-1-1) clamp complex." DNA Repair (Amst) **3**(8-9): 1009-1014.
Pascucci, B., M. Stucki, Z. O. Jonsson, E. Dogliotti and U. Hubscher (1999). "Long patch base excision repair with purified human proteins. DNA ligase I as patch size mediator for DNA polymerases delta and epsilon." J Biol Chem **274**(47): 33696-33702.
Payne, A. and G. Chu (1994). "Xeroderma pigmentosum group E binding factor recognizes a broad spectrum of DNA damage." Mutat Res **310**(1): 89-102.
Pellegrini, L., D. S. Yu, T. Lo, S. Anand, M. Lee, T. L. Blundell and A. R. Venkitaraman (2002). "Insights into DNA recombination from the structure of a RAD51-BRCA2 complex." Nature **420**(6913): 287-293.

Pennella, M. A., Y. Liu, J. L. Woo, C. A. Kim and A. J. Berk (2010). "Adenovirus E1B 55-kilodalton protein is a p53-SUMO1 E3 ligase that represses p53 and stimulates its nuclear export through interactions with promyelocytic leukemia nuclear bodies." J Virol **84**(23): 12210-12225.
Pepe, A. and S. C. West (2014). "MUS81-EME2 promotes replication fork restart." Cell Rep **7**(4): 1048-1055.
Petermann, E., A. Maya-Mendoza, G. Zachos, D. A. F. Gillespie, D. A. Jackson and K. W. Caldecott (2006). "Chk1 requirement for high global rates of replication fork progression during normal vertebrate S phase." Molecular and Cellular Biology **26**(8): 3319-3326.
Petermann, E., M. L. Orta, N. Issaeva, N. Schultz and T. Helleday (2010). "Hydroxyurea-Stalled Replication Forks Become Progressively Inactivated and Require Two Different RAD51-Mediated Pathways for Restart and Repair." Molecular Cell **37**(4): 492-502.
Petermann, E., M. Woodcock and T. Helleday (2010). "Chk1 promotes replication fork progression by controlling replication initiation." Proc Natl Acad Sci U S A **107**(37): 16090-16095.
Petersen, B. O., J. Lukas, C. S. Sorensen, J. Bartek and K. Helin (1999). "Phosphorylation of mammalian CDC6 by cyclin A/CDK2 regulates its subcellular localization." EMBO J **18**(2): 396-410.
Piatti, S., C. Lengauer and K. Nasmyth (1995). "Cdc6 Is an Unstable Protein Whose De-Novo Synthesis in G(1) Is Important for the Onset of S-Phase and for Preventing a Reductional Anaphase in the Budding Yeast Saccharomyces-Cerevisiae." Embo Journal **14**(15): 3788-3799.
Pichierri, P., F. Rosselli and A. Franchitto (2003). "Werner's syndrome protein is phosphorylated in an ATR/ATM-dependent manner following replication arrest and DNA damage induced during the S phase of the cell cycle." Oncogene **22**(10): 1491-1500.
Pilder, S., M. Moore, J. Logan and T. Shenk (1986). "The adenovirus E1B-55K transforming polypeptide modulates transport or cytoplasmic stabilization of viral and host cell mRNAs." Mol Cell Biol **6**(2): 470-476.
Poli, J., O. Tsaponina, L. Crabbe, A. Keszthelyi, V. Pantesco, A. Chabes, A. Lengronne and P. Pasero (2012). "dNTP pools determine fork progression and origin usage under replication stress." Embo Journal **31**(4): 883-894.
Pope, J. H. and W. P. Rowe (1964). "Immunofluorescent Studies of Adenovirus 12 Tumors and of Cells Transformed or Infected by Adenoviruses." J Exp Med **120**: 577-588.
Postow, L., C. Ullsperger, R. W. Keller, C. Bustamante, A. V. Vologodskii and N. R. Cozzarelli (2001). "Positive torsional strain causes the formation of a four-way junction at replication forks." J Biol Chem **276**(4): 2790-2796.
Pourquier, P., A. A. Pilon, G. Kohlhagen, A. Mazumder, A. Sharma and Y. Pommier (1997). "Trapping of mammalian topoisomerase I and recombinations induced by damaged DNA containing nicks or gaps. Importance of DNA end phosphorylation and camptothecin effects." J Biol Chem **272**(42): 26441-26447.
Prasad, R., G. L. Dianov, V. A. Bohr and S. H. Wilson (2000). "FEN1 stimulation of DNA polymerase beta mediates an excision step in mammalian long patch base excision repair." Journal of Biological Chemistry **275**(6): 4460-4466.

Pruijn, G. J., W. van Driel and P. C. van der Vliet (1986). "Nuclear factor III, a novel sequence-specific DNA-binding protein from HeLa cells stimulating adenovirus DNA replication." Nature **322**(6080): 656-659.
Puvion-Dutilleul, F., M. K. Chelbi-Alix, M. Koken, F. Quignon, E. Puvion and H. de The (1995). "Adenovirus infection induces rearrangements in the intranuclear distribution of the nuclear body-associated PML protein." Exp Cell Res **218**(1): 9-16.
Querido, E., P. Blanchette, Q. Yan, T. Kamura, M. Morrison, D. Boivin, W. G. Kaelin, R. C. Conaway, J. W. Conaway and P. E. Branton (2001). "Degradation of p53 by adenovirus E4orf6 and E1B55K proteins occurs via a novel mechanism involving a Cullin-containing complex." Genes Dev **15**(23): 3104-3117.
Querido, E., R. C. Marcellus, A. Lai, R. Charbonneau, J. G. Teodoro, G. Ketner and P. E. Branton (1997). "Regulation of p53 levels by the E1B 55-kilodalton protein and E4orf6 in adenovirus-infected cells." J Virol **71**(5): 3788-3798.
Ragland, R. L., S. Patel, R. S. Rivard, K. Smith, A. A. Peters, A. K. Bielinsky and E. J. Brown (2013). "RNF4 and PLK1 are required for replication fork collapse in ATR-deficient cells." Genes & Development **27**(20): 2259-2273.
Ralf, C., I. D. Hickson and L. Wu (2006). "The Bloom's syndrome helicase can promote the regression of a model replication fork." Journal of Biological Chemistry **281**(32): 22839-22846.
Rao, L., M. Debbas, P. Sabbatini, D. Hockenbery, S. Korsmeyer and E. White (1992). "The adenovirus E1A proteins induce apoptosis, which is inhibited by the E1B 19-kDa and Bcl-2 proteins." Proc Natl Acad Sci U S A **89**(16): 7742-7746.
Raschle, M., P. Knipscheer, M. Enoiu, T. Angelov, J. Sun, J. D. Griffith, T. E. Ellenberger, O. D. Scharer and J. C. Walter (2008). "Mechanism of replication-coupled DNA interstrand crosslink repair." Cell **134**(6): 969-980.
Reinhardt, H. C., A. S. Aslanian, J. A. Lees and M. B. Yaffe (2007). "p53-deficient cells rely on ATM- and ATR-mediated checkpoint signaling through the p38MAPK/MK2 pathway for survival after DNA damage." Cancer Cell **11**(2): 175-189.
Rekosh, D. M., W. C. Russell, A. J. Bellet and A. J. Robinson (1977). "Identification of a protein linked to the ends of adenovirus DNA." Cell **11**(2): 283-295.
Riballo, E., S. E. Critchlow, S. H. Teo, A. J. Doherty, A. Priestley, B. Broughton, B. Kysela, H. Beamish, N. Plowman, C. F. Arlett, A. R. Lehmann, S. P. Jackson and P. A. Jeggo (1999). "Identification of a defect in DNA ligase IV in a radiosensitive leukaemia patient." Curr Biol **9**(13): 699-702.
Rich, T., R. L. Allen and A. H. Wyllie (2000). "Defying death after DNA damage." Nature **407**(6805): 777-783.
Roberts, M. M., J. L. White, M. G. Grutter and R. M. Burnett (1986). "Three-dimensional structure of the adenovirus major coat protein hexon." Science **232**(4754): 1148-1151.
Robison, J. G., J. Elliott, K. Dixon and G. G. Oakley (2004). "Replication protein A and the Mre11 center dot Rad50 center dot Nbs1 complex co-localize and interact at sites of stalled replication forks." Journal of Biological Chemistry **279**(33): 34802-34810.
Rogakou, E. P., D. R. Pilch, A. H. Orr, V. S. Ivanova and W. M. Bonner (1998). "DNA double-stranded breaks induce histone H2AX phosphorylation on serine 139." J Biol Chem **273**(10): 5858-5868.

Rowe, W. P., R. J. Huebner, L. K. Gilmore, R. H. Parrott and T. G. Ward (1953). "Isolation of a cytopathogenic agent from human adenoids undergoing spontaneous degeneration in tissue culture." Proc Soc Exp Biol Med **84**(3): 570-573.
Roy, S., R. Calcedo, A. Medina-Jaszek, M. Keough, H. Peng and J. M. Wilson (2011). "Adenoviruses in lymphocytes of the human gastro-intestinal tract." PLoS One **6**(9): e24859.
Ruley, H. E. (1983). "Adenovirus early region 1A enables viral and cellular transforming genes to transform primary cells in culture." Nature **304**(5927): 602-606.
Russell, W. C. (2009). "Adenoviruses: update on structure and function." J Gen Virol **90**(Pt 1): 1-20.
Sabbatini, P., S. K. Chiou, L. Rao and E. White (1995). "Modulation of p53-mediated transcriptional repression and apoptosis by the adenovirus E1B 19K protein." Mol Cell Biol **15**(2): 1060-1070.
Saijo, M., I. Kuraoka, C. Masutani, F. Hanaoka and K. Tanaka (1996). "Sequential binding of DNA repair proteins RPA and ERCC1 to XPA in vitro." Nucleic Acids Research **24**(23): 4719-4724.
Salone, B., Y. Martina, S. Piersanti, E. Cundari, G. Cherubini, L. Franqueville, C. M. Failla, P. Boulanger and S. I (2003). "Integrin alpha 3 beta 1 is an alternative cellular receptor for adenovirus serotype 5." Journal of Virology **77**(24): 13448-13454.
Sanchez, Y., C. Wong, R. S. Thoma, R. Richman, Z. Wu, H. Piwnica-Worms and S. J. Elledge (1997). "Conservation of the Chk1 checkpoint pathway in mammals: linkage of DNA damage to Cdk regulation through Cdc25." Science **277**(5331): 1497-1501.
Sarbajna, S., D. Davies and S. C. West (2014). "Roles of SLX1-SLX4, MUS81-EME1, and GEN1 in avoiding genome instability and mitotic catastrophe." Genes Dev **28**(10): 1124-1136.
Sartori, A. A., C. Lukas, J. Coates, M. Mistrik, S. Fu, J. Bartek, R. Baer, J. Lukas and S. P. Jackson (2007). "Human CtIP promotes DNA end resection." Nature **450**(7169): 509-U506.
Satoh, M. S. and T. Lindahl (1992). "Role of poly(ADP-ribose) formation in DNA repair." Nature **356**(6367): 356-358.
Schaack, J., W. Y. Ho, P. Freimuth and T. Shenk (1990). "Adenovirus terminal protein mediates both nuclear matrix association and efficient transcription of adenovirus DNA." Genes Dev **4**(7): 1197-1208.
Schaley, J., R. J. O'Connor, L. J. Taylor, D. Bar-Sagi and P. Hearing (2000). "Induction of the cellular E2F-1 promoter by the adenovirus E4-6/7 protein." J Virol **74**(5): 2084-2093.
Schlacher, K., N. Christ, N. Siaud, A. Egashira, H. Wu and M. Jasin (2011). "Double-Strand Break Repair-Independent Role for BRCA2 in Blocking Stalled Replication Fork Degradation by MRE11 (vol 145, pg 529, 2011)." Cell **145**(6): 993-993.
Schon, O., A. Friedler, M. Bycroft, S. M. V. Freund and A. R. Fersht (2002). "Molecular mechanism of the interaction between MDM2 and p53." Journal of Molecular Biology **323**(3): 491-501.
Schreiner, S., C. Burck, M. Glass, P. Groitl, P. Wimmer, S. Kinkley, A. Mund, R. D. Everett and T. Dobner (2013). "Control of human adenovirus type 5 gene expression by cellular Daxx/ATRX chromatin-associated complexes." Nucleic Acids Res **41**(6): 3532-3550.
Schreiner, S., P. Wimmer, P. Groitl, S. Y. Chen, P. Blanchette, P. E. Branton and T. Dobner (2011). "Adenovirus type 5 early region 1B 55K oncoprotein-dependent degradation of cellular factor Daxx is required for efficient transformation of primary rodent cells." J Virol **85**(17): 8752-8765.

Schwab, R. A., A. N. Blackford and W. Niedzwiedz (2010). "ATR activation and replication fork restart are defective in FANCM-deficient cells." Embo Journal **29**(4): 806-818.
Seimiya, H. and S. Smith (2002). "The telomeric poly(ADP-ribose) polymerase, tankyrase 1, contains multiple binding sites for telomeric repeat binding factor 1 (TRF1) and a novel acceptor, 182-kDa tankyrase-binding protein (TAB182)." Journal of Biological Chemistry **277**(16): 14116-14126.
Shi, W., Z. Feng, J. Zhang, I. Gonzalez-Suarez, R. P. Vanderwaal, X. Wu, S. N. Powell, J. L. Roti Roti, S. Gonzalo and J. Zhang (2010). "The role of RPA2 phosphorylation in homologous recombination in response to replication arrest." Carcinogenesis **31**(6): 994-1002.
Shieh, S. Y., J. Ahn, K. Tamai, Y. Taya and C. Prives (2000). "The human homologs of checkpoint kinases Chk1 and Cds1 (Chk2) phosphorylate p53 at multiple DNA damage-inducible sites." Genes & Development **14**(3): 289-300.
Shivji, K. K., M. K. Kenny and R. D. Wood (1992). "Proliferating cell nuclear antigen is required for DNA excision repair." Cell **69**(2): 367-374.
Shivji, M. K. K., M. K. Kenny and R. D. Wood (1992). "Proliferating Cell Nuclear Antigen Is Required for DNA Excision Repair." Cell **69**(2): 367-374.
Shtrichman, R., R. Sharf, H. Barr, T. Dobner and T. Kleinberger (1999). "Induction of apoptosis by adenovirus E4orf4 protein is specific to transformed cells and requires an interaction with protein phosphatase 2A." Proc Natl Acad Sci U S A **96**(18): 10080-10085.
Sidorova, J. M., N. Z. Li, A. Folch and R. J. Monnat (2008). "The RecQ helicase WRN is required for normal replication fork progression after DNA damage or replication fork arrest." Cell Cycle **7**(6): 796-807.
Sirbu, B. M., W. H. McDonald, H. Dungrawala, A. Badu-Nkansah, G. M. Kavanaugh, Y. Chen, D. L. Tabb and D. Cortez (2013). "Identification of proteins at active, stalled, and collapsed replication forks using isolation of proteins on nascent DNA (iPOND) coupled with mass spectrometry." J Biol Chem **288**(44): 31458-31467.
Sleeth, K. M., R. L. Robson and G. L. Dianov (2004). "Exchangeability of mammalian DNA ligases between base excision repair pathways." Biochemistry **43**(40): 12924-12930.
Smeets, D. F. and F. A. van de Klundert (1990). "Common fragile sites in man and three closely related primate species." Cytogenet Cell Genet **53**(1): 8-14.
Sobeck, A., S. Stone, V. Costanzo, B. de Graaf, T. Reuter, J. de Winter, M. Wallisch, Y. Akkari, S. Olson, W. Wang, H. Joenje, J. L. Christian, P. J. Lupardus, K. A. Cimprich, J. Gautier and M. E. Hoatlin (2006). "Fanconi anemia proteins are required to prevent accumulation of replication-associated DNA double-strand breaks." Mol Cell Biol **26**(2): 425-437.
Song, C. Z., P. M. Loewenstein, K. Toth and M. Green (1995). "Transcription factor TFIID is a direct functional target of the adenovirus E1A transcription-repression domain." Proc Natl Acad Sci U S A **92**(22): 10330-10333.
Sonoda, E., M. S. Sasaki, J. M. Buerstedde, O. Bezzubova, A. Shinohara, H. Ogawa, M. Takata, Y. Yamaguchi-Iwai and S. Takeda (1998). "Rad51-deficient vertebrate cells accumulate chromosomal breaks prior to cell death." EMBO J **17**(2): 598-608.
Sorensen, C. S., R. G. Syluasen, J. Falck, T. Schroeder, L. Ronnstrand, K. K. Khanna, B. B. Zhou, J. Bartek and J. Lukas (2003). "Chk1 regulates the S phase checkpoint by coupling the physiological turnover and ionizing radiation-induced accelerated proteolysis of Cdc25A." Cancer Cell **3**(3): 247-258.

Soria, C., F. E. Estermann, K. C. Espantman and C. C. O'Shea (2010). "Heterochromatin silencing of p53 target genes by a small viral protein." Nature **466**(7310): 1076-U1085.
Sparks, J. L., H. Chon, S. M. Cerritelli, T. A. Kunkel, E. Johansson, R. J. Crouch and P. M. Burgers (2012). "RNase H2-Initiated Ribonucleotide Excision Repair." Molecular Cell **47**(6): 980-986.
Srinivasan, S. V., D. Dominguez-Sola, L. C. Wang, O. Hyrien and J. Gautier (2013). "Cdc45 Is a Critical Effector of Myc-Dependent DNA Replication Stress." Cell Reports **3**(5): 1629-1639.
Steegenga, W. T., N. Riteco, A. G. Jochemsen, F. J. Fallaux and J. L. Bos (1998). "The large E1B protein together with the E4orf6 protein target p53 for active degradation in adenovirus infected cells." Oncogene **16**(3): 349-357.
Stelter, P. and H. D. Ulrich (2003). "Control of spontaneous and damage-induced mutagenesis by SUMO and ubiquitin conjugation." Nature **425**(6954): 188-191.
Stewart, G. S., R. S. Maser, T. Stankovic, D. A. Bressan, M. I. Kaplan, N. G. Jaspers, A. Raams, P. J. Byrd, J. H. Petrini and A. M. Taylor (1999). "The DNA double-strand break repair gene hMRE11 is mutated in individuals with an ataxia-telangiectasia-like disorder." Cell **99**(6): 577-587.
Stewart, G. S., S. Panier, K. Townsend, A. K. Al-Hakim, N. K. Kolas, E. S. Miller, S. Nakada, J. Ylanko, S. Olivarius, M. Mendez, C. Oldreive, J. Wildenhain, A. Tagliaferro, L. Pelletier, N. Taubenheim, A. Durandy, P. J. Byrd, T. Stankovic, A. M. R. Taylor and D. Durocher (2009). "The RIDDLE Syndrome Protein Mediates a Ubiquitin-Dependent Signaling Cascade at Sites of DNA Damage." Cell **136**(3): 420-434.
Stich, H. F., T. C. Hsu and F. Rapp (1964). "Viruses + Mammalian Chromosomes .I. Localization of Chromosome Aberrations after Infection with Herpes Simplex Virus." Virology **22**(4): 439-&.
Stillman, B. W., J. B. Lewis, L. T. Chow, M. B. Mathews and J. E. Smart (1981). "Identification of the gene and mRNA for the adenovirus terminal protein precursor." Cell **23**(2): 497-508.
Stracker, T. H., C. T. Carson and M. D. Weitzman (2002). "Adenovirus oncoproteins inactivate the Mre11-Rad50-NBS1 DNA repair complex." Nature **418**(6895): 348-352.
Stracker, T. H., D. V. Lee, C. T. Carson, F. D. Araujo, D. A. Ornelles and M. D. Weitzman (2005). "Serotype-specific reorganization of the Mre11 complex by adenoviral E4orf3 proteins." Journal of Virology **79**(11): 6664-6673.
Stucki, M., J. A. Clapperton, D. Mohammad, M. B. Yaffe, S. J. Smerdon and S. P. Jackson (2005). "MDC1 directly binds phosphorylated histone H2AX to regulate cellular responses to DNA double-strand breaks." Cell **123**(7): 1213-1226.
Subramanian, T., B. Tarodi and G. Chinnadurai (1995). "p53-independent apoptotic and necrotic cell deaths induced by adenovirus infection: suppression by E1B 19K and Bcl-2 proteins." Cell Growth Differ **6**(2): 131-137.
Sugasawa, K., J. M. Y. Ng, C. Masutani, S. Iwai, P. J. van der Spek, A. P. M. Eker, F. Hanaoka, D. Bootsma and J. H. J. Hoeijmakers (1998). "Xeroderma pigmentosum group C protein complex is the initiator of global genome nucleotide excision repair." Molecular Cell **2**(2): 223-232.
Sugiyama, T. and S. C. Kowalczykowski (2002). "Rad52 protein associates with replication protein A (RPA)-single-stranded DNA to accelerate Rad51-mediated displacement of RPA and presynaptic complex formation." J Biol Chem **277**(35): 31663-31672.

Sun, H., J. K. Karow, I. D. Hickson and N. Maizels (1998). "The Bloom's syndrome helicase unwinds G4 DNA." Journal of Biological Chemistry **273**(42): 27587-27592.
Sun, Y. L., X. F. Jiang, S. J. Chen, N. Fernandes and B. D. Price (2005). "A role for the Tip60 histone acetyltransferase in the acetylation and activation of ATM." Proceedings of the National Academy of Sciences of the United States of America **102**(37): 13182-13187.
Suwa, A., M. Hirakata, Y. Takeda, S. A. Jesch, T. Mimori and J. A. Hardin (1994). "DNA-Dependent Protein-Kinase (Ku Protein-P350 Complex) Assembles on Double-Stranded DNA." Proceedings of the National Academy of Sciences of the United States of America **91**(15): 6904-6908.
Takahashi, P., A. Polson and D. Reisman (2011). "Elevated transcription of the p53 gene in early S-phase leads to a rapid DNA-damage response during S-phase of the cell cycle." Apoptosis **16**(9): 950-958.
Takahashi, S., K. Kontani, Y. Araki and T. Katada (2007). "Caf1 regulates translocation of ribonucleotide reductase by releasing nucleoplasmic Spd1-Suc22 assembly." Nucleic Acids Res **35**(4): 1187-1197.
Takahashi, Y., V. Lallemand-Breitenbach, J. Zhu and H. de The (2004). "PML nuclear bodies and apoptosis." Oncogene **23**(16): 2819-2824.
Takata, M., M. S. Sasaki, E. Sonoda, C. Morrison, M. Hashimoto, H. Utsumi, Y. Yamaguchi-Iwai, A. Shinohara and S. Takeda (1998). "Homologous recombination and non-homologous end-joining pathways of DNA double-strand break repair have overlapping roles in the maintenance of chromosomal integrity in vertebrate cells." EMBO J **17**(18): 5497-5508.
Tanaka, H., H. Arakawa, T. Yamaguchi, K. Shiraishi, S. Fukuda, K. Matsui, Y. Takei and Y. Nakamura (2000). "A ribonucleotide reductase gene involved in a p53-dependent cell-cycle checkpoint for DNA damage." Nature **404**(6773): 42-49.
Tanaka, M., K. Hayashi, H. Sakura, M. Miwa, T. Matsushima and T. Sugimura (1978). "Demonstration of high molecular weight poly (adenosine diphosphate ribose)." Nucleic Acids Res **5**(9): 3183-3194.
Tang, J., J. D. Gary, S. Clarke and H. R. Herschman (1998). "PRMT 3, a type I protein arginine N-methyltransferase that differs from PRMT1 in its oligomerization, subcellular localization, substrate specificity, and regulation." J Biol Chem **273**(27): 16935-16945.
Tapias, A., J. Auriol, D. Forget, J. H. Enzlin, O. D. Scharer, F. Coin, B. Coulombe and J. M. Egly (2004). "Ordered conformational changes in damaged DNA induced by nucleotide excision repair factors." Journal of Biological Chemistry **279**(18): 19074-19083.
Tercero, J. A. and J. F. Diffley (2001). "Regulation of DNA replication fork progression through damaged DNA by the Mec1/Rad53 checkpoint." Nature **412**(6846): 553-557.
Thangavel, S., M. Berti, M. Levikova, C. Pinto, S. Gomathinayagam, M. Vujanovic, R. Zellweger, H. Moore, E. H. Lee, E. A. Henclrickson, P. Cejka, S. Stewart, M. Lopes and A. Vindigni (2015). "DNA2 drives processing and restart of reversed replication forks in human cells." Journal of Cell Biology **208**(5): 545-562.
Thomas, D. C., J. D. Roberts and T. A. Kunkel (1991). "Heteroduplex repair in extracts of human HeLa cells." J Biol Chem **266**(6): 3744-3751.
Tibbetts, R. S., K. M. Brumbaugh, J. M. Williams, J. N. Sarkaria, W. A. Cliby, S. Y. Shieh, Y. Taya, C. Prives and R. T. Abraham (1999). "A role for ATR in the DNA damage-induced phosphorylation of p53." Genes & Development **13**(2): 152-157.

Tibbetts, R. S., D. Cortez, K. M. Brumbaugh, R. Scully, D. Livingston, S. J. Elledge and R. T. Abraham (2000). "Functional interactions between BRCA1 and the checkpoint kinase ATR during genotoxic stress." Genes Dev **14**(23): 2989-3002.
Traven, A., A. Hammet, N. Tenis, C. L. Denis and J. Heierhorst (2005). "Ccr4-not complex mRNA deadenylase activity contributes to DNA damage responses in Saccharomyces cerevisiae." Genetics **169**(1): 65-75.
Trenz, K., E. Smith, S. Smith and V. Costanzo (2006). "ATM and ATR promote Mre11 dependent restart of collapsed replication forks and prevent accumulation of DNA breaks." EMBO J **25**(8): 1764-1774.
Tsai, C. J., S. A. Kim and G. Chu (2007). "Cernunnos/XLF promotes the ligation of mismatched and noncohesive DNA ends." Proceedings of the National Academy of Sciences of the United States of America **104**(19): 7851-7856.
Tsuji, T., E. Lau, G. G. Chiang and W. Jiang (2008). "The Role of Dbf4/Drf1-Dependent Kinase Cdc7 in DNA-Damage Checkpoint Control." Molecular Cell **32**(6): 862-869.
Tucker, M., R. R. Staples, M. A. Valencia-Sanchez, D. Muhlrad and R. Parker (2002). "Ccr4p is the catalytic subunit of a Ccr4p/Pop2p/Notp mRNA deadenylase complex in Saccharomyces cerevisiae." EMBO J **21**(6): 1427-1436.
Tucker, M., M. A. Valencia-Sanchez, R. R. Staples, J. Chen, C. L. Denis and R. Parker (2001). "The transcription factor associated Ccr4 and Caf1 proteins are components of the major cytoplasmic mRNA deadenylase in Saccharomyces cerevisiae." Cell **104**(3): 377-386.
Tuduri, S., L. Crabbe, C. Conti, H. Tourriere, H. Holtgreve-Grez, A. Jauch, V. Pantesco, J. De Vos, A. Thomas, C. Theillet, Y. Pommier, J. Tazi, A. Coquelle and P. Pasero (2009). "Topoisomerase I suppresses genomic instability by preventing interference between replication and transcription." Nature Cell Biology **11**(11): 1315-U1125.
Turnell, A. S. and R. J. Grand (2012). "DNA viruses and the cellular DNA-damage response." Journal of General Virology **93**: 2076-2097.
Ueda, K., A. Omachi, M. Kawaichi and O. Hayaishi (1975). "Natural occurrence of poly(ADP-ribosyl) histones in rat liver." Proc Natl Acad Sci U S A **72**(1): 205-209.
Uhnoo, I., G. Wadell, L. Svensson and M. E. Johansson (1984). "Importance of enteric adenoviruses 40 and 41 in acute gastroenteritis in infants and young children." J Clin Microbiol **20**(3): 365-372.
Valentine, R. C. and H. G. Pereira (1965). "Antigens and structure of the adenovirus." J Mol Biol **13**(1): 13-20.
Vallur, A. C. and N. Maizels (2010). "Distinct Activities of Exonuclease 1 and Flap Endonuclease 1 at Telomeric G4 DNA." Plos One **5**(1).
van der Vliet, P. C. and A. J. Levine (1973). "DNA-binding proteins specific for cells infected by adenovirus." Nat New Biol **246**(154): 170-174.
Vayda, M. E., A. E. Rogers and S. J. Flint (1983). "The structure of nucleoprotein cores released from adenovirions." Nucleic Acids Res **11**(2): 441-460.
Virtanen, A., P. Gilardi, A. Naslund, J. M. LeMoullec, U. Pettersson and M. Perricaudet (1984). "mRNAs from human adenovirus 2 early region 4." J Virol **51**(3): 822-831.
Volker, M., M. J. Mone, P. Karmakar, A. van Hoffen, W. Schul, W. Vermeulen, J. H. J. Hoeijmakers, R. van Driel, A. A. van Zeeland and L. H. F. Mullenders (2001). "Sequential assembly of the nucleotide excision repair factors in vivo." Molecular Cell **8**(1): 213-224.

Walker, J. R., R. A. Corpina and J. Goldberg (2001). "Structure of the Ku heterodimer bound to DNA and its implications for double-strand break repair." Nature **412**(6847): 607-614.
Wang, B., S. Matsuoka, P. B. Carpenter and S. J. Elledge (2002). "53BP1, a mediator of the DNA damage checkpoint." Science **298**(5597): 1435-1438.
Wang, P. J., A. Chabes, R. Casagrande, X. C. Tian, L. Thelander and T. C. Huffaker (1997). "Rnr4p, a novel ribonucleotide reductase small-subunit protein." Mol Cell Biol **17**(10): 6114-6121.
Wang, X. W., Q. M. Zhan, J. D. Coursen, M. A. Khan, H. U. Kontny, L. J. Yu, M. C. Hollander, P. M. O'Connor, A. J. Fornace and C. C. Harris (1999). "GADD45 induction of a G(2)/M cell cycle checkpoint." Proceedings of the National Academy of Sciences of the United States of America **96**(7): 3706-3711.
Ward, I. M. and J. Chen (2001). "Histone H2AX is phosphorylated in an ATR-dependent manner in response to replicational stress." J Biol Chem **276**(51): 47759-47762.
Ward, J. F., J. W. Evans, C. L. Limoli and P. M. Calabro-Jones (1987). "Radiation and hydrogen peroxide induced free radical damage to DNA." Br J Cancer Suppl **8**: 105-112.
Watson, J. D. and F. H. Crick (1953). "Molecular structure of nucleic acids; a structure for deoxyribose nucleic acid." Nature **171**(4356): 737-738.
Weibezahn, K. F. and T. Coquerelle (1981). "Radiation induced DNA double strand breaks are rejoined by ligation and recombination processes." Nucleic Acids Res **9**(13): 3139-3150.
Weiden, M. D. and H. S. Ginsberg (1994). "Deletion of the E4 region of the genome produces adenovirus DNA concatemers." Proc Natl Acad Sci U S A **91**(1): 153-157.
Weiden, M. D. and H. S. Ginsberg (1994). "Deletion of the E4 Region of the Genome Produces Adenovirus DNA Concateners." Proceedings of the National Academy of Sciences of the United States of America **91**(1): 153-157.
Weinfeld, M., M. A. Chaudhry, D. D'Amours, J. D. Pelletier, G. G. Poirier, L. F. Povirk and S. P. Lees-Miller (1997). "Interaction of DNA-dependent protein kinase and poly(ADP-ribose) polymerase with radiation-induced DNA strand breaks." Radiat Res **148**(1): 22-28.
Weiss, S. J., G. W. King and A. F. LoBuglio (1977). "Evidence for hydroxyl radical generation by human Monocytes." J Clin Invest **60**(2): 370-373.
Westmoreland, T. J., J. R. Marks, J. A. Olson, Jr., E. M. Thompson, M. A. Resnick and C. B. Bennett (2004). "Cell cycle progression in G1 and S phases is CCR4 dependent following ionizing radiation or replication stress in Saccharomyces cerevisiae." Eukaryot Cell **3**(2): 430-446.
Whitehouse, C. J., R. M. Taylor, A. Thistlethwaite, H. Zhang, F. Karimi-Busheri, D. D. Lasko, M. Weinfeld and K. W. Caldecott (2001). "XRCC1 stimulates human polynucleotide kinase activity at damaged DNA termini and accelerates DNA single-strand break repair." Cell **104**(1): 107-117.
Whyte, P., K. J. Buchkovich, J. M. Horowitz, S. H. Friend, M. Raybuck, R. A. Weinberg and E. Harlow (1988). "Association between an oncogene and an anti-oncogene: the adenovirus E1A proteins bind to the retinoblastoma gene product." Nature **334**(6178): 124-129.
Wickham, T. J., P. Mathias, D. A. Cheresh and G. R. Nemerow (1993). "Integrins alpha v beta 3 and alpha v beta 5 promote adenovirus internalization but not virus attachment." Cell **73**(2): 309-319.

Wilsker, D., E. Petermann, T. Helleday and F. Bunz (2008). "Essential function of Chk1 can be uncoupled from DNA damage checkpoint and replication control." Proceedings of the National Academy of Sciences of the United States of America **105**(52): 20752-20757.
Wong, A. K. C., R. Pero, P. A. Ormonde, S. V. Tavtigian and P. L. Bartel (1997). "RAD51 interacts with the evolutionarily conserved BRC motifs in the human breast cancer susceptibility gene brca2." Journal of Biological Chemistry **272**(51): 31941-31944.
Woo, J. L. and A. J. Berk (2007). "Adenovirus ubiquitin-protein ligase stimulates viral late mRNA nuclear export." J Virol **81**(2): 575-587.
Wood, R. D. (1999). "DNA damage recognition during nucleotide excision repair in mammalian cells." Biochimie **81**(1-2): 39-44.
Woodward, A. M., T. Gohler, M. G. Luciani, M. Oehlmann, X. Q. Ge, A. Gartner, D. A. Jackson and J. J. Blow (2006). "Excess Mcm2-7 license dormant origins of replication that can be used under conditions of replicative stress." Journal of Cell Biology **173**(5): 673-683.
Woolstencroft, R. N., T. H. Beilharz, M. A. Cook, T. Preiss, D. Durocher and M. Tyers (2006). "Ccr4 contributes to tolerance of replication stress through control of CRT1 mRNA poly(A) tail length." J Cell Sci **119**(Pt 24): 5178-5192.
Wu, L. and I. D. Hickson (2003). "The Bloom's syndrome helicase suppresses crossing over during homologous recombination." Nature **426**(6968): 870-874.
Wu, Y. L., K. Shin-ya and R. M. Brosh (2008). "FANCJ helicase defective in Fanconia anemia and breast cancer unwinds G-quadruplex DNA to defend genomic stability." Molecular and Cellular Biology **28**(12): 4116-4128.
Xue, Y., R. Gibbons, Z. Yan, D. Yang, T. L. McDowell, S. Sechi, J. Qin, S. Zhou, D. Higgs and W. Wang (2003). "The ATRX syndrome protein forms a chromatin-remodeling complex with Daxx and localizes in promyelocytic leukemia nuclear bodies." Proc Natl Acad Sci U S A **100**(19): 10635-10640.
Yabe, Y., J. J. Trentin and G. Taylor (1962). "Cancer induction in hamsters by human type 12 adenovirus. Effect of age and of virus dose." Proc Soc Exp Biol Med **111**: 343-344.
Yan, J., J. Zhu, H. Zhong, Q. Lu, C. Huang and Q. Ye (2003). "BRCA1 interacts with FHL2 and enhances FHL2 transactivation function." FEBS Lett **553**(1-2): 183-189.
Yano, K., K. Morotomi-Yano, S. Y. Wang, N. Uematsu, K. J. Lee, A. Asaithamby, E. Weterings and D. J. Chen (2008). "Ku recruits XLF to DNA double-strand breaks." EMBO Rep **9**(1): 91-96.
Yarbro, J. W. (1968). "Further studies on the mechanism of action of hydroxyurea." Cancer Res **28**(6): 1082-1087.
Yew, P. R. and A. J. Berk (1992). "Inhibition of p53 transactivation required for transformation by adenovirus early 1B protein." Nature **357**(6373): 82-85.
Yew, P. R., X. Liu and A. J. Berk (1994). "Adenovirus E1B oncoprotein tethers a transcriptional repression domain to p53." Genes Dev **8**(2): 190-202.
Ying, S. M., S. Minocherhomji, K. L. Chan, T. Palmai-Pallag, W. K. Chu, T. Wass, H. W. Mankouri, Y. Liu and I. D. Hickson (2013). "MUS81 promotes common fragile site expression." Nature Cell Biology **15**(8): 1001-U1253.
Yoo, S. and W. S. Dynan (1999). "Geometry of a complex formed by double strand break repair proteins at a single DNA end: recruitment of DNA-PKcs induces inward translocation of Ku protein." Nucleic Acids Res **27**(24): 4679-4686.

Yu, X. C., S. A. Fu, M. Y. Lai, R. Baer and J. J. Chen (2006). "BRCA1 ubiquitinates its phosphorylation-dependent binding partners CtIP." Genes & Development **20**(13): 1721-1726.
Yu, Y., W. Wang, Q. Ding, R. Ye, D. Chen, D. Merkle, D. Schriemer, K. Meek and S. P. Lees-Miller (2003). "DNA-PK phosphorylation sites in XRCC4 are not required for survival after radiation or for V(D)J recombination." DNA Repair (Amst) **2**(11): 1239-1252.
Zantema, A., J. A. Fransen, A. Davis-Olivier, F. C. Ramaekers, G. P. Vooijs, B. DeLeys and A. J. Van der Eb (1985). "Localization of the E1B proteins of adenovirus 5 in transformed cells, as revealed by interaction with monoclonal antibodies." Virology **142**(1): 44-58.
Zegerman, P. and J. F. Diffley (2010). "Checkpoint-dependent inhibition of DNA replication initiation by Sld3 and Dbf4 phosphorylation." Nature **467**(7314): 474-478.
Zellweger, R., D. Dalcher, K. Mutreja, M. Berti, J. A. Schmid, R. Herrador, A. Vindigni and M. Lopes (2015). "Rad51-mediated replication fork reversal is a global response to genotoxic treatments in human cells." Journal of Cell Biology **208**(5): 563-579.
Zeman, M. K. and K. A. Cimprich (2014). "Causes and consequences of replication stress." Nat Cell Biol **16**(1): 2-9.
Zhan, Q. M., M. J. Antinore, X. W. Wang, F. Carrier, M. L. Smith, C. C. Harris and A. J. Forance (1999). "Association with Cdc2 and inhibition of Cdc2/cyclin B1 kinase activity by the p53-regulated protein Gadd45." Oncogene **18**(18): 2892-2900.
Zhang, Y., F. Yuan, S. R. Presnell, K. Tian, Y. Gao, A. E. Tomkinson, L. Gu and G. M. Li (2005). "Reconstitution of 5'-directed human mismatch repair in a purified system." Cell **122**(5): 693-705.
Zhao, H. and H. Piwnica-Worms (2001). "ATR-mediated checkpoint pathways regulate phosphorylation and activation of human Chk1." Mol Cell Biol **21**(13): 4129-4139.
Zhao, H., J. L. Watkins and H. Piwnica-Worms (2002). "Disruption of the checkpoint kinase 1/cell division cycle 25A pathway abrogates ionizing radiation-induced S and G(2) checkpoints." Proceedings of the National Academy of Sciences of the United States of America **99**(23): 14795-14800.
Zheng, Z. M. (2010). "Viral oncogenes, noncoding RNAs, and RNA splicing in human tumor viruses." Int J Biol Sci **6**(7): 730-755.
Zhong, H., A. Bryson, M. Eckersdorff and D. O. Ferguson (2005). "Rad50 depletion impacts upon ATR-dependent DNA damage responses." Hum Mol Genet **14**(18): 2685-2693.
Zhong, S., P. Salomoni and P. P. Pandolfi (2000). "The transcriptional role of PML and the nuclear body." Nat Cell Biol **2**(5): E85-90.
Zou, L. and S. J. Elledge (2003). "Sensing DNA damage through ATRIP recognition of RPA-ssDNA complexes." Science **300**(5625): 1542-1548.
Zubieta, C., G. Schoehn, J. Chroboczek and S. Cusack (2005). "The structure of the human adenovirus 2 penton." Mol Cell **17**(1): 121-135.
Zur Hausen, H. (1967). "Induction of specific chromosomal aberrations by adenovirus type 12 in human embryonic kidney cells." J Virol **1**(6): 1174-1185.